Identification of common genetic variants as modifiers of risk of vestibular schwannoma

A thesis submitted to the University of Manchester for the degree of Doctor of Philosophy in the Faculty of Biology, Medicine and Health

2021

Katherine V. Sadler

School of Biological Sciences, Division of Evolution, Infection and Genomics

Table of Contents

Word count: 35,767

List of Figures

Supplementary Figures

List of Tables

Supplementary Tables

List of Abbreviations

ACGS - Association for Clinical Genomic Sciences

ACMG-AMP - American College of Medical Genetics and Genomics and the Association for Molecular Pathology

ASO - Antisense Oligonucleotide

bp - Base Pair

BSA - Bovine Serum Albumin

BVS - Bilateral Vestibular Schwannoma

Cas - CRISPR-associated

CNS - Central Nervous System

CNV - Copy Number Variant

COSMIC - Catalog of Somatic Mutations in Cancer

CRISPR - Clustered Regularly Interspaced Short Palindromic Repeats

dbSNP - Single Nucleotide Polymorphism Database

DECIPHER - Database of Chromosomal Imbalance and Phenotype in Humans using Ensembl Resources

DEPC- Diethyl Pyrocarbonate

DPBS - Dulbecco's Phosphate Buffered Saline

DMEM - Dulbecco's Modified Eagle Medium

DMSO - Dimethyl Sulfoxide

DNA - Deoxyribonucleic Acid

dNTP - Deoxynucleoside triphosphate

DQC - Dish QC

DTT - Dithiothreitol

EDTA - Ethylenediaminetetraacetic Acid

ERM - Ezrin, Radixin, and Moesin

ExAC - Exome Aggregation Consortium

FACS - Fluorescence Activated Cell Sorting

FBS - Fetal Bovine Serum

FERM - Four Point One, Ezrin, Radixin, and Moesin

GDL - Genomic Diagnostic Laboratory

GFP - Green Fluorescent Protein

gnomAD - Genome Aggregation Database

gRNA - Guide RNA

GWAS - Genome-Wide Association Study

HDR - Homology Directed Repair

HGMD - Human Gene Mutation Database

HGVS - Human Genome Variation Society

HRP - Horseradish Peroxidase

ICE - Inference of CRISPR Edits

LB - Luria-Bertani

LD - Linkage Disequilibrium

lncRNA - Long Non-Coding RNA

LOH - Loss of Heterozygosity

LOVD - Leiden Open Variation Database

MAF - Minor Allele Frequency

Mb - Megabases

MCGM - Manchester Centre for Genomic Medicine

MLPA - Multiplex Ligation-Dependent Probe Analysis

MOI - Multiplicity of Infection

MR - Mitotic Recombination

MRI - Magnetic-Resonance Imaging

NCARC - Northern Care Alliance Research Collection

NCBI - National Center for Biotechnology Information

NF2 - Neurofibromatosis Type 2

NGS - Next Generation Sequencing

NHEJ - Non-Homologous End Joining

NHS - National Health Service

NICE - National Institute for Health and Care Excellence

OR - Odds Ratio

PAM - Protospacer Adjacent Motif

PBS - Phosphate Buffered Saline

PCA - Principle Component Analysis

PCR - Polymerase Chain Reaction

pegRNA - Prime Editing Guide RNA

PRS - Polygenic Risk Score

PV - Pathogenic Variant

QC - Quality Control

REVEL - Rare Exome Variant Ensemble Learner

RIPA - Radioimmunoprecipitation Assay

RNA - Ribonucleic Acid

RNP - Ribonucleoprotein

SIFT - Sorting Intolerant From Tolerant

SNP - Single Nucleotide Polymorphism

SNV - Single Nucleotide Varinat

SRFT - Salford Royal Foundation Trust

sVS - Sporadic Vestibular Schwannoma

TAE - Tris Base, Acetic Acid, EDTA

TALENs - Transcription Activator-Like Effector Nucleases

TBE - Tris, Borate, EDTA

TBS - Tris-Buffered Saline

TE - Tris, EDTA

TERT - Telomerase Reverse Transcriptase

Tm - Melting Temperature

UCSC - University of California Santa Cruz

UVS - Unilateral Vestibular Schwannoma

VS - Vestibular Schwannoma

WES - Whole Exome Sequencing

WGS - Whole Genome Sequencing

WT - Wild-Type

Abstract

Identification of common genetic variants as modifiers of risk of vestibular schwannoma. Katherine V. Sadler; the University of Manchester, Doctor of Philosophy, 2021.

Vestibular schwannomas (VS) are benign tumours that arise on the vestibular branch of the vestibulocochlear nerve. Accounting for approximately 9% of all non-malignant central nervous system tumours, VS frequently cause hearing loss amongst other symptoms in patients. VS are known to occur in the context of tumour suppressor syndromes, neurofibromatosis type 2 (NF2) and *LZTR1*-associated schwannomatosis. However, most VS present sporadically in patients without further features of NF2 or schwannomatosis. Currently, no germline variants are associated with predisposition to sporadic VS in the absence of NF2 and schwannomatosis disease. This study aims to further the understanding of the genetic landscape that surrounds VS predisposition through different branches of research into the biological features of VS.

Characterisation of genotypic features for both germline and somatic samples in sporadic and syndromic forms of VS was conducted through a review of molecular testing in VS patients. Biallelic inactivation of *NF2* is frequently observed in somatic sporadic VS samples, suggesting that loss of *NF2* function is a common pathway in the development of all VS tumours. Interpretation of missense variants in *NF2* remains challenging. Through collation of known *NF2* missense variants and corresponding evidence for their clinical interpretation, I highlight the need for incorporation of disease-specific features into variant interpretation guidelines to improve clinical actionability.

In a genome-wide association study performed in 911 cases and 5,500 controls I identify a novel risk locus on chromosome 9p21.3 in association with sporadic VS risk. Pathway analysis of the genes encompassed by this region highlights a potential mechanism for susceptibility to VS development when somatic loss of *NF2* occurs.

Through disease modelling of a known VS susceptibility variant in *NF2*, I also demonstrate that splice-modulating therapies hold promise in the treatment of NF2 disease caused by deep intronic variants.

This study provides new insights and further characterisation of the genomic features that predispose to, and result in, VS tumourigenesis. These findings point towards promising new areas of research into VS predisposition, unified by dysregulation of the oncogenic signalling pathways that involve function of the *NF2* protein.

Lay abstract

Vestibular schwannomas (VS) are a benign type of tumour that develop on the lining of the hearing and balance nerves in the brain. Although VS are not malignant, their growth can damage surrounding structures within the brain, frequently causing hearing loss and other medical complications. VS can occur in some patients that have the conditions neurofibromatosis type 2 (NF2) and schwannomatosis. However, most VS patients present sporadically, out of the blue, and do not have NF2 or schwannomatosis. Currently, the genetic features that contribute to the risk of sporadic VS development are unknown. This study aims to provide a better understanding of the genetic features that contribute to VS risk and development.

By reviewing genetic testing results, I characterise the types of genetic changes found in the blood and tumour samples from VS patients. I found that the gene associated with NF2 is frequently non-functional (doesn't work) in sporadic VS tumour samples. This suggests that there are other inherited genetic features that make patients vulnerable to loss of the *NF2* gene.

I collated a list of known DNA changes in the *NF2* gene and looked for evidence to determine if these changes could be causative of NF2 disease. I conclude that more details on the medical features of patients would help determine if *NF2* gene changes are disease causing.

In a large case-control study I compared genetic differences between VS patients and healthy control samples. I found a region on chromosome 9 that seems to be associated with an increased chance of developing a VS tumour. The genes found in this region can be linked to the *NF2* gene and other cancer-associated signalling networks.

I also investigated a known VS causing genetic change in a cell model. The gene change is positioned within a non-coding part of the *NF2* gene. Because it is non-coding, I tried to correct the genetic change by treating cells with a synthetic piece of DNA that binds to, and masks, the genetic change. This treatment seemed to correct the way that the *NF2* gene is read and made into a protein.

This study provides new insights and further descriptions of the genetic features that increase the risk of VS tumours. I point towards promising new areas of research linked to cancer signalling pathways that involve the protein made by the *NF2* gene.

Declaration

No portion of the work referred to in the thesis has been submitted in support of an application for another degree or qualification of this or any other university or other institute of learning.

Copyright statement

i. The author of this thesis (including any appendices and/or schedules to this thesis) owns certain copyright or related rights in it (the "Copyright") and s/he has given The University of Manchester certain rights to use such Copyright, including for administrative purposes.

ii. Copies of this thesis, either in full or in extracts and whether in hard or electronic copy, may be made **only** in accordance with the Copyright, Designs and Patents Act 1988 (as amended) and regulations issued under it or, where appropriate, in accordance with licensing agreements which the University has from time to time. This page must form part of any such copies made.

iii. The ownership of certain Copyright, patents, designs, trademarks and other intellectual property (the "Intellectual Property") and any reproductions of copyright works in the thesis, for example graphs and tables ("Reproductions"), which may be described in this thesis, may not be owned by the author and may be owned by third parties. Such Intellectual Property and Reproductions cannot and must not be made available for use without the prior written permission of the owner(s) of the relevant Intellectual Property and/or Reproductions.

iv. Further information on the conditions under which disclosure, publication and commercialisation of this thesis, the Copyright and any Intellectual Property and/or Reproductions described in it may take place is available in the University IP Policy (see http://documents.manchester.ac.uk/DocuInfo.aspx?DocID=24420), in any relevant Thesis restriction declarations deposited in the University Library, The University Library's regulations (see http://www.library.manchester.ac.uk/about/regulations/) and in The University's policy on Presentation of Theses.

Acknowledgments

I would first like to express my gratitude to my supervisory team, Dr. Miram Smith and Prof. Gareth Evans, for all the support, guidance and time they have given to me over the past few years. It has been a great privilege to learn from you both; the extensive knowledge and enthusiasm you have for your areas of expertise is inspiring. I would like to thank Dr. Miriam Smith for teaching me many of the laboratory techniques and methods used to produce this thesis, in addition to all of the input and feedback you have given. I would like to thank Prof. Gareth Evans for all of his guidance and vital input into study designs and manuscripts.

My appreciation and thanks goes out to my project advisor Prof. Kevin Munro who provided me with support and advice over the course of this project. I am grateful to Dr. Antony Adamson, and the Genome Editing Unit team at the University of Manchester, for their input in experimental design and generous sharing of resources that have contributed greatly to the progress of this project. Also, a big thanks to Dr. John Bowes for sharing your statistical expertise for the benefit of this work.

I would like to thank all of the patients who contributed samples to the research undertaken, to the Biomedical Research Centre for funding this project and to all my collaborators over the past few years. A particular thanks to the Skull Base Team and Geoffrey Jefferson Brain Research Centre at Salford Royal Foundation Trust for providing samples, advice and support.

I am thankful to all of my lab group members, your support and skills have been invaluable over the course of my project and it has been a pleasure to work alongside you. A special thanks goes to Charlie Rowlands, Cristina Perez-Becerril and Leslie Molina-Ramirez-Keogh, without your expertise and friendship none of this would have been possible.

To my dearest friends Amy Cunningham, Ella Kidd, Mike Sheard, Charlie Rowlands, Jade Harris, Hannah Behague, Ria Hall, Emily Gatehouse and Brad Gregory, I want to thank you all from the bottom of my heart for the emotional, and physical, support that you have given me over the entirety of our friendships. I wouldn't have reached here without you all and I am forever grateful.

Finally, a huge thank you to Mum, Dad and Alexandra, your love and support is what motivates me every day.

Author contributions

3. Sporadic vestibular schwannoma: a molecular testing summary

J Med Genet, 58(4):227-233

Katherine V Sadler, Naomi L Bowers, Claire Hartley, Philip T Smith, Simon Tobi, Andrew J Wallace, Andrew King, Simon K W Lloyd, Scott Rutherford, Omar N Pathmanaban, Charlotte Hammerbeck-Ward, Simon Freeman, Emma Stapleton, Amy Taylor, Adam Shaw, Dorothy Halliday, Miriam Jane Smith, D Gareth Evans.

Patient data was compiled and analysed by myself, DGE and MJS. I generated the statistics and drafted the manuscript with guidance from DGE and MJS. DGE designed the study. Molecular testing was carried out by myself, MJS, NLB, ST, CH, AJW and PTS. All other authors contributed data or patients to the study. All authors reviewed the manuscript and approved the final version.

4. Re-evaluation of missense variant classifications in *NF2*

Katherine V Sadler, Charlie F Rowlands, Philip T Smith, Claire L Hartley, Naomi L Bowers, Nicola Y Roberts, Jade L Harris, Andrew J Wallace, D Gareth Evans, Ludwine M Messiaen, and Miriam J Smith.

Data curation was conducted by myself, CFR, DGE, LMM and MJS. MJS and LMM conceptualised the study. Analysis of data was performed by myself, PTS, CLH, NLB, NYR, JLH and AJW. I performed the study investigation and evidence collection. The original draft was written by myself, alongside figure creation. All authors contributed to review and editing of the final article.

5. Genome-wide association analysis identifies a susceptibility locus for sporadic vestibular schwannoma at 9p21

Katherine V Sadler, John Bowes, Charlie F Rowlands, Cristina Perez-Becerril, Andrew T King, Scott A Rutherford, Omar N Pathmanaban, Charlotte Hammerbeck-Ward, Simon K W Lloyd, Simon R Freeman, Ricky Williams, Cathal J Hannan, Daniel Lewis, D Gareth Evans and Miriam J Smith.

Patient data was accumulated by myself, DGE and MJS. Patient DNA samples were quality assessed and prepared for genotyping by myself. Genotyping was conducted at two external facilities, the Oxford Genomics Centre at the Wellcome Centre for Human Genetics and YourGene Health. Genotyping data was cleaned and analysed by myself, under guidance from JB, CFR and CP-B. All other authors contributed patient samples and assisted in sample acquisition. I drafted the manuscript and generated statistics with advice from DGE and MJS.

6. Generation of an *in vitro* model for vestibular schwannoma predisposition in a biologically relevant cell type for pre-clinical therapy screening

Katherine V Sadler, Cristina Perez-Becerril, Antony D Adamson, David Chapman, D Gareth Evans, and Miriam J Smith.

I performed all experimental procedures, except fluorescence activated cell sorting (FACS). CP-B provided assistance in my learning of new laboratory techniques and troubleshooting of experiments. ADA provided advice on study design and shared vectors of behalf of the Genome Editing Unit team at the University of Manchester. DC performed FACS. MJS conceptualised the study. The antisense oligonucleotide was designed by a technical assistant at Gene Tools (Philomath, OR, USA). I drafted the original manuscript and generated the figures under guidance from DGE and MJS.

Rationale for alternative format

The body of work comprising this thesis is presented in a mixed alternative format, with all results chapters written in the style of journal publications. Each experimental chapter has been presented as an individual paper, with three of the four results chapters suitable for submission to a peer-reviewed journal. Chapter 3 has been published in the Journal of Medical Genetics (*J Med Genet*, 58(4):227-233) and chapter 4 has been recently published in Human Mutation (http://doi.org/10.1002/humu.24370). Chapter 5 is prepared for submission and awaits the results of a genotype screening investigation to bolster the impact of its findings. Chapter 6 has been prepared in a journal style format but is not yet suitable for publication.

This thesis has been divided into different, but complementary, branches of research that focus on the detection of highly penetrant pathogenic variants in known vestibular schwannoma (VS)-associated genes, the identification of novel low penetrance risk variants through genome-wide association analysis, and the development of a gene therapy model for a known VS-associated pathogenic variant in *NF2*. The differing experimental approaches employed in each of these branches of research lends itself to a publication-style format of chapters, where each chapter provides a different perspective on furthering the understanding of VS risk and development. Presentation of this thesis in journal format provides a more comprehensive and linear story between each chapter of research than traditional format. The chapters of this thesis progress from identification of pathogenic variants in highly penetrant VS-associated genes, highlighting the potential role of common genetic modifiers of VS risk, to identification of low effect size variants in novel genes in association with VS risk, concluding with the development of VS disease models.

Chapter 3 consists of a summary of molecular testing undertaken in the germline and somatic samples of sporadic VS patients. The article highlights that a significant minority of sVS patients represent undiagnosed cases of NF2 and schwannomatosis as result of pathogenic germline variants in *NF2* and *LZTR1*, respectively. Moreover, *NF2* analysis in somatic VS samples supports existing hypotheses of proposed multi-gene involvement in VS tumourigenesis. Somatic biallelic inactivation of *NF2* is frequently observed in sporadic VS patients, which is suggestive of other genetic factors that render individuals susceptible to *NF2* loss of function and subsequent VS development.

Chapter 4 provides a re-evaluation of variant classification evidence for known *NF2* missense variants. Clinical classification of missense variants remains challenging due to lack of evidence for pathogenicity and function. This paper highlights the need for phenotypic information to be reported in association with published variants, alongside variant-specific functional analysis to enable more definitive variant interpretation. The variable presentation of NF2 disease in families possessing pathogenic *NF2* missense variants may be contributed to by low effect size genetic risk modifiers yet to be identified.

In chapter 5 we present a genome-wide association study that identifies a novel risk locus on chromosome 9p21.3 in association with sporadic VS risk. A number of genes are localised to this region, *CDKN2B-AS1* and *CDKN2A/B*, also referred to as the INK4 locus. Dysregulation of gene products within the INK4 locus have been associated with multiple pathologies, and associations between the INK4 locus and multiple oncogenic pathways provides compelling evidence that the 9p21.3 region is truly associated with risk of VS tumourigenesis.

Chapter 6 outlines the different methodological approaches undertaken to develop a VS-associated disease model to assess the clinical potential of antisense oligonucleotide (ASO) therapy in the treatment of deep intronic pathogenic variants in *NF2*. A variety of technologies were employed in an attempt to generate and characterise the *NF2* c.516+232 G>A variant. Whilst generation of a CRISPR edited cell line remained unsuccessful, we observed restoration of wild-type splicing in cells transduced with the *NF2* variant and treated with a sequence-specific ASO, highlighting this technique as a potential NF2 therapy.

The chapters presented in this body of work are unified through their contribution to furthering the understanding of the genetic landscape that surrounds vestibular schwannoma tumour predisposition.

1. Introduction

1.1. Clinical summary of vestibular schwannoma

Vestibular schwannomas (VSs) are benign nerve sheath tumours that arise on both the superior and inferior branches of the vestibular portions of the vestibulocochlear nerve (Stivaros *et al.*, 2015). Whilst VS histology is benign, the effects of tumour growth within the internal auditory canal can disrupt surrounding nerves, resulting in hearing loss, tinnitus and vestibular disequilibrium. Less frequent symptoms of VS can include headaches, vertigo, visual blurring and disturbances in facial sensitivity (Kentala and Pyykkö, 2001). Previously referred to as acoustic neuromas, a consensus renaming of 'vestibular schwannoma' was established in 1991 ('National Institutes of Health Consensus Development Conference Statement on Acoustic Neuroma, December 11-13, 1991. The Consensus Development Panel,' 1994). VS tumours develop from the macroglial Schwann cells that provide structural support to neurons within the brain, rather than the neurons themselves. Moreover, VSs almost never occur on the cochlear division of the eighth cranial nerve (Martin, Leonard and Radzyner, 2003).

Accounting for approximately 9% of all non-malignant CNS tumours (Ostrom *et al.*, 2021), VS annual incidence has been estimated to range from 1 in 64,000 to 1 in 90,000 (Kshettry *et al.*, 2015; Kleijwegt *et al.*, 2016; Evans *et al.*, 2018c), which may equate to a lifetime risk as high as 1 in 800. With a similar overall occurrence in males and females, risk of VS increases with age and peak diagnosis is between 50-70 years (Kshettry *et al.*, 2015; Kleijwegt *et al.*, 2016).

A number of studies have investigated possible environmental risk factors for VS development, with little conclusive evidence (Fisher *et al.*, 2014; Brenner *et al.*, 2002; Berkowitz *et al.*, 2015; Han *et al.*, 2012; Schlehofer *et al.*, 2007). However, previous exposure to cranial radiotherapy has been found to have a significant association with subsequent VS development (Ron *et al.*, 1988). As cranial radiotherapy is experienced so rarely within the general population, it is suggestive that genetic factors influence risk of VS development.

1.1.1. Patient management

1.1.1.1. Radiotherapy and surgery

Currently, treatment options for VS patients are mainly limited to radiotherapy, surgical resection and surveillance. Both radiotherapy and surgical removal of VS carry significant associated morbidities, requiring careful consideration for the patient and their care team. Damage of surrounding nerves by radiation exposure, or from surgical intervention, can result in deterioration or complete loss of hearing in some patients, with an increased risk in larger (Hasegawa et al., 2013; Kruyt et al., 2018), or tumour predisposition syndrome-associated VS tumours (Mathieu et al., 2007). Tumour size, patient age and other co-morbidities are important factors to consider in the suitability of radiation or surgical approaches in VS treatment (Rutherford and King, 2005). When VS are slow growing, risks associated with invasive treatments can outweigh those from no clinical action. Tumour surveillance through serial magnetic resonance imaging (MRI) scans is proven to be appropriate in patients considered to have tumours with low growth rate (Bakkouri et al., 2009). Fast growing VS are usually identified in initial 6 month follow-up scans (Halliday et al., 2018) and growth rate during this period is predictive of continued growth (Tschudi, Linder and Fisch, 2000).

1.1.1.2. Bevacizumab

Antiangiogenic vascular endothelial growth factor (VEGF) inhibitors, such as bevacizumab, are approved in the treatment of multiple cancer types and have been demonstrated to slow growth, or in some cases reduce size of VS tumours in patients with tumour predisposition syndrome neurofibromatosis type 2 (NF2) (Plotkin *et al.*, 2009; Plotkin *et al.*, 2012). However, in the UK, bevacizumab treatment is only offered to NF2 patients with rapidly growing schwannomas (Morris *et al.*, 2016).

1.1.1.3. Genetic risk stratification

Identifying novel genetic contributors to VS risk may provide insight into the variable tumour growth rate, age at onset, and clinical severity observed between patients. Utilising genetic modifiers in prognosis would

better enable the stratification of patients into optimal treatment strategies prospectively, and identify new therapy targets. With so few management options available, there is a clinical demand for the development of more non-invasive treatment strategies for VS patients.

1.2. Vestibular schwannoma predisposition

1.2.1. Neurofibromatosis type 2

Neurofibromatosis type 2 is an autosomal dominant tumour predisposition syndrome that results from disruption of the *NF2* gene. *NF2* may be disrupted constitutionally in all cells of the body, or only in a proportion of cells in mosaic individuals. Symptomatic presentation of NF2 is often in the second or third decade of life (Evans *et al.*, 2005; Evans, 2009). Development of bilateral vestibular schwannomas (BVS) is observed in 90-95% of NF2 patients (Evans *et al.*, 1992; Parry *et al.*, 1994; Mautner *et al.*, 1996). Presentation of BVS in the context of NF2 disease is estimated to account for only 5% of total VS incidence (Evans *et al.*, 2005), the remainder are attributed to sporadic cases or other tumour disorders. In addition to the vestibular symptoms associated with VS growth, NF2 patients may also develop neuropathies, cutaneous features, cataracts, and schwannomas on other nerves, as well as other tumour types such as meningioma and ependymoma (Asthagiri *et al.*, 2009; Evans *et al.*, 2018b). See table 1 for the current Manchester clinical diagnostic criteria for NF2 (Evans *et al.*, 1992; Smith *et al.*, 2017). Recent studies estimate NF2 birth incidence as 1 in 28,000 (Evans *et al.*, 2018a).

NF2 has a propensity to occur as mosaic disease (Evans *et al.*, 1998b), which can lead to variable symptomatic presentation in affected individuals and therefore confound clinical diagnosis with related disorders, such as schwannomatosis (section 1.2.2). Whilst observable rates of NF2 mosaicism are around 22% of cases, rates of *NF2* variant detection in second generation affected individuals suggests mosaicism rates may be as high as 60% (Evans *et al.*, 2019).

Current and revised Manchester Criteria for neurofibromatosis type 2 (NF2)
1. Bilateral vestibular schwannomas <70 **OR**
2. Family history* of NF2 **AND** unilateral VS <70 **OR**
3. Family history* of NF2 **OR** UVS **AND** any two of: meningioma, glioma, neurofibroma, schwannoma, cataract, cerebral calcification (if UVS + ≥2 non intradermal schwannomas need negative *LZTR1* testing) **OR**
4. Multiple meningiomas (two or more) **AND** any two of: UVS, glioma, neurofibroma, schwannoma, cerebral calcification **OR**
5. Constitutional or mosaic pathogenic *NF2* mutation in blood or identical mutations in two distinct tumours
*VS = Vestibular Schwannoma, UVS = Unilateral Vestibular Schwannoma * First degree relative*

Table 1. Current and revised Manchester Criteria for neurofibromatosis type 2

1.2.1.1. Genotype-phenotype correlations

Genotype-phenotype correlations have been observed in NF2. The majority of identified *NF2* pathogenic variants create a truncated or non-functional protein, resulting in a more severe phenotype than observed in cases of missense variants (Ruttledge *et al.*, 1996; Evans, 2009). Similarly, splice-site variants positioned earlier in the *NF2* transcript have been associated with more severe NF2 presentation than variants closer to the protein C-terminus (Baser *et al.*, 2005; Kluwe *et al.*, 1998). The two predominant isoforms of *NF2* have variant C-terminal ends of the gene protein product, resulting from alternate splicing of the final two exons (Shimizu *et al.*, 2002). The association of C-terminus variants with a less severe NF2 phenotype may be due to functional redundancy between the different isoforms of *NF2*.

Structural variants and variants within regulatory elements result in more variable disease presentation, likely dependent on the function of the protein region affected (Evans, 2009). Clinical interpretation of *NF2* missense variants remains challenging, due to limited availability of evidence from phenotypic and functional data. It is unclear whether there are genotype-phenotype correlations within missense variants; pathogenicity of an amino acid alteration is not necessarily determined by its position within a transcript, but rather its location within protein tertiary structures (Suckow *et al.*, 1996). There is clinical need for

consistent application of variant interpretation in a disease-specific context for *NF2* missense variants, for utilisation in patient management.

1.2.1.2. *NF2* protein

Located on chromosome 22q12, *NF2* encodes the active tumour suppressor protein merlin, which belongs to the ezrin, radixin, and moesin (ERM) protein superfamily (Trofatter *et al.*, 1993). Merlin has both open and closed conformations, dictated by the respective phosphorylation or dephosphorylation of serine residues within the protein. It is the closed dephosphorylated conformation of merlin that displays tumour suppressor activity (Shaw *et al.*, 2001). Conversely, other members of the ERM protein superfamily are activated upon the phosphorylation of critical residues (Gautreau, Louvard and Arpin, 2000).

Merlin has been associated with the regulation of multiple cell signalling pathways, including the RAS pathway (Petrilli and Fernández-Valle, 2016). Multiple pathologies are associated with the persistent activation of RAS-associated proteins; notably, the sustained activity of the RAS pathway promotes tumourigenesis and plays a causal role across many cancer types (Simanshu, Nissley and McCormick, 2017). Merlin has been demonstrated to interact directly with RAS, and other small GTPases, through binding of its FERM (four point one ERM) domain at the N-terminus of the protein (Cui *et al.*, 2019). Activation of merlin results in contact inhibition of tumour cell growth (Morrison *et al.*, 2001), this is antagonistic of other ERM proteins where increased activity has been linked to increased cell adhesion, migration and transformation (Clucas and Valderrama, 2014). The FERM domain of merlin is encoded by the first half of the *NF2* gene (Shimizu *et al.*, 2002). The observations of genotype-phenotype correlations, between variants positioned earlier in the gene transcript and increased disease severity, may be a result of disrupted FERM domain function.

Loss of merlin activity has also been associated with the proliferation and structural modulation of Schwann cells (Muranen *et al.*, 2007) through deregulation of the phosphoinositide 3-kinase (PI3K)/AKT (Jacob *et al.*, 2008) and Hippo/YAP signalling pathways (Zhang *et al.*, 2010). Merlin

performs an inhibitory role on the PI3K/AKT pathway (Rong *et al.*, 2004), which is downstream of the MAPK (mitogen activated protein kinase) signalling cascade and can be modulated via RAS (Vivanco and Sawyers, 2002). Conversely, merlin is an upstream activator of Hippo, which inactivates downstream genes associated with cell survival and proliferation. When merlin function is lost, so is Hippo mediated inactivation of downstream gene targets associated with tumourigenesis (Harvey, Zhang and Thomas, 2013). With demonstrated roles in multiple oncogenic pathways, it is unsurprising that somatic pathogenic variants in *NF2* are regularly observed in other types of cancer (Schroeder, Angelo and Kurzrock, 2014).

1.2.1.3. Somatic *NF2* variants

Genotyping of somatic tumour samples obtained from NF2 patients has demonstrated that biallelic loss of *NF2* drives tumourigenesis (Evans, 2009), consistent with the 2-hit hypothesis described by Knudson in dominant tumour predisposition disorders (Knudson, 1971). Loss of heterozygosity (LOH) is a frequently observed second *NF2* hit in schwannoma tumours, either by mitotic recombination (MR) or through full or partial loss of chromosome 22 (Hadfield *et al.*, 2010). Rates of 22q LOH detection in NF2-associated schwannomas are approximately 67% (Hadfield *et al.*, 2010). It has been suggested that inactivation of *NF2* may be involved in the development of all schwannomas, as loss of merlin expression is observed at higher rates than detectable pathogenic variants, this is likely due to the variety of mechanisms that cause gene inactivation (Sainz *et al.*, 1994; Evans, 2009). Whilst it is clear that loss of *NF2* function plays a large role in the development of VS and other tumour types, pathogenic germline variants in *NF2* do not account for all cases of schwannoma predisposition.

1.2.2. Schwannomatosis

Unilateral vestibular schwannomas (UVS) are occasionally observed in individuals with schwannomatosis, an autosomal dominant tumour

predisposition disorder characterised by the development of multiple schwannomas, and occasionally meningiomas (Smith *et al.*, 2012a). Schwannomatosis-associated schwannomas are most frequently non-intradermal, non-vestibular and associated with painful presentation (MacCollin *et al.*, 2005). Yet, a small proportion of schwannomatosis patients present with UVS, making the clinical distinction from NF2 challenging in the absence of genomic testing. See table 2 for the current schwannomatosis clinical diagnostic criteria. Currently, there are two known genes associated with schwannomatosis manifestation.

Current schwannomatosis criteria
• ≥2 non-intradermal anatomically distinct schwannomas (at least one histologically confirmed)
• Cranial scan with no evidence of bilateral vestibular schwannoma
• *NF2* mutation negative
• One pathologically confirmed schwannoma, unilateral vestibular schwannoma (VS) or intracranial meningioma **AND** an affected first-degree relative with confirmed schwannomatosis
• A germline *SMARCB1* or *LZTR1* pathogenic variant **AND** one pathologically confirmed schwannoma or meningioma
Note: Presence of a unilateral VS or meningioma(s) does not exclude the diagnosis.

Table 2. Current schwannomatosis criteria

1.2.2.1. *SMARCB1*-associated schwannomatosis

Pathogenic variants in *SMARCB1* were first associated with familial schwannomatosis in 2007 (Hulsebos *et al.*, 2007). Located on chromosome 22q, 6Mb centromeric to *NF2* (figure 1), *SMARCB1* encodes a subunit of the SWI/SNF (SWItch/Sucrose Non-Fermentable) chromatin remodelling complex, which holds a critical role in transcriptional regulation (Roberts and Orkin, 2004). Approximately 20% of human tumours have been associated with pathogenic variants in SWI/SNF complex subunits (Kadoch *et al.*, 2013). Biallelic inactivation of *SMARCB1* has been observed in a majority of malignant rhabdoid tumours (Biegel, 2006), and loss of *SMARCB1* expression has been associated with a number of other cancers (Sévenet *et al.*, 1999; Genovese *et al.*, 2017; Yoshida *et al.*, 2018). Germline *SMARCB1* mutations are estimated to account for 40-60% of familial

schwannomatosis cases (Boyd *et al.*, 2008; Hadfield *et al.*, 2008; Smith *et al.*, 2012b), and 10% of sporadic incidences (Rousseau *et al.*, 2011). Whilst cranial nerve schwannomas are frequently observed in *SMARCB1*-associated schwannomatosis they are non-vestibular (Smith *et al.*, 2012b). There is an absence of confirmed VS cases in patients possessing germline *SMARCB1* pathogenic variants (Evans *et al.*, 2018c), with a single possible case reported (Wu, Kong and Bi, 2015).

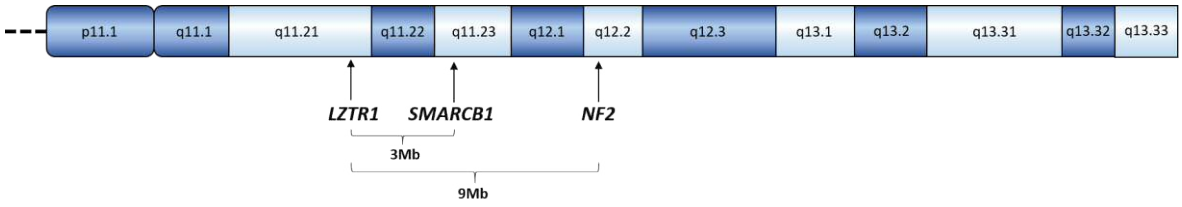

Figure 1. Chromosome 22q.

1.2.2.2. *LZTR1*-associated schwannomatosis

In 2014, germline loss-of-function variants in *LZTR1* were found in up to 80% of *SMARCB1* mutation negative schwannomatosis patients (Piotrowski *et al.*, 2014). Subsequent studies in larger cohorts have estimated that germline *LZTR1* mutations are found in 26-43% of schwannomatosis cases (Smith *et al.*, 2015; Paganini *et al.*, 2015). Also located on chromosome 22q, 3Mb centromeric to *SMARCB1* (figure 1), *LZTR1* encodes a member of the BTB (broad-complex, tramtrack, and bric-a-brac) protein superfamily located exclusively at the Golgi matrix (Nacak *et al.*, 2006; Frattini *et al.*, 2013). Alongside schwannomatosis, pathogenic *LZTR1* variants have been identified in cases of glioblastoma (Frattini *et al.*, 2013), as well as autosomal dominant and recessive forms of developmental disorder Noonan syndrome, which is not associated with tumour predisposition (Johnston *et al.*, 2018; Motta *et al.*, 2018). Noonan syndrome is part of a larger disease group of RASopathies that result from disruption of the RAS-MAPK (rat sarcoma virus - mitogen-activated protein kinase) pathway (Tidyman and Rauen, 2009). Whilst the cellular role of *LZTR1* has not been fully delineated, *LZTR1* has been demonstrated to inhibit the RAS-MAPK pathway through polyubiquitination and degradation of RAS (Bigenzahn *et*

al., 2018; Abe *et al.*, 2020). A well described oncogenic pathway, deregulation of RAS-MAPK signalling through loss of *LZTR1* function provides a suggested mechanism of *LZTR1* driven tumourigenesis (Steklov *et al.*, 2018). As loss of *SMARCB1* and *LZTR1* function do not account for all incidences of schwannomatosis, it is speculated that other schwannomatosis causal genes exist (Smith *et al.*, 2015). Conversely to *SMARCB1*-associated schwannomatosis, UVS have been observed in a number of *LZTR1*-associated schwannomatosis patients (Smith *et al.*, 2012a; Smith *et al.*, 2015). However, identification of germline *LZTR1* mutations in cases of solitary VS are low, at around 3% (Pathmanaban *et al.*, 2017; Sadler *et al.*, 2020).

1.2.2.3. Multi-gene contributions to schwannoma development

Whilst germline *SMARCB1* and *LZTR1* mutations predispose to schwannoma development, somatic genotyping of tumours in schwannomatosis patients frequently reveals the additional biallelic inactivation of *NF2* (Boyd *et al.*, 2008; Hadfield *et al.*, 2008; Paganini *et al.*, 2015). Recurrent observations of somatic chromosome 22q LOH in *trans* with a retained germline *SMARCB1* or *LZTR1* mutation, with a further acquired mutation on the remaining *NF2* allele, have led to proposals of multi-hit models of tumourigenesis in schwannomatosis (figure 2) (Sestini *et al.*, 2008; Kehrer-Sawatzki *et al.*, 2017). Rates of 22q LOH in non-NF2 schwannomas have been previously reported as 57-63% (Hadfield *et al.*, 2010; Lassaletta *et al.*, 2013). The co-involvement of *NF2* within schwannomatosis tumour development suggests an overlap of gene functions and that *NF2* may be central in a common pathway of schwannoma development.

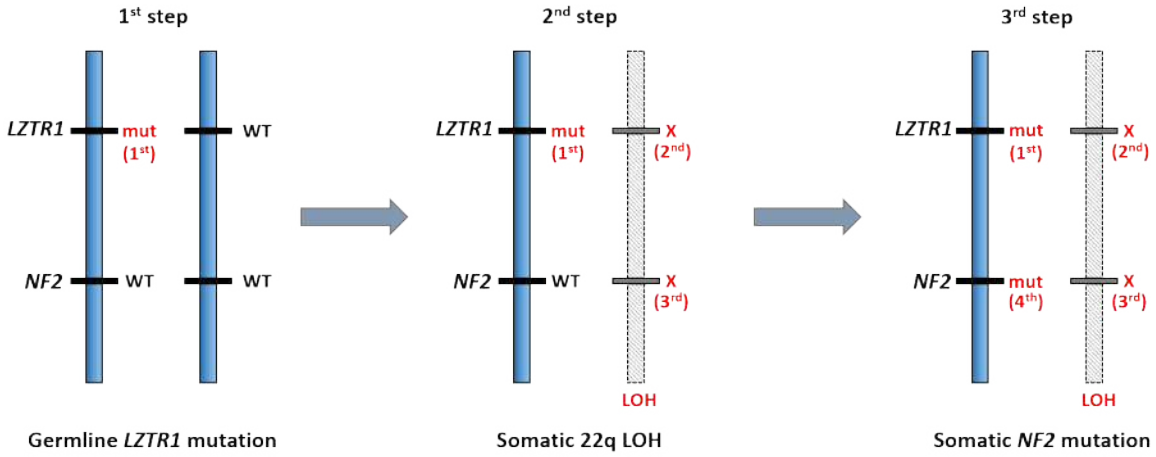

Figure 2. Multi-hit model of tumourigenesis in *LZTR1*-schwannomatosis.

The proposed 4-hit/3-step model begins with a germline *LZTR1* mutation (1st hit), followed by somatic 22q LOH that results in loss of both *LZTR1* (2nd hit) and *NF2* (3rd hit) on the *trans* allele. Finally, a somatic *NF2* mutation is acquired (4th hit), resulting in schwannoma tumourigenesis. LOH – loss of heterozygosity, mut – mutation, WT – wild-type. Adapted from Kehrer-Sawatzki *et al.* (2017).

1.2.3. Interpretation of variants in schwannoma predisposition genes

Variants identified in disease-associated genes require characterisation and classification to determine their functional effect and the likelihood the variant confers a pathogenic effect that contributes to a specific disease phenotype. Assessment of variants in a clinical setting must be reproducible and interpretation guidelines enable consistent reporting of variants. In 2015 the ACMG-AMP (American College of Medical Genetics and Genomics and the Association for Molecular Pathology) guidelines for variant interpretation (Richards *et al.*, 2015) were published and enabled reproducible interpretation of variants through an evidence framework. The National Health Service (NHS) within the UK currently employs the ACGS (Association for Clinical Genomic Sciences) Best Practice Guidelines for Variant Classification in Rare Disease 2020, which build upon the original framework proposed by Richards *et al.* (2015) (ACGS best practice guidelines, 2020 https://www.acgs.uk.com/quality/best-practice-guidelines/#VariantGuidelines. Accessed 23 August 2021). Whilst these guidelines greatly assist in the consistency of clinical reporting of genetic

variants, lines of evidence to support pathogenicity are broad and not applicable to all disorders or genes. Moreover, missense variants remain challenging to interpret due to limited functional and clinical information. Considering the impact of gene variants in a disease-specific context can provide novel lines of evidence for use in pathogenicity classification. Disease-specific guidelines are now in development, which incorporate additional disease-associated features into variant classification; for example, LOH and retention of a missense variant in a tumour would be informative for *NF2* variant classification. Clinical interpretation using the aforementioned guidelines assumes that identified variants are highly penetrant and located in genes with known pathological associations. Interpretation of low penetrance variants with variable expressivity are much more challenging to address.

1.3. Sporadic vestibular schwannoma

The vast majority of vestibular schwannoma cases occur sporadically and unilaterally in individuals without further features of NF2 or schwannomatosis. Whilst the average age of sporadic vestibular schwannoma (sVS) presentation is in the fourth to fifth decades of life (Evans, 2009), cases of apparently sVS under 25 years are observed with low rates of germline variant detection (Pathmanaban *et al.*, 2017). A small proportion of apparently sVS patients represent undetected cases of NF2 or schwannomatosis (Sadler *et al.*, 2020). Identifying cases of apparent sVS that are actually due to germline tumour predisposition variants is critical for accurate risk prediction and prognosis in patients.

Observations of familial clustering of UVS have led to suggestions that UVS risk may be an inheritable characteristic, possibly due to hypomorphic variants in known schwannoma-associated genes, or novel genetic associations (Bikhazi *et al.*, 1997; Hemminki and Li, 2003; Evans *et al.*, 2018c). However, estimated population incidence of sVS has increased since initial observations (Bikhazi *et al.*, 1997) and limited evidence has subsequently been accrued to support familial UVS risk (Evans *et al.*, 2018c).

Pathogenic variants in *NF2* are frequently observed in sVS tumours (Hadfield *et al.*, 2010). Yet the reported frequency of *NF2* mutation detection in VS samples ranges widely, from 15-84% (de Vries, van der Mey and Hogendoorn, 2015). The range of detection frequencies may be attributable to variable growth and stability between patient tumours at the time of surgical resection. It has been demonstrated that inflammatory cells can account for the majority of cells in growing sVS tumours, resulting in cellular contamination of samples (Lewis *et al.*, 2018). Proliferating macrophages in growing VS hinder somatic variant detection, as the infiltrating cells will not possess the somatic pathogenic *NF2* variant driving tumourigenesis. The contamination of samples with inflammatory cells may hold an explanation for absence of pathogenic variant detection in some VS tumours. Still, bilallelic inactivation of *NF2* is common in sVS tumours and identification of *NF2* variants may increase further with improvements in detection and interpretation techniques (Hadfield *et al.*, 2010; Carlson *et al.*, 2018; Sadler *et al.*, 2020).

The range in age of presentation in cases of sVS, the observation of potential UVS inherited risk, and the characteristic biallelic inactivation of *NF2* in sVS tumour samples suggests there are genetic moderators of sVS risk yet uncharacterised. The existence of genetic variants that modify VS risk is further supported by the variable penetrance and expressivity observed within multi-generational NF2 affected families. Individuals possessing the same pathogenic *NF2* variant may present with VS at wide ranging ages, with differing tumour burdens and disease progression (Evans *et al.*, 1998a). The missing heritability of VS risk may be attributable to the existence of low effect size variants that mediate functional consequences on known VS associated pathways. Common genetic variants rarely confer pathogenic effects on gene function, but they may alter gene regulation or expression that results in low penetrance phenotypic effects. Moreover, inheriting combinations of common genetic variants in multiple genes can contribute to polygenic specific risks, sometimes equivalent to risks conferred by monogenic disorders (Khera *et al.*, 2018).

1.4. Identifying novel genetic associations with vestibular schwannoma

1.4.1. Gene expression studies of vestibular schwannoma

A number of gene expression profiling studies have been performed in vestibular schwannoma (Welling *et al.*, 2002; Hanemann *et al.*, 2006), with some focussing specifically on sVS samples (Cayé-Thomasen *et al.*, 2010; Aarhus *et al.*, 2010; Sass *et al.*, 2017). Whilst both up and down regulation of many genes and multiple signalling pathways have been identified, the reported effects on gene expression have sometimes been conflicting (Cayé-Thomasen *et al.*, 2010; Aarhus *et al.*, 2010). For example, Aarhus *et al.* (2010) observed downregulation of both *AKT1* and *VEGF* in an expression study in VS samples, discordant with earlier literature reporting upregulation of *AKT1* (Jacob *et al.*, 2008) and *VEGF* (Hanemann *et al.*, 2006) in VS. These inconsistent findings may be due to clinical non-specificity of the tumour samples analysed, inappropriate choices of control samples or the heterogeneous nature of tumour gene expression profiles (Cayé-Thomasen *et al.*, 2010). Yet, network linking of deregulated genes has identified RAS/ERK (extracellular signal-regulated kinases), and other components of the MAPK signalling cascade, as a core network of differentially expressed genes in VS (Aarhus *et al.*, 2010), substantiating the MAPK signalling pathway as a central mechanism of VS pathogenesis, previously outlined in section 1.2.1.2.

1.4.2. Genetic sequencing analysis of vestibular schwannoma

Whole exome sequencing (WES) and whole genome sequencing (WGS) are powerful methods that can facilitate large-scale mutation characterisation in pathological samples. Both WES and WGS have been applied in the investigation of genetic variants in sporadic VS samples (Håvik *et al.*, 2018; Carlson *et al.*, 2018). Overall, VS tumours display low mutational burden, harbouring relatively low numbers of somatic mutations in WES analysis (Håvik *et al.*, 2018). A consistent and unsurprising finding is that a high proportion of identified mutations in VS tumours are found in *NF2*. However, pathogenic variants in recurrent genes have also been identified. In a study by Håvik *et al.* (2018), WES identified *CDC27* and *USP8* mutations in 11% and

7% of VS samples respectively. Whilst both genes are associated with roles in cell cycle progression and regulation (Naviglio *et al.*, 1998; Jörgensen *et al.*, 2001), there are no observations of germline pathogenic variants in *CDC27* and *USP8* in VS patients and therefore likely represent acquired somatic events, rather than inherited predisposition.

Studies of gene expression and large-scale sequencing analysis have largely focussed on the genetic profiling of somatic tumour samples, rather than the germline genotypes of the patients who develop VS. With the absence of germline pathogenic variant detection in sVS patients, the identification of potential moderate, and low risk inherited genetic factors for VS remains an ongoing goal.

1.4.3. Genome-wide association studies

Genomic variation exists on multiple levels, from modulation of gene expression by chemical modification, through to chromosome rearrangement. The most commonly observed variation within the genome is single nucleotide polymorphisms (SNPs) (Abecasis *et al.*, 2010), single base changes that usually represent normal variability between individuals with limited functional impact. However, SNPs can also represent variants of small effect size that subtly contribute to altered gene expression and manifestation of pathological phenotypes. Identifying robust associations between common genetic variants and disease is challenging, due to the statistical power required for demonstrating significant differences observed between case and control populations. Investigations into common low risk variants are most frequently performed in large cohort genome-wide association studies (GWAS). For over ten years GWAS have been performed with the aim of identifying novel genetic associations within complex disorders (Visscher *et al.*, 2012). GWAS are usually conducted by SNP genotyping large numbers of case and control samples. Comparing genotype frequencies between cases and controls can reveal enrichment of certain alleles in a population, which may confer risk of, or protection from, the phenotype of interest.

GWAS take advantage of linkage disequilibrium (LD) within the genome, measured as squared correlation (r^2), to characterise genome-wide SNP variation using a subset of physically tagged SNPs. Associated tagged SNPs are not necessarily functional, but may be in LD with functional SNPs, highlighting loci of interest for further characterisation. SNP genotyping is often conducted through array platforms designed to characterise variants with known functional associations or in regions of LD that enable inference, or imputation, of surrounding genotypes. Imputation is the process of predicting genotypes of untagged SNPs through haplotype analysis of tagged SNPs; haplotype reference panels and LD metrics can be used to infer genotypes of variants in the surrounding region (Marchini and Howie, 2010). Commercial arrays enable genotyping of between 200,000 and 2 million SNPs (Visscher *et al.*, 2017). For example, the UK Biobank Axiom® Array contains 820,967 SNP and indel markers, specifically chosen to capture the genotypes of known functional SNPs and variants that enable the utilisation of LD to infer alleles in surrounding regions (ThermoFisher UK Biobank Axiom® Array Content Summary [Online]). The genotype markers within the UK Biobank Axiom® Array have been curated for optimal performance in a North Western European population, largely to reflect the genetic background of samples obtained within the UK. Matching cases and controls for ancestry, and adjusting for population substructures that may occur due to geographical and cultural boundaries, is a major consideration in GWAS design. Differing populations also differ in allelic frequencies of genetic variants, which can confound associations identified within studies (Zondervan and Cardon, 2007). In addition to ancestral matching of cases and controls, it is essential that a case phenotype is adequately defined and a minimum sample size calculated for sufficient statistical power in association discovery (Zondervan and Cardon, 2007). Sample size calculations are based on the predicted effect size, or odds ratio (OR), of variants of interest.

For genome-wide association analysis, each characterised SNP is examined independently for association with the phenotype. In GWAS investigating a binary phenotype, affected vs unaffected, this is usually performed through a logistic regression model (Bush and Moore, 2012). Logistic regression models

enable the incorporation of clinical covariates to provide adjusted OR values, such as age or sex adjusted risk. Performance of so many independent SNP associations creates a multiple testing burden, which increases the rate of false positive results and therefore needs to be corrected for during analysis (Bush and Moore, 2012). Resolving multiple testing burden using statistical methods, such as LD-adjusted Bonferroni correction, lowers the required *p*-value for an association be considered statistically significant, *p*-values of ~$5x10^{-8}$ are generally considered significant for most commercial genotyping platforms (Li *et al.*, 2012). Currently there are no published studies that have implemented GWAS methodology for the identification of novel variants in association with VS.

1.5. Clinical impact of identifying genetic modifiers of risk

1.5.1. Risk prediction models

A major driving force behind the investigation of novel genetic associations in disease is driven by the prospect of delivering clinically actionable findings. Risk prediction models have been utilised in the stratification of patients for multiple disorders over the past few decades, typically incorporating information on environmental risk factors, physiological observations and family histories of patients. The wider availability of genomic testing now enables genotypic data to be incorporated into disease risk prediction. Though it is challenging to incorporate complex trait risks into patient management, the benefits of stratifying patients based on polygenic risk scores (PRS) has been demonstrated in a number of conditions (Abraham *et al.*, 2016; van Veen *et al.*, 2018). The simplest form of polygenic risk scoring calculates the sum of effect sizes for multiple SNPs on disease risk. Risk variants are often collated from GWAS associations. By combining effect sizes from multiple variants the clinical utility of genotype data for low effect size alleles is increased (Lambert, Abraham and Inouye, 2019). Identification of novel genomic risk variants in association with VS predisposition could facilitate the development of a PRS, or alternative patient stratification pathway, to enable more tailored VS patient management.

1.5.2. Identification of therapeutic targets

Detecting further genetic associations with VS risk may identify novel associated cellular pathways, highlighting potential targets for therapeutic interventions. Immunohistochemical investigations have demonstrated expression of VEGF and its receptors in VS samples (Brieger *et al.*, 2003; Saito *et al.*, 2003), with observed correlation between VEGF expression and tumour growth rate (Cayé-Thomasen *et al.*, 2003). Whilst the antiangiogenic VEGF inhibitor, bevacizumab, is offered to NF2 patients with rapidly growing schwannomas (Morris *et al.*, 2016), there is a lack of robust investigation into the efficacy of bevacizumab in cases of sporadic VS, though examples of successful treatment exist (Karajannis *et al.*, 2019).

MicroRNA (miRNA) expression profiling of VS tumours has identified a number of candidate molecules in association with VS growth rate (Sass *et al.*, 2020). A miRNA deregulation expression signature has been characterised in schwannomas, with significant downregulation of miR-7 and upregulation of miR-21 observed in VS samples (Cioffi *et al.*, 2010; Saydam *et al.*, 2011). Moreover, overexpression of miR-7 has been demonstrated to inhibit schwannoma cell growth (Saydam *et al.*, 2011). With known oncogene targets, deregulation of miR-7 highlights a potentially targetable pathway of VS tumourigenesis. Targeting therapies that modulate associated miRNA expression may prove effective in the reduction or stabilisation of VS growth (Yin *et al.*, 2021). Yet, there are no currently developed therapies for regulation of miRNA expression in VS tumours.

Though tumour expressed molecules, such as VEGF, provide clinically actionable targets, they are usually not specific to VS. Concerns of toxicity and persistent side-effects have been highlighted in patients treated with bevacizumab (Morris *et al.*, 2017), which is concerning for younger patients facing long-term treatment. Identification of VS-specific genetic features might enable the development of tailored chemotherapies that circumvent off-target effects observed in other drug treatments.

1.6. Disease modelling

Identification of VEGF expression, an existing therapeutic target, in VS tumours enabled the rapid repurposing of bevacizumab for NF2 patient treatment (Plotkin *et al.*, 2009). However, novel targets often necessitate the development of new therapies, requiring robust functional studies and large-scale clinical trials before medical translation is possible. Prior to studies in patients, prospective drug molecules are screened for efficacy and toxicity in pre-clinical cell line and animal models. Whilst the landscape of inherited genetic risk factors associated with sporadic VS remains uncharacterised, disease models of NF2 and *LZTR1*-associated schwannomatosis remain most relevant for use in VS therapeutic development. *NF2* and *LZTR1* gene knockout cell line models are commercially available for research, as well as accurate phenocopy mouse models of NF2 (Gehlhausen *et al.*, 2015). However, as previously discussed, both *NF2* (section 1.2.1) and *LZTR1* (section 1.2.2.2) are implicated in other pathologies outside of schwannoma development and can therefore also produce non-VS phenotypes. The genotype-phenotype correlations observed in NF2 also raise the issue of variant-specific effects on disease progression. Conclusions drawn from functional work in gene knockout models may be non-specific and result in limited translational success of therapeutics. The importance of determining variant-specific effects on gene function are highlighted in the ACGS (Association for Clinical Genomic Sciences) Best Practice Guidelines for Variant Classification in Rare Disease 2020 as a valuable line of evidence in variant interpretation (ACGS best practice guidelines, 2020 https://www.acgs.uk.com/quality/best-practice-guidelines/#VariantGuidelines. Accessed 23 August 2021).

The nature and position of a variant determines which mechanisms of therapeutic intervention may be possible. Pathogenic variants located in coding regions of the genome can represent challenging gene therapy targets, as disruption of the wild-type (WT) gene product needs to be avoided. However, non-coding variants offer more flexibility as potential gene therapy targets. For example, pathogenic intronic variants can cause aberrant splicing, creating non-functional proteins and subsequent disease (Lacerra *et al.*, 2000). Concealment of intronic variants from the spliceosome complex by targeted molecule binding can restore WT splicing and functional gene products (Hammond and Wood, 2011). Successful splice-

modulating therapies have been developed in a number of disorders (Hammond and Wood, 2011; Spitali and Aartsma-Rus, 2012), including NF2 (Castellanos *et al.*, 2013). Castellanos *et al.* (2013) demonstrated that delivery of a mutation-specific antisense oligonucleotide (ASO) *in vitro* restored WT splicing in a patient-derived cell model of NF2, caused by deep intronic variant *NF2* c.1447-240 T>A resulting in cryptic exon inclusion. Around 1% of *NF2* pathogenic variants are deep intronic (Castellanos *et al.*, 2013; Perez-Becerril, Evans and Smith, 2021). With examples of familial NF2 caused by deep intronic variants (De Klein *et al.*, 1998), splice modulating therapies hold great potential for this field of research.

Still, with so many possible types of pathogenic mutation, often confined in singular families, conducting functional work and model development for every identified variant is a daunting task. Development of streamlined mutagenesis workflows for the study of variant-specific effects is needed for effective therapeutic screening in pre-clinical models.

1.6.1. Developing variant-specific models

Generating patient-derived cell lines to create variant-specific models for therapy screening is a possibility. However, alongside the ethical considerations of using patient tissue, primary cell lines often prove challenging to derive and maintain. Moreover, patient-derived cell lines contain genetic variants that are specific to the individual of origin. Patient-specific common SNPs can alter the genomic context of a pathogenic variant of interest (Anttila *et al.*, 2018), such as regulation of gene expression, which could cause variable replication of findings between cell models.

Use of a standardised cell line to maintain consistencies in genomic context would negate some of the issues surrounding experiment replicability, but requires variant generation through mutagenesis methods.

1.6.2. Plasmid-based methods of mutagenesis

Site-directed mutagenesis is a powerful tool for studying the effects of specific nucleotide changes on gene function, both for SNP variants and deletions/ insertions. A common *in vitro* technique, site-directed mutagenesis utilises complementary base pairing of oligonucleotide primers designed to contain a mismatch region of the variant of interest,

incorporating the specified mutation into plasmid constructs containing the gene/ transcript of interest, which can then be transfected into a cell line, preferably of a disease-relevant cell type (Carrigan, Ballar and Tuzmen, 2011). Similarly, generation and transfection of synthetic plasmid pseudo-constructs enable the study of variant-specific effects on gene expression and gene products *in vitro*. Gene pseudo-constructs contain only part of a gene sequence for exogenous expression in transfected cells, as the full gene transcript is too large to be integrated into a plasmid. However, plasmid-based methods are mainly transient experiments, where the variant of interest is not incorporated into the host cell genome (Recillas-Targa, 2006). The plasmid, and therefore gene expression of the construct, will be lost after a number of cell divisions. Cells transfected with plasmids often overexpress construct products and are therefore not representative of normal physiological expression levels of the gene in a cell. Overexpression can be due to the use of highly active promoters and introduction of multiple plasmids to a cell. Though stable transfection can be achieved through the use of selectable markers (Glover, Lipps and Jans, 2005), it is an inefficient and time intensive process unsuitable for workflows demanding generation of multiple variants in short time periods. Moreover, pseudo-constructs of variant genes will not possess information on the genomic context of the region of interest, likely affecting gene regulation and expression.

Ideal mutagenesis methods would edit DNA sequences directly in the genome of target cells, creating a permanent change stably inherited by daughter cells. With research progress and technological advancement, permanent gene editing techniques are now easily accessible and applied widely across the field of genomic medicine.

1.6.3. CRISPR gene editing

Clustered regularly interspaced short palindromic repeats (CRISPR) are repetitive sequence elements found within some prokaryote genomes. CRISPR elements perform an essential role in the adaptive immunity of organisms such as bacteria and archaea, relying on the activity of CRISPR-associated (Cas) nucleases (Bolotin *et al.*, 2005; Marraffini and Sontheimer, 2010). In response to viral or plasmid infection, fragments of invading foreign

nucleic acids are integrated into a host genome, providing a genomic record of previously encountered pathogens and facilitating subsequent detection (Al-Attar *et al.*, 2011). Host production of guide RNA (gRNA), that contain the integrated pathogen nucleic acid sequence, directs endonuclease cleavage of the pathogen through complementary base pairing (Moon et al., 2019). The system of gRNA-directed cleavage can be manipulated for the purposes of gene editing (Jinek *et al.*, 2012). Synthesis of target sequence-specific gRNAs direct DNA breakage at a region of interest, inducing cellular responses to DNA damage that facilitate introduction of sequence variants.

Creation of double stranded DNA breaks at target loci induces endogenous cellular DNA repair mechanisms, such as non-homologous end joining (NHEJ) and homology directed repair (HDR). NHEJ is an error prone process characterised by the ligation of double stranded DNA fragments, often resulting in indels at the cleavage site (Carroll, 2014). This method of CRISPR-directed DNA cleavage is imprecise but effective at gene expression knockdown in disease models (Hsu, Lander and Zhang, 2014). To take advantage of HDR for gene editing purposes, an exogenous DNA repair template containing the variant of interest is introduced into the cell. The template is recognised as a reference sequence by DNA repair enzymes, which incorporate the variant into repaired genomic DNA (Carroll, 2014). Whilst HDR CRISPR methods can accurately introduce specific genetic variants, it is an inefficient process in higher eukaryotes and mechanistically competes with NHEJ, often resulting in the acquisition of indels at the target site (Hsu, Lander and Zhang, 2014).

Modifications to CRISPR-associated nucleases that direct DNA cleavage have expanded the possible applications of CRISPR gene editing techniques. Cas9-nickase is a mutated form of the Cas9 protein, which creates single stranded breaks, or ‘nicks’, at DNA target sites (Schubert *et al.*, 2021). Single stranded DNA breakage does not induce NHEJ and therefore reduces the risk of indel formation (Davis and Maizels, 2014). Variants can then be created or introduced at the target site through chemical modification of bases, or provision of an alternative sequence template.

1.6.3.1. CRISPR base editing

Base editing utilises Cas9-nickase to create a DNA break at a target sequence; bound to a deaminase enzyme, base editors are capable of directing C>T and A>G base conversions (Komor *et al.*, 2016; Gaudelli *et al.*, 2017). However, with the inability to create all possible types of base conversion, and narrow activity windows of deaminase enzymes, base editors are significantly limited in the suitability of target sequences (Molla and Yang, 2019).

1.6.3.2. CRISPR prime editing

Prime editing is another CRISPR-based method that employs Cas9-nickase, with an additional sequence template that introduces a variant of interest. Prime editing is enabled through the design of an extended prime editing guide RNA (pegRNA), which both specifies the target site and encodes the desired edit (Anzalone *et al.*, 2019). Able to perform targeted insertions, deletions and all base type substitutions, in principle prime editing could correct 89% of known human pathogenic variants (Anzalone *et al.*, 2019). The prime editor complex is comprised of a reverse transcriptase fused to a Cas9-nickase, which binds to the pegRNA specifying the genomic target site through a complementary sequence at the 5' end of the molecule. DNA 'nicking' occurs on the opposite DNA strand bound to the 5' end of the pegRNA (Jinek *et al.*, 2012). The extended 3' sequence of pegRNA is designed to be the reverse complement sequence upstream of the nicking site. Complementary base pairing of the 3' end of the pegRNA upstream of the DNA break enables an edited reverse transcriptase template sequence to be directly copied into the target locus (Anzalone *et al.*, 2019). See figure 3 for a schematic of pegRNA-directed gene editing. With significantly lower off-target effects and similar efficiency to HDR methods, prime editing promises to be an important tool in the future of gene editing research.

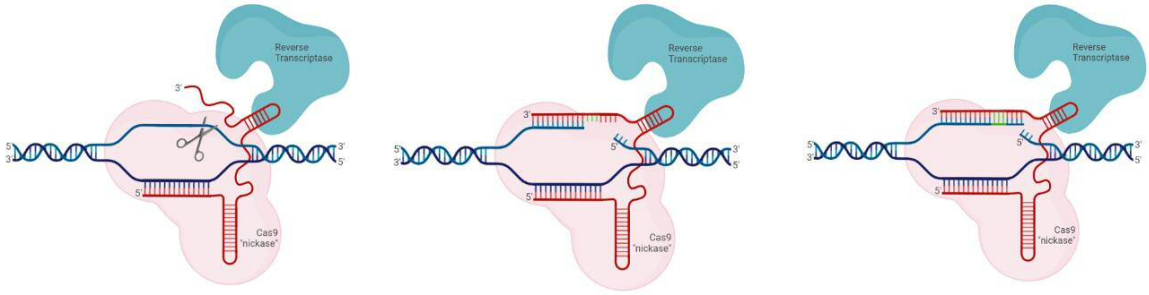

Figure 3. CRISPR prime editing.

From left to right, the 5' end of pegRNA (red) binds complementarily to target genomic site, directing single stranded nicking by Cas9-nickase on opposite DNA strand containing PAM site. 3' end of pegRNA binds complementarily upstream of the nicked site. A reverse transcription template, containing the exogenous DNA edit (green), is then polymerised into the target site. Endonuclease exposure cleaves the 5' flap left in the endogenous DNA strand, DNA repair results in stably edited DNA. Figure created with Biorender.com.

1.7. Aims

The overall aim of this project is to improve characterisation of the genomic landscape of vestibular schwannoma pathogenesis.

The work has been divided into different but complementary branches of research that span the detection and interpretation of variants in genes known to predispose to VS development, the identification of novel low penetrance risk variants, and the generation of a disease model for a known VS-associated pathogenic variant in *NF2*. It is intended that this body of work will contribute to the field by furthering the understanding of the genetic landscape that surrounds vestibular schwannoma tumour predisposition.

Three major strands of research were undertaken for this study:

1. Identify and characterise rare, high impact variants in VS patient germline and tumour samples.

Though there are currently no genes known to be associated with sporadic VS predisposition, variable phenotypic features in NF2 and schwannomatosis patients can present as apparent sVS cases. A proportion of sVS patients represent

undetected cases of tumour predisposition syndromes (Pathmanaban *et al.*, 2017), diagnosis of which is crucial for effective patient management. Moreover, biallelic inactivation of *NF2* is a common observation in sVS somatic samples (Hadfield *et al.*, 2010), determining the frequency and types of pathogenic *NF2* variants in sVS tumours may help delineate a common pathway of VS tumourigenesis.

Variants identified in VS predisposition genes, *NF2* and *LZTR1*, require characterisation to assess pathogenicity and determine what clinical impact the finding has on a patient. Characterisation of variants in a clinical setting must be reproducible, and variant interpretation guidelines enable consistent reporting of variants (ACGS best practice guidelines, 2020 https://www.acgs.uk.com/quality/best-practice-guidelines/#VariantGuidelines. Accessed 23 August 2021). However, missense variants remain challenging to interpret due to limited functional and clinical information. Considering the impact of gene variants in a disease-specific manner can provide further context for novel lines of evidence in pathogenicity classification.

To identify cases of undetected VS tumour predisposition syndromes in a population of apparently sVS patients we intend to test for variants in the *NF2* gene, as well as *LZTR1* and *SMARCB1* when possible, in germline samples from patients. *NF2* testing will also be conducted in available somatic tumour DNA samples, to better characterise the role of *NF2* deregulation in sVS development. Identified variants will be interpreted following the ACGS best practice guidelines (2020). Moreover, a comprehensive list of identified missense variants in *NF2* will be re-evaluated and classified in accordance with existing guidelines, highlighting opportunities to apply disease-specific forms of evidence to support or refute pathogenicity of variants.

2. Identification of common genetic variants in association with VS risk through genome-wide association analysis.

Rates of germline pathogenic variant identification in apparent sVS are low (Pathmanaban *et al.*, 2017). However, suspected missing heritability (Hemminki

and Li, 2003), variable clinical presentation features, and somatic genotypes of VS tumours (Hadfield *et al.*, 2010) is suggestive that genetic modifiers of VS risk remain uncharacterised. The hypothesis behind this branch of the project is that the missing heritability and variable presentation observed in VS cases can be explained, at least in part, by common low penetrance, small effect size inherited genetic variants. Though likely present within the general population, these variants may significantly modify the risk of VS development, age at onset and tumour burden when inherited in combination within an individual.

To identify novel genetic variants in association with VS risk, a genome-wide association study in sVS patients, negative for germline pathogenic *NF2* variants, will be conducted. Loci containing SNP variants reaching significant levels of association with VS risk will be further characterised through review of existing literature and investigations of associated variant frequencies in NF2 patients with VS. It is intended that variants identified in association with VS presentation can be utilised in clinical risk prediction models. Stratifying individuals based on genetic risk of VS would enable more personalised care management and prognosis, and identify the most appropriate treatment options for patients.

3. Generation of an *in vitro* model for VS predisposition in a biologically relevant cell type for pre-clinical therapy screening.

Identification of novel genetic disease associations can highlight potential targets for therapeutic development. New therapies require extensive functional study prior to clinical trials and medical translation. Cell models are a valuable tool for investigating the effects of promising drug compounds and it is important that studied cell types are relevant to the disease of interest. Whilst the inherited risk of sVS remains uncharacterised, a VS-associated *NF2* mutational model remains most relevant in the study of VS therapy development. The use of antisense oligonucleotides to mask the effects of deep intronic pathogenic variants hold great therapeutic potential.

We hypothesise that design of an antisense oligonucleotide to prevent inclusion of a cryptic exon caused by a deep intronic pathogenic variant in *NF2* (c.516+232 G>A) will restore WT gene splicing.

We intend on introducing a permanent edit of *NF2* c.516+232 G>A in the genome of an immortalised Schwann cell line ipn02.3 2λ through CRISPR based methodology. Additional characterisation of the mutation and investigation of therapeutic options will be conducted using a plasmid construct of the variant *NF2* gene. Modulation of splicing to restore gene function would demonstrate the possibility of a personalised gene therapy in NF2 patients with the same variant.

2. Methods

2.1. Ethical approval

Ethical approval of the use of anonymised samples from the Manchester Centre for Genomic Medicine (MCGM) archive was obtained from the North West 7– Greater Manchester Central Research Ethics Committee, IRAS ID: 36817, Rec Ref: 10/H1008/74. Prospectively recruited patients were provided with an information leaflet and ethics form pertaining to the study prior to obtaining written consent for participation.

2.2. Patient samples

The large majority of patients were retrospectively identified from the local laboratory database within the MCGM. Further samples were provided by referring clinicians through the Northern Care Alliance Research Collection (NCARC) biobank.

2.2.1. Local sample collection

2.2.1.1. Blood

Peripheral blood samples were collected in EDTA (ethylenediaminetetraacetic acid) tubes and transported to the NHS Genomic Diagnostic Laboratory of St Mary's Hospital MFT for DNA extraction and storage. Blood samples are transported at room temperature and stored at 4°C prior to DNA extraction.

2.2.1.2. Tumour

Vestibular schwannoma tumour samples were obtained during surgery. Samples were not obtained from tumours deemed unnecessary for surgical intervention. Tumour tissue was transported fresh at room temperature, or frozen on dry ice, and stored at -20°C prior to DNA extraction.

2.2.2. Local DNA storage

Patient DNA samples extracted by the NHS Genomic Diagnostic Laboratory were stored in the MCGM DNA Archive, temporarily at 4°C before moved to long term storage at -20°C.

2.2.3. Blood samples from NCARC

A proportion of patient samples were recruited prospectively by clinical staff and research practitioners in the neurology team and Skull Base Unit at Salford Royal NHS Foundation Trust (SRFT). Blood samples obtained in SRFT were collected in EDTA and committed to the NCARC tissue repository. Samples were transported frozen and stored at -20°C prior to DNA extraction.

2.3. Genomic sample preparation

2.3.1. DNA extraction from blood

2.3.1.1. Manual

DNA was extracted manually from blood samples using the Gentra Puregene kit (QIAGEN, Hilden, Germany). DNA extraction using the Whole Blood standard protocol was followed, consisting of a series of precipitation and washing steps to obtain pure, high volume DNA in approximately 12-14 hours including an overnight incubation.

2.3.1.2. Automated

DNA samples extracted from blood by the NHS Genomic Diagnostic Laboratory MCGM were performed according to manufacturer protocol using the Chemagic Magnetic Separation Module I instrument, based on M-PVA magnetic bead technology (PerkinElmer, Waltham, MA, USA).

2.3.2. DNA extraction from cultured cells

DNA was extracted from cultured cells using the Gentra Puregene kit (QIAGEN, Hilden, Germany), following the Cultured Cells protocol adapted for adherent cells. Volumes and parameters were scaled for cell density as suggested in the protocol.

2.3.3. DNA extraction from tissue

Tumour DNA extraction was performed by the NHS Genomic Diagnostic Laboratory MCGM using the column-based Cobas® DNA Sample Preparation Kit (Roche, Basel, Switzerland).

2.3.4. Plasmid DNA extraction

Plasmid DNA extraction from transformed *E.coli* was conducted using ZymoPURE Plasmid Mini/Midi/Maxi prep kits (Zymo Research, Irvine, CA, USA), in addition to the QIAGEN Plasmid Midiprep kit (QIAGEN, Hilden, Germany). Overnight cultures of 2-5ml were used for Miniprep DNA extractions, 50ml for Midiprep and 150ml for Maxiprep. Expected yields of high-copy plasmid DNA are as follows, 100 µg in 25µl (Zymo Research Miniprep), 100-400 µg in 100 µl (QIAGEN and Zymo Research Midiprep, respectively), 500 µg in 200 µl (Zymo Research Maxiprep).

Both Zymo Research and QIAGEN plasmid DNA isolation kits utilise a method of alkaline lysis of bacterial cultures. Bacterial lysates are neutralised with high salt solution that precipitates genomic DNA, whilst plasmid DNA remains in solution. Cell debris is removed by centrifugation pelleting (miniprep) or through filtration (midi/maxiprep). The remaining supernatant is loaded onto a silica membrane column, to which the plasmid DNA will bind and can subsequently be eluted into water or buffer as appropriate.

2.3.5. DNA concentration

If required, Zymo Genomic DNA Clean & Concentrator™-25 (Zymo Research, Irvine, CA, USA) was used according to manufacturer's instructions to increase DNA concentrations from sample extractions, samples were eluted into 35µl of elution buffer.

2.3.6. DNA, RNA and protein extraction from cells

Simultaneous DNA, RNA and protein extraction was achieved using the QIAGEN AllPrep® DNA/RNA/Protein Mini Kit (QIAGEN, Hilden, Germany). A maximum of $1x10^7$ cells were lysed directly in each well of 6-well culture plates. Subsequent RNA, total protein and genomic DNA were extracted according to manufacturer's instructions.

RNA extraction was also performed using the Monarch® Total RNA Miniprep kit (New England Biolabs, Hitchin, UK) according to manufacturer's instructions. Again, a maximum of $1x10^7$ cells were lysed directly in each well of 6-well culture plates. Genomic DNA was removed from samples, and RNA recovered, according the manufacturer's instructions.

2.3.7. Protein extraction from cells

Protein extractions were also conducted using RIPA (radioimmunoprecipitation assay) (Sigma Aldrich, St Louis, MO, USA) buffer for cell lysis. Cultured cell media was aspirated and cells were rinsed gently with Dulbecco's Phosphate Buffered Saline (1X with calcium, magnesium, catalog number: 14040117) (DPBS) (Gibco, Waltham, MA, USA), which was again aspirated (more details of cell culture in section 2.7). 1ml of ice cold RIPA buffer was added to 0.5-5x10^7 cells, with addition of phosphatase inhibitors PhosSTOP™ at 1X concentration (Roche, Basel, Switzerland). Adherent cells were detached from culture plates by scraping and the RIPA buffer cell solution was transferred to a microcentrifuge tube and incubated on ice for 30 minutes with regular mixing. Following incubation, tubes were centrifuged at 16,000xg for 20 minutes at 4 °C, the resulting supernatant was collected in a fresh tube and the pellet discarded.

2.3.8. DNA, RNA and protein quantification

Extracted DNA and RNA samples were quantified using both the NanoDrop 8000 spectrophotometer (Thermo Fisher Scientific Inc, Waltham, MA, USA) and µDrop Plate for the Multiskan™ GO Plate Reader (Thermo Fisher Scientific Inc., Waltham, MA, USA). Protein samples were quantified using a Pierce™ BCA (bicinchoninic acid) Protein Assay kit (Thermo Fisher Scientific Inc, Waltham, MA, USA) following protocol for use in a µDrop Plate.

2.4. Molecular techniques

2.4.1. Polymerase chain reaction (PCR)

2.4.1.1. Primer design

Primers were designed using the NCBI (National Center for Biotechnology Information) Primer-BLAST online tool (https://www.ncbi.nlm.nih.gov/tools/primer-blast/index.cgi), default settings were used unless stated otherwise. Primers were ordered from Merck, Sigma Aldrich (St Louis, MO, USA) at a concentration of 100µM.

2.4.1.2. PCR reactions

Standard PCR reactions were performed for DNA amplification using the 2X Green GoTaq® Mastermix, which contains GoTaq® DNA Polymerase, 400µM dATP, 400µM dGTP, 400µM dCTP, 400µM dTTP, 3mM MgCl2 and yellow and blue loading dyes (Promega, Madison, WI, USA). With a total volume of 20µl the reaction included, 10µl Green GoTaq, 10ng DNA, 1µl forward primer (5µM), 1µl reverse primer (5µM) and double distilled H_2O to 20µl. Reactions were performed on the Veriti® Thermal Cycler (Applied Biosystems, Waltham, MA, USA). Standard PCR parameters were as follows in table 3:

Stage	Temperature °C	Time
1	95	3 minutes
2 (35 cycles)	95	30 seconds
	56-64*	30 seconds
	72	45 seconds
3	72	4 minutes
	4	Hold

Table 3. Thermal cycler parameters for PCR

*Temperature dependent upon optimum annealing temperature for primer pair

2.4.1.3. Agarose gel electrophoresis

PCR products were confirmed using agarose-TBE (Tris/Borate/EDTA) gels. Expected products sized below 2Kb were electrophoresed on 1.5% gels (1.5g agarose, 100ml 1X TBE buffer), larger expected products were electrophoresed on a 1% gel (1g agarose, 100ml 1X TBE buffer). UltraPure agarose (Invitrogen, Carlsbad, CA, USA) was dissolved in 1X TBE buffer by heating in a microwave for 2 minutes on full power. Gels were stained with SafeView (NBS Biologicals, Huntingdon, UK), 7.5µl was added to cooled agarose before polymerisation in a gel casting tray with small well combs (30 wells per comb). As Green GoTaq® Mastermix (Promega, Madison, WI, USA) already contains loading dye and glycerol, 5µl of the PCR product was run on the gel in an electrophoresis tank submerged in 1X TBE buffer at

120V for 25-35 minutes, or until the dye-front had run to the end of the gel. Samples were run alongside an appropriate DNA ladder, 100bp GeneRuler (Thermo Fisher Scientific, Waltham, MA, USA), or 1Kb Hyperladder™ (Bioline, London, UK). Gels were visualised and imaged using UV trans-illumination on a Bio-Rad XR+ gel documentation system.

2.4.1.4. PCR purification

Purification of PCR products is necessary to remove unincorporated components from the initial amplification cycling. PCR products were purified using column-based or bead-based methods. Column-based QIAquick PCR purification kit (QIAGEN, Hilden, Germany) was performed according to manufacturer's instructions, eluting into 50µl of elution buffer. Bead purification was performed using Agencourt AMPure XP paramagnetic beads (Beckman Coulter, Pasadena, CA, USA), or AppMag PCR Clean Up Beads (Appleton Woods Ltd., Birmingham, UK). Beads were added at 1.8x volume of the PCR product. Automated processing of samples, according to manufacturer instructions, was conducted by the NHS service at MCGM on the Biomek NX robotics instrument (Beckman Coulter, Pasadena, CA, USA) with elution of the purified product in 100µl dH_2O.

2.4.2. Sanger sequencing

2.4.2.1. Cycle sequencing

Sequencing reactions were performed using the BigDye™ Terminator v3.1 Cycle Sequencing Kit (Thermo Fisher Scientific Inc, Waltham, MA, USA). With a total volume of 10µl per sample the reaction included 5.275µl water, 1.875µl 5X sequencing buffer, 1.6µl primer (5µM), 0.25µl BigDye™ Terminator v3.1 enzyme mastermix, 1µl PCR product. Sequencing reactions were run using the thermal cycler parameters in table 4.

Stage	Temperature °C	Time
1	98	30 seconds
2 (32 cycles)	98	10 seconds
	55	10 seconds
	60	4 minutes
3	4	Hold

Table 4. Thermal cycler parameters for cycle sequencing

2.4.2.2. CleanSEQ purification

Sequencing reaction products were purified using either Agencourt CleanSEQ paramagnetic bead solution (Beckman Coulter, Brea, CA, USA) or AppMag Dye Terminator Removal Clean Up Beads (Appleton Woods Ltd., Birmingham, UK). For both products, 5µl of bead solution was added to 10µl of sequencing reaction. Samples were then processed by the NHS service at MCGM according to manufacturer instructions on an automated Biomek NX robotics instrument (Beckman Coulter, Pasadena, CA, USA).

2.4.2.3. Sanger sequencing analysis

Sequencing analysis was performed using Applied Biosystems™ 3730xl DNA Analyzer (Thermo Fisher Scientific, Waltham, MA, USA). Sanger sequencing chromatograms were viewed and analysed using the programs, Chromas (Technelysium, South Brisbane, Australia) and CodonCode Aligner (CodonCode Corporation, Centerville, MA, USA).

2.4.3. Next generation sequencing

Next generation sequencing (NGS) was conducted by the NHS Genomic Diagnostic Laboratory MCGM on either the Illumina MiSeq™ or HiSeq™ platform, according to manufacturer's instructions (Illumina, San Diego, CA, USA). Library preparation was performed using the SureSelect Human All Exon Kit (Agilent, Santa Clara, CA, USA).

2.4.4. UK Biobank Axiom™ array

The UK Biobank Axiom™ Array contains 820,967 SNP and indel markers. Genotyping on UK Biobank Axiom™ 96 well arrays (Thermo Fisher Scientific,

Waltham, MA, USA) was conducted by two service providers, Oxford Genomics Centre and Yourgene Health, using the same Axiom 2.0 Assay manual workflow. Genotypes were called and quality checked in-house using Axiom analysis suite software v4.0.3.3 following the Axiom Best Practice Genotyping Analysis Workflow, which uses an adapted version of the BRLMM-P algorithm. Full details of array genotyping quality parameters and interpretation are given in results section 5.

2.4.5. cDNA synthesis from RNA extractions

RNA samples were treated with ezDNase™ Enzyme (Thermo Fisher Scientific, Waltham, MA, USA) to digest remaining genomic DNA. Between 1-5µg of RNA was input to the reaction, max volume 8µl. Total reaction components per sample were as follows, 1µl 10X ezDNase Buffer, 1µl ezDNase, up to 8µl RNA, nuclease-free water to make 10µl total reaction volume. Samples were incubated at 37°C for 2 minutes, then chilled on ice. Samples were then used directly as input for cDNA synthesis.

cDNA synthesis was performed using the SuperScript™ IV Reverse Transcriptase kit (Thermo Fisher Scientific, Waltham, MA, USA). Samples were first annealed to primers using the following reagents, 1µl 50µM Oligo d(T) primer, 1µl 10mM dNTP (deoxynucleoside triphosphate) mix, 10µl of ezDNase reaction, 1µl DEPC-treated (Diethyl Pyrocarbonate) water. The total reaction volume of 13µl was heated at 65°C for 5 minutes, then incubated on ice for 1 minute. Reverse transcription reaction components were then added to the primer annealed samples as follows, 4µl 5X SSIV Buffer, 1µl 100mM DTT (Dithiothreitol), 1µl RNaseOUT™ Recombinant RNase Inhibitor, 1µl SuperScript® IV Reverse Transcriptase (200 U/µl). Samples were incubated at 50°C for 10 minutes, then inactivated by 80°C incubation for 10 minutes. Remaining RNA was removed through addition of 1µl *E.coli* RNase H, with 37°C incubation for 20 minutes. Reverse transcription samples were then amplified by PCR as detailed in section 2.4.1.2.

2.5. Computational resources

2.5.1. Databases and online tools

Variant frequencies and ExAC (Exome Aggregation Consortium) constraint metrics were obtained from the Genome Aggregation Database (gnomAD v2.1.1) www.gnomad.broadinstitute.org (Lek *et al.*, 2016). The DECIPHER (Database of Chromosomal Imbalance and Phenotype in Humans using Ensembl Resources) database https://www.deciphergenomics.org/ (Firth *et al.*, 2009) was used to investigate regional constraint in proteins. Minor allele frequency calculations were performed using alleleFrequencyApp www.cardiodb.org/allelefrequencyapp (Whiffin *et al.*, 2017). Sequence alignment was conducted using Clustal Omega http://www.ebi.ac.uk/Tools/msa/clustalo (Sievers *et al.*, 2011). Leiden Open Variation Database (LOVD) (www.lovd.nl) (Fokkema *et al.*, 2021), ClinVar NCBI (www.ncbi.nlm.nih.gov/clinvar) (Landrum *et al.*, 2018), Human Gene Mutation Database (HGMD) (www.hgmd.cf.ac.uk/ac/all.php) (Stenson *et al.*, 2020), dbSNP https://www.ncbi.nlm.nih.gov/projects/SNP (Sherry *et al.*, 2001), Clinical Interpretation of Variants in Cancer (CIViC) (https://civicdb.org/home), Mastermind Genomic Search Engine (https://www.genomenon.com/mastermind), COSMIC (Catalog of Somatic Mutations in Cancer) www.cancer.sanger.ac.uk (Tate *et al.*, 2019) and CanVar-UK www.canvaruk.org were used to gain variant-specific information. UCSC (University of California Santa Cruz) LiftOver tool was used for any genomic co-ordinate conversions between genome builds GRCh37/hg19 and GRCh38/hg38 www.genome.ucsc.edu/cgi-bin/hgLiftOver (Kent *et al.*, 2002). The Michigan Imputation Server https://imputationserver.sph.umich.edu/index.html#!pages/home (Das *et al.*, 2016) was employed for phasing and imputation of GWAS-associated data, further details of use are found in section 5. Online platform FUMA (Functional Mapping and Annotation) GWAS https://fuma.ctglab.nl/ (Watanabe *et al.*, 2017) was used to visualise and explore GWAS summary statistics.

2.5.2. *In silico* pathogenicity prediction tools

Multiple *in silico* tools were used for variant effect prediction, they include: Align-GVGD (Mathe *et al.*, 2006), SIFT (Kumar, Henikoff and Ng, 2009), PolyPhen-2 (Adzhubei *et al.*, 2010), MutationTaster2 (Schwarz *et al.*, 2014), SpliceAI (Jaganathan *et al.*, 2019), SpliceSiteFinder-like tool (Zhang, 1998), MaxEntScan (Yeo and Burge, 2004), REVEL (Rare Exome Variant Ensemble Learner) (Ioannidis *et al.*, 2016), ClinPred (Alirezaie *et al.*, 2018). Many of these tools were accessed through the clinical prediction software Alamut Visual version 2.15 (SOPHiA GENETICS, Lausanne, Switzerland).

2.6. Bacteriological methods

2.6.1. Bacterial culture

E.coli cultures were grown in Luria-Bertani (LB) broth (10g/L tryptone, 5g/L yeast extract, 5g/L NaCl) (Sigma-Aldrich, St. Louis, MO, USA), or on LB plates (addition of 1.5% w/v agar). Ampicillin (50µg/ml) was added to LB. Plated cultures were incubated inverted and stationary at 37°C, liquid cultures were incubated in loose-lid tubes, or flasks, at 37°C with 220 rpm shaking. Culture stocks were stored in LB-ampicillin broth with 50% glycerol (v/v) at -80°C.

2.6.2. Transformation

New England Biolabs® (NEB) Stable Competent *E.coli* (New England Biolabs, Hitchin, UK) strain was used for all transformations. Bacterial cells were thawed on ice for 20-30 minutes. 100ng of plasmid assembly was added to 50µl of competent cells, mixed gently and incubated on ice for 25 minutes. Cells were heat shocked in a waterbath for 30 seconds at 42°C, then incubated on ice for a further 2 minutes. Transformed cells were then spread on LB-ampicillin plates and incubated overnight.

2.7. Cell culture

2.7.1. Initiation of cell culture

Cell cultures were initiated from frozen cell pellets. 1ml cell aliquots were thawed quickly in a water bath at 37^{o}C, then transferred into 9ml of Dulbecco's Modified Eagle's Medium (1X, high glucose, pyruvate, no glutamine, catalog number: 21969035) (DMEM) (Gibco, Waltham, MA, USA),

supplemented with 10% Foetal Bovine Serum (FBS) (HyClone, Cytiva, Marlborough, MA, USA) and L-glutamine (100X) (Gibco, Waltham, MA, USA). Cells were then centrifuged for 5 minutes at 500rpm. Supernatant was removed and cells resuspended in 12ml of DMEM, supplemented with FBS and L-glutamine. Resuspended cells were then transferred to a 10cm² dish and incubated at 37°C, 5% CO_2. Once confluent, cells were seeded into 75cm² culture flasks (section 2.7.2).

2.7.2. Routine cell culture

Adherent immortalised Schwann cell line, ipn02.3 2λ, was used for all experiments. Cell line ipn02.3 was immortalised via the viral delivery of human TERT (telomerase reverse transcriptase) and murine Cdk4, generated in the laboratory of Dr Margaret Wallace, University of Florida (Li *et al.*, 2016). Cells were cultured and maintained in DMEM (Gibco, Waltham, MA, USA) supplemented with 10% FBS (HyClone, Cytiva, Marlborough, MA, USA), L-glutamine (100X) (Gibco, Waltham, MA, USA) and penicillin (5U/µL)/ streptomycin (5µg/µL) (Gibco, Waltham, MA, USA). Supplemented media was passed through a 0.2µm filter prior to culture use, to minimise risk of mycoplasma infection.

Cells were seeded in 75cm² culture flasks and incubated at 37°C, 5% CO_2. Passage of cells was performed every 3-4 days at 80-100% confluency. Media was aspirated and cells rinsed with Dulbecco's Phosphate Buffered Saline (1X with calcium, magnesium, catalog number: 14040117) (DPBS) (Gibco, Waltham, MA, USA) prior to addition of 2ml 0.25% trypsin-EDTA (Gibco, Waltham, MA, USA) for 2 minutes to detach cells from flask. Trypsin was neutralised with 8ml of FBS-supplemented media. New cultures were seeded at a 1 in 12 dilution in fresh media. To determine cell density a haemocytometer was used to count cells. An average cell count was taken for the four outer squares of the counting chamber. Cell count was multiplied by 10^4 to obtain cells/ml.

2.7.3. Freezing cell stocks

Confluent cells in 75cm² culture flasks were detached using 2ml 0.25% trypsin-EDTA (Gibco, Waltham, MA, USA) for 2 minutes, neutralised with FBS-

supplemented media and collected in a 15ml tube. Cells were pelleted by centrifugation for 5 minutes at 500 rpm, then resuspended in 3-6ml of 90% DMEM (supplemented with FBS and L-glutamine)/ 10% DMSO (dimethyl sulfoxide). Cells were frozen in cryotubes at -80^{o}C in 1ml aliquots.

2.7.4. Transfection methods

2.7.4.1. TransIT-X2®

TransIT-X2® dynamic delivery system (Mirus Bio, Madison, WI, USA) was tested for transfection of CRISPR RNP (ribonucleoprotein) complexes. RNP complexes consisted of EnGen® Spy Cas9 NLS (20µM) (New England Biolabs, Hitchin, UK) and synthetic gRNA (100µM) diluted to 50µM (Sigma-Merck, Darmstadt, Germany). Control gRNA targeting the AAVS1 locus (Chen *et al.*, 2018) was used for RNP mix ratio optimisation. RNP ratios tested were 2:1 and 3:1, gRNA:Cas9. Optimisation of TransIT-X2® reagent volume and cell density was also performed. Optimisation of RNP ratio and TransIT-X2® volume was conducted in 24-well culture plates. 0.5ml cells were plated 24 hours prior to transfection at a density of 0.8-3.0 x10^{5} cells/ml, cells were approximately 80% confluent on the day of transfection. Transfection optimisation components are outlined in table 5, Opti-MEM™ Reduced Serum Medium was used as transfection media (catalog number: 31985062, Gibco, Waltham, MA, USA). RNP components were combined and incubated for 10 minutes at room temperature prior to transfection.

Optimisation parameters	gRNA (50µM)	EnGen® Spy Cas9 NLS (20µM)	TransIT-X2®	Opti-MEM™
RNP 2:1 TransIT-X2® 1µl	0.12µl	0.15µl	1µl	50µl
RNP 2:1 TransIT-X2® 1.5µl	0.12µl	0.15µl	1.5µl	50µl
RNP 3:1 TransIT-X2® 1µl	0.18µl	0.15µl	1µl	50µl
RNP 3:1 TransIT-X2® 1.5µl	0.18µl	0.15µl	1.5µl	50µl

Table 5. Component reagents of TransIT-X2® transfection optimisation

Cell media was aspirated and replaced with FBS-supplemented DMEM 24 hours post-transfection. DNA was extracted from transfected cells 48 hours post-transfection, as described in section 2.3.2. Sanger sequencing was performed on extracted DNA and chromatograms were analysed using Synthego ICE (inference of CRISPR edits) tool version 2.0 https://ice.synthego.com [accessed March 2021] to assess editing efficiency. Optimisation remained unsuccessful at creating Cas9 directed DNA cleavage after multiple troubleshooting attempts.

2.7.4.2. Nucleofection

Nucleofection was implemented to increase transfection efficiency. Initial optimisation of Nucleofection was performed using the Lonza Amaxa Cell Line Optimisation Nucleofector™ kit (Lonza Group Ltd. Basel, Switzerland) following standard protocol. Subsequent Nucleofections were conducted using the Lonza Amaxa Nucleofector™ kit V (Lonza Group Ltd. Basel, Switzerland). The single cuvette Nucleofector™ 2b Device (Lonza Group Ltd. Basel, Switzerland) was used for all Nucleofections. Nucleofection program D-033 was used unless otherwise stated. Post-Nucleofection two additional steps were performed prior to cell plating; a 10 minute room temperature incubation to increase transfection efficiency, followed by addition of RPMI 1640 with L-glutamine (Lonza Group Ltd. Basel, Switzerland) low-calcium recovery media incubated for a further 10 minutes at 37^{o}C to maximise cell survival.

2.7.4.3. Lentivirus transduction

Pseudo-constructs were designed for a reporter system to assess the impact of *NF2* deep intronic variant c.516+232 G>A, on protein translation. All vector maps can be found in the appendices. Constructs were assembled and packaged by VectorBuilder (VectorBuilder Inc. Chicago, IL, USA). Constructs were delivered into ipn02.3 2λ Schwann cells through lentivirus packaging following the VectorBuilder protocol for transducing adherent cells. Lentiviruses used by VectorBuilder are “self-inactivating” and are kept at -80^{o}C for long term storage.

A positive control (pLV[Exp]-EGFP:T2A:Puro-EF1A>mCherry) supplied by VectorBuilder was used to determine the multiplicity of infection (MOI) optimisation for target cells. MOI is the number of infectious virus particles per cell, e.g. MOI = 1, is equal to 1 transducing unit (TU), or virus particle, per cell. Standard MOI concentrations range from 1-10 TU/cell. Green fluorescent protein analysis (further details in section 2.7.5) was conducted in cells transduced with an MOI of 1, 5 and 10 of the pLV[Exp]-EGFP:T2A:Puro-EF1A>mCherry positive control virus. MOI = 5 demonstrated efficient transduction and was therefore used for subsequent transductions unless stated otherwise. Lentivirus stock concentrations were $>10^8$ TU/ml. For transductions of MOI = 5 for $6x10^5$ cells, 30µl of stock lentivirus was used.

Cells were plated 24 hours prior to lentivirus transduction, $3x10^5$ cells were plated per well of a 6-well plate. Plates were incubated over night at 37°C, 5% CO_2. After 24 hours of incubation cells were at 30-50% confluency, approximately $6x10^5$ cells. For transduction, virus was defrosted on ice and then added to 0.5ml supplemented DMEM at the MOI concentration stated. Old culture media was aspirated from cells and virus-containing media added, cells were then incubated at 37°C, 5% CO_2 for 9 hours. After incubation, virus-containing media was removed and fresh supplemented DMEM added. Fluorescence analysis (section 2.7.5) of cells was performed >24 hours after transduction and for DNA/RNA/protein extraction >48 hours (section 2.3).

2.7.5. Fluorescence analysis

Fluorescent markers were used to confirm successful transfection for optimisation of protocols and for selection of cells. Two methods of fluorescence analysis were used.

2.7.5.1. Fluorescence microscopy

For fluorescent microscopy analysis, cells were cultured on 12mm cover glass slips placed in 24-well plates. Media was aspirated and cells rinsed with DPBS. Cover glasses were removed and mounted on microscope slides using Vectashield® Hard Set™ mounting medium with DAPI (Vector

Laboratories, Inc. Burlingame, CA, USA). Slides were viewed on an Axio Imager.Z2 fluorescence microscope (ZEISS, Oberkochen, Germany).

2.7.5.2. Fluorescence activated cell sorting (FACS)

FACS was performed by the University of Manchester Flow Cytometry Core Facility to obtain green fluorescent protein (GFP) positive cell populations, indicating successful transfection. FACS was conducted using the BD FACSAria™ Fusion Flow Cytometer, (BD Biosciences, Franklin Lakes, NJ, USA) cell counting and gating parameters were set using BD Biosciences FACSDiva™ software.

2.8. CRISPR

2.8.1. Cas9 double stranded DNA cleavage

To assess the capacity of the target variant site (*NF2* c.516+232 G>A) for Cas9 directed double strand cleavage, three gRNAs were designed to target NGG PAM (protospacer adjacent motif) sites in the surrounding region when assembled in a RNP complex with Cas9 (details in table 6). A known high DNA cutting efficiency target gRNA (AAVS1) (Ogata, Kozuka and Kanda, 2003) was used as a positive control to assess transfection success. Primers were designed to create two different sized fragments for amplification and sequencing characterisation of the control and target regions (table 7). Synthego ICE version 2.0 analysis https://ice.synthego.com [accessed March 2021] was used to assess editing efficiency. Details of RNP reagent optimisation using the AAVS1 positive control gRNA are outlined in table 8.

gRNA name	gRNA sequence (5'>3')
AAVS1 ctrl	CTCCCTCCCAGGATCCTCTC
NF2 sgRNA1	AAAGGTTTTTGGAGTTAGTT
NF2 sgRNA2 (antisense)	TTTACAGGCCATGCTAGTCC
NF2 sgRNA3	TGGGGTCACCAGGACTAGCA

Table 6. Ribonucleoprotein gRNA designs to target *NF2* c.516+232 G>A region

Primer name	Primer sequence (5'>3')
AAVS1_F	CCTTCTTGTAGGCCTGCATC
AAVS1_R	TGACGCACGGAGGAACAATA
AAVS1_TIDE_F	ACTAGGGACAGGATTGGTGACA
NF2_F	GAGCTGGGAGGGAATGAGAT
NF2_R	CATCTCAGGCCTTCACATGC
NF2_ICE_F	GCCTGCTCTCCCTTTCTTCT

Table 7. Primer sequences for amplification and sequencing of control and target regions

Optimisation ratio gRNA:Cas9	gRNA (30µM)	EnGen® Spy Cas9 NLS (20µM)	Nucleofector solution	Volume of cell suspension ($1x10^6$ cells)
RNP 3:1	4µl	2µl	78µl	16.7µl
RNP 6:1	8µl	2µl	74µl	16.7µl
RNP 9:1	12µl	2µl	70µl	16.7µl

Table 8. Component reagents of RNP Nucleofection optimisation

2.8.2. Prime editing

Design of the target prime editing gRNA vector was conducted using pegFinder http://pegfinder.sidichenlab.org/ (Chow *et al.*, 2021) for NGG PAM sites. Oligonucleotide fragment designs for introduction of the *NF2* c.516+232 G>A variant through pegRNA vector assembly are detailed in table 9, *NF2* transcript NM_000268.4 (isoform 1) was used for design reference. The pegRNA vector was assembled using the pU6-pegRNA-GG-acceptor, a gift from David Liu (Addgene plasmid #132777) and NEB® Golden Gate Assembly Kit (Bsa1-HF®v2) (New England Biolabs, Hitchin, UK) detailed in section 2.8.2.1 (Anzalone *et al.*, 2019). Prime editing gRNA vector pU6-Sp-pegRNA-RNF2_+5GtoT, a gift from David Liu (Addgene plasmid #135957) (Anzalone *et al.*, 2019), was used as a positive control. PegRNA vectors were co-transfected with prime editor vector pCMV-PE2-P2A-GFP, a gift from David Liu (Addgene plasmid #132776) (Anzalone *et al.*, 2019), which contains modified spyCas9 for Cas9-directed DNA cleavage. All vector maps can be found in the appendices. Vectors were initially transfected into target cells at

a 3:1 ratio (3µg prime editor: 1µg pegRNA vector) as well as a 4:3 (4µg prime editor: 3µg pegRNA vector) ratio in attempts to increase efficiency.

Oligo name	Sequence	Modification
sgF	caccgTGGGGTCACCAGGACTAGCAgttttaga	-
sgR	tagctctaaaacTGCTAGTCCTGGTGACCCCAc	-
scaffF	GCTAGAAATAGCAAGTTAAAATAAGGCTAGTC CGTTATCAACTTGAAAAAGTGGCACCGAGTCG	5’ Phosphorylated
scaffR	GCACCGACTCGGTGCCACTTTTTCAAGTTGATA ACGGACTAGCCTTATTTTAACTTGCTATTTC	5’ Phosphorylated
extensF	gtgcACGTTAGAAAAAACATTTACAGGCCATGC TAGTCCTGGTGA	-
extensR	aaaaTCACCAGGACTAGCATGGCCTGTAAATGT TTTTTCTAACGT	-

Table 9. Prime editing vector Golden Gate assembly fragments

2.8.2.1. Golden Gate pegRNA plasmid assembly

NEB® Golden Gate Assembly Kit (Bsa1-HF®v2) (New England Biolabs, Hitchin, UK) was used to assemble prime editing pegRNAs in the backbone vector pU6-pegRNA-GG-acceptor, a gift from David Liu (Addgene plasmid #132777). Vector maps found in appendices. PegRNA design and vector details are described in section 2.8.2. Vector Bsa1 restriction enzyme digestion, assembly, and transformation was performed as described previously (Anzalone *et al.*, 2019).

2.8.2.1.1. Acceptor plasmid digestion and isolation

Digestion reaction components were as follows, 2000ng pU6-pegRNA-GG-acceptor plasmid, 1µl Bsa1-HF®v2 restriction enzyme (New England Biolabs, Hitchin, UK), 3µl 10x Cutsmart Buffer and H_2O to 30µl total reaction volume. The digestion components were incubated at 37°C for 5 hours. Following this, 5µl of purple gel loading dye (6X) (New England Biolabs, Hitchin, UK) was added to 30µl of plasmid backbone digestion and loaded on a 0.8% agarose gel alongside a Quick-Load® Purple 1 kb Plus

DNA Ladder (New England Biolabs, Hitchin, UK). The target ~2.2kb fragment was viewed on a UV trans-illuminator and excised from the gel using a scalpel. Zymoclean Gel DNA Recovery kit (Zymo Research, Irvine, CA, USA) was used according to manufacturer's instructions to isolate the plasmid fragment.

2.8.2.1.2. Annealing of oligonucleotide pairs

PegRNA oligonucleotide fragments (described in section 2.8.2 table 9) were annealed to their reverse complementary pair using the following reaction components, 1µl forward oligo (100µM), 1µl reverse oligo (100µM), 23µl annealing buffer (H_2O supplemented with 10mM Tris-Cl pH 8.5 and 50 mM NaCl). Reactions were placed in a Veriti® Thermal Cycler (Applied Biosystems, Waltham, MA, USA) at 95 °C for 3 minutes, then cooled gradually (0.1 °C/s) to 22°C. Annealed oligonucleotides were then diluted 1:4 through addition of 75µl H_2O to make a final oligonucleotide concentration of 1µM.

2.8.2.1.3. Plasmid assembly

The components of the Golden Gate plasmid assembly reaction are seen in table 10. Reaction components were incubated at room temperature for 10 minutes, then placed in a Veriti® Thermal Cycler (Applied Biosystems, Waltham, MA, USA) for 15 minutes at 37°C, then 15 minutes at 80°C, then held at 12°C. Correct plasmid assembly was confirmed by Sanger sequencing (section 2.4.2) using the following primers:

pU6_forward: GAGGGCCTATTTCCCATGATT

pU6_reverse: GGGAAACGCCTGGTATCTTT

Correctly assembled plasmids were transformed into competent cells as described in section 2.6.2.

Component	Volume
Digested pU6-pegRNA-GG-acceptor plasmid 2.2kb isolated fragment (30ng/µl)	1µl
Annealed sgF and sgR oligonucleotide pair (1µM)	1µl
Annealed extensF and extensR oligonucleotide pair (1µM)	1µl
Annealed scaffoldF and scaffoldR oligonucleotide pair (1µM)	1µl
Bsa1-HF®v2 restriction enzyme (NEB)	0.25µl
T4 DNA ligase (NEB)	0.5µl
10x T4 DNA ligase buffer (NEB)	1µl
H_2O	4.25µl
Total reaction volume	10µl

Table 10. Components of the Golden Gate plasmid assembly reaction

NEB – New England Biolabs, NEB® Golden Gate Assembly Kit (Bsa1-HF®v2).

2.8.2.1.4. Analysis of prime editing success

Primers to characterise and assess editing at the *NF2* target region are described in table 7. Characterisation of the positive control (pU6-Sp-pegRNA-RNF2_+5GtoT) prime editing target site was performed using the primer sequences below:

RNF2_Forward: GCTGTGCAGACAAACGGAAC

RNF2_Reverse: TATGCCCCTTGGCAGTCATC

2.9. Western blotting

An input of 15µg of total protein was used per Western blot sample. Samples were combined with 2X Laemmli Sample buffer (Bio-Rad, Hercules, CA, USA), with added 2-Mercaptoethanol (Bio-Rad, Hercules, CA, USA), to make a 1X final concentration (1:1 volume buffer to sample). Precast Mini-PROTEAN® TGX Stain-Free Gels 7.5-12% (Bio-Rad, Hercules, CA, USA) were used, submerged in 1X TGS running buffer (Bio-Rad, Hercules, CA, USA) in an electrophoretic tank. Protein standard Precision Plus Protein™ WesternC™ (Bio-Rad, Hercules, CA, USA) was loaded alongside samples. Gels were electrophoresed at 200V for 20-40 minutes, depending on the expected protein size. Proteins were transferred onto an Immun-Blot® PVDF Membrane (Bio-Rad, Hercules, CA, USA) using a semi-dry

transfer system, transfer occurred for 35 minutes at 48 mA per membrane (0.8 mA/cm2). Transfer buffer, Bjerrum Schafer-Nielsen (48 mM Tris, 39 mM Glycinne, 20% Methanol, pH = 9.2) (Bio-Rad, Hercules, CA, USA) was used. After transfer, membranes were blocked through incubation with 3% non-fat milk in TBS (Tris-Buffered Saline) (Bio-Rad, Hercules, CA, USA) 0.1% TWEEN® (Sigma Aldrich, St Louis, MO, USA) buffer for 1 hour. Membranes were incubated with 1:1000 dilutions of primary antibody Monoclonal ANTI-FLAG® M2 produced in mouse (Sigma Aldrich, St Louis, MO, USA). Antibody dilutions were made in 2% bovine serum albumin (BSA) (Sigma Aldrich, St Louis, MO, USA) in TBS 0.1% TWEEN®. Protein detection was achieved through incubation with a 1:3000 dilution of secondary antibody, Donkey Anti-Mouse IgG (H+L) Horseradish Peroxidase (HRP) Conjugate (Thermo Fisher Scientific Inc, Waltham, MA, USA) and 1:30,0000 dilution of Precision Protein™ StrepTactin-HRP Conjugate (Bio-Rad, Hercules, CA, USA). Protein visualisation was enhanced using the Clarity™ Western ECL Substrate (Bio-Rad, Hercules, CA, USA). Blots were visualised and imaged using a Bio-Rad XR+ gel documentation system.

If repeat antibody incubation was required, Immun-Blot® PVDF Membranes were stripped of existing bound antibodies using Re-Blot Plus Mild Solution (10X) (MilliporeSigma, Burlington, MA, USA). Re-Blot Plus Mild Solution (10X) solution was diluted to 1X with distilled water. For one blot, 15ml of 1X Re-Blot Plus Mild Solution incubated with shaking at room temperature for 15 minutes. Blot membranes were washed briefly with TBS and visualised using the Clarity™ Western ECL Substrate to confirm antibody stripping.

For normalisation of protein band intensities, incubation with beta-actin antibody (Catalog number: MA5-16410) (Thermo Fisher Scientific Inc, Waltham, MA, USA) was conducted. Membranes were blocked with 2% BSA for 1 hour. Beta-actin was used at a 1:1000 dilution in 1% BSA (Sigma Aldrich, St Louis, MO, USA) TBS 0.1% TWEEN® with 40 minutes of incubation. Secondary antibody, Goat Anti-Rabbit IgG (H+L) HRP Conjugate (Thermo Fisher Scientific Inc, Waltham, MA, USA), was diluted to 1:2000 with addition of 1:50,0000 Precision Protein™ StrepTactin-HRP Conjugate (Bio-Rad, Hercules, CA, USA) in 1% BSA (Sigma Aldrich, St Louis, MO, USA) TBS 0.1% TWEEN® incubated for 1 hour.

2.10. Antisense oligonucleotide

An antisense oligonucleotide (ASO) was designed and produced by Gene Tools (Philomath, OR, USA) to mask translation of the cryptic exon created by the *NF2* c.516+232 G>A deep intronic variant. Complementary to the antisense sequence of the variant region, the following 29mer morpholino was designed to have melting temperature (Tm) of 90.6°C for optimal RNA affinity in human cells (37°C).

ASO sequence (5' > 3') – CTCAACTGCATCTGAAAAAACAACCACGT

Following lentivirus transduction of wild-type and mutant *NF2* c.516+232 G>A constructs, as detailed in section 2.7.4.3, samples were Nucleofected (section 2.4.7.2) with the ASO to investigate if wild-type splicing is rescued by masking of the cryptic exon. Approximately $1x10^6$ ipn02.3 2λ Schwann cells were used per sample reaction. Cells were centrifuged at 100xg for 10 minutes, supernatant was then removed and cells resuspended in Nucleofector solution from the Lonza Amaxa Nucleofector™ kit V (Lonza Group Ltd. Basel, Switzerland). ASO stock of 1mM was added to resuspended cells in Nucleofector solution to make a 5µM or 10µM concentration of ASO in delivery solution with a total volume of 100µl. Reactions were transferred to single cuvettes for the Nucleofector™ 2b Device (Lonza Group Ltd. Basel, Switzerland) and Nucleofected using program D-033. Cell recovery and plating was conducted as described in section 2.4.7.2. DNA, RNA and protein was extracted (section 2.3.6) from samples 48 hours post-Nucleofection.

3. Sporadic vestibular schwannoma: a molecular testing summary

ORIGINAL RESEARCH

Sporadic vestibular schwannoma: a molecular testing summary

Katherine V Sadler ,[1] Naomi L Bowers,[2] Claire Hartley,[3] Philip T Smith,[4] Simon Tobi,[4] Andrew J Wallace,[5] Andrew King,[6] Simon K W Lloyd,[7] Scott Rutherford,[6] Omar N Pathmanaban,[8] Charlotte Hammerbeck-Ward,[8] Simon Freeman,[9] Emma Stapleton,[7] Amy Taylor ,[10] Adam Shaw,[11] Dorothy Halliday,[12,13] Miriam Jane Smith ,[2] D Gareth Evans [14]

For numbered affiliations see end of article.

Correspondence to
Professor D Gareth Evans, Clinical Genetics, Manchester University NHS Foundation Trust, Manchester M13 9WL, UK; gareth.evans@mft.nhs.uk

MJS and DGE are joint senior authors.

Received 19 March 2020
Revised 1 May 2020
Accepted 3 May 2020

ABSTRACT

Objectives Cases of sporadic vestibular schwannoma (sVS) have a low rate of association with germline pathogenic variants. However, some individuals with sVS can represent undetected cases of neurofibromatosis type 2 (NF2) or schwannomatosis. Earlier identification of patients with these syndromes can facilitate more accurate familial risk prediction and prognosis.

Methods Cases of sVS were ascertained from a local register at the Manchester Centre for Genomic Medicine. Genetic analysis was conducted in *NF2* on blood samples for all patients, and tumour DNA samples when available. *LZTR1* and *SMARCB1* screening was also performed in patient subgroups.

Results Age at genetic testing for vestibular schwannoma (VS) presentation was younger in comparison with previous literature, a bias resulting from updated genetic testing recommendations. Mosaic or constitutional germline *NF2* variants were confirmed in 2% of patients. Pathogenic germline variants in *LZTR1* were found in 3% of all tested patients, with a higher rate of 5% in patients <30 years. No pathogenic *SMARCB1* variants were identified within the cohort. Considering all individuals who received tumour DNA analysis, 69% of patients were found to possess two somatic pathogenic *NF2* variants, including those with germline *LZTR1* pathogenic variants.

Conclusions Undiagnosed schwannoma predisposition may account for a significant minority of apparently sVS cases, especially at lower presentation ages. Loss of *NF2* function is a common event in VS tumours and may represent a targetable common pathway in VS tumourigenesis. These data also support the multi-hit mechanism of *LZTR1*-associated VS tumourigenesis.

INTRODUCTION

Vestibular schwannomas (VS) are benign nerve sheath tumours that arise on the vestibular branch of the vestibulocochlear (eighth) cranial nerve. VS can occur both unilaterally and bilaterally, developing on both the superior and inferior branches of the vestibular nerve.[1] While VS histology is benign, tumour growth within the internal auditory canal can result in nerve disruption, causing hearing loss, tinnitus and vestibular disequilibrium.[2] Larger tumours growing among eloquent structures within the cerebellopontine angle can also produce facial pain, brainstem compression and hydrocephalus. These morbidities cause a decline in patients' quality of life.

With a lifetime risk of approximately 1 in 1000 individuals,[3] VS accounts for nearly 8% of all brain and central nervous system tumours.[4] Recent epidemiological studies suggest VS annual incidence ranges from 1 in 64 000 to 1 in 90 000 people,[5–7] which may equate to a lifetime risk as high as 1 in 800. VS is known to occur within the context of tumour suppressor syndromes, neurofibromatosis type 2 (NF2) and rarely schwannomatosis. NF2 has a propensity to occur as mosaic disease,[8] variable presentation of which can result in significant phenotypic overlap between the two disorders. While the development of bilateral VS is strongly associated with NF2 disease, NF2-associated VS only accounts for 5% of all VS cases[9]; the majority of VS cases occur sporadically in otherwise healthy individuals.[3]

Cases of apparent sporadic vestibular schwannoma (sVS) have been demonstrated to have a low rate of association with germline predisposition mutations detectable in blood.[10] Nonetheless, somatic biallelic inactivation of the *NF2* gene is frequently observed in sVS tumours.[11] Recent literature suggesting that NF2 mosaicism rates in patients fulfilling NF2 diagnostic criteria are twice as high as previous estimates may hold an explanation for the high incidence of *NF2* inactivation in sVS tumours.[8] With the incidence of de novo NF2 mosaicism now thought to be as high as 60%, it is likely that a considerable proportion of patients with sVS possess undetected NF2 mosaicism. These patients may have remained undetected due to low allele fractions and therefore may present with a milder NF2 phenotype, such as a solitary VS. This suggestion is supported by the higher rates of mosaicism observed in patients with VS who present at older ages >60 years (80.7%), compared with those <20 years (21.7%).[8]

Pathogenic variants (PVs) in two additional genes are known to predispose to multiple schwannomas, *LZTR1* and *SMARCB1*,[12 13] although only *LZTR1*, and not *SMARCB1*, has been associated with VS development.[10 14] Biallelic loss of *NF2* is also observed in the tumours of patients with germline *LZTR1* and *SMARCB1* associated schwannomas,

To cite: Sadler KV, Bowers NL, Hartley C, *et al*. *J Med Genet* Epub ahead of print: [please include Day Month Year]. doi:10.1136/jmedgenet-2020-107022

leading to a four-hit/three-step multi-hit hypothesis of schwannoma tumourigenesis.[15 16] Loss of heterozygosity (LOH) on the long arm of chromosome 22 is a frequent second mutational hit within VS tumours, often encompassing the genes *NF2*, *SMARCB1* and *LZTR1*. It is estimated that LOH occurs in over half of all sVS tumours, with up to 14% of cases attributed to mitotic recombination (MR).[11] Frequent observation of *NF2* disruption in sVS tumours, in addition to higher estimated rates of NF2 mosaicism, gives reason to suspect a common pathway of VS tumourigenesis may exist through loss of *NF2* function.

In this article we review the molecular testing conducted in both germline and somatic samples obtained from patients with sVS. Through consideration of previous molecular studies, and with additional context of *LZTR1* and *SMARCB1* testing, we hope to gain greater insight into the spectrum of PVs observed in sVS. Delineating the relationships between *NF2*, *LZTR1* and *SMARCB1* and understanding their contributions to VS tumourigenesis may suggest new therapeutic approaches in the management of VS tumours.

MATERIALS AND METHODS

Patient samples

Patients were identified from a local register at the Manchester Centre for Genomic Medicine. The register contains demographic, clinical and genetic information from 505 individuals with features suggestive of possible NF2 or schwannomatosis disease, who did not fulfil clinical diagnosis for either disorder at initial presentation. The samples included within this analysis consisted of all patients within the database who initially presented with sVS, had no affected family members from a previous generation and had received germline *NF2* mutational analysis. A total of 394 patients were identified; 196 were male, 196 were female and 2 individuals of unknown sex.

Molecular analysis

All individuals underwent lymphocyte DNA analysis for *NF2*; further analysis of *LZTR1* and *SMARCB1* was conducted in subsets of patients negative for germline *NF2* variants. The number of patients within these subsets was smaller, a result of the more recent association between *LZTR1* and VS,[12] sample availability, and absence of routine *SMARCB1* testing due to reduced association with VS.[14] Request for further analysis in schwannomatosis-associated genes is left to a clinician's discretion. Within the cohort, 188 patients also received *NF2* molecular analysis on somatic DNA extracted from at least one tumour sample. Somatic mutational testing was subject to sample availability, as not all VS tumours are suitable for surgical resection and some DNA samples were of insufficient quality or quantity for analysis. Prior to 2013 Sanger sequencing was employed to analyse exon and intron/exon boundaries. Since 2013 next generation sequencing (NGS) on Illumina MiSeq has been used to sequence the exonic regions covered by Sanger with 1000× coverage, in addition to ~1000 bases of flanking intronic sequence per exon, resulting in increased variant detection. Identified sequence variants are confirmed via Sanger. Approximately 49% of germline samples analysed were sequenced prior to 2013. Multiple ligation-dependent probe amplification was used to detect CNVs. Microsatellite markers were used to detect loss of heterozygosity (LOH) events within tumour samples. Similar analysis of CNVs and LOH was conducted in the *LZTR1* and *SMARCB1* loci. Chromosome analysis confirmed ring chromosome 22 in one patient. Patients were considered to have mosaic NF2 when a PV was identified in lymphocyte DNA at a reduced level below 30% allele frequency, or where an identical *NF2* variant was identified in two anatomically distinct tumours.

Table 1 Germline pathogenic *NF2* variants identified in patients with sporadic vestibular schwannoma

Patient number	Age at presentation (years)	Variant	Variant type	Mosaic (fraction)
135	18	Ring chromosome 22	Structural	Yes (ND)
147	18	c.447+1G>A	Canonical splice site	Yes (ND)
168	23	Large deletion *NF2* promoter to exon 4	Large deletion	Yes (ND)
184	20	c.675+1G>A	Canonical splice site	Yes (2%)
189	29	c.655G>A; p.(Val219Met)	Missense	Yes (1.8%)
218	13	Whole gene deletion	Large deletion	No
298	22	c.892C>T; p.(Gln298*)	Nonsense	Yes (3%)
353	22	c.259_272del14; p.(Lys88Hisfs*11)	Frameshift	Yes (ND)

ND, exact percentage not determined.

RESULTS

The average age at which patients presented with VS was 30 years, ranging from 0.2 to 74 years. The average age of VS presentation in male and female patients was 29 and 30 years, respectively. Patients with unknown sex or age of VS presentation were not included within these averages.

Germline variants

Sequencing results of *NF2* were obtained from the germline samples of 394 patients; 233 individuals were <30 years. Variants causing disruption of *NF2* were identified in eight (2%) patients. One patient possessed a non-mosaic large deletion of *NF2*, and seven individuals had mosaic NF2 disease with differing variant types. The average age of VS presentation in patients with germline *NF2* variants was 21 years. A summary of these patients is given in table 1. Follow-up information was available from six individuals. In both patients 135 and 353, a solitary VS remained the only phenotypic feature at follow-up 4 years after initial presentation. Four of the mosaic individuals later presented with features of NF2. The average interval between initial sVS presentation and fulfilment of NF2 phenotypic criteria in these patients was 4 years, ranging from 1 to 10 years. No follow-up data were available from patients 218 and 298.

From the cohort of 394, two groups of patients were also screened for germline *LZTR1* variants. Group 1 included 75 individuals diagnosed with VS under 30 years, who received *LZTR1* testing subsequent to negative *NF2* screening. Patient age ranged from 0.2 to 24 years. Group 2 comprised 86 NF2-negative patients, over 30 years at VS diagnosis not previously offered *LZTR1* screening. Patient age ranged from 30 to 72 years. The two patient groups reflect testing practice consistent with current recommendations.[10 17] Figure 1 outlines the patient testing groups.

In group 1, 5 out of 75 (7%) patients were found to possess six *LZTR1* variants; two identified variants in one patient were classified as variants of unknown significance. The remaining variants were considered pathogenic and these four patients

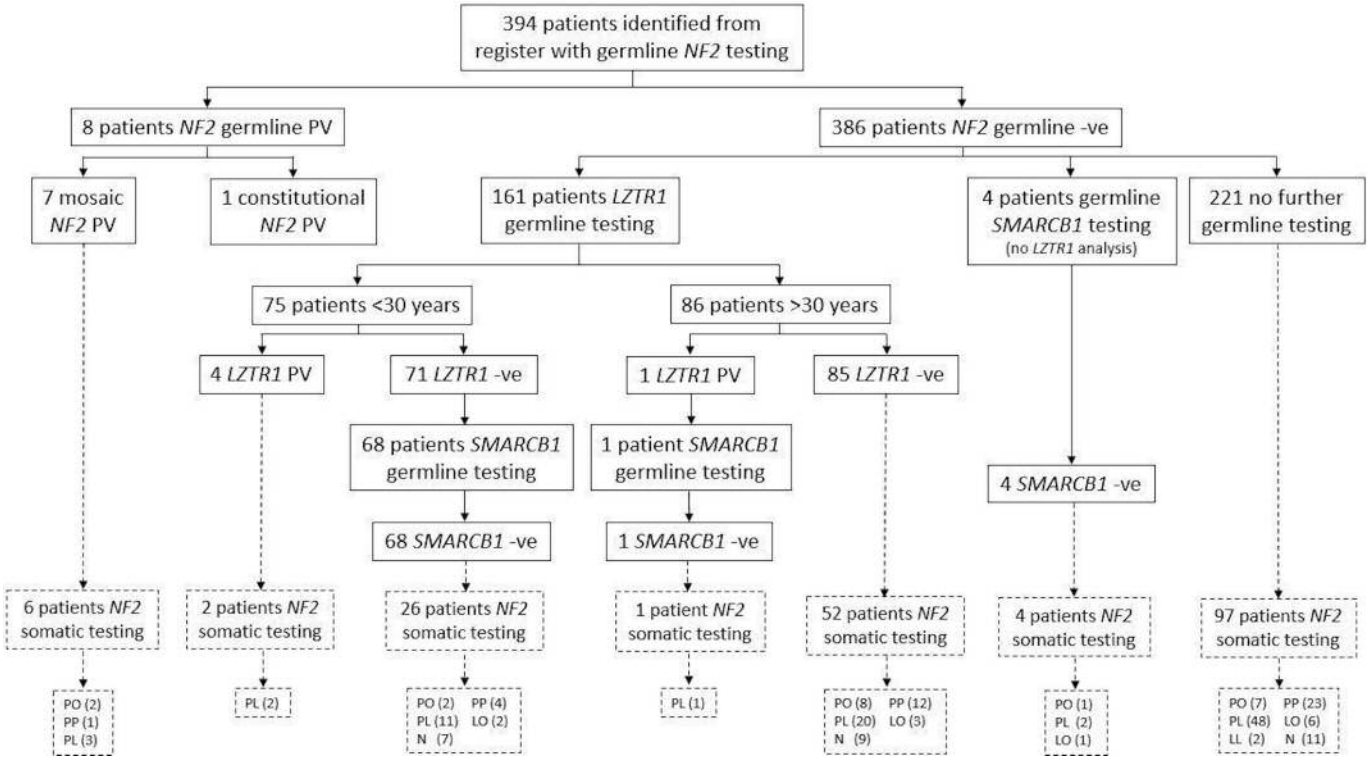

Figure 1 A total of 394 patients received germline *NF2* testing, with further subsets of patients receiving *LZTR1* and *SMARCB1* analysis. The number of patients in each testing group and their germline results are summarised in the solid line boxes within the flow diagram. Boxes with dashed outlines contain information on the 188 patients who received somatic molecular testing on at least one tumour sample. A variety of pathogenic mutational events combinations were detected. The number of individuals with each mutational combination is stated in brackets. The most common combination of events was a pathogenic single nucleotide variant with LOH of the *trans*-allele. LL, two LOH events detected; LO, one LOH event detected; LOH, loss of heterozygosity; N, no pathogenic variants identified; PL, point variant and LOH event detected; PO, one point variant identified in sample; PP, two point variants identified; PVs, pathogenic variants.

were subsequently diagnosed with *LZTR1*-associated schwannomatosis, totalling 5% of the <30 years *LZTR1* tested cohort.

Screening in group 2 identified one individual (1%) aged 34 at diagnosis, with a single PV in *LZTR1*. Table 2 provides an overview of *LZTR1* PVs, age at VS presentation and patient screening group.

Age at VS symptomatic presentation was known for four of the patients with germline *LZTR1* PVs, with an average of 22 years. Age at presentation was unknown in patient 350; however, confirmation of VS diagnosis occurred at age 22. In all of these patients the PV was non-mosaic.

Seventy-three (19%) patients received germline *SMARCB1* testing; no PVs in *SMARCB1* were identified. From the total cohort of 394, no pathogenic germline variants were identified in 380 (96%) patients.

Somatic tumour variants

Out of the 394 patients with germline *NF2* testing, 188 (48%) also received molecular analysis of *NF2* in at least one tumour sample. From the eight patients with identifiable germline *NF2* variants, six underwent tumour analysis. In two of these tumour samples, LOH was found to be the second pathogenic hit on the *trans*-allele. In the patient with ring chromosome 22, a pathogenic single nucleotide variant disrupting a splice site was identified as a second *NF2* hit. In patient 189, a nonsense variant causing a premature stop codon was identified. The remaining two patients did not have identifiable second mutational events. Table 3 provides a summary of the NF2-affected patients' tumour analysis.

Two of the five patients who possessed germline pathogenic *LZTR1* variants underwent tumour analysis. In both patients' tumour samples, two mutational events affecting *NF2* were identified. The *NF2* PVs comprised a single nucleotide base change, not present in blood, and LOH of the region on the *trans*-allele.

When considering all analysed tumours (188), 101 (54%) patients had identifiable LOH events, 76 (40%) had no identified LOH, and 11 (6%) patients remained with equivocal LOH involvement. Out of the individuals with LOH in their tumours,

Table 2 Germline pathogenic *LZTR1* variants identified in patients with sporadic vestibular schwannoma

Patient number	Age at presentation (years)	Variant	Variant type	*LZTR1* screening group
82	24	c.772delT; p.(Phe258Leufs*93)	Frameshift	1
227	17	c.628C>T; p.(Arg210*)	Nonsense	1
238	13	c.352dup; p.(Arg118Profs*28)	Frameshift	1
350	<22	Whole gene deletion	Large deletion	1
133	34	c.1799delA; p.(Asn600Thrfs*4)	Frameshift	2

Table 3 Pathogenic somatic variants identified in tumours from patients with germline *NF2* variants

Patient number	Germline pathogenic *NF2* variants	Second pathogenic *NF2* hit identified in tumour	Mitotic recombination
135	Ring chromosome 22	c.1122+2T>A	No
147	c.447+1G>A	LOH	Yes
184	c.675+1G>A	Not identified	No
189	c.655G>A; p.(Val219Met)	c.169C>T; p.(Arg57*)	No
298	c.892C>T; p.(Gln298*)	Not identified	No
353	c.259_272del14; p.(Lys88Hisfs*11)	LOH	No

LOH, loss of heterozygosity.

73 were tested for MR, from which 12 (16%) were found to possess an MR event. At least one PV involving the *NF2* locus was identified in 161 (86%) patient tumours; this includes LOH. Moreover, 129 (69%) patients were found to have two in-trans *NF2* PVs within a single tumour. In 69% (89) of patients with an identifiable second PV, loss of *NF2* was a result of LOH. In total, 27 (14%) patients had no *NF2* PVs identified within their tumour samples. The proportions of mutational event combinations, as well as variant types identified in tumour samples, are highlighted in figures 1 and 2.

Three patients received molecular testing on two or more anatomically distinct tumours (table 4). The subsequent tumours occurred years after the first apparent sVS, so these events were uncommon. In patient 96 LOH of the *NF2* locus was identified in both the sVS tumour sample and a subsequent meningioma; microsatellite markers suggested the same allele was lost in both tumours. Two PVs affecting *NF2* were identified in the VS sample of patient 141, yet no identifiable PVs in *NF2* were found in either the plexiform tumour or spinal schwannoma later obtained from the patient. In patient 189, the same pathogenic missense variant was identified in the initial sVS sample and a subsequent meningioma, confirming mosaic NF2. A second PV hit was identified in the VS sample, but no further PVs were identified in the second tumour.

DISCUSSION

The cohort used for our summary of molecular testing in patients with sVS is an overlapping and updated data set of that used by Evans *et al*[3] in 2005. In comparison with the report on the initial cohort, the average age at VS incidence has lowered from 54 to 30 years. The decrease in incidence age is due to bias within the local patient register, attributable to updated genetic testing recommendations for patients diagnosed with VS <30 years of age.[17] This recommendation is supported by literature suggesting that patients presenting at younger ages are more likely to have predisposing PVs identified.[10] These findings, combined with a greater awareness of VS tumours and their associated familial risks, have likely accompanied a drive to refer patients for genetic testing earlier in their care management. This bias is highlighted by the wider Manchester Skull Base database that contains 1410 patients with sVS, in whom the average age is 53 years. It may seem unexpected to have identified germline pathogenic *NF2* variants in an sVS cohort, especially the individual with a non-mosaic constitutional PV. However, the individuals included within this review did not fulfil the NF2 criteria at the point of referral. The patients with identified germline *NF2* variants developed VS at a younger average age (21 years), with the non-mosaic individual presenting at just 13 years, indicative of a tumour predisposition disorder. Identification of germline NF2 mosaicism in patients 184, 189 and 298 was aided through prior tumour analysis, as lymphocyte pathogenic allele fractions were extremely low at 2%, 1.8% and 3%, respectively (table 1). Follow-up information was available from six of the

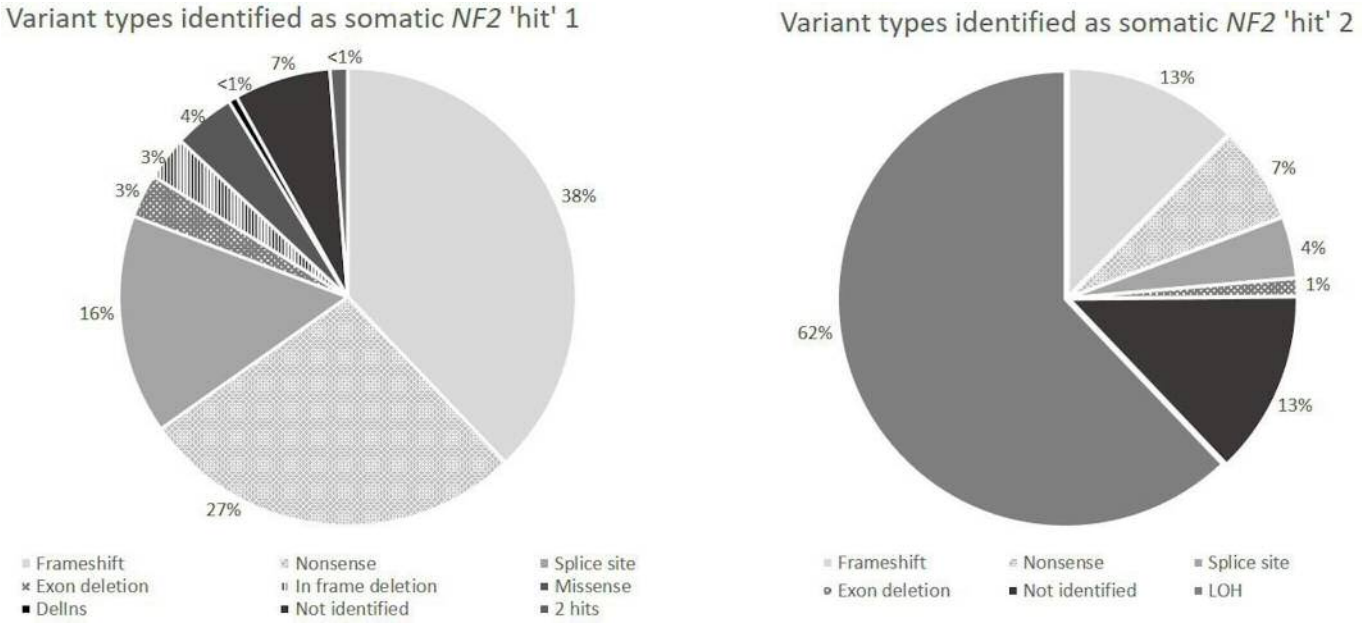

Figure 2 At least one pathogenic *NF2* variant was identified in somatic tumour samples from 161 patients. The proportions of variant types identified within their samples as either a presumed first, or second, pathogenic hit disrupting *NF2* are depicted in the figure. Frameshift variants were the most common pathogenic point variant types found for both first and second *NF2* hits. LOH events affecting the *NF2* locus were by far the most common variant type identified as a second, or likely second, pathogenic hit in tumour samples. Patients with no identified first pathogenic hit will have had LOH detected as a presumed second hit. Two *NF2* pathogenic variants, in addition to an LOH event, were identified in two patients, noted as 'two hits'. LOH, loss of heterozygosity.

Table 4 Pathogenic *NF2* variants identified in tumour DNA from patients with two or more anatomically distinct tumours

Patient number	First tumour, *NF2* variant 1	First tumour, *NF2* variant 2	Second tumour, *NF2* variant 1	Second tumour, *NF2* variant 2	Third tumour, *NF2* variants
96	–	LOH	–	LOH	N/A
141	c.1574+1G>A	LOH	–	–	–
189	c.655G>A; p.(Val219Met)	c.169C>T; p.(Arg57*)	c.655G>A; p.(Val219Met)	–	N/A

'–' indicates no identified variant.
LOH, loss of heterozygosity; N/A, not applicable.

eight patients with germline NF2. In both patients 135 and 353, a solitary VS remained the only phenotypic feature at follow-up 4 years after initial presentation; therefore, clinical diagnostic criteria of NF2 would not have been met without results from genetic testing. Four of the mosaic individuals later presented with features of NF2, such as bilateral VS and multiple meningioma, consistent with clinical diagnosis. In these patients the interval of time between initial sVS presentation and fulfilment of clinical NF2 criteria was wide-ranging, from 1 to 10 years. This is likely attributable to the variable presentation of mosaic NF2 disease. No follow-up data were available from patients 218 and 298; as patient 218 possesses a constitutional *NF2* PV, it would be expected that this individual would develop subsequent features of NF2.

Overall, 3% of all patients who received *LZTR1* testing were found to possess a germline PV, with a higher rate of 5% in patients <30 years. In comparison, only 2% of all patients and 3% of patients <30 years tested for NF2 had an identifiable PV. This demonstrates that *LZTR1*-associated schwannomatosis can account for some of the apparently sVS population, and suggests that a subset of patients with sVS who have not had germline *LZTR1* testing may have undiagnosed schwannomatosis. This finding supports our previous suggestions that *LZTR1* molecular analysis should be considered in individuals with a unilateral VS (UVS) in the absence of other NF2 features when diagnosed at a young age.[18] These suggestions were based on observations in patients with UVS presenting with at least one other schwannoma, where a similar proportion of patients (5%) with germline *LZTR1* PVs were identified, reflecting the risk of further tumour development in patients with sVS with germline *LZTR1* PVs. In the current study, *LZTR1* analysis of patients with sVS >30 years, screening group 2, suggests a lower rate of schwannomatosis detection and subsequently reduced benefits of *LZTR1* screening in this older group. However, the diagnosis of *LZTR1*-associated schwannomatosis in patient 133, presenting at age 34, may warrant consideration of *LZTR1* screening in patients over 30 years. The average age at VS presentation for patients with germline pathogenic *LZTR1* variants was 22 years, comparable with the patients found to have NF2. This observation may provide better testing suggestions in young patients presenting with sVS.

No patients with sVS were found to harbour an *SMARCB1* variant. This is consistent with previous observations.[19 20] Additionally, 96% of the cohort did not possess an identifiable germline PV, supporting existing literature that suggests patients with sVS have a low rate of association with germline predisposing variants.[10] However, risk of potential NF2 still exists within this patient group, especially at lower presentation ages. It is recommended that patients with sVS <30 years with negative germline NF2 testing receive follow-up cranial MRI at 5, 10 and 20 years after assessment. Patients can be subsequently discharged if no further features of NF2 develop.[17]

In analysis of tumours from the patients, at least one *NF2* PV was identified in 86% of samples; in 69% of the cohort two *NF2* PVs were identified. The rate of *NF2* gene disruption observed within this cohort is higher than reported in similar studies[11]; this may be attributable to improvements in sequencing technology detection rates over the past decade.[21] LOH of the region encompassing *NF2* was found to have occurred in 54% of analysed tumours, reflective of frequencies published in 2010 by Hadfield *et al*,[11] where 56% of analysed tumours displayed LOH. Likewise, the 16% frequency of MR events within our sVS cohort is similar (14%). One of the patients with a germline *NF2* PV, patient 147, had an MR event identified within their tumour sample (table 3). No MR events were detected in patients with germline *LZTR1* PVs. This could suggest an alternative mechanism of LOH within these individuals. A similar phenomenon has been suggested in patients with *SMARCB1*-associated schwannomatosis.[11] However, the small size of this cohort means any conclusions drawn from the data are limited.

Mutational event combinations and the types of variants identified as disrupting *NF2* have also been summarised for patient tumour testing. For the majority of patients (46%) who received molecular analysis on a tumour sample, both a pathogenic point variant and LOH event were identified. This was similar across all patient testing groups, summarised in figure 1. While frameshift variants were the most common point variant types found for both first and second presumed *NF2* hits (figure 2), LOH events affecting the *NF2* locus were by far the most common variant type identified as a second, or likely second, pathogenic hit in tumour samples. LOH of the *trans*-allele is a common phenomenon for tumour predisposition associated genes, and LOH of the *NF2* locus is frequently observed in VS tumours.[11] By summarising the types of identified somatic *NF2* PVs in figure 2, it becomes apparent that missense variants make up a small fraction (4%) of PVs observed in VS samples. Two *NF2* PVs, in addition to an LOH event, were identified in single tumour samples from two patients. It is likely that the two point variants exist in '*cis*' on the same allele and that LOH on the *trans*-allele is a second pathogenic hit. It is also possible that detection of the three PVs is due to sampling of a multifocal tumour.

Both of the individuals with germline *LZTR1* PVs who received tumour DNA testing were also found to have two *NF2* PVs within their tumour samples, consisting of a point variant and LOH. This discovery is supportive of the multi-hit hypothesis proposed as a mechanism of schwannoma tumourigenesis,[15 16 22] and suggests that loss of a second copy of *NF2* is a frequent event in VS that may form a common pathway in the development of all VS tumours.[23] Further work is needed to delineate the role of *NF2* loss of function in VS tumour development, and in understanding how germline *LZTR1* PVs may predispose to somatic *NF2* loss. A possibility is that a variant germline *LZTR1* allele has reduced tumour suppressor activity. If LOH of chromosome 22q occurs, some degree of increased Schwann cell proliferation

may take place, in turn increasing the likelihood of a somatic mutational event occurring in the remaining *NF2* allele. This is similar to the mechanism of *SMARCB1*-associated VS tumourigenesis suggested by Hadfield *et al*.[11]

A small proportion of patients (14%) had no identifiable pathogenic *NF2* variants in tumour analysis. However, failure to detect *NF2* variants in VS tumours does not necessarily mean that no pathogenic *NF2* variants are present. There is reason to suspect that some variants remain undetected within tumour samples, due to low fractions of tumour cells in comparison with inflammatory cell infiltrates. In a study by Lewis *et al*,[24] inflammatory macrophage cells were found to be the predominant cell type within growing VS samples, rather than tumour cells. During tumour sample analysis DNA from inflammatory cells is also sequenced, reducing the fraction of the total DNA obtained from tumour cells and therefore reducing variant detection rates. These findings suggest an explanation for the variable rates of variant detection in tumours across studies,[24–26] and allude to the possibility of more *NF2*-driven VS tumours not yet detected due to macrophage contamination. If possible, it may prove valuable to investigate the growth status of the tumours from the 27 patients without identifiable somatic pathogenic *NF2* variants, as poorer variant detection rates would be expected in tumours deemed to be growing rather than static.[24]

Three patients received molecular analysis on two anatomically distinct tumours (table 4). Only LOH of one allele was detected in each of the two somatic samples from patient 96, who first presented with VS at age 20 years and a meningioma at age 41. PVs in *NF2* are frequently observed in meningioma tumours.[27] The young age of the patient and the development of two anatomically distinct tumours are suggestive of a tumour predisposition disorder. Failure to detect a germline variant, or two pathogenic hits within the patient tumour samples, suggests the existence of undetected mosaic variants (<10% allele fraction), or of more complex variants affecting the *NF2* locus that require alternative detection methods.[8] In patient 141, two PVs affecting *NF2* were identified within the initial VS tumour analysed, yet no variants were identified in the two subsequent tumour samples obtained from a plexiform and spinal schwannoma. As only a small proportion of schwannomas possess no identifiable pathogenic *NF2* variants, it is suggestive that the absence of detectable variants within the secondary samples may be due to technical complications, such as tumour contamination with macrophages, rather than no existing variants. The same pathogenic missense variant was identified in both somatic samples obtained from patient 189, confirming mosaic NF2. While a second PV was identified in the initial sVS sample that developed at age 29, no further PVs were found in the subsequent meningioma. This patient went on to develop a contralateral VS almost 10 years after the first, at 38 years.

A limitation of this review is that not all patients received molecular analysis of *LZTR1* and *SMARCB1*, for the reasons outlined in the Materials and methods section. Screening of *NF2* PV-negative patients for variants in both these genes may identify more cases of schwannomatosis, with an estimated detection rate of 3%. Second, the molecular testing conducted in the cohort took place over a number of years and consequently occurred on different sequencing platforms with varying detection rates, with almost half of germline samples tested prior to NGS implementation in 2013. Current NGS platforms do not cover all intronic and promoter regions, and therefore incidence of NF2 may have been underestimated due to undetectable variants or extremely low allele fractions in mosaic cases. Moreover, somatic mutational analysis was conducted in 48% of the cohort, subject to sample availability. It is possible this non-uniform sampling may have introduced bias towards genetic testing of aggressive tumours more likely to be resected. Nonetheless, this molecular testing summary provides insight into the prevalence of schwannomatosis in apparently sVS patients, and suggests the existence of a common pathway of VS tumourigenesis through loss of *NF2* function that requires further delineation.

Author affiliations
[1]Manchester Centre for Genomic Medicine, The University of Manchester, Manchester, UK
[2]Genetic Medicine, University of Manchester, Manchester, UK
[3]Genetic Medicine, Regional Genetic Laboratories, Manchester, UK
[4]Centre for Genomic Medicine, Manchester University NHS Foundation Trust, Manchester, UK
[5]Manchester University NHS Foundation Trust, Manchester, UK
[6]Neurosurgery, Salford Royal Hospital, Manchester, UK
[7]Department of Otolaryngology, Manchester Royal Infirmary, Manchester, UK
[8]Department of Neurosurgery, Salford Royal NHS Foundation Trust, Salford, UK
[9]ENT, Manchester Royal infirmary, Manchester, UK
[10]Clinical Genetics, East Anglian Medical Genetics Service, Cambridge, UK
[11]Department of Genetics, Guy's and St Thomas' NHS Foundation Trust, London, UK
[12]Oxford Centre for Genetic Medicine, Oxford University Hospitals NHS Foundation Trust, Oxford, UK
[13]Neurosciences, NF2 Unit, Oxford, UK
[14]Clinical Genetics, Manchester University NHS Foundation Trust, Manchester, UK

Contributors DGE designed the study. Patient data were compiled and analysed by KVS, DGE and MJS. Molecular testing was carried out by KVS, MJS, NLB, ST, CH, AJW and PTS. All other authors contributed data or individuals to the study. All authors reviewed the manuscript and approved the final version.

Funding We would like to acknowledge the NHS England funded highly specialised NF2 service. DGE is an NIHR Senior Investigator. This research was supported by the Manchester NIHR Biomedical Research Centre (IS-BRC1215-20007).

Competing interests None declared.

Patient consent for publication Not required.

Ethics approval Ethical approval for use of anonymised samples from the Manchester Centre for Genomic Medicine archive was obtained from the North West-Greater Manchester Central Research Ethics Committee (reference 10/H1008/74).

Provenance and peer review Not commissioned; externally peer reviewed.

Data availability statement All data relevant to the study are included in the article or uploaded as supplementary information. Anonymised data from the study are available on request.

ORCID iDs
Katherine V Sadler http://orcid.org/0000-0002-5693-4932
Amy Taylor http://orcid.org/0000-0001-9811-330X
Miriam Jane Smith http://orcid.org/0000-0002-3184-0817
D Gareth Evans http://orcid.org/0000-0002-8482-5784

REFERENCES

1 Stivaros SM, Stemmer-Rachamimov AO, Alston R, Plotkin SR, Nadol JB, Quesnel A, O'Malley J, Whitfield GA, McCabe MG, Freeman SR, Lloyd SK, Wright NB, Kilday J-P, Kamaly-Asl ID, Mills SJ, Rutherford SA, King AT, Evans DG. Multiple synchronous sites of origin of vestibular schwannomas in neurofibromatosis type 2. *J Med Genet* 2015;52:557–62.
2 Kentala E, Pyykkö I. Clinical picture of vestibular schwannoma. *Auris Nasus Larynx* 2001;28:15–22.
3 Evans DGR, Moran A, King A, Saeed S, Gurusinghe N, Ramsden R. Incidence of vestibular schwannoma and neurofibromatosis 2 in the North West of England over a 10-year period: higher incidence than previously thought. *Otol Neurotol* 2005;26:93–7.
4 Ostrom QT, Gittleman H, Liao P, Vecchione-Koval T, Wolinsky Y, Kruchko C, Barnholtz-Sloan JS. CBTRUS statistical report: primary brain and other central nervous system tumors diagnosed in the United States in 2010-2014. *Neuro Oncol* 2017;19:v1–88.
5 Kshettry VR, Hsieh JK, Ostrom QT, Kruchko C, Barnholtz-Sloan JS. Incidence of vestibular schwannomas in the United States. *J Neurooncol* 2015;124:223–8.
6 Kleijwegt M, Ho V, Visser O, Godefroy W, van der Mey A. Real incidence of vestibular schwannoma? estimations from a national registry. *Otol Neurotol* 2016;37:1411–7.
7 Evans DG, Wallace AJ, Hartley C, Freeman SR, Lloyd SK, Thomas O, Axon P, Hammerbeck-Ward CL, Pathmanaban O, Rutherford SA, Kellett M, Laitt R, King AT,

Bischetsrieder J, Blakeley J, Smith MJ. Familial unilateral vestibular schwannoma is rarely caused by inherited variants in the NF2 gene. *Laryngoscope* 2019;129:967–73.
8 Evans DG, Hartley CL, Smith PT, King AT, Bowers NL, Tobi S, Wallace AJ, Perry M, Anup R, Lloyd SKW, Rutherford SA, Hammerbeck-Ward C, Pathmanaban ON, Stapleton E, Freeman SR, Kellett M, Halliday D, Parry A, Gair JJ, Axon P, Laitt R, Thomas O, Afridi SK, Obholzer R, Duff C, Stivaros SM, Vassallo G, Harkness EF, Smith MJ, English Specialist NF research group. Incidence of mosaicism in 1055 de novo NF2 cases: much higher than previous estimates with high utility of next-generation sequencing. *Genet Med* 2020;22.
9 Carlson ML, Smadbeck JB, Link MJ, Klee EW, Vasmatzis G, Schimmenti LA. Next generation sequencing of sporadic vestibular schwannoma: necessity of biallelic NF2 inactivation and implications of accessory Non-NF2 variants. *Otol Neurotol* 2018;39:e860–71.
10 Pathmanaban ON, Sadler KV, Kamaly-Asl ID, King AT, Rutherford SA, Hammerbeck-Ward C, McCabe MG, Kilday J-P, Beetz C, Poplawski NK, Evans DG, Smith MJ. Association of genetic predisposition with solitary schwannoma or meningioma in children and young adults. *JAMA Neurol* 2017;74:1123–9.
11 Hadfield KD, Smith MJ, Urquhart JE, Wallace AJ, Bowers NL, King AT, Rutherford SA, Trump D, Newman WG, Evans DG. Rates of loss of heterozygosity and mitotic recombination in NF2 schwannomas, sporadic vestibular schwannomas and schwannomatosis schwannomas. *Oncogene* 2010;29:6216–21.
12 Piotrowski A, Xie J, Liu YF, Poplawski AB, Gomes AR, Madanecki P, Fu C, Crowley MR, Crossman DK, Armstrong L, Babovic-Vuksanovic D, Bergner A, Blakeley JO, Blumenthal AL, Daniels MS, Feit H, Gardner K, Hurst S, Kobelka C, Lee C, Nagy R, Rauen KA, Slopis JM, Suwannarat P, Westman JA, Zanko A, Korf BR, Messiaen LM. Germline loss-of-function mutations in LZTR1 predispose to an inherited disorder of multiple schwannomas. *Nat Genet* 2014;46:182–7.
13 Hulsebos TJM, Plomp AS, Wolterman RA, Robanus-Maandag EC, Baas F, Wesseling P. Germline mutation of INI1/SMARCB1 in familial schwannomatosis. *Am J Hum Genet* 2007;80:805–10.
14 Smith MJ, Bowers NL, Bulman M, Gokhale C, Wallace AJ, King AT, Lloyd SKL, Rutherford SA, Hammerbeck-Ward CL, Freeman SR, Evans DG. Revisiting neurofibromatosis type 2 diagnostic criteria to exclude LZTR1-related schwannomatosis. *Neurology* 2017;88:87–92.
15 Sestini R, Bacci C, Provenzano A, Genuardi M, Papi L. Evidence of a four-hit mechanism involving SMARCB1 and NF2 in schwannomatosis-associated schwannomas. *Hum Mutat* 2008;29:227–31.
16 Hadfield KD, Newman WG, Bowers NL, Wallace A, Bolger C, Colley A, McCann E, Trump D, Prescott T, Evans DGR. Molecular characterisation of SMARCB1 and NF2 in familial and sporadic schwannomatosis. *J Med Genet* 2008;45:332–9.
17 Evans DG, Raymond FL, Barwell JG, Halliday D. Genetic testing and screening of individuals at risk of NF2. *Clin Genet* 2012;82:416–24.
18 Smith MJ, Isidor B, Beetz C, Williams SG, Bhaskar SS, Richer W, O'Sullivan J, Anderson B, Daly SB, Urquhart JE, Fryer A, Rustad CF, Mills SJ, Samii A, du Plessis D, Halliday D, Barbarot S, Bourdeaut F, Newman WG, Evans DG. Mutations in LZTR1 add to the complex heterogeneity of schwannomatosis. *Neurology* 2015;84:141–7.
19 Smith MJ, Wallace AJ, Bowers NL, Eaton H, Evans DGR. SMARCB1 mutations in schwannomatosis and genotype correlations with rhabdoid tumors. *Cancer Genet* 2014;207:373–8.
20 Evans DG, Bowers NL, Tobi S, Hartley C, Wallace AJ, King AT, Lloyd SKW, Rutherford SA, Hammerbeck-Ward C, Pathmanaban ON, Freeman SR, Ealing J, Kellett M, Laitt R, Thomas O, Halliday D, Ferner R, Taylor A, Duff C, Harkness EF, Smith MJ. Schwannomatosis: a genetic and epidemiological study. *J Neurol Neurosurg Psychiatry* 2018;89:1215–9.
21 Contini E, Paganini I, Sestini R, Candita L, Capone GL, Barbetti L, Falconi S, Frusconi S, Giotti I, Giuliani C, Torricelli F, Benelli M, Papi L. A systematic assessment of accuracy in detecting somatic mosaic variants by deep amplicon sequencing: application to NF2 gene. *PLoS One* 2015;10:e0129099.
22 Kehrer-Sawatzki H, Kluwe L, Friedrich RE, Summerer A, Schäfer E, Wahlländer U, Matthies C, Gugel I, Farschtschi S, Hagel C, Cooper DN, Mautner V-F. Phenotypic and genotypic overlap between mosaic NF2 and schwannomatosis in patients with multiple non-intradermal schwannomas. *Hum Genet* 2018;137:543–52.
23 de Vries M, van der Mey AGL, Hogendoorn PCW. Tumor biology of vestibular schwannoma: a review of experimental data on the determinants of tumor genesis and growth characteristics. *Otol Neurotol* 2015;36:1128–36.
24 Lewis D, Roncaroli F, Agushi E, Mosses D, Williams R, Li K-loh, Zhu X, Hinz R, Atkinson R, Wadeson A, Hulme S, Mayers H, Stapleton E, Lloyd SKL, Freeman SR, Rutherford SA, Hammerbeck-Ward C, Evans DG, Pathmanaban O, Jackson A, King AT, Coope DJ. Inflammation and vascular permeability correlate with growth in sporadic vestibular schwannoma. *Neuro Oncol* 2019;21:314–25.
25 de Vries M, Hogendoorn PCW, Briaire-de Bruyn I, Malessy MJA, van der Mey AGL. Intratumoral hemorrhage, vessel density, and the inflammatory reaction contribute to volume increase of sporadic vestibular schwannomas. *Virchows Arch* 2012;460:629–36.
26 de Vries M, Briaire-de Bruijn I, Malessy MJA, de Bruïne SFT, van der Mey AGL, Hogendoorn PCW. Tumor-Associated macrophages are related to volumetric growth of vestibular schwannomas. *Otol Neurotol* 2013;34:347–52.
27 Dumanski JP, Rouleau GA, Nordenskjöld M, Collins VP. Molecular genetic analysis of chromosome 22 in 81 cases of meningioma. *Cancer Res* 1990;50:5863–7.

4. Re-evaluation of missense variant classifications in *NF2*

Re-evaluation of Missense Variant Classifications in *NF2*

Katherine V. Sadler[1,2], Charlie F. Rowlands[1,2], Philip T. Smith[1], Claire L. Hartley[1], Naomi L. Bowers[1], Nicola Y. Roberts[1], Jade L. Harris[1], Andrew J. Wallace[1], D. Gareth Evans[1,2], Ludwine M. Messiaen[3], and Miriam J. Smith[1,2].

1. Manchester Centre for Genomic Medicine, St Mary's Hospital, Manchester Academic Health Sciences Centre (MAHSC), Manchester, UK
2. Division of Evolution, Infection and Genomics, School of Biological Sciences, Faculty of Biology, Medicine and Health, University of Manchester, Manchester, UK
3. Department of Genetics, University of Alabama at Birmingham, Birmingham, AL, USA

4.1. Abstract

Missense variants in the *NF2* gene result in variable NF2 disease presentation. Clinical classification of missense variants often represents a challenge, due to lack of evidence for pathogenicity and function. This study provides a summary of *NF2* missense variants, with variant classifications based on currently available evidence. *NF2* missense variants were collated from pathology-associated databases and existing literature. Association for Clinical Genomic Sciences Best Practice Guidelines (2020) were followed in the application of evidence for variant interpretation and classification. The majority of *NF2* missense variants remain classified as variants of uncertain significance. However, *NF2* missense variants identified in gnomAD occurred at a consistent rate across the gene, while variants compiled from pathology-associated databases displayed differing rates of variation by exon of *NF2*. The highest rate of NF2 disease-associated variants was observed in exon 7, whilst lower rates were observed towards the C-terminus of the *NF2* protein, merlin. Further phenotypic information associated with variants, alongside variant-specific functional analysis, is necessary for more definitive variant interpretation. Our data identified differences in frequency of *NF2* missense variants by exon between gnomAD population data and NF2 disease-associated variants, suggesting a potential genotype-phenotype correlation; further work is necessary to substantiate this.

4.2. Introduction

Neurofibromatosis type 2 (NF2; MIM# 101000) is an autosomal dominant tumour predisposition condition, resulting from disruption of the *NF2* gene. Located on chromosome 22q12, *NF2* encodes the active tumour suppressor protein merlin [1]. NF2 predisposes individuals to schwannoma development, with bilateral vestibular schwannomas (VS) being a characteristic feature (Evans et al., 1992). NF2 patients frequently experience hearing loss and tinnitus as a result of VS growth; patients may also develop neuropathies, cutaneous features, cataracts, and schwannomas on other nerves, as well as meningiomas and ependymomas [2]. NF2 birth incidence has been recently estimated as 1 in 28,000 [3].

The majority of pathogenic variants identified in *NF2* result in truncation of the protein product, often causing loss of protein expression or creating non-

functional proteins [4]. Genotype-phenotype correlations have been observed in NF2, where protein truncating variants, such as frameshift or nonsense, result in more severe disease presentation than missense variants [5,6]. In cases where truncating variants result in a severe phenotype, a dominant negative action of the variant protein has been proposed [7]. Variants in regulatory elements, such as splice sites and larger structural variants e.g. ring chromosome 22, often result in variable disease presentation [4]. Still, splice site variants positioned earlier in the *NF2* transcript have been associated with more severe disease presentation [8,9]. Investigation of missense variant genotype-phenotype correlations presents a unique challenge, as function of an amino acid residue is not necessarily related to its position within a transcript, but rather its location within protein tertiary structures [10].

Missense variants often represent clinical dilemmas for diagnostic services due to challenges of obtaining evidence for pathogenicity and function. Diagnostic classification of missense variants largely relies upon population frequency data and *in silico* predictive tools, as well as familial and functional data when available. Release of the ACMG-AMP (American College of Medical Genetics and Genomics and the Association for Molecular Pathology) guidelines for variant interpretation[11] enabled more reproducible interpretation of variants by providing an evidence framework, facilitating more consistent clinical reporting. Subsequent revision of these guidelines has followed and the ACGS (Association for Clinical Genomic Sciences) Best Practice Guidelines for Variant Classification in Rare Disease 2020 is the framework now currently employed by the National Health Service (NHS) within the UK (ACGS best practice guidelines, 2020 https://www.acgs.uk.com/quality/best-practice-guidelines/#VariantGuidelines. Accessed 23 August 2021). The ACGS 2020 guidelines combine the detailed guidance of Richards *et al.* (2015), with clarifications and developments proposed by other research groups [12]. Key developments in the ACGS (2020) guidelines from the ACMG-AMP include: defining variant-specific, rather than gene-specific, effects from functional studies, resolving scoring inconsistencies from combining evidence criteria, and the sub-division of pathogenic, likely pathogenic and variant of uncertain significance (VUS) classifications. Further disease-specific guidelines are currently in development through ClinGen and other curation networks, which

incorporate additional disease-associated features into variant classification; for example, loss of heterozygosity (LOH) and retention of a missense variant in a tumour would be informative for *NF2* variant classification. Recently proposed improvements in NF2 genetic severity scores suggest incorporation of merlin functional assays conducted in patient fibroblasts [13], this evidence would be similarly valuable for *NF2* variant classification.

Whilst missense variants only account for ~9% of diagnosed NF2 cases [14], they represent >25% of observed *NF2* variants in gnomAD. This disparity may be attributed to tolerability of the NF2 protein to missense variation, but might also suggest reduced phenotype severity and disease penetrance in individuals who possess missense variants. This suggestion is supported by observed phenotypic variation in familial cases of NF2, such as the c.1604T>C p.(Leu535Pro) missense variant [14]. The p.(Leu535Pro) variant has been found to segregate with disease in an extended NF2 family, where all affected individuals presented with VS at ages ranging between 16 to 80 years. A small number of this family developed other tumour types, namely meningiomas and an ependymoma. Meningiomas are often considered a mark of severity in NF2 disease and are employed as prognostic features for genomic counselling [15]; this inconsistent presentation of disease severity within one family epitomises the challenge of defining the effect and function of such missense variants.

The aim of this study was to re-evaluate and classify a comprehensive list of *NF2* missense variants from pathology-associated databases, with further focus on variants identified in association with features of NF2 disease. Variants were classified according to ACGS 2020 guidelines, collating clinical and functional information where available; the intention being to provide a robust summary of current evidence that supports or refutes pathogenicity of these variants.

4.3. Materials and methods

4.3.1. Systematic compilation of missense variants

Compilation of known *NF2* missense variants from human disease databases was conducted systematically, primarily by clinical and public database searches, followed by literature searches for published variants. Clinical database information was obtained from NF2 registries located in the

Manchester Centre for Genomic Medicine, St. Mary's Hospital, Manchester, England, UK and The University of Alabama at Birmingham, AL, USA. The publically accessible variant databases included were Leiden Open Variation Database (LOVD) (www.lovd.nl) [16], ClinVar NCBI (www.ncbi.nlm.nih.gov/clinvar) [17], the Human Gene Mutation Database (HGMD) (www.hgmd.cf.ac.uk/ac/all.php) [18], Clinical Interpretation of Variants in Cancer (CIViC) (https://civicdb.org/home) and Mastermind Genomic Search Engine (https://www.genomenon.com/mastermind). Details of duplicate variants were merged to retain relevant clinical information. A literature search was conducted through PubMed using combinations of the following MeSH terms: missense mutation, *NF2* gene, *NF2* gene product, DNA mutational analysis, central NF2/neurofibromatosis. A total of 124 unique publications were searched for novel variants. Figure 4 shows a flow chart detailing the order of variant compilation and numbers of variants included and excluded at each step. An extra literature mining step was conducted using LitVar to capture any missing variants [19]. A total of 395 unique variants were included within the study.

A subset of variants identified in patients with a confirmed Manchester Criteria NF2 diagnosis (Supp. Table 1) or known NF2-associated features, e.g. unilateral VS, meningioma, ependymoma, were grouped for further analysis. A total of 97 NF2 disease-associated variants were included, 69 of these variants appear in public databases, 17 were identifiable in the literature, the remaning 11 were exclusive to local databases and are now in submission to public variant databases (Figure 4).

Variants outside the exonic regions of the primary *NF2* transcript RefSeq NM_000268.4 (isoform 1) were excluded from analysis, as well as variants described as nonsense, frameshifts, insertions, deletions, indels and synonymous.

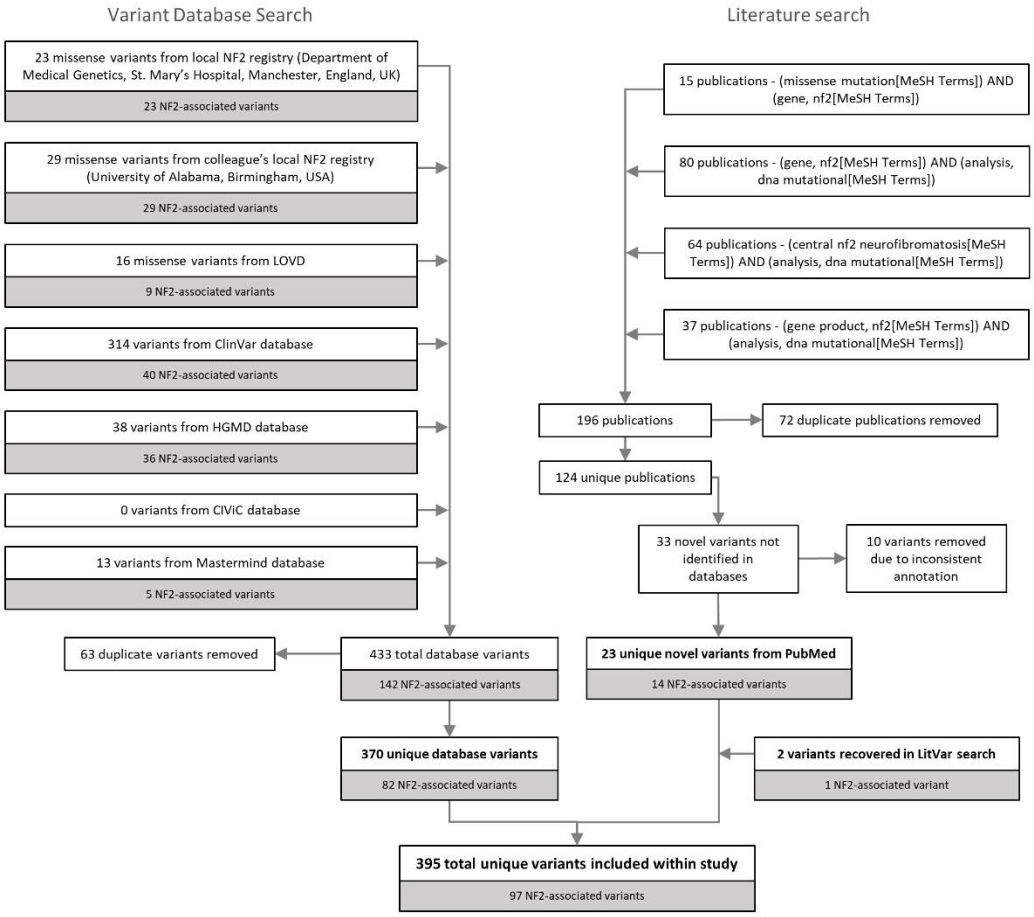

Figure 4. Flow chart outlining variant compilation.

4.3.2. Variant Classification Tools

Evidence for clinical classification of variants was obtained and interpreted following the ACGS best practice guidelines (2020). Classification scores and posterior probabilities were also calculated for each variant [12,20]. See Table 11 for a summary of both the ACMG-AMP (2015) and revised ACGS (2020) variant classification frameworks.

The *NF2* transcript RefSeq NM_000268.4 was used for all *in silico* tool use. Variants were imported into the clinical prediction software Alamut Visual version 2.15 (SOPHiA GENETICS, Lausanne, Switzerland), in which multiple variant database information and *in silico* tools are embedded. Results from the following tools were exported from Alamut and factored into classification analysis: Align-GVGD [21], SIFT [22], PolyPhen-2 [23], MutationTaster2 [24], SpliceSiteFinder-like tool [25], MaxEntScan [26]. Variant frequencies and ExAC constraint metrics were obtained from gnomAD v2.1.1 (gnomad.broadinstitute.org) [27].

ACMG-AMP classification	ACMG-AMP evidence†	ACGS posterior probability threshold ‡¶	Points §	ACGS classification		ACGS evidence¶
Pathogenic	1 Very Strong ***AND*** ≥1 Strong ***OR*** ≥2 Moderate ***OR*** 1 Moderate + 1 Supporting ***OR*** ≥2 Supporting	PP > 0.99	>10	Pathogenic	a	1 Very Strong ***AND*** ≥1 Strong ***OR*** ≥1 Moderate ***OR*** ≥2 Supporting
	≥2 Strong ¥				b	≥3 Strong
	1 Strong ***AND*** ≥3 Moderate ***OR*** 2 Moderate ***AND*** ≥2 Supporting ***OR*** 1 Moderate ***AND*** ≥4 Supporting				c	2 Strong ***AND*** ≥1 Moderate ***OR*** ≥2 Supporting
					d	1 Strong ***AND*** ≥3 Moderate ***OR*** ≥2 Moderate ***AND*** ≥2 Supporting ***OR*** ≥1 Moderate ***AND*** ≥4 Supporting
Likely pathogenic	1 Very Strong ***AND*** 1 Moderate ¥	0.99 ≥ PP > 0.90	6-9	Likely pathogenic	a	≥2 Strong
	1 Strong ***AND*** 1–2 Moderate					
	1 Strong ***AND*** ≥2 Supporting				b	1 Strong ***AND*** 1-2 Moderate ***OR*** ≥2 Supporting
	≥3 Moderate					
	2 Moderate ***AND*** ≥2 Supporting				c	≥3 Moderate ***OR*** 2 Moderate ***AND*** ≥2 Supporting ***OR*** 1 Moderate ***AND*** ≥4 Supporting
	1 Moderate ***AND*** ≥4 Supporting					
Uncertain significance		0.812 ≤ PP < 0.90	5	VUS	Hot	1 Strong + 1 Supporting ***OR*** 2 Moderate + 1 Supporting ***OR*** 1 Moderate + 3 Supporting
		0.675 ≤ PP < 0.812	4		Warm	1 Strong ***OR*** 2 Moderate ***OR*** 1 Moderate + 2 Supporting ***OR*** 4 Supporting
		0.50 ≤ PP < 0.675	3		Tepid	1 Moderate + 1 Supporting ***OR*** 3 Supporting
		0.325 ≤ PP < 0.50	2		Cool	1 Moderate ***OR*** 2 Supporting
		0.188 ≤ PP < 0.325	1		Cold	1 Supporting
		0.10 ≤ PP < 0.188	0		Ice cold	
Likely benign	1 Strong ***AND*** 1 Supporting	0.001 ≤ PP < 0.10	-1 to -6	Likely benign		
	≥2 Supporting					
Benign	1 Stand-Alone	PP < 0.001	<-6	Benign		
	≥2 Strong					

Table 11. A summary comparison of the ACMG-AMP and ACGS variant classification guidelines. Additional scoring suggestions made by Tavtigian et al. (2018) and Tavtigian et al. (2020). †Richards et al. (2015) Table 5; ‡Tavtigian et al. (2018) Table 1; §Tavtigian et al. (2020) Table 2; ¶ACGS best practice guidelines (2020) Table 3 and Figure 6; ¥ Inconsistent evidence weighting, identified in Tavtigian et al. (2018) and resolved in ACGS (2020) guidelines.

UCSC LiftOver tool was used for any genomic co-ordinate conversions between genome builds GRCh37/hg19 and GRCh38/hg38 (genome.ucsc.edu/cgi-bin/hgLiftOver) [28].

4.3.3. Population and frequency data

Maximum credible population allele frequency was determined using the alleleFrequencyApp (cardiodb.org/allelefrequencyapp) [29], and was calculated to be 1.88e-07 for NF2, based on the following input parameters: monoallelic inheritance, disease incidence of 1 in 28,000 [3], allelic heterogeneity 0.01 and penetrance 0.95, accounting for the known rate of recurrent pathogenic variants and late disease onset. Strong benign evidence (BS1) was applied to any variants with an allele frequency equal to or higher than NF2 disease incidence (1/28,000). With a low maximum credible population allele frequency calculated (1.88e-07), moderate pathogenicity evidence (PM2) based on frequency data was not applied to any variant observed in gnomAD as frequency values of observed variants exceeded this value.

4.3.4. Functional data

With a predicted missense constraint Z score of 2.29 in ExAC, *NF2* is considered moderately intolerant of variation. However, only Z scores ≥3.09 are considered significant within the ACGS guidelines and therefore variants in *NF2* are ineligible for application of evidence for missense constraint (PP2).

The DECIPHER database [30] was used to investigate possible mutational hotspots or identify regional constraint within functional domains of the NF2 protein. However, no specific structural regions displayed significant association with missense constraint. Therefore ACGS evidence of mutational hotspots and functional domains without benign variation (PM1) was not applied to any of the variants in this study.

Whilst functional work has been conducted and published on a number of variants included within this study, evidence from functional studies (PS3) was only applied to five specific variants as repeated and rigorous publications describing variant-specific effects on protein function were available for them. No functional data from RNA analysis was available for variants predicted to impact splicing.

4.3.5. Computational data

Multiple *in silico* tools were used for variant effect prediction; meta-predictor REVEL (Rare Exome Variant Ensemble Learner) was used as the deciding score for evidence use (PP3, BP4) if other tools were in conflict [31], as it is one of the best performing meta-predictors [32]. REVEL scores ≥0.7 were considered pathogenic and ≤0.4 benign. ClinPred [33] meta-predictor scores were also produced for variants, although were not included as evidence for ACGS variant classification.

Splice prediction tools were also interpreted and applied as evidence, as suggested in the ACGS 2020 guidelines. Variants that received MaxEntScan [26] predictions of >15% score reduction compared to reference allele, and SpliceSiteFinder-Like [25] predictions with >5% reduction, had PP3 computational evidence of pathogenicity applied in their classification.

4.3.6. Clinical information

If phenotype was described, patients who fitted Manchester Criteria for NF2 disease (Supp. Table 1) [34,35] were considered to have phenotypic specificity for a disease of single aetiology (PP4), applied as supporting evidence of pathogenicity. Where possible, family history and segregation data was applied to the evidence framework.

4.3.7. Other databases

COSMIC (www.cancer.sanger.ac.uk) [36] was used in the investigation of variants that were observed in somatic samples. CanVar-UK cancer predisposition gene variant database (www.canvaruk.org) was used in the search for further variant information, as well as links to structured search engine requests.

4.4. Results

4.4.1. Summary of variant classifications

From the 395 total variants interpreted in this study, 375 were classified as VUS. The majority of VUSs (73%) were identified exclusively from ClinVar without accompanying phenotypic information, these variants were observed in large-scale classification studies without focus on NF2 disease [37]. Variants, shown in Table 12, were placed into further VUS temperature categories in line with ACGS recommendations (Table 11). A complete list of variants and the evidence categories applied to their classification can be found in supplementary table Appendix I.

Whilst 395 variants were collated in total, only 97 were identified in cases with confirmed NF2-associated phenotypic features (Table 12). All variants classified as likely pathogenic and pathogenic were identified in association with NF2 disease presentation, and were therefore assigned to both data groups in Table 12.

Seventeen *NF2* missense variants had *in silico* computational evidence of pathogenicity (PP3) applied by splicing prediction tool scores, SpliceSiteFinder-Like [25] and MaxEntScan [26], in the absence of a pathogenic REVEL metascore. SpliceAI produced a confident prediction on splicing impact in only five of these variants. All seventeen of these potential splicing variants remain classified as VUS.

Interestingly, one variant, c.1532A>G, predicted to produce the missense change, p.(Asp511Gly), and not predicted to affect splicing by the MaxEntScan and SpliceSiteFinder-Like tools, was shown to affect splicing by RNA analysis (methods described in Piotrowski et al., 2014 [38]). This variant results in an out of frame mis-spliced transcript, r.1533_1575del, p.(Asp511Valfs*24). Confirmation of aberrant splicing allowed application of strong evidence for pathogenicity from in vitro studies (PS3), resulting in a likely pathogenic classification.

Classifications	Variants in *NF2*	
	All database variants	**NF2 disease-associated**
Benign	0	0
Likely benign	12	6
VUS (ice cold)	85	14
VUS (cold)	87	10
VUS (cool)	96	16
VUS (tepid)	83	21
VUS (warm)	17	16
VUS (hot)	7	6
Likely pathogenic	6	6
Pathogenic	2	2
Total	395	97

Table 12. Variant classifications for identified missense variants in *NF2*.

Further grouping into NF2 disease-associated *NF2* variants in the right hand column. VUS = Variant of Uncertain Significance.

4.4.2. Conflict with existing classifications

When all variant classifications were compared to existing ClinVar interpretations, 17 variants were in conflict with current submissions, seen in Table 13. The vast majority of these variants were downgraded in pathogenicity class.

Sequence change	Amino acid change	ClinVar (number of submissions)	ACGS Classification	NF2 phenotype observed
c.2T>C	p.(Met1Thr)	Likely pathogenic (1)	VUS (warm)	Unknown
c.613A>G	p.(Met205Val)	VUS (3)/ Benign (1)	Likely benign	Associated
c.641T>C	p.(Leu214Pro)	VUS (1)/ Likely pathogenic (1)	VUS (hot)	Yes
c.658A>T	p.(Asn220Tyr)	Pathogenic (1)	Likely pathogenic (c)	Yes
c.1052G>A	p.(Arg351His)	VUS (2)	Likely benign	Associated
c.1079T>C	p.(Leu360Pro)	Pathogenic (1)	Likely pathogenic (b)	Associated
c.1385G>A	p.(Arg462His)	VUS (2)	Likely benign	Unknown
c.1387G>A	p.(Glu463Lys)	VUS (1)/ Likely benign (2)	Likely benign	Unknown
c.1439C>T	p.(Thr480Met)	VUS (2)	Likely benign	Yes
c.1451T>C	p.(Met484Thr)	VUS (1)/ Likely benign (1)/ Benign (1)/ not provided (1)	Likely benign	Unknown
c.1540A>G	p.(Met514Val)	VUS (4)/ benign (1)	Likely benign	Yes
c.1550T>C	p.(Leu517Pro)	Pathogenic (1)	VUS (warm)	Yes
c.1613A>C	p.(Gln538Pro)	Pathogenic (1)	Likely pathogenic (b)	Yes
c.1639G>A	p.(Glu547Lys)	VUS (1)/ Likely benign (2)	Likely benign	Associated
c.1701C>G	p.(Asp567Glu)	VUS (3)	Likely benign	Unknown
c.1753G>A	p.(Ala585Thr)	VUS (3)	Likely benign	Unknown
c.1774T>C	p.(Phe592Leu)	VUS (4)/ Likely benign (1)	Likely benign	Unknown

Table 13. Variants with conflicting classification to existing submissions in ClinVar.

Likely pathogenic (b/c) = variant sub-classifications as per table 11. Associated – observed in individual with features associated with NF2 but without fulfilling Manchester NF2 criteria. Yes – observed in individual fulfilling Manchester NF2 criteria. *NF2* transcript RefSeq NM_000268.4.

4.4.3. Rate of variation across *NF2*

The number of variants identified in each exon of *NF2* was compared to exon size in amino acids. Missense variants recorded within gnomAD occurred at a highly consistent rate across the *NF2* transcript, Figure 5. When considering all 395 *NF2* variants identified in this study rates per exon differed, yet the average trendline remained consistent across the gene (Figure 5). Exon 4 possessed the lowest rate of variation by size and exon 7 the highest. Considering the 97 NF2-associated variants, rates of variation changed for a number of exons but remained highest in exon 7. Approximately half of all variants in exons 2, 4 and 7 were identified in association with an NF2 phenotype. The lowest rates of NF2-associated variants were observed in exons 3, 9 and 17. Notably, the average trendline for NF2-associated variants decreased towards the end of the gene (Figure 5).

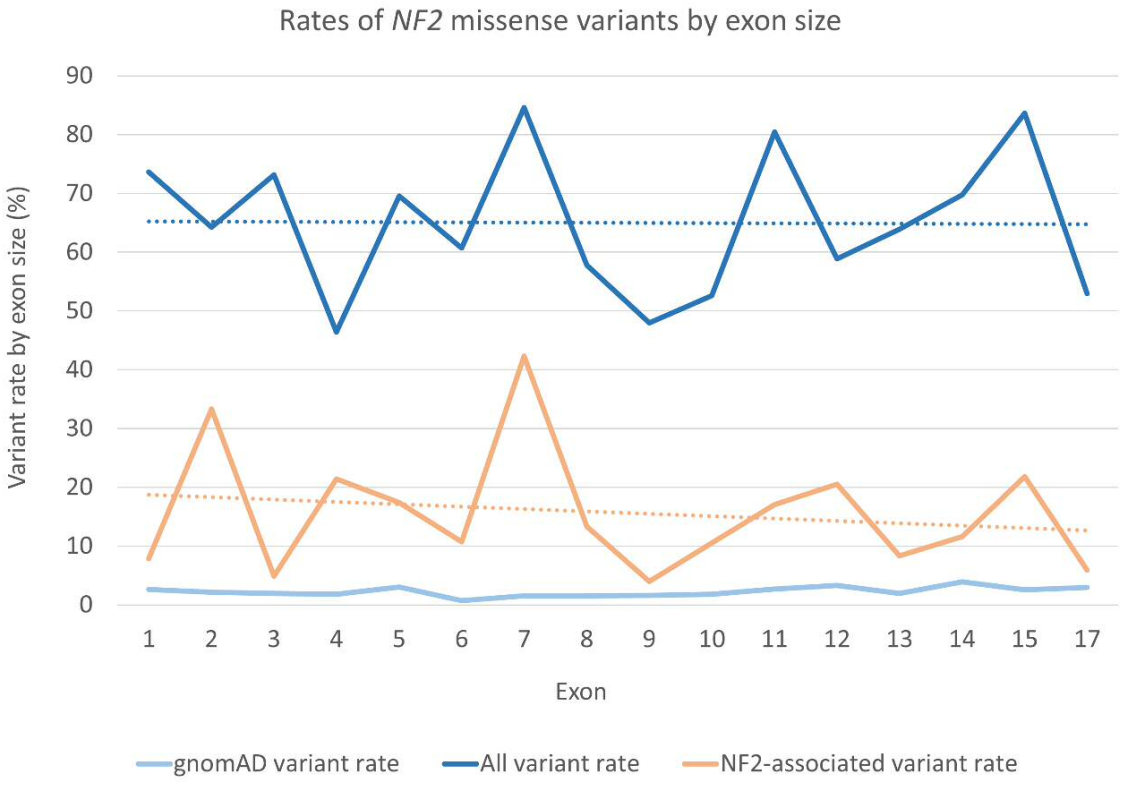

Figure 5. A comparison of rates of NF2 missense variants in gnomAD v2.1.1 (controls), all variants identified within this study, and NF2 disease-associated variants.
Rates were calculated as a percentage of the number of variants in comparison to exon size in amino acids. Assumed benign variation in the gnomAD v2.1.1 (controls) dataset remains consistent across the gene. In contrast, there is an increased rate of variation in a number of exons for variants identified in pathology databases.

Identified variants were plotted across a schematic of isoform 1 of the *NF2* gene structure to highlight potential mutational hotspots (Figure 6); context of secondary and tertiary structure motifs was also included [39]. Missense variants occur across all exons of *NF2*, yet localised clustering of NF2-associated variants are observed in some exons, such as the 5' region of exon 15. The high rates of NF2-associated variants across exons 2 and 7 are observable in Figure 6.

4.4.4. Somatic variants

From the 395 variants collated within this study, 39 had been observed exclusively in somatic samples. Many of the somatic samples were obtained from schwannoma and meningioma tumours, however, 15 of the variants were identified exclusively in non-NF2 related tumour types, such as liver, breast and lung cancers, supplementary table Appendix I.

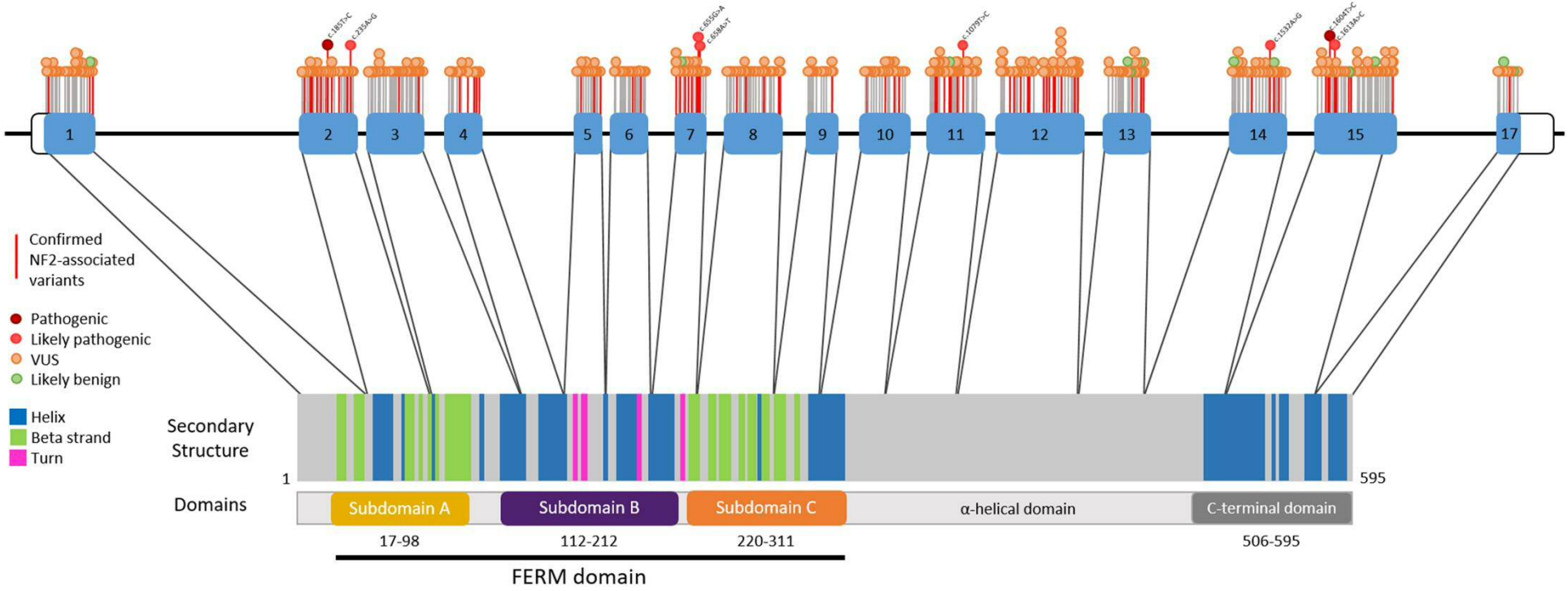

Figure 6. *NF2* isoform 1.

Missense variants with corresponding classifications are labelled on the exon-intron structure at the top of the figure. Confirmed NF2-associated variants are tagged in red. Likely pathogenic and pathogenic variants are labelled with variant nomenclature. Exon boundaries are highlighted on a schematic of the translated protein product with annotated secondary structures, as well as the tertiary domains of the protein. *NF2* transcript RefSeq NM_000268.4.

4.5. Discussion

The vast majority of missense variants identified within *NF2* are classified as variants of uncertain significance in accordance with the ACGS 2020 guidelines. Unfortunately, these variants remain as clinical interpetation dilemmas without sufficient evidence to ascribe or discount them as disease causing. Whilst the VUS temperature scale provides further insight into the possible pathogenicity of a variant, many variants remain at the "cooler" end of the scale with little compelling evidence available, see Table 11 for ACGS VUS sub-classifications. The novel temperature scaling, suggested in the ACGS 2020 guidelines, provides a system for prioritising evidence collection for variants of uncertain significance; for example, obtaining further phenotypic information on patients possessing a specific VUS may enable upgrading of variant pathogenicity at miminal cost. Approximately one third of variants observed in association with NF2 phenotypic features were grouped into "warm" or "hot" VUS and pathogenic classification boundaries; this is primarily due to the clinical and familial evidence available for these variants. Clinical information was unavailable for a large proportion of the variants included within this study and therefore other institutions may be able to reclassify variants upon application of such accompanying data. Similarly, if functional data on variant-specific effects was available, such as RNA studies on possible splicing variants, application of stronger lines of evidence (PS3) and therefore more resolute variant classification would be possible. The need for inclusion of higher performing splice prediction tools within the ACGS guidelines, alongside the utility of RNA studies is exemplified by variant c.1532A>G. Whilst MaxEntScan and SpliceSiteFinder-Like tool did not produce significant splice prediction scores, mRNA analysis from a patient sample confirmed aberrant splicing of *NF2*. The apparent missense variant actually results in frameshifted transcript, r.1533_1575del p.(Asp511Valfs*24), which is predicted to lead to nonsense mediated decay. Confirmation of aberrant splicing through functional analysis allowed application of strong evidence for pathogenicity (PS3), and upgrading of the variant classification to likely pathogenic. SpliceAI [40] splice prediction scores were obtained for each of the variants included within this study, but were not employed for classification purposes following current ACGS guidelines. SpliceAI scores were considered with the following weighting >0.8 high

confidence prediction, >0.5 confident prediction, 0.2-0.5 lower confidence prediction. Variant c.1532A>G received a high confidence SpliceAI score, predicting a donor gain splicing event, lending support for the inclusion of SpliceAI in variant prediction. A further 13 *NF2* missense variants with confident SpliceAI consequence predictions remain without functional evidence (PS3) in our variant list (supplementary table Appendix I), these variants represent promising candidates for RNA studies that may generate further evidence of pathogenicity and therefore variant reclassification.

Evidence of mutational hotspots and functional domains (PM1), was not applied to any of the variants in this study as no specific structural domains of *NF2* display missense constraint in DECIPHER, as outlined in the ACGS 2020 guidelines. However, with our observations of variant clustering in different domains of merlin, alongside a number of studies describing domain-specific interactions of the protein function [39,41], it seems likely that regional constraint could be better defined for *NF2*. Identifying areas of regional constraint would enable the application of moderate evidence for pathogenicity that might enable the revision of a number of variants into likely pathogenic and pathogenic classifications. Exploring ways to redefine regional constraint and domain function for *NF2* may prove valuable in the curation of NF2 disease-specific variant interpretation guidelines. Full details of the 395 *NF2* missense variants is available in supplementary table Appendix I.

From the 17 variants for which reclassification conflicted with the existing ClinVar classification, most were downgraded in pathogenicity when following ACGS recommendations. The majority of the downgraded variants from ClinVar had prior pathogenicity determined based on evidence considered weak by both the ACMG-AMP and ACGS guidelines. For example, the c.658A>T p.(Asn220Tyr) variant is classified as pathogenic within ClinVar based on *in silico* analysis, segregation within a single family and a singular functional study. Yet, when this evidence is considered within the ACGS framework, the c.658A>T p.(Asn220Tyr) variant should be classified as likely pathogenic, as no strong evidence is suitably applicable. Another consideration of ClinVar variant classifications is the age of the studies that were used to assign pathogenicity; a number of variants were submitted to ClinVar prior to the inception of the clinical variant interpretation

guidelines suggested by Richards *et al*. in 2015, and therefore evidence is often applied with inconsistent weighting in these earlier submissions.

When considering missense variant rates by exon size, a highly consistent rate of assumed benign variation was observed in the gnomADv2.1.1 (controls) dataset (Figure 5). In contrast, the variants collated from pathology databases for this study demonstrated differing rates of variation by exon. The comparable pattern of variant rates between 'all database variants' and 'NF2-associated variants' in Figure 5 suggests that a considerable fraction of 'all database variants' are potentially pathogenic and would be associated with an NF2 phenotype if clinical features were provided. Exon 7 possessed the highest rate of variation, with approximately half of its variants occurring within a codon possessing at least one other recorded missense variant (Figure 6). Exon 7 also contained the highest rate of NF2-associated variants. Spanning the linker region of subdomains B and C of the FERM domain in the merlin protein (Figure 6), the sequence of exon 7 in *NF2* is highly conserved across the ERM (ezrin, radixin, moesin) protein superfamily [39]. The sequence conservation of exon 7, alongside the high rate of NF2-associated missense variants, suggests that alteration of amino acid residues in this region may disrupt critical biophysical interactions of the merlin protein. For example, the exon 7 variant c.658A>T p.(Asn220Tyr) has been reported to display reduced binding to scaffolding protein EBP50 [41]; Shimizu et al. (2002) theorised that this may be due to altered residue contacts resulting in changes to subdomain orientation.

Rates of NF2-associated variants decreased towards the end of the *NF2* gene, which may suggest that variants positioned later in the gene transcript are less likely to disrupt function of the protein, similar to the genotype-phenotype correlation observed in *NF2* splice variants [8,9]. Moreover, the single NF2 disease-associated variant identified in exon 17 was observed in a somatic astrocytoma sample from one individual. Astrocytomas are observed very rarely in association with NF2 (Gene Reviews – Neurofibromatosis 2, 2018. https://www.ncbi.nlm.nih.gov/books/NBK1201/. Accessed 02 September 2021) and it is possible that this variant was acquired somatically in the tumour and is not related to NF2 disease. As the two predominant isoforms of merlin possess variant C-terminal ends [39], it is possible there is transcript redundancy that

reduces the pathological effect of variants towards the end of the gene. As only isoform 1 of *NF2* has been analysed within this study it should be considered that some variants may confer transcript-specific effects currently unaccounted for in our interpretation.

Fifteen of the *NF2* missense variants included in this study were observed exclusively in somatic samples from non-NF2 related tumours, and this is consistent with previous observations of somatic *NF2* variants in multiple cancer types, such as mesothelioma, liver and large instestine cancers [42]. Merlin is a known tumour suppressor, regulating multiple cell signalling pathways associated with cell proliferation and therefore tumourigenesis of multiple cancer types [1,43].

With the current absence of NF2 disease-specific guidelines for variant classification, we propose additional presentation features that could be considered for *NF2* variant interpretation under the ACGS 2020 framework. Individuals meeting Manchester NF2 criteria with an identifiable germline *NF2* rare missense variant in the absence of other detectable variants, in addition to somatic *NF2* LOH with retention of the missense variant on the *trans*-allele, would provide moderate evidence for pathogenicity of a missense variant. Furthermore, observed mosaicism of an identical *NF2* rare missense variant in two tumour samples, or at low frequency in blood, would be strong evidence for pathogenicity of the variant in the absence of other variant identification. An example of the utility for this suggested evidence criteria can be seen for variant c.655G>A p.(Val219Met), which has been described in somatic samples and cases of mosaic NF2 identified through multiple tumour genotyping [14]. Since missense variants generally lead to a milder phenotype, they are more likely to be seen as non-mosaic variants [44]. The frequent observation of c.655G>A p.(Val219Met) mosaicism – five mosaic NF2 patients seen in Manchester laboratory - suggests the variant may confer a severe functional effect, as low level mosaic patients still present with a clinical NF2 phenotype. Application of the suggested NF2 disease-specific evidence for mosaicism would enable reclassification of this variant from likely pathogenic (c) to pathogenic (d). Both of these specific genotypic observations could be incorporated into ACGS 2020 variant interpretation guidelines by increasing the strength of the PP4 evidence class to moderate or

strong, 'patient phenotype or family history is highly specific for a disease with a single genetic aetiology'.

In conclusion, most *NF2* missense variants remain classified as variants of uncertain significance after application of current ACGS guidelines. Our observation of differing missense variant rates by exon of *NF2*, with fewer NF2-associated variants towards the C-terminus of merlin, is suggestive of a potential genotype-phenotype correlation, although further work is necessary to substantiate this. Whilst we provide a comprehensive list of *NF2* missense variants, it is not exhaustive, and we encourage other researchers within the field to submit novel variants to public databases. This is particularly significant with the anticipation of ClinGen NF2 disease-specific variant interpretation guidelines. There is an unmet demand for both clinical descriptions in association with reported variants, alongside functional analysis of variant-specific effects on merlin, including RNA studies, which are necessary for more definitive variant interpretation.

4.6. Web Resources

ACGS best practice guidelines (2020), https://www.acgs.uk.com/quality/best-practice-guidelines/#VariantGuidelines

Align-GVGD, http://agvgd.hci.utah.edu/

AlleleFrequencyApp, cardiodb.org/allelefrequencyapp

CanVar-UK, www.canvaruk.org

CIViC, https://civicdb.org/home

ClinPred, https://sites.google.com/site/clinpred/

ClinVar NCBI, www.ncbi.nlm.nih.gov/clinvar

COSMIC, www.cancer.sanger.ac.uk

DECIPHER, https://www.deciphergenomics.org/

ExAC, https://exac.broadinstitute.org/

gnomAD v2.1.1, gnomad.broadinstitute.org

Human Gene Mutation Database, www.hgmd.cf.ac.uk/ac/all.php

Leiden Open Variation Database, www.lovd.nl

LitVar, https://www.ncbi.nlm.nih.gov/CBBresearch/Lu/Demo/LitVar/#!?query

Mastermind Genomic Search Engine, https://www.genomenon.com/mastermind

MutationTaster2, https://www.mutationtaster.org/

PolyPhen-2, http://genetics.bwh.harvard.edu/pph2/

REVEL, https://sites.google.com/site/revelgenomics/

UCSC LiftOver tool, genome.ucsc.edu/cgi-bin/hgLiftOver

4.7. Acknowledgements

The authors wish to acknowledge the National Health Service (NHS) England funded highly specialised NF2 service, Prof Evans is an NIHR Senior Investigator. This research was supported by the Manchester National Institute for Health Research (NIHR) Biomedical Research Centre (IS-BRC-1215-20007).

4.8. Ethics declaration

Ethical approval for the use of anonymised samples from the Manchester Centre for Genomic Medicine archive was obtained from the North West – Greater Manchester Central Research Ethics Committee (reference 10/H1008/74).

Ethical approval for the use of de-identified data from the UAB Medical Genomics Laboratory was obtained from the UAB Institutional Review Board, project number 080926009.

4.9. References

1. Trofatter JA, MacCollin MM, Rutter JL, et al. A novel moesin-, ezrin-, radixin-like gene is a candidate for the neurofibromatosis 2 tumour suppressor. *Cell*. Nov 1993;75(4):826.
2. Asthagiri AR, Parry DM, Butman JA, et al. Neurofibromatosis type 2. *Lancet*. Jun 2009;373(9679):1974-86. doi:10.1016/S0140-6736(09)60259-2
3. Evans DG, Bowers NL, Tobi S, et al. Schwannomatosis: a genetic and epidemiological study. *J Neurol Neurosurg Psychiatry*. Nov 2018;89(11):1215-1219. doi:10.1136/jnnp-2018-318538
4. Evans DG. Neurofibromatosis type 2 (NF2): a clinical and molecular review. *Orphanet J Rare Dis*. Jun 2009;4:16. doi:10.1186/1750-1172-4-16
5. Ruttledge MH, Andermann AA, Phelan CM, et al. Type of mutation in the neurofibromatosis type 2 gene (NF2) frequently determines severity of disease. *Am J Hum Genet*. Aug 1996;59(2):331-42.
6. Smith MJ, Higgs JE, Bowers NL, et al. Cranial meningiomas in 411 neurofibromatosis type 2 (NF2) patients with proven gene mutations: clear positional effect of mutations, but absence of female severity effect on age at onset. *J Med Genet*. Apr 2011;48(4):261-5. doi:10.1136/jmg.2010.085241
7. Evans DG. Neurofibromatosis type 2. *Handb Clin Neurol*. 2015;132:87-96. doi:10.1016/B978-0-444-62702-5.00005-6
8. Baser ME, Kuramoto L, Woods R, et al. The location of constitutional neurofibromatosis 2 (NF2) splice site mutations is associated with the severity of NF2. *J Med Genet*. Jul 2005;42(7):540-6. doi:10.1136/jmg.2004.029504
9. Kluwe L, MacCollin M, Tatagiba M, et al. Phenotypic variability associated with 14 splice-site mutations in the NF2 gene. *Am J Med Genet*. May 18 1998;77(3):228-33.
10. Suckow J, Markiewicz P, Kleina LG, Miller J, Kisters-Woike B, Müller-Hill B. Genetic studies of the Lac repressor. XV: 4000 single amino acid substitutions and analysis of the resulting phenotypes on the basis of the protein structure. *J Mol Biol*. Aug 30 1996;261(4):509-23. doi:10.1006/jmbi.1996.0479
11. Richards S, Aziz N, Bale S, et al. Standards and guidelines for the interpretation of sequence variants: a joint consensus recommendation of the American College of Medical Genetics and Genomics and the Association for Molecular Pathology. *Genet Med*. May 2015;17(5):405-24. doi:10.1038/gim.2015.30
12. Tavtigian SV, Greenblatt MS, Harrison SM, et al. Modeling the ACMG/AMP variant classification guidelines as a Bayesian classification framework. *Genet Med*. 09 2018;20(9):1054-1060. doi:10.1038/gim.2017.210
13. Catasús N, Garcia B, Galván-Femenía I, et al. Revisiting the UK Genetic Severity Score for NF2: a proposal for the addition of a functional genetic component. *J Med Genet*. Aug 04 2021;doi:10.1136/jmedgenet-2020-107548
14. Heineman TE, Evans DG, Campagne F, Selesnick SH. In Silico Analysis of NF2 Gene Missense Mutations in Neurofibromatosis Type 2: From Genotype to Phenotype. *Otol Neurotol*. Jun 2015;36(5):908-14. doi:10.1097/MAO.0000000000000639
15. Halliday D, Emmanouil B, Pretorius P, et al. Genetic Severity Score predicts clinical phenotype in NF2. *J Med Genet*. 10 2017;54(10):657-664. doi:10.1136/jmedgenet-2017-104519

16. Fokkema IFAC, Kroon M, López Hernández JA, et al. The LOVD3 platform: efficient genome-wide sharing of genetic variants. *Eur J Hum Genet*. Sep 15 2021;doi:10.1038/s41431-021-00959-x
17. Landrum MJ, Lee JM, Benson M, et al. ClinVar: improving access to variant interpretations and supporting evidence. *Nucleic Acids Res*. 01 2018;46(D1):D1062-D1067. doi:10.1093/nar/gkx1153
18. Stenson PD, Mort M, Ball EV, et al. The Human Gene Mutation Database (HGMD. *Hum Genet*. Oct 2020;139(10):1197-1207. doi:10.1007/s00439-020-02199-3
19. Allot A, Peng Y, Wei CH, Lee K, Phan L, Lu Z. LitVar: a semantic search engine for linking genomic variant data in PubMed and PMC. *Nucleic Acids Res*. 07 02 2018;46(W1):W530-W536. doi:10.1093/nar/gky355
20. Tavtigian SV, Harrison SM, Boucher KM, Biesecker LG. Fitting a naturally scaled point system to the ACMG/AMP variant classification guidelines. *Hum Mutat*. Jul 2020;doi:10.1002/humu.24088
21. Mathe E, Olivier M, Kato S, Ishioka C, Hainaut P, Tavtigian SV. Computational approaches for predicting the biological effect of p53 missense mutations: a comparison of three sequence analysis based methods. *Nucleic Acids Res*. 2006;34(5):1317-25. doi:10.1093/nar/gkj518
22. Kumar P, Henikoff S, Ng PC. Predicting the effects of coding non-synonymous variants on protein function using the SIFT algorithm. *Nat Protoc*. 2009;4(7):1073-81. doi:10.1038/nprot.2009.86
23. Adzhubei IA, Schmidt S, Peshkin L, et al. A method and server for predicting damaging missense mutations. *Nat Methods*. Apr 2010;7(4):248-9. doi:10.1038/nmeth0410-248
24. Schwarz JM, Cooper DN, Schuelke M, Seelow D. MutationTaster2: mutation prediction for the deep-sequencing age. *Nat Methods*. Apr 2014;11(4):361-2. doi:10.1038/nmeth.2890
25. Zhang MQ. Statistical features of human exons and their flanking regions. *Hum Mol Genet*. May 1998;7(5):919-32. doi:10.1093/hmg/7.5.919
26. Yeo G, Burge CB. Maximum entropy modeling of short sequence motifs with applications to RNA splicing signals. *J Comput Biol*. 2004;11(2-3):377-94. doi:10.1089/1066527041410418
27. Lek M, Karczewski KJ, Minikel EV, et al. Analysis of protein-coding genetic variation in 60,706 humans. *Nature*. 08 2016;536(7616):285-91. doi:10.1038/nature19057
28. Kent WJ, Sugnet CW, Furey TS, et al. The human genome browser at UCSC. *Genome Res*. Jun 2002;12(6):996-1006. doi:10.1101/gr.229102
29. Whiffin N, Minikel E, Walsh R, et al. Using high-resolution variant frequencies to empower clinical genome interpretation. *Genet Med*. 10 2017;19(10):1151-1158. doi:10.1038/gim.2017.26
30. Firth HV, Richards SM, Bevan AP, et al. DECIPHER: Database of Chromosomal Imbalance and Phenotype in Humans Using Ensembl Resources. *Am J Hum Genet*. Apr 2009;84(4):524-33. doi:10.1016/j.ajhg.2009.03.010
31. Ioannidis NM, Rothstein JH, Pejaver V, et al. REVEL: An Ensemble Method for Predicting the Pathogenicity of Rare Missense Variants. *Am J Hum Genet*. Oct 2016;99(4):877-885. doi:10.1016/j.ajhg.2016.08.016
32. Wilcox EH, Sarmady M, Wulf B, et al. Evaluating the impact of in silico predictors on clinical variant classification. Genet Med. Dec 23 2021;doi:10.1016/j.gim.2021.11.018

33. Alirezaie N, Kernohan KD, Hartley T, Majewski J, Hocking TD. ClinPred: Prediction Tool to Identify Disease-Relevant Nonsynonymous Single-Nucleotide Variants. *Am J Hum Genet*. 10 2018;103(4):474-483. doi:10.1016/j.ajhg.2018.08.005
34. Evans DG, Huson SM, Donnai D, et al. A clinical study of type 2 neurofibromatosis. *Q J Med*. Aug 1992;84(304):603-18.
35. Smith MJ, Bowers NL, Bulman M, et al. Revisiting neurofibromatosis type 2 diagnostic criteria to exclude LZTR1-related schwannomatosis. *Neurology*. Jan 2017;88(1):87-92. doi:10.1212/WNL.0000000000003418
36. Tate JG, Bamford S, Jubb HC, et al. COSMIC: the Catalogue Of Somatic Mutations In Cancer. *Nucleic Acids Res*. 01 2019;47(D1):D941-D947. doi:10.1093/nar/gky1015
37. Nykamp K, Anderson M, Powers M, et al. Sherloc: a comprehensive refinement of the ACMG-AMP variant classification criteria. *Genet Med*. 10 2017;19(10):1105-1117. doi:10.1038/gim.2017.37
38. Piotrowski A, Xie J, Liu YF, et al. Germline loss-of-function mutations in LZTR1 predispose to an inherited disorder of multiple schwannomas. Nat Genet. Feb 2014;46(2):182-7. doi:10.1038/ng.2855
39. Shimizu T, Seto A, Maita N, Hamada K, Tsukita S, Hakoshima T. Structural basis for neurofibromatosis type 2. Crystal structure of the merlin FERM domain. *J Biol Chem*. Mar 22 2002;277(12):10332-6. doi:10.1074/jbc.M109979200
40. Jaganathan K, Kyriazopoulou Panagiotopoulou S, McRae JF, et al. Predicting Splicing from Primary Sequence with Deep Learning. Cell. 01 2019;176(3):535-548.e24. doi:10.1016/j.cell.2018.12.015
41. Stokowski RP, Cox DR. Functional analysis of the neurofibromatosis type 2 protein by means of disease-causing point mutations. *Am J Hum Genet*. Mar 2000;66(3):873-91. doi:10.1086/302812
42. Schroeder RD, Angelo LS, Kurzrock R. NF2/merlin in hereditary neurofibromatosis 2 versus cancer: biologic mechanisms and clinical associations. *Oncotarget*. Jan 15 2014;5(1):67-77. doi:10.18632/oncotarget.1557
43. Cui Y, Groth S, Troutman S, et al. The NF2 tumour suppressor merlin interacts with Ras and RasGAP, which may modulate Ras signaling. *Oncogene*. 09 2019;38(36):6370-6381. doi:10.1038/s41388-019-0883-6
44. Evans DG, Bowers N, Huson SM, Wallace A. Mutation type and position varies between mosaic and inherited NF2 and correlates with disease severity. *Clin Genet*. Jun 2013;83(6):594-5. doi:10.1111/cge.12007

4.10. Supplementary material

Current and revised Manchester Criteria for neurofibromatosis type 2 (NF2)
1. Bilateral vestibular schwannomas <70 **OR**
2. Family history* of NF2 **AND** unilateral VS <70 **OR**
3. Family history* of NF2 **OR** UVS **AND** any two of: meningioma, glioma, neurofibroma, schwannoma, cataract, cerebral calcification (if UVS + ≥2 non intradermal schwannomas need negative *LZTR1* testing) **OR**
4. Multiple meningiomas (two or more) **AND** any two of: UVS, glioma, neurofibroma, schwannoma, cerebral calcification **OR**
5. Constitutional or mosaic pathogenic *NF2* mutation in blood or identical mutations in two distinct tumours
*VS = Vestibular Schwannoma, UVS = Unilateral Vestibular Schwannoma * First degree relative*

Supplementary table 1. Current and revised Manchester Criteria for neurofibromatosis type 2.

5. Genome-wide association analysis identifies a susceptibility locus for sporadic vestibular schwannoma at 9p21

Genome-wide association analysis identifies a susceptibility locus for sporadic vestibular schwannoma at 9p21

Katherine V Sadler[1,2], John Bowes[2], Charlie F Rowlands[1,2], Cristina Perez-Becerril[1,2], Andrew T King[3], Scott A Rutherford[3], Omar N Pathmanaban[3], Charlotte Hammerbeck-Ward[3], Simon K W Lloyd[4], Simon R Freeman[4], Ricky Williams[5], Cathal J Hannan[2,3,6], Daniel Lewis[3], D Gareth Evans[1,2] and Miriam J Smith[1,2].

[1]Manchester Centre for Genomic Medicine, St Mary's Hospital, Manchester Academic Health Sciences Centre (MAHSC), Manchester, UK

[2]Division of Evolution, Infection and Genomics, School of Biological Sciences, Faculty of Biology, Medicine and Health, University of Manchester, Manchester, UK

[3]Department of Neurosurgery, and Neuroradiology Manchester Centre for Clinical Neurosciences, Salford Royal NHS Foundation Trust, Manchester Academic Health Sciences Centre (MAHSC), Manchester, UK

[4]Department of Otolaryngology, Manchester Royal Infirmary, Manchester Academic Health Sciences Centre (MAHSC), University of Manchester, Manchester, UK

[5]Brain Tumour Biobank, Salford Royal NHS Foundation Trust, Manchester Academic Health Science Centre, Manchester, UK

[6]Division of Cardiovascular Sciences, School of Medical Sciences, Faculty of Biology Medicine and Health, University of Manchester, Manchester, UK

5.1. Abstract

Background

Vestibular schwannomas (VS) are benign nerve sheath tumours that arise on the vestibulocochlear nerve. VSs are known to occur in the context of tumour suppressor syndromes NF2 and *LZTR1*-schwannomatosis. However, the majority of VS present sporadically without identification of germline pathogenic variants.

Methods

To identify novel genetic associations with risk of VS development, we conducted a genome-wide association study (GWAS) in a combined cohort of 911 sporadic VS cases collated from the NF2 service in the North West of England, UK and 5,500 control samples from the UK Biobank resource. We also present this data in prospective stage 1 and stage 2 analyses, carried out independently due to data availability and to investigate the possible replication of associated loci.

Results

One risk locus was identified at a suggestive level of significance within both stage 1 and stage 2 data sets and reached genome-wide significance in our combined analysis (9p21.3, rs1556516, *P* = 1.47e-13, odds ratio = 0.67, AF = 0.52). 9p21.3 is a GWAS association hotspot, and a number of genes are localised to this region, *CDKN2B-AS1* and *CDKN2A/B*, also referred to as the INK4 locus.

Conclusions

Dysregulation of gene products within the INK4 locus have been associated with multiple pathologies and the genes in this region have been observed to directly impact the expression of one another. Recurrent associations of the INK4 locus with components of well described oncogenic pathways provides compelling evidence that the 9p21.3 region is truly associated with risk of VS tumourigenesis.

5.2. Background

Vestibular schwannomas (VS) are benign tumours that develop on the vestibular portion of the vestibulocochlear nerve. Arising from Schwann cells of the myelin sheath surrounding nerves in the internal auditory canal, VS growth frequently causes hearing loss, tinnitus and vestibular disequilibrium in affected individuals. Less frequent symptoms include headaches, vertigo, vision disruption and facial nerve weakness [1]. Annual incidence of VS has been estimated to range from 1 in 64,000 to 1 in 90,000 [2-4] and VS account for approximately 9% of all non-malignant central nervous system tumours [5].

VSs are known to occur within the context of tumour suppressor syndromes, NF2 and schwannomatosis [6-8]. However, the majority of VSs occur sporadically in otherwise healthy individuals [2]. No environmental factors have been robustly linked to risk of VS development, except for exposure to cranial radiotherapy [9], which occurs extremely infrequently in the general population. Some incidences of solitary VS appear to cluster within families [10,11]. Moreover, phenotype and clinical outcome variability between, and within, NF2 and schwannomatosis affected families suggests the existence of genetic variants that modify VS risk and clinical course [12,13]. It is hypothesised that the missing heritability and variable presentation observed in VS cases can be explained, at least in part, by common low penetrance, small effect size inherited genetic variants.

The aim of this study was to identify novel genetic variants in association with VS risk by conducting a genome-wide association study (GWAS) in sporadic VS (sVS) patients, negative for germline pathogenic *NF2* variants. It is intended that variants identified in association with VS presentation are utilised for clinical risk prediction. Stratifying individuals based on genetic risk of VS would enable more personalised care management and prognosis, identifying optimal treatment strategies for patients. Identification of new genetic associations may also identify novel therapeutic targets for the treatment of VS.

5.3. Methods

5.3.1. Subjects

All case samples were ascertained through the highly specialised NF2 service in the North West of England, UK. Samples were collated from both the Manchester Centre for Genomic Medicine and Salford Royal Foundation Trust. Cases had presentation of sporadic VS without family history and were negative for identifiable germline pathogenic *NF2* variants. Patients with germline pathogenic *LZTR1* variants were also excluded, however *LZTR1* screening was not conducted in all case samples.

All control samples were obtained from the UK Biobank (UKBB) project. The UK Biobank is a large-scale biomedical database containing genotype and extensive phenotype data on half a million UK-based individuals between the ages of 49 and 60 years [14]. Control samples were filtered to include participants with self-declared ethnicity as 'White'. Individuals were excluded for the following ICD10 descriptions: 'Benign neoplasms of cranial nerves' (D33.3) and 'Neurofibromatosis' (Q85.0). Approximately 50,000 of the earliest UKBB samples were genotyped on the UK BiLEVE array, whilst this platform has similar SNP coverage to the UK Biobank Axiom® Array, these samples were also excluded to maximise shared SNP coverage between cases and controls. With no ICD code specifically defined for VS, no case samples were ascertained from UK Biobank.

Stage 1 analysis included 475 sVS case samples and 2,750 control samples obtained through UKBB. Stage 2 analysis included 436 sVS case samples and 2,750 control samples obtained through UKBB. For combined analysis, a total of 911 sVS case samples and 5,500 control samples comprised the study.

5.3.2. Ethics

Ethical approval of the use of anonymised samples from the Manchester Centre for Genomic Medicine archive and the collection of blood samples from patients with informed consent, was obtained from the North West 7–Greater Manchester Central Research Ethics Committee, IRAS ID: 36817, Rec Ref: 10/H1008/74.

5.3.3. Genotyping

DNA was extracted from blood samples following conventional methods and quantified by Nanodrop 8000 Spectrophotometer (Thermo Fisher). Genotyping was conducted by two service providers. Stage 1 case samples were genotyped by Oxford Genomics Centre. Stage 2 case samples were genotyped by Yourgene Health. Both service providers use the same Axiom 2.0 Assay manual workflow on UK Biobank Axiom™ 96 well arrays. The UK Biobank Axiom™ Array contains 820,967 SNP and indel markers.

Array intensity data CEL files were imported into Axiom Analysis Suite v4.0.3.3 with the Axiom_UKB_WCSG.r5 library. Axiom Best Practice Genotyping Analysis Workflow, which incorporates R package SNPolisher, was applied for genotype clustering and evaluation of clustering quality. Quality of genotyping was considered for each individual sample, in addition to plate batches. As recommended by Axiom, samples with a Dish QC (DQC) metric < 0.82 and call rate < 97% were considered to have failed genotyping. Quality metrics were calculated for each locus, based on call frequency, Hardy-Weinberg equilibrium (HWE), cluster separation, width and positioning. Probes meeting the defined quality metrics were exported in PED format. Genotypes are referenced against genome build GRCh37/ hg19.

Case and control genotypes were subject to further QC filters prior to analysis. We considered only autosomal SNPs and SNPs were removed according to the following parameters, call rate < 98%, MAF < 0.01 and HWE-departure (P < 1e-04). Samples were excluded for call rate < 98% and heterozygosity deviating ±3 SD from the mean. A summary of sample and total intersecting SNP numbers for each analyses can be seen in supplementary table 2.

5.3.4. Statistical Analysis

Case and control genotype data was merged after sample and SNP QC, statistical analysis of relatedness and ancestry was conducted on the merged dataset. Statistical analyses were largely conducted using R (v3.4.2) and PLINK (v1.9). Identity-by-descent (IBD) analysis was performed using KING

(v1.9) software, calculating relatedness between each pair of individuals to identify duplicate or closely related samples (2nd degree kinship). Samples with the lowest call rates were removed in these related pairs.

Stage 1 analysis identified one case sample as a duplicate and four pairs of samples were considered closely related, one pair of cases and three pairs of controls. Stage 2 analysis identified three pairs of closely related individuals, two pairs of cases and one pair of controls. In combined analysis, one duplicate case sample was identified, in addition to 2nd degree or closer relatives in both cases (five pairs) and controls (four pairs).

Flashpca_x84-64 (v2.0) was used to calculate eigenvectors and perform principle component analysis (PCA). Merging of case and control data with HapMap 3 data identified outliers with non-Western European (CEU) ancestry (supplementary figure 1). LD metrics were based on HapMap 3 recombination rate data, SNPs were pruned from the dataset using PLINK and regions of high LD excluded. PCA was used to identify population stratification within study participants and the first three principle components of PCA analysis were associated with case-control status. After QC exclusion for IDB and ancestral outliers, total case and control numbers for each analyses are seen in supplementary table 3.

The McCarthy Group HRC checking tool (v4.2) was used to identify ambiguous SNPs and forward-strand align genotypes to the Haplotype Reference Consortium (HRC) and 1000 Genomes reference.

5.3.5. Imputation

Phasing and imputation of non-typed SNPs and haplotype phasing of genotype data was conducted through the Michigan Imputation Server (minimac4 v1.5.7), Eagle (v2.3) and HRC r.1.1 2016 (GRCh37/hg19). Imputed data was annotated with NCBI data, and duplicate and low confidence SNPs ($r^2 < 0.5$) were removed (bcftools, vcftools).

5.3.6. Association Analysis

Association between individual SNPs and risk of VS was assessed using Cochran-Armitage linear regression under a frequentist additive effect model

in SNPTEST (v2.5.2). Odds ratios and 95% CIs were determined using a logistic regression model, conditioned on the first three principle components. SNPTEST output was filtered to include variants with a MAF >1%. Summary statistics were uploaded to FUMA for data visualisation and exploration.

5.3.7. Investigation of rs1556516 genotype effect on VS presentation age

We performed a Kaplan-Meier survival analysis, followed by a log-rank test, to assess if risk allele G at SNP rs1556516 conferred an increased risk of earlier age at VS presentation within cases from our combined cohort. From the 776 cases that passed GWAS quality filters (supplementary table 3), age at onset information was available for 668 individuals. Cases were grouped by genotype, 'CC', 'CG', 'GG'. Analysis was performed using GraphPad Prism version 9.1.2 for Windows, GraphPad Software, San Diego, California USA.

5.3.8. URLs

UKBB, http://www.ukbiobank.ac.uk/; PLINK v1.9, http://pngu.mgh.harvard.edu/purcell/plink/; McCarthy Group Checking Tool HRC/1000G (v4.2), https://www.well.ox.ac.uk/~wrayner/tools/; KING v1.9, https://people.virginia.edu/~wc9c/KING/manual.html; Flashpca_x86-64 v2.0, https://github.com/gabraham/flashpca; HapMap3, https://www.sanger.ac.uk/resources/downloads/human/hapmap3.html; bcftools, http://samtools.github.io/bcftools/bcftools.html; NCBI, https://www.ncbi.nlm.nih.gov; vcftools, https://vcftools.github.io/index.html; Michigan Imputation Server, https://imputationserver.sph.umich.edu/index.html; SNPTEST v2.5.2, https://www.well.ox.ac.uk/~gav/snptest/; FUMA, https://fuma.ctglab.nl/; GraphPad Prism (v9.1.2) www.graphpad.com

5.4. Results

5.4.1. Cohort Analysis

We performed a GWAS in a cohort of sVS patients. The cohort was prospectively analysed in two stages, due to data availability. Genotype data from both stages was also merged and analysed for a combined association analysis. Quality filters, ancestral and principle component analysis (PCA) was

conducted. PCA using HapMap3 data showed that cases and controls were largely well matched for genetic ancestry (supplementary figure 1). Analysis groups were as follows:

Stage 1 of association analysis consisted of 475 sVS cases and 2,750 UK Biobank (UKBB) control samples. After quality filters were applied 407 cases, 2,624 controls and 503,935 cohort intersecting SNPs remained for stage 1 association analysis.

Stage 2 was composed of 436 cases and 2,750 UKBB control samples. Following quality filtering 378 cases, 2,616 control samples and 517,686 SNPs remained for stage 2 association analysis.

Combined analysis included 911 cases of sVS and 5,500 UKBB control samples. After filtering on quality, 870 cases, 5,273 controls and 492,266 cohort intersecting SNPs remained for a combined association analysis.

5.4.2. Association Analysis

Imputation of non-typed SNPs was conducted through the Michigan Imputation Server [15] using the Haplotype Reference Consortium (HRC) panel. Association testing between each SNP and risk of VS was performed using a Cochran-Armitage linear regression test. Odds ratios (ORs) and 95% confidence intervals (CIs) for SNPs with minor allele frequency (MAF) >1% were derived using a logistic regression model. Genome-wide, PCA adjusted, *P*-values for combined cohort association analysis are plotted in figure 7. Genome-wide *P*-value plots for stage 1 and stage 2 analysis are available as supplementary figures 2 and 3, respectively.

Association analysis conducted in the stage 1 cohort identified a single genome-wide significant (*P*-value < $5x10^{-8}$) risk locus at 10q25.1. Lead SNP rs112277746 (*P* = 1.05e-09, OR = 3.04, 95% CI: 2.03-4.56) is located in an intergenic region intersecting no annotated genes. Rs112277746 is in high linkage disequilibrium (LD), r^2 = 0.94, with SNP rs111843780 (*P* = 7.50e-09, OR = 2.89, 95% CI: 1.95-4.29). Again, SNP rs111843780 is located in an intergenic region. Summary statistics for the stage 1 10q25.1 risk locus are found in supplementary table 4.

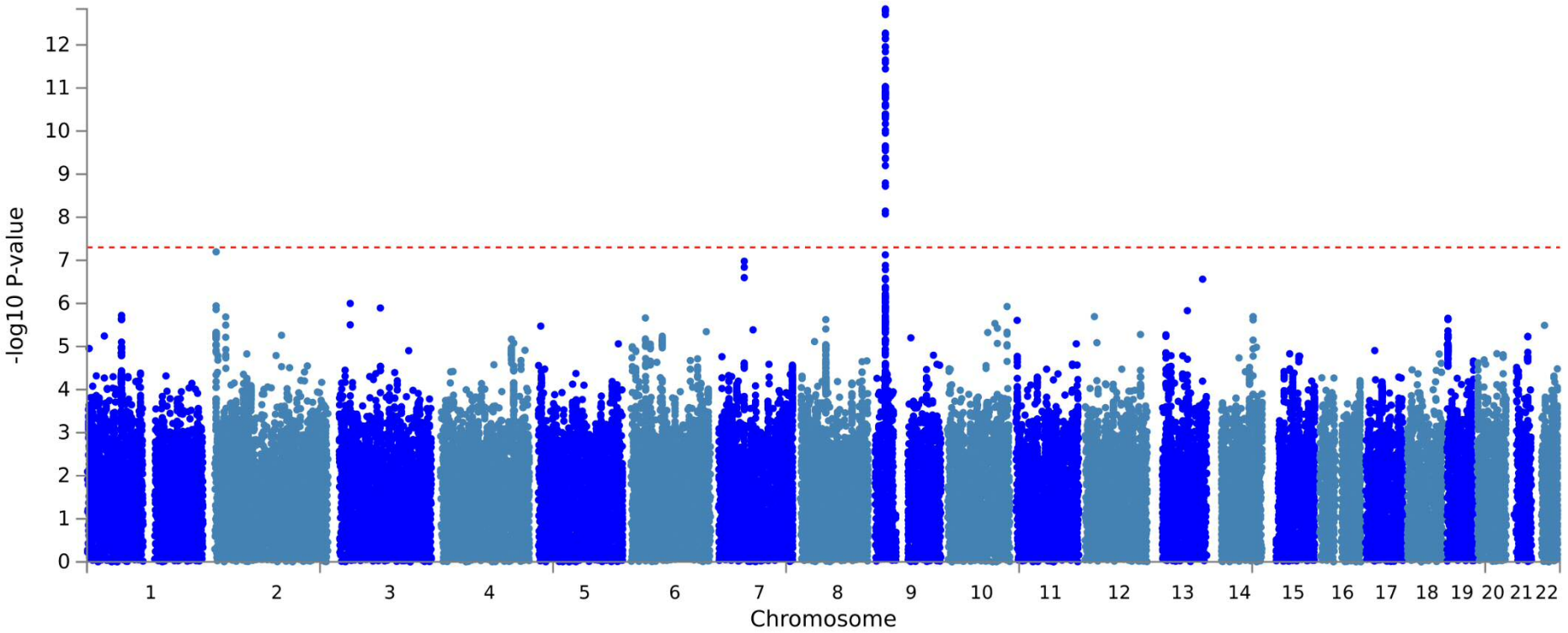

Figure 7. Manhattan plot of MAF >1% SNP *P*-values in the GWAS combined cohort across the autosomes.

Red dashed line represents *P*-value = $5x10^{-8}$.

Association analysis in stage 2 of the cohort identified two genome-wide significant risk loci at 2q21.1 (rs565735761, *P* = 3.69e-11, OR = 2.93) and 11p15.5 (rs143328874, *P* = 1.27e-08, OR = 2.66). Both SNPs map to intronic regions of annotated genes *PLEKHB2* and *TSPAN32*, respectively. 95% CI ranges were relatively large for both the 2q21.1 (95% CI: 1.77-4.83) and 11p15.5 (95% CI: 1.82-3.89) loci. Summary statistics for both stage 2 risk loci are found in supplementary table 5. The region of association identified in stage 1 was not replicated in this group.

Our combined cohort analysis identified one genome-wide significant region (*P*-value < $5x10^{-8}$) in association with VS risk at 9p21.3, seen in figure 7. The lead SNP in this region of association was rs1556516 (*P* = 1.47e-13, OR = 0.67, 95% CI: 0.60-0.75), mapping to intron 14 of *CDKN2B-AS1*. The OR values <1 at this locus suggest that the reference allele is the risk allele for the phenotype. Eleven SNPs are in linkage (r^2 = 1) with sentinel SNP rs1556516, and a further 40 are highly correlated (r^2 > 0.9), with a total of 54 SNPs possessing *P*-values < $5x10^{-8}$ within this region (supplementary table 6). Though the locus at 9p21.3 did not reach genome-wide significance in stage 1 (*P* = 2.66e-07, OR = 0.68, 95% CI: 0.59-0.79) or stage 2 (*P* = 8.19e-08, OR = 0.67, 95% CI: 0.57-0.78) of association analysis, the *P*-value of SNP rs1556516 indicated a suggestive level of genome-wide significance (*P*-value < $1x10^{-6}$) in both cohorts, and is therefore of interest for replication studies [16,17]. *P*-values and summary statistics of the lead SNP in the 9p21.3 locus can be seen for stage 1, stage 2 and combined analysis in table 14. Moreover, a characteristic tower of associated SNPs within the 9p21.3 locus can be seen in the genome-wide *P*-value plots for stage 1 and stage 2 (supplementary figures 2 and 3).

SNP	Locus	Chromosome	Position	Other allele	Reference allele	Stage	MAF	OR (95% CI)	β	SE	*P* - value	Annotated genes	Associated traits
rs1556516	9p21.3	9	22100176	C	G	1	0.484	0.680 (0.59-0.79)	-0.392	0.076	2.66e-07	*CDKN2B-AS1*	Heart failure, parental longevity.
						2	0.473	0.667 (0.57-0.78)	-0.428	0.079	8.19e-08		
						Combined	0.477	0.672 (0.60-0.75)	-0.410	0.055	1.47e-13		

Table 14. Summary statistics of genomic risk locus 9p21.3

Stage 1, stage 2 and combined association analysis shown.

MAF – minor allele frequency; OR – odds ratio; SE – standard error of β. Note: MAF is not risk allele frequency.

A number of genes are localised in the region of LD at the 9p21.3 risk locus surrounding rs1556516. In addition to gene *CDKN2B-AS1*, SNPs in high LD are also located in nearby tumour suppressor genes *CDKN2A* and *CDKN2B*, also referred to as the INK4 locus. A localised plot of SNP *P*-values at the 9p21.3 risk locus can be seen in supplementary figure 4. *CDKN2B-AS1*, also referred to as *ANRIL*, is a long non-coding RNA (lncRNA) that downregulates *CDKN2B* expression when transcribed, through *cis*-acting heterochromatin formation [18,19]. *ANRIL* has been previously reported as a major GWAS hotspot [20], with multiple associations reported for cardiovascular phenotypes [21,22] and neoplasms [23], including glioma [24]. *CDKN2A* encodes p16(INK4a) and p14(ARF), these gene products possess different reading frames within the *CDKN2A* gene and are therefore distinct proteins and not isoforms of one another. Protein p16(INK4a) acts as a negative regulator of cyclin-dependent kinases associated with cellular proliferation [25]. Among other roles, p14(ARF) inactivates the protein MDM2, which is a negative regulator of tumour suppressor protein p53 [25]. Loss of p14(ARF) expression leads to an increase in MDM2-mediated degradation of p53, and germline mutations in p14(ARF) has been found to predispose carriers to multiple benign and malignant neoplasms [26]. Interestingly, regulation of the p16/INK4a locus has been associated with radio-sensitivity in gliomas [27]. It would be valuable to establish if this locus has a similar association in VS.

In the combined association analysis, a total of 37 genomic risk loci possessed *P*-values < $1x10^{-6}$, suggestive of association with the phenotype. A list of genomic risk loci from the combined association analysis with suggestive *P*-values are available in supplementary table 7.

The second strongest association in the combined analysis was observed at 2p25.3 (rs73910511, *P* = 6.345e-08, OR = 2.48), mapping to intron 2 of *EIPR1*. Three further SNPs are highly correlated with the sentinel SNP (r^2 < 0.8), rs116439544, rs7606684 and rs116430374, all positioned within intronic regions of *EIPR1*. *EIPR1* acts as a regulator of insulin secretion and distribution of mature dense-core vesicles (DCVs) [28]. DCVs are regulated secretory vesicles found in neurons and endocrine cells involved in the modulation of neurotransmission [29]. Allele-specific methylation of *EIPR1* has

been proposed as a mediator of psychiatric disorder susceptibility in phenotypically discordant monozygotic twins [30].

The third strongest evidence of association in the combined analysis was identified at 7p11.2 (rs11238349, *P* = 1.05e-07, OR = 1.33), positioned in intron 1 of *EGFR*. Two further SNPs are in high LD with lead SNP rs11238349 (r^2 > 0.94), rs2302535 (*P* = 1.45e-07, OR = 1.33) and rs12535578 (*P* = 2.52e-07, OR = 1.32) both also positioned in intron 1 of *EGFR*. *EGFR* is an oncogenic transmembrane cell signalling protein involved in a range of cellular functions, including cell motility, differentiation, proliferation and survival [31]. With described roles in lung cancer [32], breast cancer [33] and glioma [34], *EGFR* may also represent a VS predisposition gene.

5.4.3. Investigation of rs1556516 genotype effect on VS presentation age

To assess if risk allele G at SNP rs1556516 conferred an increased risk of earlier age at VS presentation within cases, we performed a Kaplan-Meier survival analysis, results are shown figure 8. The 668 cases with age at onset data were grouped by genotype, CC = 115 cases, CG = 294 cases, GG = 259 cases. Age at onset was plotted against the proportion of patients within the genotype group with VS presentation. A log-rank test found no significant difference between the survival curves (P = 0.1537). The mean ($\bar{x}$) and interquartile ranges (IQR) of age at VS onset in years were similar for each genotype group CC ($\bar{x}$ = 42.3, IQR = 29.5), CG ($\bar{x}$ = 40.2, IQR = 28), GG ($\bar{x}$ = 42.4, IQR = 33.5).

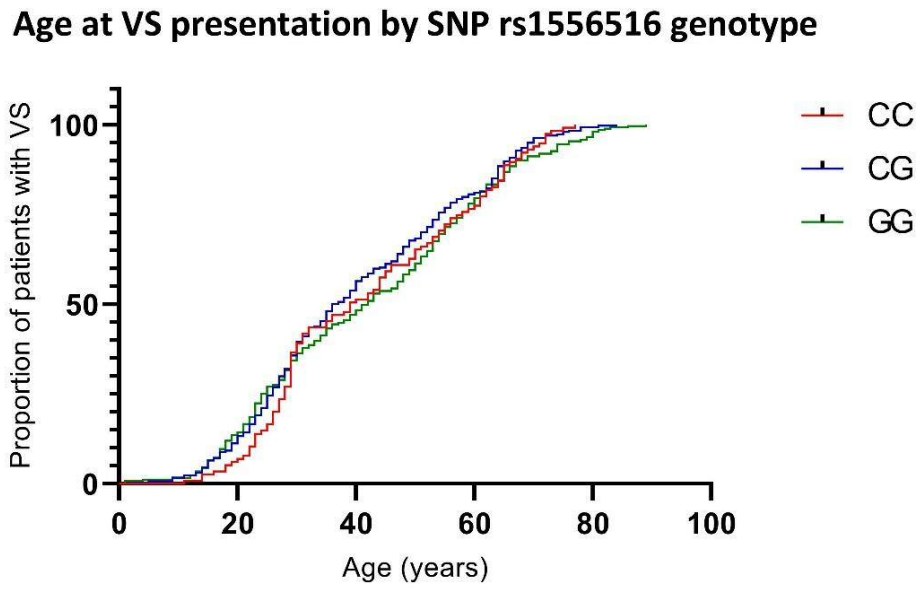

Figure 8. Kaplan-Meier survival curve of age at VS presentation by genotype group at SNP rs1556516.

5.5. Discussion

We have conducted a primary GWAS investigating novel genomic risk loci in association with VS development, which identified a susceptibility locus for sporadic VS risk. Though genome-wide significance (*P*-value < $5x10^{-8}$) at several potential risk loci identified in stages 1 or 2 was not replicated in the reciprocal sub-sets, the genome-wide significant risk locus at 9p21.3 (*P*-value = 1.47e-13) identified in the combined cohort reached *P*-values (< $1x10^{-6}$) suggestive of association with VS risk in both stage 1 and 2 of analysis, with highly similar OR values. Whilst this does not meet the criteria for a formal replication set, the data are compellingly similar in association outcomes at the 9p21.3 locus.

ANRIL silencing has been associated with cell growth arrest and increased expression of the proteins encoded by *CDKN2A/B* within the INK4 locus [35]. Deletion and deregulation of the INK4 region adjacent to *ANRIL* has been previously associated with multiple cancer types [36,37] and somatic loss of heterozygosity (LOH) of the locus has been observed frequently in tumour samples, including neurofibromatosis type 1 (NF1) plexiform neurofibromas [38-40]. Mouse models developed with knockouts of the different proteins encoded within the INK4 locus exhibit predisposition to spontaneous tumour development in comparison to their wild-type litter mates [41].

ANRIL has also been implicated in the dysregulation of inflammatory genes, including *IL6* and *IL8* [35]. Inflammatory stimuli such as TNF-α and IL-1β, activate transcription factor NF-κB, which has been demonstrated to interact directly with the promoter of *ANRIL*, inducing transcription [35]. Pro-inflammatory cytokines, including IL-1β and IL-6, have been demonstrated to exhibit increased expression in human VS tissue compared to normal vestibular nerve samples [42]. Moreover, TNF-α expression has been observed in, and associated with, the proliferation of Schwann cells, which may act in an autocrine model of cell signalling [42]. It is also hypothesised that the expression of pro-inflammatory cytokines in the tumour microenvironment results in the recruitment of inflammatory cells, such as macrophages, causing increased VS tumour growth [43,44].

NF-κB signalling has been observed to modulate drug response in lung cancers associated with activating *EGFR* mutations, in which increased NF-κB expression is associated with resistance to EGFR tyrosine kinase inhibitor drugs [45]. Constitutive signalling of EGFR is associated with activation of a number of oncogenic signalling cascades, including the PI3K/AKT/mTOR and RAS/RAF pathways [46]. RAS has been found to act as a positive regulator of gene products in the INK4 locus, and homozygous deletion of the *CDKN2A* (INK4a/ARF) locus is a frequent finding in melanoma tumours, many of which harbour *NRAS* or *BRAF* mutations [25]. The gene product of *NF2*, merlin, is a negative regulator of NF-κB activity [47] and performs an inhibitory role in the PI3K/AKT/mTOR pathway [48], which can be modulated via RAS signalling [49]. The recurrent observations of component dysregulation within these overlapping pathways has also been similarly described in glioblastoma [50], and provides compelling evidence that the 9p21.3 risk locus is truly associated with VS tumourigenesis.

Whilst there are currently no published GWAS investigating VS risk, a preprint article released in June 2021 by Shringarpure *et al.* outlines a large-scale GWAS investigating a number of self-reported rare disorders, including VS (https://doi.org/10.1101/2021.06.09.21258643). In this study, 1,216 cases with self-reported VS presentation and 168,029 controls were obtained from 23andMe, Inc. One genome-wide significant hit was identified in association with VS on chromosome 9p, lead SNP rs7341786 (*P* = 1.4e-15, OR = 1.395) positioned in *CDKN2B-AS1*. This finding was validated in a UK Biobank case cohort selected

using the phenotype “Benign neoplasm of cranial nerves”. The self-reported nature of cases in the discovery cohort and non-specific phenotyping in the validation set leaves this study vulnerable to non-specific associations. Moreover, known VS predisposing conditions, NF2 and schwannomatosis, were not used as exclusionary criteria for cases. However, within our study SNP rs7341786 also reached genome-wide significance (*P* = 4.46e-11, OR = 0.70). As we present our findings in respect to the reference sequence we report an OR <1 as the reference allele G was found to confer risk of VS. As the preprint article has not been critically reviewed and published we cannot employ it for validation of our findings. However, replication of significant association at *CDKN2B-AS1* suggests the lead risk locus within our study is genuine.

Our investigation into the effect of lead associated SNP rs1556516 on VS presentation age found no significant difference between genotype and age at VS presentation (figure 8). This suggests that the increased risk of VS conferred by SNP rs1556516 is not age-dependent and may be influenced by other variables such as genotypes at other loci or environmental stimuli. SNP rs1556516 may confer an increased risk to subtle dysregulation of a single component within the highly complex aforementioned oncogenic pathways. As multiple regulatory networks often exist within signalling pathways [48,49] it is reasonable to assume that variants within them do not always result in linear outcome correlations. Moreover, it is possible that rs1556516 represents a proxy SNP for an uncharacterised risk variant in high LD with this marker.

There are a number of limitations associated with the staged analysis conducted in this study. Case samples were obtained from similar sources in both stage 1 and stage 2. Similarly, controls for both stages were obtained from the same database. The shared source of samples in stage 1 and stage 2 may introduce bias within the association analysis. Moreover, the separation into stage 1 and stage 2 analysis results in a small number of case samples, reducing the statistical power of effect detection. However, the staged analysis was conducted prospectively as stage 1 data was available before genotyping was conducted in stage 2 case samples at a different facility. As a risk locus of genome-wide significance was observed in stage 1 we chose to analyse stage 2 independently to investigate if the same region of association could be replicated. The ability to detect suggestive and

significant risk loci associations in the smaller sub-sets of analyses suggests that the effect size of the associated alleles is greater than assumed in the initial power calculation for the study.

We acknowledge the limitation of the cohort size for the staged analysis and therefore provide a combined analysis cohort with an appropriate total number of case samples for sufficient statistical power. As sVS is a relatively rare disorder, sample availability is limited and therefore the prospect of conducting an independent validation association analysis, in the UK, is limited. Performance of replication GWAS in sVS requires collaboration with other specialised institutions internationally to form a validation cohort.

In conclusion, we have identified a susceptibility locus for sporadic VS at chromosome 9p21. Gene products within this region have demonstrated oncogenic roles, with pathway associations linked to VS tumourigenesis. Further investigation of the 9p21.3 locus in somatic VS samples may represent an interesting line of future work. LOH of the region encompassing *NF2* is a frequent observation in somatic VS samples but does not account for all cases [51]. It is possible that LOH of the 9p21.3 locus may represent a mutational hit in VS tumours without observed *NF2* loss. Whilst we did not detect an association between the 9p21.3 susceptibility locus genotype and VS age at onset within this cohort, the region may act as a risk modifier in other patient groups. Future work to delineate the effect of this region on VS risk may be performed in NF2 patients, exploring a potential association between genotype at the 9p21.3 locus and VS presentation age.

5.6. Acknowledgements

This research was funded by the Manchester National Institute for Health Research (NIHR) Biomedical Research Centre (IS-BRC-1215-20007). The views expressed are those of the author(s) and not necessarily those of the NHS, the NIHR or the Department of Health.

This research has been conducted using data from the UK Biobank resource, a major biomedical database. Project ID: 50720.

We thank the Oxford Genomics Centre at the Wellcome Centre for Human Genetics (funded by Wellcome Trust grant reference 090532/Z/09/Z) for the generation of Genotyping data.

5.7. References

1. Kentala E, Pyykkö I. Clinical picture of vestibular schwannoma. Auris Nasus Larynx. Jan 2001;28(1):15-22.

2. Evans DG, Moran A, King A, Saeed S, Gurusinghe N, Ramsden R. Incidence of vestibular schwannoma and neurofibromatosis 2 in the North West of England over a 10-year period: higher incidence than previously thought. Otol Neurotol. Jan 2005;26(1):93-7.

3. Kshettry VR, Hsieh JK, Ostrom QT, Kruchko C, Barnholtz-Sloan JS. Incidence of vestibular schwannomas in the United States. J Neurooncol. Sep 2015;124(2):223-8. doi:10.1007/s11060-015-1827-9

4. Kleijwegt M, Ho V, Visser O, Godefroy W, van der Mey A. Real Incidence of Vestibular Schwannoma? Estimations From a National Registry. Otol Neurotol. 10 2016;37(9):1411-7. doi:10.1097/MAO.0000000000001169

5. Ostrom QT, Cioffi G, Waite K, Kruchko C, Barnholtz-Sloan JS. CBTRUS Statistical Report: Primary Brain and Other Central Nervous System Tumours Diagnosed in the United States in 2014-2018. Neuro Oncol. 10 05 2021;23(12 Suppl 2):iii1-iii105. doi:10.1093/neuonc/noab200

6. Evans DG, Huson SM, Donnai D, et al. A clinical study of type 2 neurofibromatosis. Q J Med. Aug 1992;84(304):603-18.

7. Parry DM, Eldridge R, Kaiser-Kupfer MI, Bouzas EA, Pikus A, Patronas N. Neurofibromatosis 2 (NF2): clinical characteristics of 63 affected individuals and clinical evidence for heterogeneity. Am J Med Genet. Oct 1994;52(4):450-61. doi:10.1002/ajmg.1320520411

8. Smith MJ, Isidor B, Beetz C, et al. Mutations in LZTR1 add to the complex heterogeneity of schwannomatosis. Neurology. Jan 2015;84(2):141-7. doi:10.1212/WNL.0000000000001129

9. Ron E, Modan B, Boice JD, et al. Tumours of the brain and nervous system after radiotherapy in childhood. N Engl J Med. Oct 1988;319(16):1033-9. doi:10.1056/NEJM198810203191601

10. Hemminki K, Tretli S, Sundquist J, Johannesen TB, Granström C. Familial risks in nervous-system tumours: a histology-specific analysis from Sweden and Norway. Lancet Oncol. May 2009;10(5):481-8. doi:10.1016/S1470-2045(09)70076-2

11. Evans DG, Wallace AJ, Hartley C, et al. Familial unilateral vestibular schwannoma is rarely caused by inherited variants in the NF2 gene. Laryngoscope. Oct 2018;doi:10.1002/lary.27554

12. Heineman TE, Evans DG, Campagne F, Selesnick SH. In Silico Analysis of NF2 Gene Missense Mutations in Neurofibromatosis Type 2: From Genotype to Phenotype. Otol Neurotol. Jun 2015;36(5):908-14. doi:10.1097/MAO.0000000000000639

13. Smith MJ, Kulkarni A, Rustad C, et al. Vestibular schwannomas occur in schwannomatosis and should not be considered an exclusion criterion for clinical diagnosis. Am J Med Genet A. Jan 2012;158A(1):215-9. doi:10.1002/ajmg.a.34376

14. Sudlow C, Gallacher J, Allen N, et al. UK biobank: an open access resource for identifying the causes of a wide range of complex diseases of middle and old age. PLoS Med. Mar 2015;12(3):e1001779. doi:10.1371/journal.pmed.1001779

15. Das S, Forer L, Schönherr S, et al. Next-generation genotype imputation service and methods. Nat Genet. 10 2016;48(10):1284-1287. doi:10.1038/ng.3656

16. Wang H, Thomas DC, Pe'er I, Stram DO. Optimal two-stage genotyping designs for genome-wide association scans. Genet Epidemiol. May 2006;30(4):356-68. doi:10.1002/gepi.20150

17. Skol AD, Scott LJ, Abecasis GR, Boehnke M. Optimal designs for two-stage genome-wide association studies. Genet Epidemiol. Nov 2007;31(7):776-88. doi:10.1002/gepi.20240

18. Yu W, Gius D, Onyango P, et al. Epigenetic silencing of tumour suppressor gene p15 by its antisense RNA. Nature. Jan 10 2008;451(7175):202-6. doi:10.1038/nature06468

19. Cunnington MS, Santibanez Koref M, Mayosi BM, Burn J, Keavney B. Chromosome 9p21 SNPs Associated with Multiple Disease Phenotypes Correlate with ANRIL Expression. PLoS Genet. Apr 2010;6(4):e1000899. doi:10.1371/journal.pgen.1000899

20. Pasmant E, Sabbagh A, Vidaud M, Bièche I. ANRIL, a long, noncoding RNA, is an unexpected major hotspot in GWAS. FASEB J. Feb 2011;25(2):444-8. doi:10.1096/fj.10-172452

21. Consortium WTCC. Genome-wide association study of 14,000 cases of seven common diseases and 3,000 shared controls. Nature. Jun 07 2007;447(7145):661-78. doi:10.1038/nature05911

22. Helgadottir A, Thorleifsson G, Magnusson KP, et al. The same sequence variant on 9p21 associates with myocardial infarction, abdominal aortic aneurysm and intracranial aneurysm. Nat Genet. Feb 2008;40(2):217-24. doi:10.1038/ng.72

23. Pasmant E, Laurendeau I, Héron D, Vidaud M, Vidaud D, Bièche I. Characterization of a germ-line deletion, including the entire INK4/ARF locus, in a melanoma-neural system tumour family: identification of ANRIL, an antisense noncoding RNA whose expression coclusters with ARF. Cancer Res. Apr 15 2007;67(8):3963-9. doi:10.1158/0008-5472.CAN-06-2004

24. Shete S, Hosking FJ, Robertson LB, et al. Genome-wide association study identifies five susceptibility loci for glioma. Nat Genet. Aug 2009;41(8):899-904. doi:10.1038/ng.407

25. Kim WY, Sharpless NE. The regulation of INK4/ARF in cancer and aging. Cell. Oct 20 2006;127(2):265-75. doi:10.1016/j.cell.2006.10.003

26. Sargen MR, Merrill SL, Chu EY, Nathanson KL. CDKN2A mutations with p14 loss predisposing to multiple nerve sheath tumours, melanoma, dysplastic naevi and internal malignancies: a case series and review of the literature. Br J Dermatol. Oct 2016;175(4):785-9. doi:10.1111/bjd.14485

27. Simon M, Voss D, Park-Simon TW, Mahlberg R, Köster G. Role of p16 and p14ARF in radio- and chemosensitivity of malignant gliomas. Oncol Rep. Jul 2006;16(1):127-32.

28. Topalidou I, Cattin-Ortolá J, Hummer B, Asensio CS, Ailion M. EIPR1 controls dense-core vesicle cargo retention and EARP complex localization in insulin-secreting cells. Mol Biol Cell. 01 01 2020;31(1):59-79. doi:10.1091/mbc.E18-07-0469

29. Gondré-Lewis MC, Park JJ, Loh YP. Cellular mechanisms for the biogenesis and transport of synaptic and dense-core vesicles. Int Rev Cell Mol Biol. 2012;299:27-115. doi:10.1016/B978-0-12-394310-1.00002-3

30. Li Q, Wang Z, Zong L, et al. Allele-specific DNA methylation maps in monozygotic twins discordant for psychiatric disorders reveal that disease-associated switching at the EIPR1 regulatory loci modulates neural function. Mol Psychiatry. May 07 2021;doi:10.1038/s41380-021-01126-w

31. Wang K, Yamamoto H, Chin JR, Werb Z, Vu TH. Epidermal growth factor receptor-deficient mice have delayed primary endochondral ossification because of defective osteoclast recruitment. J Biol Chem. Dec 17 2004;279(51):53848-56. doi:10.1074/jbc.M403114200

32. Tai AL, Sham JS, Xie D, et al. Co-overexpression of fibroblast growth factor 3 and epidermal growth factor receptor is correlated with the development of nonsmall cell lung carcinoma. Cancer. Jan 01 2006;106(1):146-55. doi:10.1002/cncr.21581

33. Weinberg F, Peckys DB, de Jonge N. EGFR Expression in HER2-Driven Breast Cancer Cells. Int J Mol Sci. Nov 27 2020;21(23)doi:10.3390/ijms21239008

34. Kinnersley B, Labussière M, Holroyd A, et al. Genome-wide association study identifies multiple susceptibility loci for glioma. Nat Commun. Oct 01 2015;6:8559. doi:10.1038/ncomms9559

35. Zhou X, Han X, Wittfeldt A, et al. Long non-coding RNA ANRIL regulates inflammatory responses as a novel component of NF-κB pathway. RNA Biol. 2016;13(1):98-108. doi:10.1080/15476286.2015.1122164

36. Arcellana-Panlilio MY, Egeler RM, Ujack E, et al. Evidence of a role for the INK4 family of cyclin-dependent kinase inhibitors in ovarian granulosa cell tumours. Genes Chromosomes Cancer. Oct 2002;35(2):176-81. doi:10.1002/gcc.10108

37. Wiedemeyer R, Brennan C, Heffernan TP, et al. Feedback circuit among INK4 tumour suppressors constrains human glioblastoma development. Cancer Cell. Apr 2008;13(4):355-64. doi:10.1016/j.ccr.2008.02.010

38. Kumar R, Smeds J, Lundh Rozell B, Hemminki K. Loss of heterozygosity at chromosome 9p21 (INK4-p14ARF locus): homozygous deletions and mutations in the p16 and p14ARF genes in sporadic primary melanomas. Melanoma Res. Apr 1999;9(2):138-47. doi:10.1097/00008390-199904000-00005

39. Tate JG, Bamford S, Jubb HC, et al. COSMIC: the Catalogue Of Somatic Mutations In Cancer. Nucleic Acids Res. 01 2019;47(D1):D941-D947. doi:10.1093/nar/gky1015

40. Pasmant E, Sabbagh A, Masliah-Planchon J, et al. Role of noncoding RNA ANRIL in genesis of plexiform neurofibromas in neurofibromatosis type 1. J Natl Cancer Inst. Nov 2011;103(22):1713-22. doi:10.1093/jnci/djr416

41. Sharpless NE, Ramsey MR, Balasubramanian P, Castrillon DH, DePinho RA. The differential impact of p16(INK4a) or p19(ARF) deficiency on cell growth and tumourigenesis. Oncogene. Jan 15 2004;23(2):379-85. doi:10.1038/sj.onc.1207074

42. Taurone S, Bianchi E, Attanasio G, et al. Immunohistochemical profile of cytokines and growth factors expressed in vestibular schwannoma and in normal vestibular nerve tissue. Mol Med Rep. Jul 2015;12(1):737-45. doi:10.3892/mmr.2015.3415

43. Lewis D, Roncaroli F, Agushi E, et al. Inflammation and Vascular Permeability Correlate With Growth in Sporadic Vestibular Schwannoma. Neuro Oncol. Nov 2018;doi:10.1093/neuonc/noy177

44. Hannan CJ, Lewis D, O'Leary C, et al. The inflammatory microenvironment in vestibular schwannoma. Neurooncol Adv. 2020 Jan-Dec 2020;2(1):vdaa023. doi:10.1093/noajnl/vdaa023

45. Bivona TG, Hieronymus H, Parker J, et al. FAS and NF-κB signalling modulate dependence of lung cancers on mutant EGFR. Nature. Mar 24 2011;471(7339):523-6. doi:10.1038/nature09870

46. Shostak K, Chariot A. EGFR and NF-κB: partners in cancer. Trends Mol Med. Jun 2015;21(6):385-93. doi:10.1016/j.molmed.2015.04.001

47. Ammoun S, Provenzano L, Zhou L, et al. Axl/Gas6/NFκB signalling in schwannoma pathological proliferation, adhesion and survival. Oncogene. Jan 16 2014;33(3):336-46. doi:10.1038/onc.2012.587

48. Rong R, Tang X, Gutmann DH, Ye K. Neurofibromatosis 2 (NF2) tumour suppressor merlin inhibits phosphatidylinositol 3-kinase through binding to PIKE-L. Proc Natl Acad Sci U S A. Dec 28 2004;101(52):18200-5. doi:10.1073/pnas.0405971102

49. Vivanco I, Sawyers CL. The phosphatidylinositol 3-Kinase AKT pathway in human cancer. Nat Rev Cancer. Jul 2002;2(7):489-501. doi:10.1038/nrc839

50. Cancer Genome Atlas Research Network. Comprehensive genomic characterization defines human glioblastoma genes and core pathways. Nature. Oct 23 2008;455(7216):1061-8. doi:10.1038/nature07385

51. Hadfield KD, Smith MJ, Urquhart JE, et al. Rates of loss of heterozygosity and mitotic recombination in NF2 schwannomas, sporadic vestibular schwannomas and schwannomatosis schwannomas. Oncogene. Nov 2010;29(47):6216-21. doi:10.1038/onc.2010.363

5.8. Supplementary data

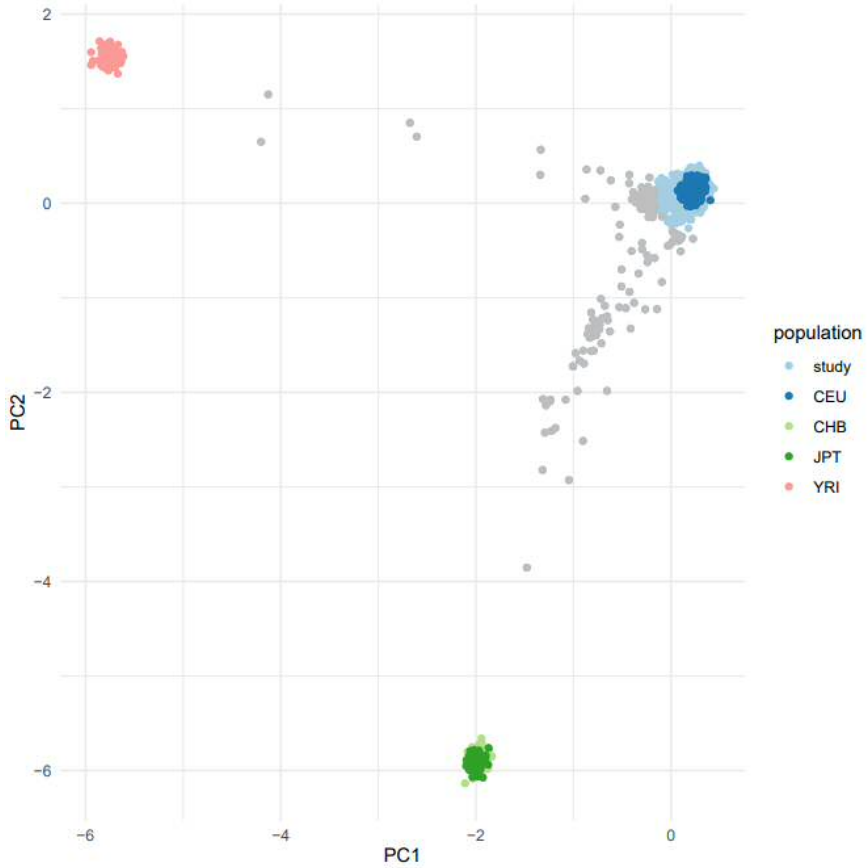

Supplementary figure 1. Combined cohort case population analysis using HapMap3 data. Grey and light blue markers indicate study samples in the combined analysis. Grey samples were deemed ancestral outliers and were excluded from downstream association analysis.

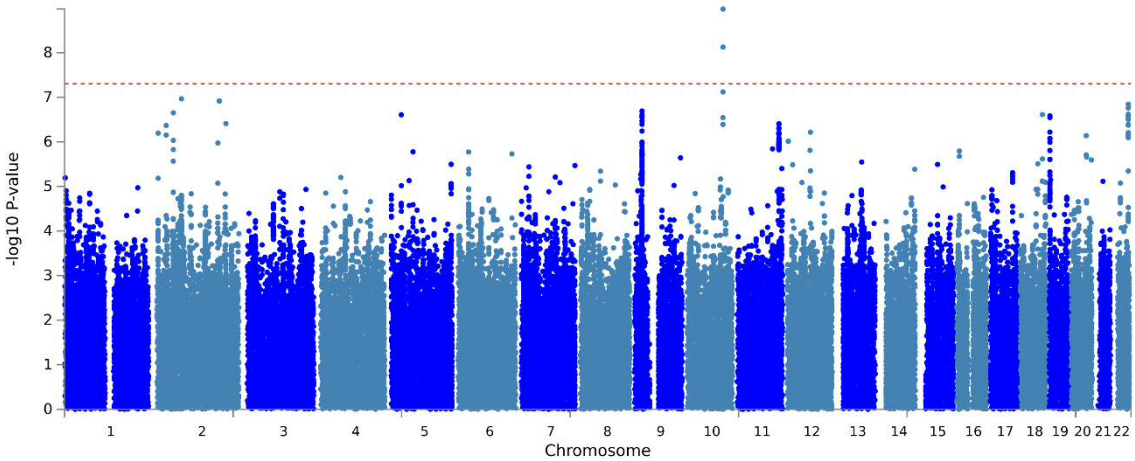

Supplementary figure 2. Manhattan plot of MAF >1% SNP *P*-values in the GWAS stage 1 cohort. Red dashed line represents *P*-value = $5x10^{-8}$.

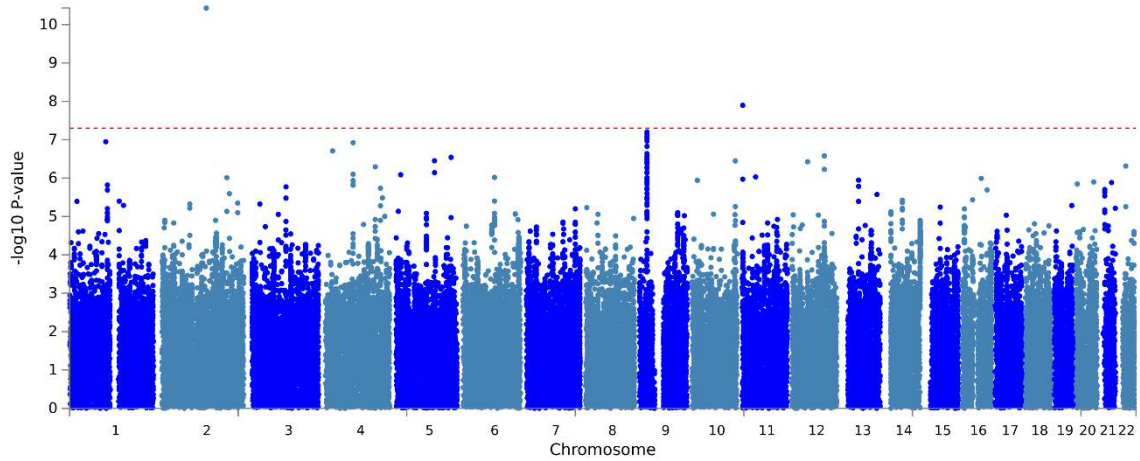

Supplementary figure 3. Manhattan plot of MAF >1% SNP *P*-values in the GWAS stage 2 cohort. Red dashed line represents *P*-value = $5x10^{-8}$.

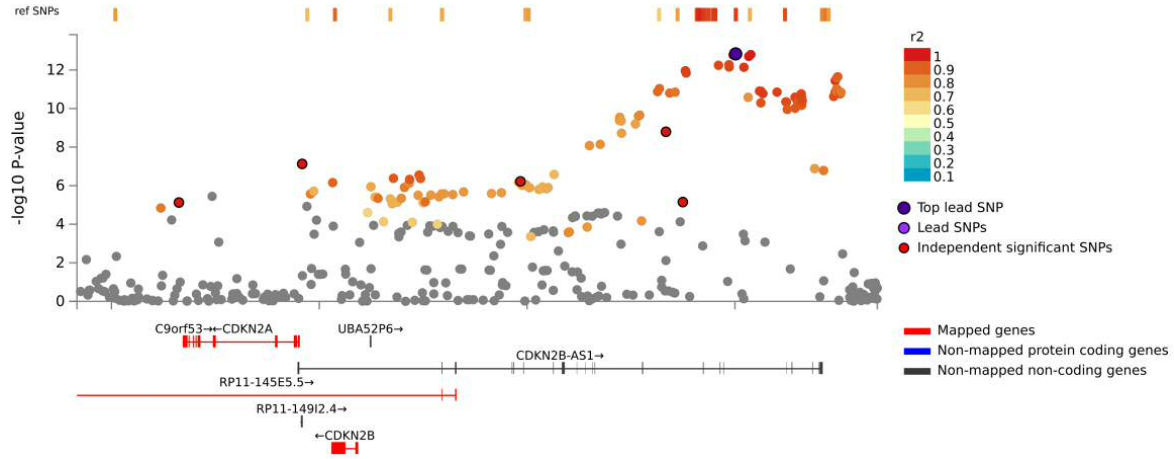

Supplementary figure 4. Localised plot of SNP *P*-values in the combined association analysis at the 9p21.3 risk locus.

Analysis	Case samples	Control samples	SNPs
Stage 1	456	2,639	503,935
Stage 2	417	2,635	517,686
Combined	870	5,273	492,266

Supplementary table 2. Cohort summaries, sample and SNP numbers following initial QC.

Analysis	Cases	Controls
Stage 1	407	2,624
Stage 2	378	2,616
Combined	776	5,221

Supplementary table 3. Cohort summaries, sample numbers post IBD and ancestral analysis.

SNP	Locus	Chromosome	Position	Other allele	Reference allele	Stage	MAF	OR (95% CI)	β	SE	*P* - value	Annotated genes	Associated traits
rs111843780	10q25.1	10	107370215	T	A	1	0.02	2.894 (1.95-4.29)	1.645	0.285	7.5E-09	Intergenic	-
rs112277746	10q25.1	10	107394416	A	C	1	0.019	3.042 (2.03-4.56)	1.867	0.306	1.05E-09	Intergenic	-

Supplementary table 4. Summary statistics for the stage 1 association risk locus 10q25.1.

SNP	Locus	Chromosome	Position	Other allele	Reference allele	Stage	MAF	OR (95% CI)	β	SE	*P* - value	Annotated genes	Associated traits
rs565735761	2q21.1	2	131942065	G	A	2	0.013	2.926 (1.77-4.83)	3.426	0.518	3.69E-11	*PLEKHB2*	-
rs143328874	11p15.5	11	2330246	C	T	2	0.023	2.657 (1.82-3.89)	1.583	0.278	1.27E-08	*TSPAN32*	-

Supplementary table 5. Summary statistics for risk loci in stage 2 association analysis.

rsID	Chromosome	Position	Ref allele	Other allele	All MAF	Cases MAF	Controls MAF	All OR	All OR lower	All OR upper	Frequentist Additive *P*-value
rs10811647	9	22065002	C	G	0.40	0.34	0.41	0.73	0.65	0.82	8.37E-09
rs10811650	9	22067593	A	G	0.40	0.34	0.41	0.73	0.65	0.82	7.18E-09
rs10757269	9	22072264	A	G	0.46	0.39	0.47	0.72	0.64	0.80	4.23E-10
rs9632884	9	22072301	G	C	0.46	0.39	0.47	0.71	0.64	0.80	2.84E-10
rs9632885	9	22072638	G	A	0.46	0.39	0.47	0.72	0.64	0.80	4.40E-10
rs10757270	9	22072719	A	G	0.41	0.34	0.42	0.72	0.64	0.80	1.90E-09
rs1831733	9	22076071	T	C	0.45	0.38	0.47	0.72	0.64	0.80	6.33E-10
rs10757271	9	22076795	A	G	0.47	0.39	0.48	0.71	0.64	0.79	2.44E-10
rs10811652	9	22077085	A	C	0.47	0.39	0.48	0.71	0.64	0.79	2.20E-10
rs10116277	9	22081397	G	T	0.46	0.38	0.47	0.69	0.62	0.77	1.32E-11
rs6475606	9	22081850	C	T	0.47	0.39	0.48	0.69	0.62	0.77	9.26E-12
rs1333040	9	22083404	C	T	0.43	0.50	0.42	0.72	0.65	0.81	1.61E-09
rs1537370	9	22084310	C	T	0.46	0.38	0.47	0.70	0.62	0.78	1.57E-11
rs1970112	9	22085598	T	C	0.45	0.38	0.47	0.69	0.62	0.78	1.42E-11
rs10738606	9	22088090	A	T	0.47	0.39	0.48	0.68	0.61	0.76	1.11E-12
rs10738607	9	22088094	A	G	0.47	0.39	0.48	0.68	0.61	0.76	1.10E-12
rs10757272	9	22088260	C	T	0.47	0.39	0.48	0.68	0.61	0.76	1.44E-12
rs10757274	9	22096055	A	G	0.47	0.39	0.49	0.68	0.61	0.75	5.73E-13
rs4977574	9	22098574	A	G	0.47	0.39	0.49	0.68	0.61	0.75	5.33E-13
rs2891168	9	22098619	A	G	0.47	0.39	0.48	0.68	0.61	0.76	7.06E-13
rs1537371	9	22099568	C	A	0.48	0.39	0.49	0.67	0.60	0.75	1.68E-13
rs1556516	9	22100176	G	C	0.48	0.39	0.49	0.67	0.60	0.75	1.47E-13
rs7859727	9	22102165	C	T	0.47	0.39	0.48	0.68	0.61	0.76	7.22E-13
rs1537372	9	22103183	G	T	0.42	0.34	0.43	0.70	0.62	0.78	2.62E-11
rs1537373	9	22103341	T	G	0.48	0.39	0.49	0.67	0.60	0.75	1.98E-13
rs1333042	9	22103813	A	G	0.48	0.39	0.49	0.67	0.60	0.75	1.58E-13
rs7859362	9	22105927	T	C	0.49	0.41	0.50	0.70	0.63	0.78	1.24E-11
rs10757275	9	22106225	G	A	0.48	0.41	0.49	0.70	0.63	0.78	5.08E-11
rs6475609	9	22106271	A	G	0.49	0.41	0.50	0.70	0.63	0.78	1.27E-11

Supplementary table 6. SNPs with *P*-values < $5x10^{-8}$ in combined association analysis at the 9p21 risk locus. Continued next page.

rs1333043	9	22106731	T	A	0.49	0.42	0.50	0.70	0.63	0.78	1.68E-11
rs1412834	9	22110131	T	C	0.49	0.42	0.51	0.70	0.63	0.78	1.40E-11
rs7341786	9	22112241	A	C	0.50	0.42	0.51	0.70	0.63	0.78	4.46E-11
rs7341791	9	22112427	A	G	0.50	0.42	0.51	0.70	0.63	0.78	4.58E-11
rs10511701	9	22112599	T	C	0.49	0.41	0.50	0.71	0.64	0.79	1.11E-10
rs10733376	9	22114469	G	C	0.49	0.42	0.51	0.70	0.63	0.78	2.58E-11
rs10738609	9	22114495	A	G	0.48	0.41	0.49	0.71	0.64	0.79	9.63E-11
rs2383206	9	22115026	A	G	0.49	0.42	0.50	0.70	0.63	0.78	4.03E-11
rs944797	9	22115286	T	C	0.49	0.42	0.50	0.70	0.63	0.78	4.04E-11
rs1004638	9	22115589	A	T	0.49	0.42	0.51	0.70	0.63	0.78	2.49E-11
rs2383207	9	22115959	A	G	0.50	0.42	0.51	0.70	0.63	0.78	1.73E-11
rs1537374	9	22116046	A	G	0.49	0.42	0.51	0.70	0.63	0.78	2.66E-11
rs1537375	9	22116071	T	C	0.49	0.41	0.50	0.71	0.63	0.79	6.78E-11
rs1537376	9	22116220	T	C	0.49	0.42	0.50	0.70	0.63	0.78	4.04E-11
rs10738610	9	22123766	A	C	0.48	0.40	0.49	0.70	0.63	0.78	2.37E-11
rs1333046	9	22124123	T	A	0.48	0.40	0.49	0.70	0.63	0.78	1.42E-11
rs7857118	9	22124140	A	T	0.49	0.41	0.50	0.69	0.62	0.77	3.60E-12
rs10757277	9	22124450	A	G	0.47	0.39	0.48	0.70	0.62	0.78	1.18E-11
rs10811656	9	22124472	C	T	0.47	0.39	0.48	0.70	0.62	0.78	1.31E-11
rs10757278	9	22124477	A	G	0.47	0.39	0.48	0.69	0.62	0.77	9.38E-12
rs1333047	9	22124504	A	T	0.48	0.40	0.49	0.69	0.62	0.77	2.59E-12
rs10757279	9	22124630	A	G	0.47	0.39	0.48	0.70	0.62	0.78	1.04E-11
rs4977575	9	22124744	C	G	0.48	0.40	0.49	0.69	0.62	0.77	2.24E-12
rs1333048	9	22125347	A	C	0.49	0.41	0.50	0.70	0.63	0.78	1.71E-11
rs1333049	9	22125503	G	C	0.47	0.39	0.48	0.70	0.63	0.78	1.43E-11

Supplementary table 6. SNPs with *P*-values < $5x10^{-8}$ in combined association analysis at the 9p21 risk locus.

Note: minor allele frequency not necessarily risk allele.

Genomic Locus	rsID	Chr	Position	*P*-value	Start	End
1	rs145283845	1	37206287	5.71E-06	37206287	37206287
2	rs6683123	1	74106487	1.90E-06	74019038	74129905
3	rs73910511	2	3348017	6.34E-08	3312411	3432289
4	rs143566853	2	23960606	2.06E-06	23894755	24617202
5	rs113909770	2	143641551	5.49E-06	143641551	143679973
6	rs139839818	3	23775703	1.00E-06	23775703	23786838
7	rs34779176	3	88541612	1.28E-06	88502200	88595799
8	rs7668541	4	152216154	6.80E-06	151598989	152222739
9	rs11734167	4	157015269	8.33E-06	156986594	157028207
10	rs115403498	5	5167481	3.37E-06	5167481	5167481
11	rs180755891	5	171721711	8.68E-06	171721711	171726702
12	rs9394822	6	41632629	8.82E-06	41632629	41639575
13	rs2670396	6	67208679	5.79E-06	67192661	67247455
14	rs2293286	6	161550999	4.53E-06	161550999	161550999
15	rs11238349	7	55156071	1.05E-07	55131064	55161043
16	rs147936255	7	73992743	4.11E-06	73992743	73992743
17	rs76423404	8	30906111	7.69E-06	30906111	30906111
18	rs311398	8	55080059	2.37E-06	55080059	55128007
19	**rs1556516**	**9**	**22100176**	**1.47E-13**	**21950446**	**22125503**
20	rs113377951	9	76779423	6.30E-06	76779423	76779423
21	rs4934068	10	86827609	4.74E-06	86668927	86914480
22	rs7087412	10	102080338	2.92E-06	102080338	102080338
23	rs112277746	10	107394416	3.76E-06	107105955	107636903
24	rs79873818	10	128196189	1.18E-06	128196189	128224320

Supplementary table 7. Genomic risk loci with P-value < $1x10^{-6}$ in combined association analysis. Continued next page.

25	rs138641986	11	2426649	2.48E-06	2426649	2426649
26	rs140318868	11	129232051	8.67E-06	129232051	129232051
27	rs118082474	12	20186669	2.02E-06	20186669	20186669
28	rs186814577	12	25579059	8.17E-06	25537855	25668071
29	rs10850997	12	119046134	5.26E-06	119016407	119135447
30	rs4770989	13	27049046	5.35E-06	27036747	27049613
31	rs9599965	13	73081033	1.48E-06	73081033	73085550
32	rs111433582	13	105749758	2.74E-07	105749758	105749758
33	rs12886404	14	88200639	2.03E-06	88154129	88208532
34	rs111843049	19	876357	9.03E-06	876357	876357
35	rs137872210	19	2155040	2.21E-06	2103255	2248717
36	rs13050340	21	40205813	5.85E-06	40185397	40223337
37	rs2078795	22	23204972	3.23E-06	23204972	23204972

Supplementary table 7. Genomic risk loci with *P*-value < $1x10^{-6}$ in combined association analysis.

Locus with *P*-value < $5x10^{-8}$ highlighted in bold.

6. Generation of an *in vitro* model for vestibular schwannoma predisposition in a biologically relevant cell type for pre-clinical therapy screening

Generation of an *in vitro* model for vestibular schwannoma predisposition in a biologically relevant cell type for pre-clinical therapy screening

Katherine V Sadler[1,2], Cristina Perez-Becerril[1,2], Antony D Adamson[3], David Chapman[4], D Gareth Evans[1,2] and Miriam J Smith[1,2].

[1]Manchester Centre for Genomic Medicine, St Mary's Hospital, Manchester Academic Health Sciences Centre (MAHSC), Manchester, UK

[2]Division of Evolution, Infection and Genomics, School of Biological Sciences, Faculty of Biology, Medicine and Health, University of Manchester, Manchester, UK

[3]Genome Editing Unit Core Facility, Faculty of Biology, Medicine and Health, University of Manchester, Manchester, UK

[4]Flow Cytometry Core Facility, Faculty of Biology, Medicine and Health, University of Manchester, Manchester, UK

6.1. Abstract

Background

Vestibular schwannomas (VS) are benign tumours that arise from Schwann cells surrounding the vestibulocochlear nerve. The majority of VS occur sporadically without associated germline pathogenic variants. Disease models of tumour predisposition syndrome neurofibromatosis type 2 (NF2) remain most relevant for use in VS therapeutic development. We intended to introduce deep intronic variant *NF2* c.516+232 G>A in the genome of an immortalised Schwann cell line to assess the clinical potential of antisense oligonucleotide (ASO) therapy.

Methods

Designs for both homology directed repair and prime editing CRISPR techniques were explored as methods for introduction of the *NF2* c.516+232 G>A variant into Schwann cell line ipn02.3 2λ. Additionally, pseudo-constructs of the *NF2* gene were designed to generate a reporter system to assess the impact of the *NF2* c.516+232 G>A variant on gene expression. Cells containing reporter constructs were treated with a target ASO to assess if wild type (WT) splicing could be restored in variant cells.

Results

Homology directed repair and prime editing failed to generate a permanent edit of *NF2* c.516+232 G>A into the genome of immortalised Schwann cell line ipn02.3 2λ using CRISPR methodology. This may be due to inaccessibility of the target region for CRISPR-associated nucleases. However, characterisation of cells transduced with exogenous *NF2* variant constructs confirmed the *NF2* c.516+232 G>A variant results in cryptic exon inclusion within a proportion of transcripts and reduces expression of the WT protein. Moreover, we demonstrate that treatment with a sequence-specific ASO appears to restore WT splicing of *NF2*.

Conclusions

Though we were unable to generate a *NF2* c.516+232 G>A variant cell line as an *in vitro* model of VS predisposition, we provide further characterisation of the variant using a construct-based reporter system in a biologically relevant cell type. We demonstrate that ASO treatment is a potential therapy to restore WT splicing in NF2 disease caused by deep intronic variants.

6.2. Background

Vestibular schwannomas (VS) are benign neoplasms that arise on the vestibular branch of the vestibulocochlear nerve. Accounting for approximately 9% of all non-malignant central nervous system tumours [1], growth of VS frequently causes hearing loss, tinnitus and vestibular disequilibrium in affected individuals [2]. VSs are known to occur within the context of tumour suppressor syndromes, NF2 and *LZTR1*-associated schwannomatosis [3-5]. However, the majority of VS present sporadically in patients without identification of germline pathogenic variants [6,7]. Whilst the landscape of inherited genetic risk factors associated with sporadic VS remains uncharacterised, disease models of NF2 and *LZTR1*-associated schwannomatosis remain most relevant for use in VS therapeutic development.

Pathogenic intronic variants hold unique therapeutic potential due to their position within untranslated genomic regions. Cryptic splice sites and other intronic mechanisms of disease may be 'masked' using splice-modulating therapies, such as antisense oligonucleotides (ASO) [8]. Masking of aberrant splicing using such therapies can restore wild-type (WT) splice transcripts and functional gene products [9]. Examples of successful splice-modulating therapies have been developed in a number of disorders [8,9], including NF2 [10]. Castellanos *et al.* (2013) demonstrated that delivery of a mutation-specific ASO can restore WT splicing in patient-derived fibroblasts from an individual with a deep intronic pathogenic variant in *NF2* (c.1447-240 T>A). With examples of familial NF2 caused by deep intronic *NF2* variants [10,11], splice-modulating techniques hold great potential as a method of NF2 gene therapy. Development of splice-modulating therapies requires variant-specific disease models in relevant cell types to facilitate pre-clinical screening of therapeutic reagents.

Whilst it is possible to generate patient-derived cell lines to create disease models, primary cell lines are often challenging to derive and maintain, and many cell types are not readily accessible from patients. Moreover, patient-derived cell lines possess common genetic variation specific to the individual of origin, which may alter the genomic context of a pathogenic variant [12]. Common variants can modify disease risk and presentation, limiting the translation of discoveries made in patient-specific cell models. Use of a standardised cell line to maintain consistencies in genomic context would negate some of the issues surrounding

experiment replicability, but requires the introduction of genetic variants into cell lines through mutagenesis methods.

Plasmid-based techniques, such as site-directed mutagenesis or construct-based expression models, are valuable methods for studying the effects of specific nucleotide changes [13]. Transfection of plasmids designed to exogenously express gene variants enables the study of gene expression and function in disease-relevant cell types. However, plasmid-based methods are mainly transient experiments, where the variant of interest is not incorporated into the host cell genome as the plasmid is lost after a number of cell divisions [14]. Plasmids are often overexpressed in transfected cells and exogenous gene expression removes genomic context information for the region of interest, therefore these models will not be representative of normal physiological gene expression in a cell. Ideal mutagenesis methods would introduce DNA variants directly into the genome of target cells, creating permanent edits stably inherited by daughter cells.

With the development of gene editing technologies such as zinc-finger nucleases [15], TALENs (transcription activator-like effector nucleases) [16] and CRISPR [17] permanent gene editing techniques are available and applied widely across the field of genomic medicine. In many cases, CRISPR has superseded other gene editing techniques, due its relative simplicity, cost and accessibility [18]. Utilising complementary base-pairing to guide DNA cleavage by a CRISPR-associated (Cas) nuclease at sequence-specific sites, CRISPR facilitates the introduction of genetic variants into target cell genomes [17]. Cas nuclease-mediated cleavage is dependent upon the presence of a protospacer adjacent motif (PAM) for recognition of a target site, typically an NGG sequence motif [19]. Cas nuclease DNA cleavage induces endogenous cellular DNA repair mechanisms, such as non-homologous end joining (NHEJ) and homology directed repair (HDR). These mechanisms can be exploited to create gene knock-outs, through NHEJ indel formation, and gene variants, through introduction of mutation containing repair templates incorporated by HDR [20].

Subsequent modifications to Cas nucleases have expanded the possible applications of CRISPR gene editing. Cas9-nickase is a mutated form of the Cas9 nuclease that creates single stranded DNA breaks, or 'nicks' [17,21], which do not

induce NHEJ and therefore reduces the risk of indel formation [22]. Instead, variants can be created or introduced at the target site through chemical modification of bases, or provision of an alternative sequence template.

Prime editing is a CRISPR-based method that employs Cas9-nickase and an additional sequence template that introduces a variant of interest. Prime editing is enabled through the design of an extended prime editing guide RNA (pegRNA), which both specifies the target site and encodes the desired edit [23]. The prime editor complex is comprised of a reverse transcriptase fused to a Cas9-nickase, which binds to the pegRNA that specifies the target genomic site through complementary base-pairing. A reverse transcriptase template sequence incorporated within the pegRNA allows the variant sequence to be directly copied into the target locus [23]. Prime editing displays significantly lower off-target effects and similar efficiency to HDR methods, and facilitates the introduction of variants in a seamless manner, maintaining integrity of the surrounding DNA sequence at the target site. The advantages in specificity and precision that prime editing holds over other gene editing techniques makes it a promising tool in the future of gene editing research.

The aim of this study was to generate a model system for pre-clinical screening of a personalised gene therapy for a known pathogenic intronic variant in *NF2*. We intended to introduce a permanent edit of *NF2* c.516+232 G>A in the genome of an immortalised Schwann cell line, ipn02.3 2λ, through CRISPR-based methodology. The *NF2* c.516+232G>A variant is located in intron 5 of *NF2* and results in the creation of a branch point recognition sequence, activating cryptic exon inclusion 18bp downstream of the base change, NM_000268.4 r.516_517ins516+250_516+355, p.(Arg172_Val173ins*32) [11]. An in-frame stop codon, 32 amino acid residues into the cryptic exon, results in premature termination of the *NF2* protein, see figure 9. Additional characterisation of the mutation and investigation of antisense oligonucleotide splice-modulating therapy was conducted using a plasmid construct containing exons 5 and 6 and intron 5 of both the wild-type (WT) and variant *NF2* gene. Correction of splicing to restore WT protein translation would demonstrate the possibility of developing a personalised gene therapy for NF2 patients with the same variant.

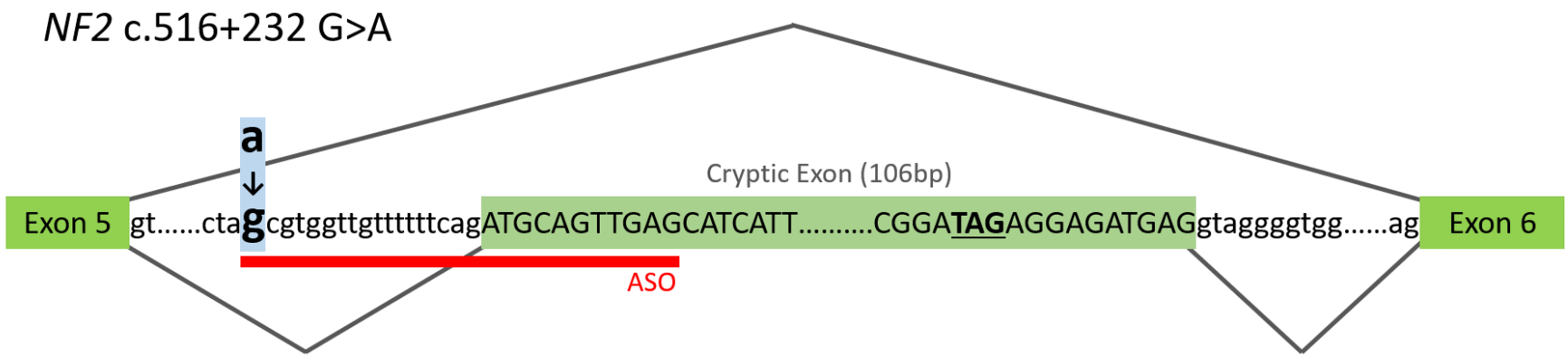

Figure 9. A schematic of the deep intronic *NF2* pathogenic variant c.516+232 G>A.

The G>A base substitution (blue box) creates a branch point recognition sequence that results in transcription of a cryptic exon 18bp downstream, NM_000268.4 r.516_517ins516+250_516+355, p.(Arg172_Val173ins*32). The cryptic exon contains an in-frame stop codon, TAG (bold underlined), causing truncation of the protein product. An antisense oligonucleotide (ASO) coloured red, was designed to bind complementarily to the variant sequence with the intention of masking cryptic exon inclusion.

6.3. Materials and methods

An overview of the main methodology workflows employed in this study can be seen in figure 10.

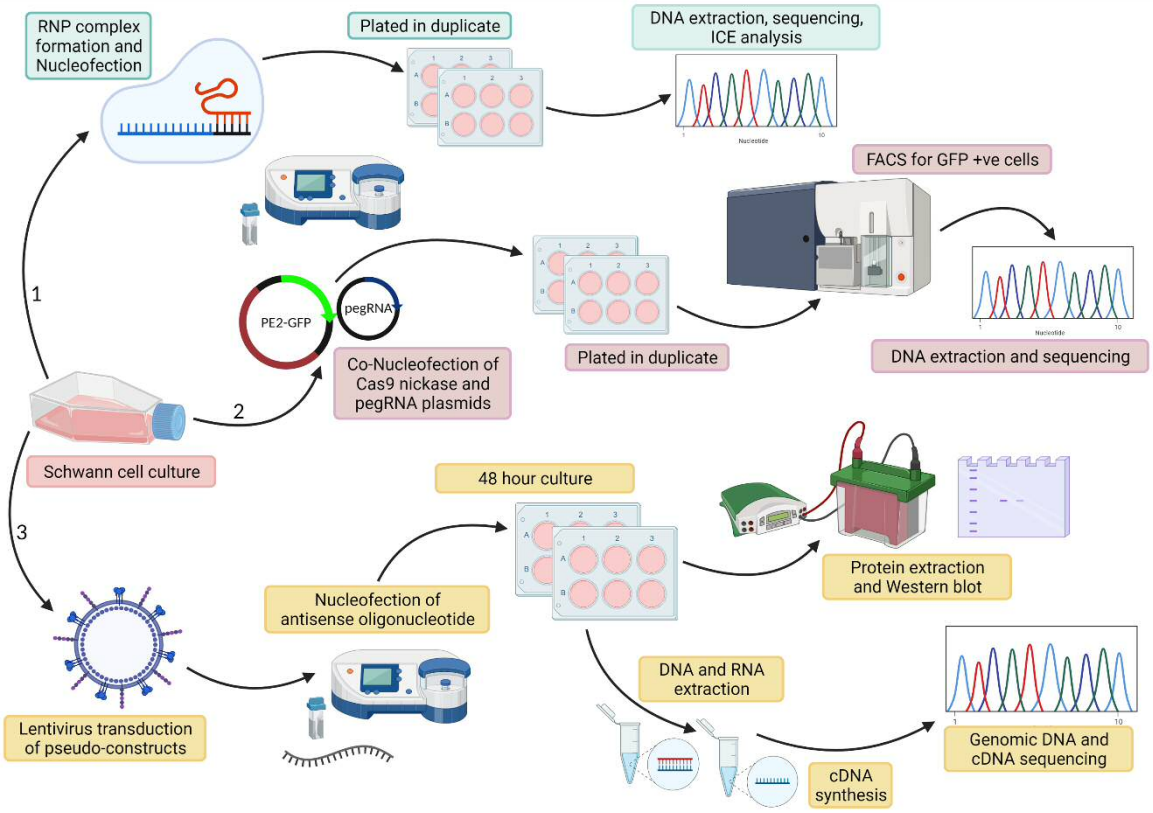

Figure 10. An overview of the three main workflows followed to create and characterise the *NF2* c.516+232 G>A variant in this study.

First, a ribonucleoprotein (RNP) CRISPR assembly and Nucleofection workflow (1) is labelled in blue at the top of the figure. Secondly, the prime editing CRISPR workflow (2) is labelled in purple in the centre of the figure. Finally, lentivirus transduction (3) and downstream analysis of variant *NF2* gene pseudo-constructs is summarised with orange labels at the bottom of the figure. ICE – inference of CRISPR edits. FACS – fluorescence activated cell sorting. GFP – green fluorescent protein. PegRNA – prime editing guide RNA. Figure created with Biorender.com

6.3.1. Cell culture

Adherent immortalised Schwann cell line ipn02.3 2λ, (generated in the laboratory of Dr Margaret Wallace, University of Florida) was used for all workflows in this study. Cells were cultured as described in section 2.7.2.

6.3.2. Genomic samples preparation

Genomic DNA, RNA, protein and plasmid DNA samples were obtained from cultured mammalian cells and transformed *E.coli* as described in section 2.3.

6.3.3. Design of gRNA for CRISPR RNP complex

To assess the capacity of the target variant site (*NF2* c.516+232 G>A) for Cas9 directed double stranded DNA cleavage, three guide RNAs (gRNA) were designed to target NGG PAM sites in the surrounding region for assembly into a RNP (ribonucleoprotein) complex (gRNA designs in table 6, section 2.8.1). Locations of the three gRNAs and anticipated design of homology arms for HDR can be seen in figure 11. A known high efficiency target gRNA (AAVS1) [24] was used as a positive control to assess transfection success (gRNA sequence in table 6, section 2.8.1). Primers were designed to create two different sized fragments for amplification and sequencing characterisation of the control and target regions (table 7, section 2.8.1). Synthego ICE (inference of CRISPR edits) analysis version 2.0 https://ice.synthego.com was used to assess editing efficiency.

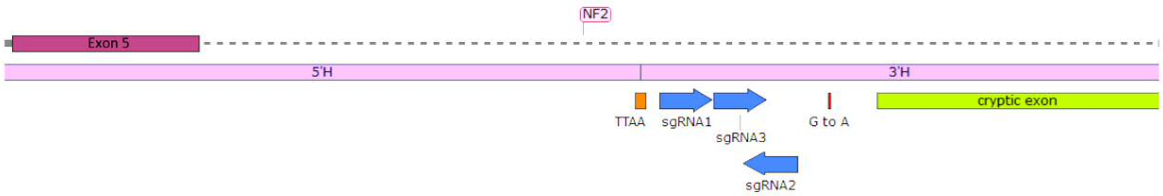

Figure 11. Diagram of the target genomic region of the *NF2* c.516+232 G>A variant. The G>A substitution is highlighted in red. Three single guide RNAs (sgRNA) are labelled with directionality in blue arrows. A TTAA sequence motif is highlighted in orange which is required for piggybac transposase excision of selection marker cassettes. 5' and 3' homology arms flanking the TTAA motif for use as a homology directed repair template are coloured purple.

6.3.4. Piggybac excision

Initial experimental designs were made for HDR facilitated CRISPR methodology, utilising a gRNA:Cas9 RNP complex for DNA cleavage. HDR templates can be designed to contain positive selection markers, such as fluorescence tags and antibiotic resistance genes, to enable efficient

downstream selection of edited cell populations. As introduction of selection markers would not maintain integrity of the genomic sequence surrounding the variant of interest, we planned an additional piggybac transposase step following HDR template inclusion. After HDR template inclusion, cells would be exposed to a piggybacase transposase, facilitating excision of the positive selection marker cassette in an edited cell population, introducing the *NF2* intronic variant in a scar-less manner [25]. To take advantage of piggybacase activity, homology arms are required to be designed flanking a TTAA sequence motif, highlighted in figure 11.

6.3.5. TransIT-X2® transfections

Initial experiments employed the TransIT-X2® dynamic delivery system (Mirus Bio, Madison, WI, USA) for transfection of CRISPR RNP complexes. RNP complexes consisted of EnGen® Spy Cas9 NLS (20µM) (New England Biolabs, Hitchin, UK) and gRNA (100µM) diluted to 50µM (Sigma-Merck, Darmstadt, Germany). Details of reagents and optimisation ratios are found in section 2.7.4.1. RNP components were combined and incubated for 10 minutes at room temperature prior to transfection. Cell media was aspirated and replaced with FBS-supplemented DMEM 24 hours post-transfection. DNA was extracted from transfected cells 48 hours post-transfection. Sanger sequencing (section 2.4.2.3) was performed on extracted DNA and chromatograms were analysed using Synthego ICE tool version 2.0 https://ice.synthego.com to assess editing efficiency.

6.3.6. Nucleofection transfections

Nucleofection was implemented to increase transfection efficiency. Initial optimisation of Nucleofection was performed as detailed in section 2.7.4.2. Subsequent Nucleofections were conducted using the Lonza Amaxa Nucleofector™ kit V (Lonza Group Ltd. Basel, Switzerland). The single cuvette Nucleofector™ 2b Device (Lonza Group Ltd. Basel, Switzerland) was used for all Nucleofections. Approximately $1x10^6$ cells are required per sample for the Nucleofector™ 2b Device. Nucleofection program D-033 was used unless otherwise stated. RNP complexes were formed directly in Nucleofector solution with a 10 minute room temperature incubation prior to addition of

cell suspensions. Full Nucleofection methodology is found in section 2.7.4.2. RNP reagent optimisation is outlined in table 8, section 2.8.1.

6.3.7. Design and assembly of pegRNA for CRISPR prime editing

Design of the *NF2* target prime editing gRNA vector was conducted using pegFinder http://pegfinder.sidichenlab.org/ [accessed 28th May 2021][26] for NGG PAM sites. Oligonucleotide fragment designs for introduction of the *NF2* c.516+232 G>A variant through pegRNA vector assembly are detailed in table 9 section 2.8.2. *NF2* transcript NM_000268.4 (isoform 1) was used for design reference. The pegRNA vector was assembled as described in section 2.8.2.1. Correct plasmid assembly was confirmed by Sanger sequencing (section 2.4.2), using the primers detailed in section 2.8.2.1.3. Correctly assembled pegRNA vectors were transformed into New England Biolabs® (NEB) Stable Competent *E.coli* (New England Biolabs, Hitchin, UK) as described in section 2.6.2. Prime editing gRNA vector pU6-Sp-pegRNA-RNF2_+5GtoT, a gift from David Liu (Addgene plasmid #135957) [23], was used as a positive control. PegRNA vectors were co-transfected with vector pCMV-PE2-P2A-GFP, a gift from David Liu (Addgene plasmid #135957) [23], as detailed in section 2.8.2. All vector maps can be found in the Appendix II.

6.3.8. Fluorescence activated cell sorting (FACS)

FACS was performed to obtain green fluorescent protein (GFP) positive cell populations, indicating successful transfection of the pCMV-PE2-P2A-GFP vector for prime editing. FACS was conducted using the BD FACSAria™ Fusion Flow Cytometer, (BD Biosciences, Franklin Lakes, NJ, USA) cell counting and gating parameters were set using BD Biosciences FACSDiva™ software.

6.3.9. Lentivirus transduction of pseudo-construct reporter system

Pseudo-constructs of the *NF2* gene between exons 5 and 6 were designed to generate a reporter system to assess the impact of *NF2* deep intronic variant c.516+232 G>A on transcription and protein translation. Fluorescent markers, antibiotic resistance genes and immunohistochemical epitope tag FLAG® were incorporated into vector designs for multiple downstream investigations. Both mCherry and Venus fluorescent markers were designed into the reporter vectors. All vector maps can be found in the appendices.

Constructs were assembled and packaged by VectorBuilder (VectorBuilder Inc. Chicago, IL, USA). Constructs were delivered into ipn02.3 2λ Schwann cells through lentivirus packaging following the VectorBuilder protocol for transducing adherent cells. Details of lentivirus transduction optimisation in section 2.7.4.3.

6.3.10. Antisense oligonucleotide

An ASO was designed and produced by Gene Tools (Philomath, OR, USA) to mask translation of the cryptic exon created by the *NF2* c.516+232 G>A deep intronic variant. Complementary to the antisense sequence of the variant region, the following 29mer morpholino was designed to have melting temperature (Tm) of 90.6°C for optimal RNA affinity in human cells (37°C).

ASO sequence (5' > 3') – CTCAACTGCATCTGAAAAAACAACCACGT

Position of the ASO at the target region can be seen in figure 9.

Twenty-four hours after lentivirus transduction of WT and mutant *NF2* c.516+232 G>A constructs (section 2.7.4.3), samples were Nucleofected with the ASO to investigate if masking of the cryptic exon rescues WT splicing. Full details of ASO Nucleofection in section 2.10. Approximately $1x10^6$ ipn02.3 2λ Schwann cells were used per Nucleofection sample. Cells were centrifuged at 100xg for 10 minutes, supernatant was then removed and cells resuspended in Nucleofector solution (Lonza Amaxa Nucleofector™ kit V) to make a total volume of 100µl of delivery solution when supplemented with ASO at concentrations of 5µM or 10µM. ASO cell suspensions were transferred to single cuvettes for the Nucleofector™ 2b Device (Lonza Group Ltd. Basel, Switzerland) and Nucleofected using program D-033. Cell recovery and plating was conducted as described in section 2.7.4.2. RNA and protein was extracted from samples 48 hours post-Nucleofection.

6.3.11. cDNA synthesis from RNA extractions

RNA was extracted from pseudo-construct transduced cell samples to investigate aberrant splicing and potential WT splicing rescue by ASO Nucleofection. cDNA synthesis was performed using the SuperScript™ IV Reverse Transcriptase kit (Thermo Fisher Scientific, Waltham, MA, USA) as

described in section 2.4.5. Primers (table 15) were designed for amplification and sequencing of construct-specific sequences, to avoid genomic *NF2* sequences.

Primer name	Sequence (5'>3')
Construct_Forward	GACGACGACGATAAGTATGG
Construct_Reverse	CACCAGAAAACTCGCCAGA

Table 15. Primers used for the characterisation of pseudo-constructs transduced and expressed in target cells.

6.3.12. Western blotting

Western blotting was used to identify variant proteins produced by the WT and mutant pseudo-constructs transduced into cells. 15µg of total protein sample was used per well. Samples were prepared and analysed as detailed in section 2.9. Western blot band intensity values were normalised using beta-actin antibody binding, as described in section 2.9.

6.4. Results

6.4.1. TransIT-X2®

Transfection of ipn02.3 2λ cells with TransIT-X2® non-liposomal polymeric reagent failed to induce Cas9-directed DNA cleavage for both the target *NF2* region and the known high efficiency positive control, AAVS1. No evidence of indel formation was observed in Sanger sequencing chromatograms analysed using the Synthego inference of CRISPR edits tool. We concluded that transfection efficiency with this reagent was too low and decided to test an alternative, higher-efficiency method of RNP transfection.

6.4.2. Nucleofection

Utilising Nucleofection as an alternative transfection method proved successful at inducing DNA cleavage with the AAVS1 positive control RNP complex. Positive control RNP complexes at a ratio of 9:1 (gRNA:Cas9) were found to be most efficient at inducing indel formation in cells, with a Synthego ICE editing efficiency score of 38%. ICE analysis of RNP ratios of 3:1 and 6:1 were scored with 20% and 22% efficiency, respectively. Chromatograms for a negative control and AAVS1 RNP treated sample can be seen in figure 12.

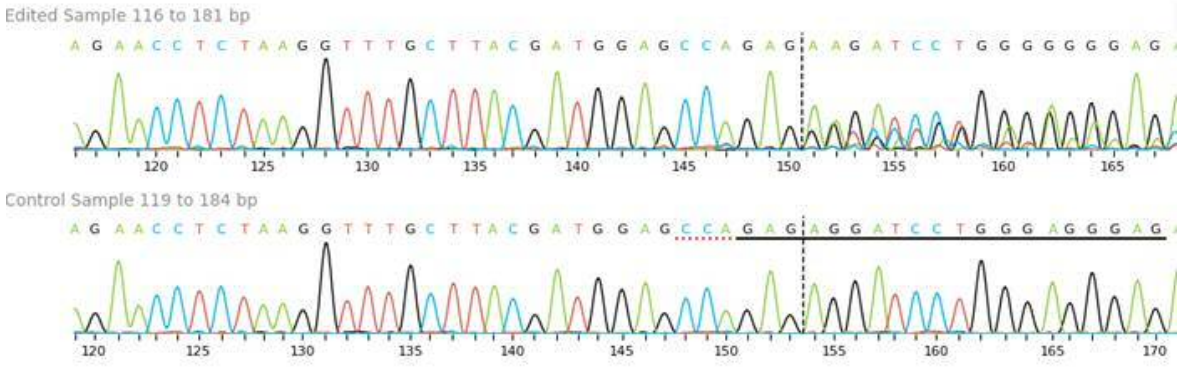

Figure 12. ICE analysis chromatograms.

A negative control sample chromatogram is shown at the bottom of the figure. A chromatogram of DNA sequencing performed in cells treated with an AAVS1 RNP 9:1 ratio complex is shown at the top of the figure. The guide RNA sequence is underlined in black in the antisense direction. The NGG PAM site is indicated by the red dashed lined. Indel formation is observable as base call frameshifts following the cleavage site, black dashed line, in the RNP treated sample chromatogram. This sample was scored with 38% editing efficiency by the Synthego ICE analysis tool.

Using the optimised parameters determined by the positive control we performed Nucleofection reactions at 9:1 RNP complex ratios for the three gRNAs designed for the *NF2* target region. After multiple repeats and troubleshooting attempts, such as increasing Cas9 concentration, varying RNP ratios and differing Nucleofection programs, no evidence of indel formation, i.e. double stranded DNA cleavage, was detected for any of the *NF2* targeting guide RNAs. Therefore, we decided to test an alternative form of CRISPR gene editing that does not require double stranded DNA cleavage.

6.4.3. CRISPR prime editing

Nucleofection of ipn02.3 2λ cells with the prime editor vector (pCMV-PE2-P2A-GFP) produced a transfection efficiency of approximately 5-10%, indicated by GFP expression using fluorescence microscopy (figure 13), described further in section 2.7.5.1. This also suggested successful transfection of the Cas9-nickase. However, Sanger sequencing of DNA extracted from transfected cells showed no evidence of variant introduction following co-Nucleofection of prime editor (pCMV-PE2-P2A-GFP) and pegRNA vectors at 3:1 ratios, detailed in section 2.8.2. It was considered that absence of edit detection in sequencing chromatograms may be due to low editing

efficiency. For subsequent Nucleofections, vector concentrations and the ratio of pegRNA to prime editor vector was increased (4:3), described in section 2.8.2. Moreover, an increased intensity Nucleofection program (T-033) was tested to determine if transfection efficiency was improved. Fluorescence microscopy analysis suggested that transfection efficiency remained similar, with approximately 10% of cells expressing GFP. In an attempt to increase the proportion of potentially edited cells in the population we chose to perform FACS to select for GFP expressing cells i.e. cells containing the pCMV-PE2-P2A-GFP vector. No fluorescence tags are incorporated within the pegRNA vectors. However, pegRNA vectors are approximately five times smaller than the prime editor vector (pCMV-PE2-P2A-GFP) and therefore should be transfected into cells more readily (see vector maps in Appendix II).

FACS was conducted 4 days after co-Nucleofection of the prime editor and pegRNA vectors, to maximise input cell numbers but retain GFP fluorescence from transient vector expression. In both the positive control sample (pU6-Sp-pegRNA-RNF2_+5GtoT) and target *NF2* pegRNA sample, approximately 5% of cells were identified as GFP positive and sorted into separate populations for onward culture in a 6-well plate. Once sorted cells reached confluency, samples were divided to maintain continued culture, in addition to DNA extraction. Sanger sequencing of DNA obtained from both the positive control and *NF2* target sample revealed no evidence of edit incorporation into the genome of cells.

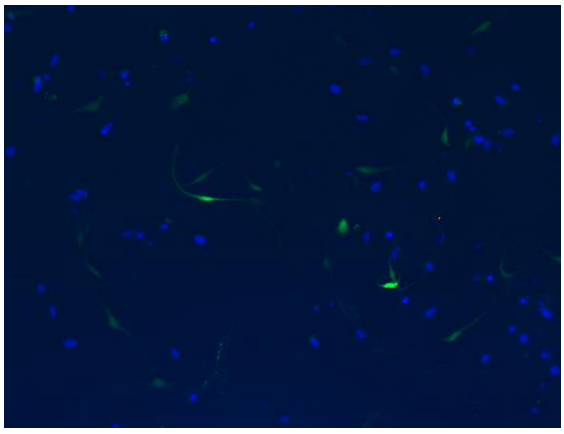

Figure 13. Fluorescence microscope image of *NF2* target pegRNA transfected cells. DAPI staining observed in nuclei of all mounted cells and GFP fluorescence in successfully Nucleofected cells. Approximately 5-10% of cells express GFP.

6.4.4. Pseudo-construct reporter system

ipn02.3 2λ cells were transduced with the WT and *NF2* variant pseudo-constructs. Fluorescence microscopy analysis was conducted to confirm successful transduction and investigate the impact of the *NF2* variant on construct expression. As fluorescent tag, mCherry, possessed an independent promoter, mCherry expression was expected to be observed in both WT and mutant transduced cells, evidence of this is observed in figure 14. Fluorescence tag Venus was positioned downstream of *NF2* exon 6, and therefore expected to have reduced or no expression in the *NF2* variant construct due to introduction of a premature stop codon upstream of Venus. Co-expression of mCherry and Venus was observed in WT transduced cells (figure 14, left). Little to no Venus expression was captured in the *NF2* variant construct transduced cells (figure 14, right). See vector maps in Appendix II.

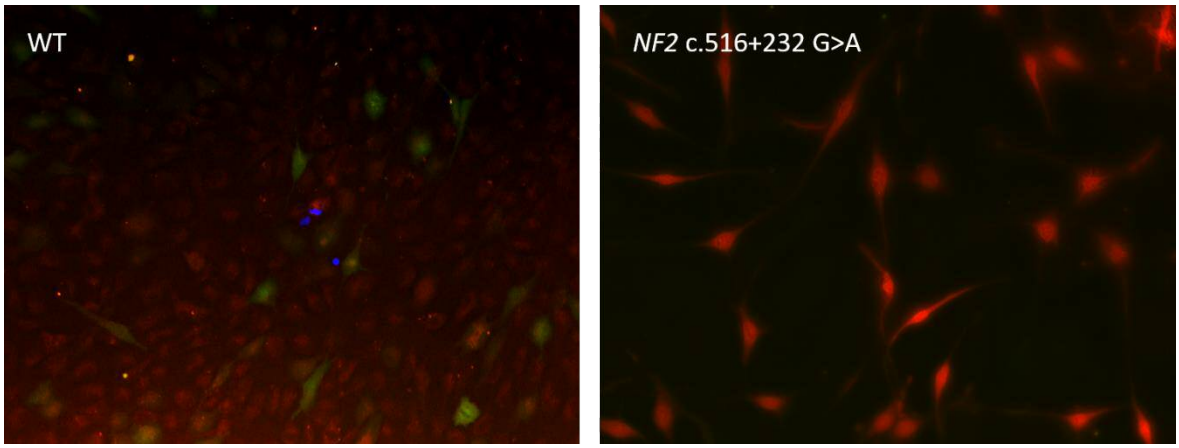

Figure 14. Fluorescence microscope images of cells transduced with constructs. Left image is a capture of cells transduced with the WT pseudo-construct of the *NF2* gene. Co-expression of mCherry (red) and Venus (green) is observed. Right image of cells transduced with the mutant *NF2* c.516+232 G>A construct. Little to no Venus expression was captured, mCherry fluorescence is prominent. DAPI staining blue.

RNA extracted from construct transduced cells was converted into cDNA for downstream PCR amplification and sequencing. cDNA was amplified using the primers detailed in table 15. Post-PCR, samples were electrophoresed and imaged to analyse amplification product sizes. Primers were designed to capture transcripts with both WT splicing and cryptic exon inclusion. Amplified products of WT splicing were expected to produce a fragment

approximately 211bp in size. The WT amplification product band can be seen in both WT and mutant construct transduced cell in figure 15. Inclusion of the cryptic exon in *NF2* c.516+232 G>A variant transcripts was expected to produce a larger amplification product of approximately 317bp in size, this is observed in the mutant construct transduced cells not treated with ASO (lane 3, figure 15). Nucleofection of the ASO appears to restore WT splicing, no cryptic exon inclusion, in the *NF2* variant construct (lane 6, figure 15).

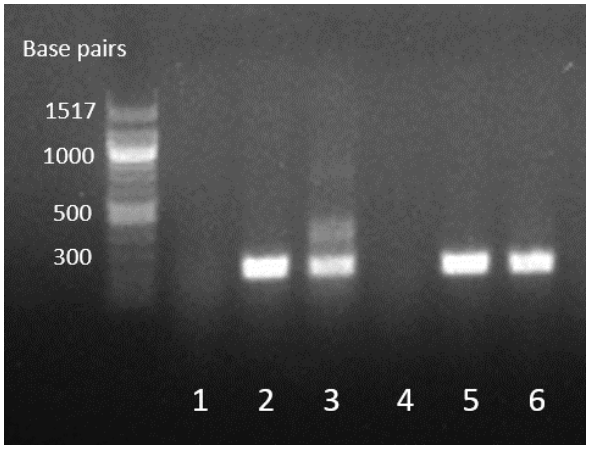

Figure 15. cDNA samples post PCR amplification.

Non-transduced cells in lanes 1 and 4. WT construct in lanes 2 and 5. *NF2* c.516+232 G>A variant construct in lanes 3 and 6. Lanes 1-3 not treated with ASO, lanes 4-6 Nucleofected with ASO 24 hours post-transduction. Bright band observed in lanes 2, 3, 5 and 6 approximately 211bp. Faint band in lane 3 approximately 317bp.

Amplified PCR products of cDNA samples were Sanger sequenced to investigate the composition of expressed transcripts. Sequencing of WT construct transduced cells (lanes 2 and 5 in figure 15) produced chromatograms consistent with WT splicing at exon boundaries. Cells transduced with the *NF2* c.516+232 G>A variant construct, not treated with the ASO, produced a chromatogram revealing two sequencing reading frames following the 3' boundary of *NF2* exon 5 (figure 16, trace A). The sequence indicates both a WT splice transcript and variant transcript are being expressed in cells transduced with the variant construct. Sequencing of cDNA obtained from variant construct transduced cells treated with the ASO, revealed a chromatogram consistent with WT splicing between *NF2* exons 5 and 6 (figure 16, trace B).

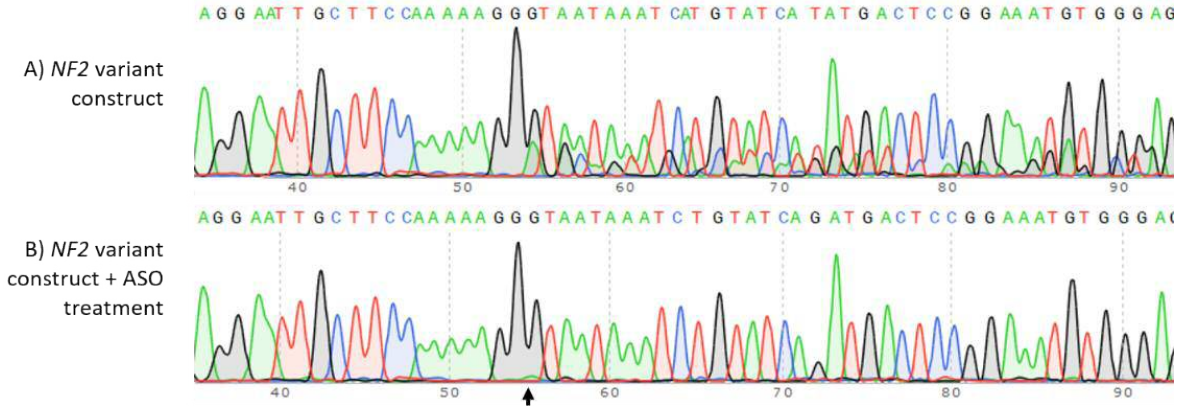

Figure 16. Chromatograms of Sanger sequencing performed in cDNA obtained from cells transduced with the *NF2* c.516+232 G>A variant construct.
Trace A, top of figure, is from cells not treated with the ASO. Trace B, bottom of figure, is from cells transduced with the variant construct with subsequent Nucleofection of the ASO. Black arrow denotes position of *NF2* exon 5 3' boundary.

Protein was extracted from transduced cells, both untreated and treated with ASO Nucleofection. Two potential protein sizes were expected to be observed in Western blot analysis. WT translation of exons 5 and 6 of *NF2*, with fusion protein Venus, was expected to produce a band of approximately 38kDa. The *NF2* c.516+232 G>A variant was expected to create a mutant truncated protein, composed of *NF2* exon 5 and part of the included cryptic exon derived from intron 5, predicted to be approximately 9kDa in size. ASO treatment was predicted to restore WT splicing and therefore translation of the WT protein in cells transduced with the mutant construct. In both the WT and mutant construct samples, a protein band correlating with the WT protein (~38kDa) was observed (figure 17). Following normalisation of blot images, the intensity of WT protein expression was found to be reduced in cells transduced with the mutant construct. Yet, the intensity of WT protein expression increased in mutant construct cells treated with the ASO in comparison to untreated cells. The truncated protein product predicted to be formed by the mutant construct (~9kDa) was not observed in any iterations of Western blots conducted.

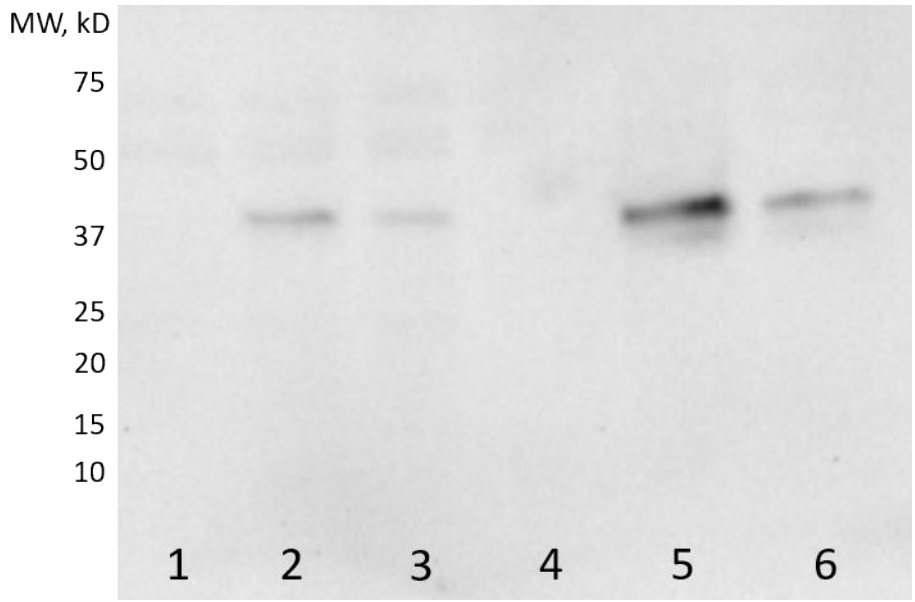

Figure 17. Western blot of proteins extracted from cells transduced with *NF2* pseudo-constructs. Bands observed correlate to a protein size of approximately 38kDa (4-20% gel). Negative control in lanes 1 and 4. WT construct in lanes 2 and 5. Mutant construct in lanes 3 and 6. Proteins in lanes 1-3 were extracted 48 hours after lentivirus transduction. Lanes 4-6 were Nucleofected with the designed ASO (10µM) targeting the mutant *NF2* sequence 24 hours after lentivirus transduction, protein was extracted 48 hours after Nucleofection. Membrane blocked with 3% non-fat milk. Primary antibody Monoclonal ANTI-FLAG® M2 produced in mouse (1:1000 dilution). Secondary antibody, Donkey Anti-Mouse IgG (H+L) Horseradish Peroxidase (HRP) Conjugate (1:3000 dilution) with Precision Protein™ StrepTactin-HRP Conjugate (1:30,000 dilution).

6.5. Discussion

6.5.1. CRISPR gene editing

Homology directed repair and prime editing CRISPR systems have so far failed to generate a permanent edit of *NF2* c.516+232 G>A into the genome of the immortalised Schwann cell line, ipn02.3 2λ. We have tested two alternative methods of transfection, including non-liposomal polymeric reagent, TransIT-X2®, which resulted in very low transfection efficiency in these cells. Subsequent use of the higher efficiency electroporation method, Nucleofection, to introduce a positive control RNP complex successfully generated indels induced by double stranded DNA cleavage at the target site. However, following extensive optimisation of reagents and Nucleofection conditions, the three gRNAs targeting the *NF2* c.516+232 region proved

unsuccessful at generating indels. It is possible that the failure of our target gRNAs is attributable to sequence specific features of their designs. A number of gRNA sequence features have been associated with variable CRISPR efficiency [27]. Observations made by Liu *et al.* (2016) suggest that gRNAs with GC nucleotide content between 40-60% are optimal for on-target performance. As one of our guide RNA designs (sgRNA1, table 6, section 2.8.1) possesses a GC content of 30%, this may be a contributory factor to its apparent inactivity. Other features, such as gRNA secondary structure and nucleotide preference at specific base positions may impact gRNA efficiency [27]. Another consideration for gRNA success is the context of the target region the guide is designed to bind. Guide RNAs designed to target promoter transcription start sites demonstrate a greater chance of successful cleavage in comparison to intergenic targets, likely due to chromatin-dictated accessibility of the region [27]. Chromatin accessibility has been identified as the strongest indicator of variable gRNA binding *in vivo* [28]. Reduced accessibility for the Cas9 nuclease at the *NF2* variant target site may offer an explanation for the cleavage inactivity of all three designed gRNAs. Though the major isoforms of *NF2*, which include exons 5 and 6, are known to be expressed in human Schwann cells [29], it is possible that epigenetic factors, such as chromatin structure and residue methylation, confer inaccessibility to the deep intronic region.

Region inaccessibility may have also contributed to our inability to induce CRISPR prime edits. As we did not detect introduction of the positive control (pU6-Sp-pegRNA-RNF2_+5GtoT) variant into target cells, it is suggestive that our prime editing methodology requires further optimisation, or that the positive control target region is also inaccessible to Cas9 nucleases in our cell type of study. As the original study describing the prime editing positive control was performed in different cell types, HEK, HeLa, K562, U2OS [23], it is possible we are observing cell-specific effects of the ipn02.3 2λ Schwann cell line. Lack of edit detection may also be due to extremely low editing efficiencies. Further iterations of the prime editor system exist that demonstrate improved editing efficiencies. Prime editor 3 systems include transfection of an additional gRNA which directs nicking of the non-edited

target DNA strand, approximately 50bp from the pegRNA mediated nick [23]. The additional nick in the WT DNA strand produced in this system can increase the likelihood of the prime editor template inclusion within the opposite target DNA strand.

6.5.2. Construct characterisation of *NF2* c.516+232 G>A variant

To further characterise the *NF2* c.516+232 G>A variant, ipn02.3 2λ cells were transduced with *NF2* WT and *NF2* variant pseudo-construct reporter plasmids containing exons 5 and 6 and intron 5 of the *NF2* gene. Analysis of cDNA revealed that cells transduced with the *NF2* variant construct produced both WT and mutant transcripts. The larger transcript fragment observed in lane 3 (*NF2* variant construct) of figure 15 correlates to a size of approximately 317bp, consistent with cryptic exon inclusion. Treatment of cells with the target ASO appeared to restore WT splicing in cells transduced with the *NF2* variant construct, with transcript fragments correlating around 211bp (lane 6, figure 15). WT splicing restoration was confirmed by Sanger sequencing of the cDNA samples and is observed in figure 16.

Analysis of protein expression through Western blotting demonstrated reduced expression of WT protein translation in cells transduced with the *NF2* variant construct, suggesting that the variant induces splicing of an alternative transcript that is not fully penetrant. This is consistent with observations made in the original study conducting functional analysis on the *NF2* c.516+232 G>A variant [11]. In addition, similar to results from tumour lysates studied by De Klein *et al.* (1998), we did not observe expression of the predicted truncated mutant protein in Western blot analysis. This may be due to instability and subsequent degradation of the variant protein structure. However, De Klein *et al.* (1998) did observe a truncated protein product when variant cDNA was transfected into COS cells.

Nucleofection of ipn02.3 2λ cells with the ASO targeting the variant region appeared to increase the expression of WT protein in cells transduced with the *NF2* variant construct, suggesting that WT splicing has been restored in a proportion of transcripts (figure 17). Sequencing of cDNA samples suggests that the majority of transcripts are restored to WT splicing (figure 16).

6.5.3. Conclusions

In conclusion, we were unable to generate a stably edited *NF2* c.516+232 G>A variant Schwann cell line as an *in vitro* model of VS predisposition. However, we have provided further characterisation of the variant's effect on splicing and protein translation using a construct-based reporter system in this biologically relevant cell type. Moreover, we have demonstrated that ASO treatment holds the potential of restoring WT splicing in cells possessing the *NF2* c.516+232 G>A variant. These results are promising for the future development of ASO therapies in the treatment of NF2 disease caused by deep intronic variants.

Future work investigating the inactivity of Cas9 at the *NF2* target site would be valuable to establish if the absence of edit detection is due to inaccessibility of the region, or low editing efficiency. Design and development of a prime editor 3 system for the *NF2* target may increase editing efficiency and therefore detectable edit incorporation. Alternatively, targeting of a genomic site with predicted accessibility, such as a promoter region, to generate *NF2* gene knockdown could be conducted. Successful gene knockdown would confirm that prime editing methodology is applicable in the ipn02.3 2λ Schwann cell line.

6.6. References

1. Ostrom QT, Cioffi G, Waite K, Kruchko C, Barnholtz-Sloan JS. CBTRUS Statistical Report: Primary Brain and Other Central Nervous System Tumours Diagnosed in the United States in 2014-2018. Neuro Oncol. 10 05 2021;23(12 Suppl 2):iii1-iii105. doi:10.1093/neuonc/noab200

2. Kentala E, Pyykkö I. Clinical picture of vestibular schwannoma. Auris Nasus Larynx. Jan 2001;28(1):15-22.

3. Evans DG, Huson SM, Donnai D, et al. A clinical study of type 2 neurofibromatosis. Q J Med. Aug 1992;84(304):603-18.

4. Parry DM, Eldridge R, Kaiser-Kupfer MI, Bouzas EA, Pikus A, Patronas N. Neurofibromatosis 2 (NF2): clinical characteristics of 63 affected individuals and clinical evidence for heterogeneity. Am J Med Genet. Oct 1994;52(4):450-61. doi:10.1002/ajmg.1320520411

5. Smith MJ, Isidor B, Beetz C, et al. Mutations in LZTR1 add to the complex heterogeneity of schwannomatosis. Neurology. Jan 2015;84(2):141-7. doi:10.1212/WNL.0000000000001129

6. Evans DG, Moran A, King A, Saeed S, Gurusinghe N, Ramsden R. Incidence of vestibular schwannoma and neurofibromatosis 2 in the North West of England over a 10-year period: higher incidence than previously thought. Otol Neurotol. Jan 2005;26(1):93-7.

7. Pathmanaban ON, Sadler KV, Kamaly-Asl ID, et al. Association of Genetic Predisposition With Solitary Schwannoma or Meningioma in Children and Young Adults. JAMA Neurol. Sep 2017;74(9):1123-1129. doi:10.1001/jamaneurol.2017.1406

8. Spitali P, Aartsma-Rus A. Splice modulating therapies for human disease. Cell. Mar 2012;148(6):1085-8. doi:10.1016/j.cell.2012.02.014

9. Hammond SM, Wood MJ. Genetic therapies for RNA mis-splicing diseases. Trends Genet. May 2011;27(5):196-205. doi:10.1016/j.tig.2011.02.004

10. Castellanos E, Rosas I, Solanes A, et al. In vitro antisense therapeutics for a deep intronic mutation causing Neurofibromatosis type 2. Eur J Hum Genet. Jul 2013;21(7):769-73. doi:10.1038/ejhg.2012.261

11. De Klein A, Riegman PH, Bijlsma EK, et al. A G-->A transition creates a branch point sequence and activation of a cryptic exon, resulting in the hereditary disorder neurofibromatosis 2. Hum Mol Genet. Mar 1998;7(3):393-8. doi:10.1093/hmg/7.3.393

12. Anttila V, Bulik-Sullivan B, Finucane HK, et al. Analysis of shared heritability in common disorders of the brain. Science. 06 22 2018;360(6395)doi:10.1126/science.aap8757

13. Carrigan PE, Ballar P, Tuzmen S. Site-directed mutagenesis. Methods Mol Biol. 2011;700:107-24. doi:10.1007/978-1-61737-954-3_8

14. Recillas-Targa F. Multiple strategies for gene transfer, expression, knockdown, and chromatin influence in mammalian cell lines and transgenic animals. Mol Biotechnol. Nov 2006;34(3):337-54. doi:10.1385/MB:34:3:337

15. Urnov FD, Miller JC, Lee YL, et al. Highly efficient endogenous human gene correction using designed zinc-finger nucleases. Nature. Jun 02 2005;435(7042):646-51. doi:10.1038/nature03556

16. Bogdanove AJ, Voytas DF. TAL effectors: customizable proteins for DNA targeting. Science. Sep 30 2011;333(6051):1843-6. doi:10.1126/science.1204094

17. Jinek M, Chylinski K, Fonfara I, Hauer M, Doudna JA, Charpentier E. A programmable dual-RNA-guided DNA endonuclease in adaptive bacterial immunity. Science. Aug 2012;337(6096):816-21. doi:10.1126/science.1225829

18. Li H, Yang Y, Hong W, Huang M, Wu M, Zhao X. Applications of genome editing technology in the targeted therapy of human diseases: mechanisms, advances and prospects. Signal Transduct Target Ther. 01 03 2020;5(1):1. doi:10.1038/s41392-019-0089-y

19. Anders C, Niewoehner O, Duerst A, Jinek M. Structural basis of PAM-dependent target DNA recognition by the Cas9 endonuclease. Nature. Sep 25 2014;513(7519):569-73. doi:10.1038/nature13579

20. Carroll D. Genome engineering with targetable nucleases. Annu Rev Biochem. 2014;83:409-39. doi:10.1146/annurev-biochem-060713-035418

21. Schubert MS, Thommandru B, Woodley J, et al. Optimized design parameters for CRISPR Cas9 and Cas12a homology-directed repair. Sci Rep. Sep 30 2021;11(1):19482. doi:10.1038/s41598-021-98965-y

22. Davis L, Maizels N. Homology-directed repair of DNA nicks via pathways distinct from canonical double-strand break repair. Proc Natl Acad Sci U S A. Mar 11 2014;111(10):E924-32. doi:10.1073/pnas.1400236111

23. Anzalone AV, Randolph PB, Davis JR, et al. Search-and-replace genome editing without double-strand breaks or donor DNA. Nature. 12 2019;576(7785):149-157. doi:10.1038/s41586-019-1711-4

24. Ogata T, Kozuka T, Kanda T. Identification of an insulator in AAVS1, a preferred region for integration of adeno-associated virus DNA. J Virol. Aug 2003;77(16):9000-7. doi:10.1128/jvi.77.16.9000-9007.2003

25. Li X, Burnight ER, Cooney AL, et al. piggyBac transposase tools for genome engineering. Proc Natl Acad Sci U S A. Jun 2013;110(25):E2279-87. doi:10.1073/pnas.1305987110

26. Chow RD, Chen JS, Shen J, Chen S. A web tool for the design of prime-editing guide RNAs. Nat Biomed Eng. 02 2021;5(2):190-194. doi:10.1038/s41551-020-00622-8

27. Liu X, Homma A, Sayadi J, Yang S, Ohashi J, Takumi T. Sequence features associated with the cleavage efficiency of CRISPR/Cas9 system. Sci Rep. Jan 27 2016;6:19675. doi:10.1038/srep19675

28. Wu X, Scott DA, Kriz AJ, et al. Genome-wide binding of the CRISPR endonuclease Cas9 in mammalian cells. Nat Biotechnol. Jul 2014;32(7):670-6. doi:10.1038/nbt.2889

29. Su F, Zhou Z, Su W, Wang Z, Wu Q. A novel alternative splicing isoform of NF2 identified in human Schwann cells. Oncol Lett. Aug 2016;12(2):977-982. doi:10.3892/ol.2016.4685

7. Discussion

7.1. Realisation of aims

The overall aim of this study was to contribute to furthering the understanding of the genetic landscape that surrounds vestibular schwannoma predisposition. Through different, but complementary, lines of investigation into the biological features of VS, we have successfully accomplished this. This body of work further characterises the genotypic features of both germline and somatic samples in patients with sporadic and syndromic forms of VS (chapter 3) (Sadler *et al.*, 2020). I also highlight the need to refine variant interpretation guidelines to include disease-specific features as evidence in variant classification in a known VS predisposition gene (chapter 4).

Identification of a risk locus on chromosome 9p21.3 in our GWAS, suggests a novel region in association with germline risk for sporadic VS, pointing to a new area of focus in VS susceptibility research (chapter 5). Disease modelling of a known VS susceptibility variant in *NF2* demonstrates that splice-modulating therapies hold promise in the treatment of NF2 disease caused by deep intronic variants (chapter 6).

7.1.1. Identification and characterisation of rare, high impact variants in VS patients

In chapter 3 we highlighted that NF2 and *LZTR1*-associated schwannomatosis accounted for 2% and 3%, respectively, of apparently sporadic VS cases in our cohort. Accurate diagnosis of these tumour predisposition syndromes is vital for effective patient management and valuable for informing cascade testing in at-risk relatives. It is possible that cases of low level NF2 mosaicism remain within the apparently sporadic VS cohort, as germline samples tested prior to 2013 will not have benefited from the increased sensitivity of NGS testing to detect low allele fractions in low level mosaics.

We provide evidence supporting previous research indicating that young people presenting with UVS, without identification of *NF2* pathogenic variants, should receive molecular testing for *LZTR1* (Smith *et al.*, 2015). With the identification of *LZTR1*-associated schwannomatosis in one patient with VS presentation over 30 years, we also provide a rationale for extending

LZTR1 molecular testing in age groups above the current referral recommendations (Evans *et al.*, 2012).

We have described characteristic genotypes for sporadic VS patients as negative for germline variants in known VS-predisposition genes, yet with frequent observation of biallelic *NF2* inactivation in tumour samples. In all apparently sporadic VS patients analysed, 69% had identifiable biallelic inactivation of *NF2* in their somatic samples, including those with germline *LZTR1* pathogenic variants. This finding in *LZTR1*-associated schwannomatosis is supportive of the multi-gene hit mechanisms of schwannoma tumourigenesis previously hypothesised (Sestini *et al.*, 2008; Hadfield *et al.*, 2008; Kehrer-Sawatzki *et al.*, 2017). The current rate of *NF2* inactivation in VS tumours may also be underestimated due to macrophage infiltration contaminating tumour DNA sampling (Lewis *et al.*, 2018). These results suggest that loss of *NF2* function is a common pathway in the development of all VS tumours.

Assessment of variants in VS predisposition genes is important for classification of pathogenicity, and to determine the likely clinical impact upon a patient. In chapter 4 the difficulties of missense variant classification in the context of *NF2* are highlighted. In comparison to truncating variants, it is challenging to predict the effect of a missense variant at the protein level, as *in silico* interpretation tools can be in conflict and variants may be observed within gnomAD. Even with the provision of thorough variant interpretation guidelines (ACGS best practice guidelines, 2020), we conclude that limited availability of functional and clinical variant-specific information severely restricts actionable interpretation of missense variants. Whilst it is challenging and time-consuming to obtain rigorous functional analyses of variant-specific effects, provision of clinical descriptions in association with reported variants is, in principle, a simple action that would significantly assist in variant interpretation. I suggest that utilisation of NF2 disease-specific features, such as LOH in tumour samples, should be formally incorporated into *NF2* variant interpretation guidelines to assist in clinical decision making.

7.1.2. Identification of common genetic variants in association with VS risk

Prior to commencing this project, germline pathogenic variants in *NF2*, *LZTR1* and possibly *SMARCB1* had been associated with VS predisposition. Pathogenic germline variants in *NF2* confer the highest risk, while the risk of VS from *LZTR1* variants is significantly lower and the association with *SMARCB1* germline variants is still controversial. As the majority of VS are observed in sporadic cases, without further features of NF2 or schwannomatosis, we hypothesised that other lower risk germline variants exist that contribute to risk of VS tumourigenesis. To identify novel genetic associations we conducted a GWAS in sporadic VS patients. A genome-wide significant risk locus was identified in our analysis, with the lead SNP rs1556516 (P = 1.47e-13), positioned within lncRNA *CDKN2B-AS1*, also known as *ANRIL*.

Earlier in 2021, a preprint article was posted. The article outlined a large-scale GWAS investigating a number of self-reported rare disorders including vestibular schwannoma (https://doi.org/10.1101/2021.06.09.21258643) and also identified a genome-wide significant region in association with VS on chromosome 9p21.3, with the lead SNP rs7341786 (P = 1.4e-15). Though the group identified a different lead SNP to our analysis, it is also positioned within *ANRIL*. We consider the phenotypic description of VS cases in the Shringarpure *et al.* (2021) study to be non-specific, as the term “Benign neoplasm of cranial nerves” was used to select a validation cohort. However, as the authors replicated the 9p21.3 association, it seems that patients with this phenotypic description represent true cases of VS, or that the association at 9p21.3 is relevant to multiple types of benign neoplasms of the cranial nerves.

A review of existing literature on the 9p21.3 region encompassing *CDK2NB-AS1*, *CDKN2A* and *CDK2N2B*, also known as the INK4 locus, suggests this region is a likely contributor to VS predisposition. *CDKN2A* encodes two gene products, p16(INK4a) and p14(ARF), both of which have known tumour suppressor actions (Kim and Sharpless, 2006). Germline mutations in *CDKN2A* have been identified in cases of familial atypical multiple mole melanoma with multiple nerve sheath tumours (Sargen *et al.*, 2016) and

regulation of the p16(INK4a) locus has been associated with radio-sensitivity in gliomas (Simon *et al.*, 2006). Component dysregulation within a number of overlapping oncogenic pathways linked to products of the INK4 locus has been similarly described in glioblastoma (Cancer Genome Atlas Research Network, 2008), and provides compelling evidence that the 9p21.3 risk locus is truly associated with VS tumourigenesis. The INK4 locus represents an exciting line of future research into VS predisposition, and potentially other benign cranial neoplasms.

7.1.3. Generation of an *in vitro* model for VS predisposition

Through the use of *NF2* pseudo-construct reporter vectors we were able to model the *NF2* c.516+232 G>A variant in a cell type biologically relevant to VS tumours. Our observations of the effect of this variant on splicing and protein translation are consistent with previous reports (De Klein *et al.*, 1998) and provide further characterisation of the cryptic exon inclusion induced by the variant, NM_000268.4 r.516_517ins516+250_516+355, p.(Arg172_Val173ins*32). Additionally, we have demonstrated that design and transfection of a variant-specific ASO into cells transduced with the *NF2* c.516+232 G>A variant can restore wild-type splicing and translation of the gene product. These results hold promise for the future development of ASO therapies in the treatment of *NF2* caused by deep intronic variants.

Currently, we have been unable to generate a stably edited *NF2* c.516+232 G>A variant Schwann cell line model of VS predisposition. This may be due to design considerations for the guide RNAs used in experimentation, need for further optimisation of reagents, or access limitations of the target genomic region. Chromatin inaccessibility has been previously implicated in prevention of CRISPR genome editing (Wu *et al.*, 2014). This seems unlikely in our case, since *NF2* is expressed in human Schwann cells (Su *et al.*, 2016); however, it is possible that there are other genomic features of the deep intronic region that impede access of the CRISPR complex.

Whilst standardised cell lines help maintain consistencies in the genomic context of variant studies, there are limitations on the conclusions that can be drawn from results obtained in cell line models. Cell lines are

immortalised and therefore contain variants that might impact cellular behaviour that is not reflective of normal physiological observations. However, cell lines remain vital tools in medical research and for the development of new disease therapies.

7.2. Conclusion

Across all of the investigations conducted within this project, a common feature of VS predisposition is dysregulation of *NF2* and the oncogenic PI3K/AKT/mTOR and RAS/RAF pathways. These pathways have been demonstrated to modulate each other, and both *NF2* and *LZTR1* hold inhibitory roles within them (Rong *et al.*, 2004; Cui *et al.*, 2019; Bigenzahn *et al.*, 2018). RAS has been found to act as a positive regulator of gene products within the INK4 locus identified in association with VS in our GWAS (Kim and Sharpless, 2006). Moreover, the INK4 locus has links to *NF2* action through regulation of inflammatory network components, namely transcription factor NF-κB. Induced by inflammatory stimuli, NF-κB has been demonstrated to bind the promoter of *ANRIL* within the INK4 locus, initiating transcription (Zhou *et al.*, 2016). Whilst the *NF2* protein has been observed to act as a negative regulator of NF-κB activity (Ammoun *et al.*, 2014). Further investigation into the role of inflammatory stimuli in the instigation of VS tumourigenesis and the associated inflammatory cell invasion observed in VS tumours (Lewis *et al.*, 2018) represents a promising field of research.

The recurrent observations of dysregulation of overlapping signalling pathways in VS-associated disease suggests a central mechanism for VS predisposition. Germline genetic variants within components of these pathways, such as the INK4 locus, may leave individuals susceptible to VS development when somatic loss of other pathway elements occur. It seems likely that *NF2* loss remains central in VS tumourigenesis in susceptible individuals. Somatic loss of heterozygosity of the *NF2* locus is a relatively frequent event due to low copy repeat regions across chromosome 22 that confer vulnerability to structural rearrangement events (Kaplan *et al.*, 1987). Acquired biallelic inactivation of *NF2* in the majority of VS tumours supports this hypothesis.

7.3. Future work

The work presented here points to other promising lines of investigation for future research on VS tumourigenesis. Further characterisation of the INK4 locus in VS patients would help delineate the role of the genes encoded by this region. Analysis of *CDKN2B-AS1* (*ANRIL*) and *CDKN2A/B* expression within sporadic VS tumour samples would provide insight into the mechanism of action for the GWAS risk locus. Similarly, it would be fascinating to characterise the 9p21.3 region in VS tumour samples to investigate if LOH of this locus is observed, and if so, how frequently. Loss of the 9p21.3 region could represent a causative mutational hit in VS tumours in which loss of *NF2* is not observed.

Variants in the INK4 locus may also confer variable phenotypic presentation in patients with NF2 and schwannomatosis. Genotyping of lead SNPs identified within our GWAS in a NF2 patient cohort may reveal correlations between genotype and disease severity. For example, variants in the INK4 locus may confer an increased risk of early disease presentation or tumour burden. Significant associations between genotype and disease severity features would facilitate better stratification of NF2 patients with more informed care management plans.

As the role of inflammation and inflammatory networks becomes more apparent in the behaviour of VS tumours, further study into the impact of inflammatory stimuli on VS tumourigenesis may prove valuable. Investigation into gene products of the INK4 locus and their roles in dysregulation of inflammatory genes and networks may highlight a mechanistic direction in which inherited VS susceptibility acts. VS associated inflammation may be driven, in part, through inheritance of common genetic modifiers, such as variants within the INK4 locus.

In future work of disease modelling VS predisposition variants, it would be valuable to establish the reasons behind our unsuccessful attempt at introducing a permanent CRISPR-mediated edit (*NF2* c.516+232G>A) within intron 5 of *NF2*, chapter 6. Utilising prime editing CRISPR methodology to target genomic regions with known chromatin accessibility, such as promoter regions, would indicate if chromatin accessibility is an obstructing feature of our target deep intronic region, and would confirm that prime editing methodology is applicable in the ipn02.3 2λ Schwann cell line. Low editing efficiency may have also hindered our attempts at

prime editing. Development of a prime editor 3 system for the *NF2* target might increase editing efficiency through the preferential inclusion of the reverse transcription template (Anzalone *et al.*, 2019), resulting in variant incorporation within the genome of target cells.

References

Online References

ThermoFisher UK Biobank Axiom® Array Content Summary

https://www.thermofisher.com/document-connect/document-connect.html?url=https://assets.thermofisher.com/TFS-Assets%2FLSG%2Fbrochures%2Fuk_axiom_biobank_contentsummary_brochure.pdf

[Accessed 25/10/21].

Literature References

Aarhus, M., Bruland, O., Sætran, H. A., Mork, S. J., Lund-Johansen, M. and Knappskog, P. M. (2010) 'Global gene expression profiling and tissue microarray reveal novel candidate genes and down-regulation of the tumour suppressor gene CAV1 in sporadic vestibular schwannomas', *Neurosurgery,* 67(4), pp. 998-1019; discussion 1019.

Abe, T., Umeki, I., Kanno, S. I., Inoue, S. I., Niihori, T. and Aoki, Y. (2020) 'LZTR1 facilitates polyubiquitination and degradation of RAS-GTPases', *Cell Death Differ,* 27(3), pp. 1023-1035.

Abecasis, G. R., Altshuler, D., Auton, A., Brooks, L. D., Durbin, R. M., Gibbs, R. A., Hurles, M. E., McVean, G. A. and Consortium, G. P. (2010) 'A map of human genome variation from population-scale sequencing', *Nature,* 467(7319), pp. 1061-73.

Abraham, G., Havulinna, A. S., Bhalala, O. G., Byars, S. G., De Livera, A. M., Yetukuri, L., Tikkanen, E., Perola, M., Schunkert, H., Sijbrands, E. J., Palotie, A., Samani, N. J., Salomaa, V., Ripatti, S. and Inouye, M. (2016) 'Genomic prediction of coronary heart disease', *Eur Heart J,* 37(43), pp. 3267-3278.

Adzhubei, I. A., Schmidt, S., Peshkin, L., Ramensky, V. E., Gerasimova, A., Bork, P., Kondrashov, A. S. and Sunyaev, S. R. (2010) 'A method and server for predicting damaging missense mutations', *Nat Methods,* 7(4), pp. 248-9.

Al-Attar, S., Westra, E. R., van der Oost, J. and Brouns, S. J. (2011) 'Clustered regularly interspaced short palindromic repeats (CRISPRs): the hallmark of an ingenious antiviral defense mechanism in prokaryotes', *Biol Chem,* 392(4), pp. 277-89.

Alirezaie, N., Kernohan, K. D., Hartley, T., Majewski, J. and Hocking, T. D. (2018) 'ClinPred: Prediction Tool to Identify Disease-Relevant Nonsynonymous Single-Nucleotide Variants', *Am J Hum Genet,* 103(4), pp. 474-483.

Ammoun, S., Provenzano, L., Zhou, L., Barczyk, M., Evans, K., Hilton, D. A., Hafizi, S. and Hanemann, C. O. (2014) 'Axl/Gas6/NFκB signalling in schwannoma pathological proliferation, adhesion and survival', *Oncogene,* 33(3), pp. 336-46.

Anders, C., Niewoehner, O., Duerst, A. and Jinek, M. (2014) 'Structural basis of PAM-dependent target DNA recognition by the Cas9 endonuclease', *Nature,* 513(7519), pp. 569-73.

Anttila, V. and Bulik-Sullivan, B. and Finucane, H. K. and Walters, R. K. and Bras, J. and Duncan, L. and Escott-Price, V. and Falcone, G. J. and Gormley, P. and Malik, R. and Patsopoulos, N. A. and Ripke, S. and Wei, Z. and Yu, D. and Lee, P. H. and Turley, P. and Grenier-Boley, B. and Chouraki, V. and Kamatani, Y. and Berr, C. and Letenneur, L. and Hannequin, D. and Amouyel, P. and Boland, A. and Deleuze, J. F. and Duron, E. and Vardarajan, B. N. and Reitz, C. and Goate, A. M. and Huentelman, M. J. and Kamboh, M. I. and Larson, E. B. and Rogaeva, E. and St George-Hyslop, P. and Hakonarson, H. and Kukull, W. A. and Farrer, L. A. and Barnes, L. L. and Beach, T. G. and Demirci, F. Y. and Head, E. and Hulette, C. M. and Jicha, G. A. and Kauwe, J. S. K.

and Kaye, J. A. and Leverenz, J. B. and Levey, A. I. and Lieberman, A. P. and Pankratz, V. S. and Poon, W. W. and Quinn, J. F. and Saykin, A. J. and Schneider, L. S. and Smith, A. G. and Sonnen, J. A. and Stern, R. A. and Van Deerlin, V. M. and Van Eldik, L. J. and Harold, D. and Russo, G. and Rubinsztein, D. C. and Bayer, A. and Tsolaki, M. and Proitsi, P. and Fox, N. C. and Hampel, H. and Owen, M. J. and Mead, S. and Passmore, P. and Morgan, K. and Nöthen, M. M. and Rossor, M. and Lupton, M. K. and Hoffmann, P. and Kornhuber, J. and Lawlor, B. and McQuillin, A. and Al-Chalabi, A. and Bis, J. C. and Ruiz, A. and Boada, M. and Seshadri, S. and Beiser, A. and Rice, K. and van der Lee, S. J. and De Jager, P. L. and Geschwind, D. H. and Riemenschneider, M. and Riedel-Heller, S. and Rotter, J. I. and Ransmayr, G. and Hyman, B. T. and Cruchaga, C. and Alegret, M. and Winsvold, B. and Palta, P. and Farh, K. H. and Cuenca-Leon, E. and Furlotte, N. and Kurth, T. and Ligthart, L. and Terwindt, G. M. and Freilinger, T. and Ran, C. and Gordon, S. D. and Borck, G. and Adams, H. H. H. and Lehtimäki, T. and Wedenoja, J. and Buring, J. E. and Schürks, M. and Hrafnsdottir, M. and Hottenga, J. J. and Penninx, B. and Artto, V. and Kaunisto, M. and Vepsäläinen, S. and Martin, N. G. and Montgomery, G. W. and Kurki, M. I. and Hämäläinen, E. and Huang, H. and Huang, J. and Sandor, C. and Webber, C. and Muller-Myhsok, B. and Schreiber, S. and Salomaa, V. and Loehrer, E. and Göbel, H. and Macaya, A. and Pozo-Rosich, P. and Hansen, T. and Werge, T. and Kaprio, J. and Metspalu, A. and Kubisch, C. and Ferrari, M. D. and Belin, A. C. and van den Maagdenberg, A. M. J. M. and Zwart, J. A. and Boomsma, D. and Eriksson, N. and Olesen, J. and Chasman, D. I. and Nyholt, D. R. and Avbersek, A. and Baum, L. and Berkovic, S. and Bradfield, J. and Buono, R. J. and Catarino, C. B. and Cossette, P. and De Jonghe, P. and Depondt, C. and Dlugos, D. and Ferraro, T. N. and French, J. and Hjalgrim, H. and Jamnadas-Khoda, J. and Kälviäinen, R. and Kunz, W. S. and Lerche, H. and Leu, C. and Lindhout, D. and Lo, W. and Lowenstein, D. and McCormack, M. and Møller, R. S. and Molloy, A. and Ng, P. W. and Oliver, K. and Privitera, M. and Radtke, R. and Ruppert, A. K. and Sander, T. and Schachter, S. and Schankin, C. and Scheffer, I. and Schoch, S. and Sisodiya, S. M. and Smith, P. and Sperling, M. and Striano, P. and Surges, R. and Thomas, G. N. and Visscher, F. and Whelan, C. D. and Zara, F. and Heinzen, E. L. and Marson, A. and Becker, F. and Stroink, H. and Zimprich, F. and Gasser, T. and Gibbs, R. and Heutink, P. and Martinez, M. and Morris, H. R. and Sharma, M. and Ryten, M. and Mok, K. Y. and Pulit, S. and Bevan, S. and Holliday, E. and Attia, J. and Battey, T. and Boncoraglio, G. and Thijs, V. and Chen, W. M. and Mitchell, B. and Rothwell, P. and Sharma, P. and Sudlow, C. and Vicente, A. and Markus, H. and Kourkoulis, C. and Pera, J. and Raffeld, M. and Silliman, S. and Boraska Perica, V. and Thornton, L. M. and Huckins, L. M. and William Rayner, N. and Lewis, C. M. and Gratacos, M. and Rybakowski, F. and Keski-Rahkonen, A. and Raevuori, A. and Hudson, J. I. and Reichborn-Kjennerud, T. and Monteleone, P. and Karwautz, A. and Mannik, K. and Baker, J. H. and O'Toole, J. K. and Trace, S. E. and Davis, O. S. P. and Helder, S. G. and Ehrlich, S. and Herpertz-Dahlmann, B. and Danner, U. N. and van Elburg, A. A. and Clementi, M. and Forzan, M. and Docampo, E. and Lissowska, J. and Hauser, J. and Tortorella, A. and Maj, M. and Gonidakis, F. and Tziouvas, K. and Papezova, H. and Yilmaz, Z. and Wagner, G. and Cohen-Woods, S. and Herms, S. and Julià, A. and Rabionet, R. and Dick, D. M. and Ripatti, S. and Andreassen, O. A. and Espeseth, T. and Lundervold, A. J. and Steen, V. M. and Pinto, D. and Scherer, S. W. and Aschauer, H. and Schosser, A. and Alfredsson, L. and Padyukov, L. and Halmi, K. A. and Mitchell, J. and Strober, M. and Bergen, A. W. and Kaye, W. and Szatkiewicz, J. P. and Cormand, B. and Ramos-Quiroga, J. A. and Sánchez-Mora, C. and Ribasés, M. and Casas, M. and Hervas, A. and Arranz, M. J. and Haavik, J. and Zayats, T. and Johansson, S. and Williams, N. and Dempfle, A. and Rothenberger, A. and Kuntsi, J. and Oades, R. D. and Banaschewski, T. and Franke, B. and Buitelaar, J. K. and Arias Vasquez, A. and Doyle, A. E. and Reif, A. and Lesch, K. P. and Freitag, C. and Rivero, O. and Palmason, H. and Romanos, M. and Langley, K. and Rietschel, M. and Witt, S. H. and Dalsgaard, S. and Børglum, A. D. and Waldman, I. and

Wilmot, B. and Molly, N. and Bau, C. H. D. and Crosbie, J. and Schachar, R. and Loo, S. K. and McGough, J. J. and Grevet, E. H. and Medland, S. E. and Robinson, E. and Weiss, L. A. and Bacchelli, E. and Bailey, A. and Bal, V. and Battaglia, A. and Betancur, C. and Bolton, P. and Cantor, R. and Celestino-Soper, P. and Dawson, G. and De Rubeis, S. and Duque, F. and Green, A. and Klauck, S. M. and Leboyer, M. and Levitt, P. and Maestrini, E. and Mane, S. and De-Luca, D. M. and Parr, J. and Regan, R. and Reichenberg, A. and Sandin, S. and Vorstman, J. and Wassink, T. and Wijsman, E. and Cook, E. and Santangelo, S. and Delorme, R. and Rogé, B. and Magalhaes, T. and Arking, D. and Schulze, T. G. and Thompson, R. C. and Strohmaier, J. and Matthews, K. and Melle, I. and Morris, D. and Blackwood, D. and McIntosh, A. and Bergen, S. E. and Schalling, M. and Jamain, S. and Maaser, A. and Fischer, S. B. and Reinbold, C. S. and Fullerton, J. M. and Guzman-Parra, J. and Mayoral, F. and Schofield, P. R. and Cichon, S. and Mühleisen, T. W. and Degenhardt, F. and Schumacher, J. and Bauer, M. and Mitchell, P. B. and Gershon, E. S. and Rice, J. and Potash, J. B. and Zandi, P. P. and Craddock, N. and Ferrier, I. N. and Alda, M. and Rouleau, G. A. and Turecki, G. and Ophoff, R. and Pato, C. and Anjorin, A. and Stahl, E. and Leber, M. and Czerski, P. M. and Cruceanu, C. and Jones, I. R. and Posthuma, D. and Andlauer, T. F. M. and Forstner, A. J. and Streit, F. and Baune, B. T. and Air, T. and Sinnamon, G. and Wray, N. R. and MacIntyre, D. J. and Porteous, D. and Homuth, G. and Rivera, M. and Grove, J. and Middeldorp, C. M. and Hickie, I. and Pergadia, M. and Mehta, D. and Smit, J. H. and Jansen, R. and de Geus, E. and Dunn, E. and Li, Q. S. and Nauck, M. and Schoevers, R. A. and Beekman, A. T. and Knowles, J. A. and Viktorin, A. and Arnold, P. and Barr, C. L. and Bedoya-Berrio, G. and Bienvenu, O. J. and Brentani, H. and Burton, C. and Camarena, B. and Cappi, C. and Cath, D. and Cavallini, M. and Cusi, D. and Darrow, S. and Denys, D. and Derks, E. M. and Dietrich, A. and Fernandez, T. and Figee, M. and Freimer, N. and Gerber, G. and Grados, M. and Greenberg, E. and Hanna, G. L. and Hartmann, A. and Hirschtritt, M. E. and Hoekstra, P. J. and Huang, A. and Huyser, C. and Illmann, C. and Jenike, M. and Kuperman, S. and Leventhal, B. and Lochner, C. and Lyon, G. J. and Macciardi, F. and Madruga-Garrido, M. and Malaty, I. A. and Maras, A. and McGrath, L. and Miguel, E. C. and Mir, P. and Nestadt, G. and Nicolini, H. and Okun, M. S. and Pakstis, A. and Paschou, P. and Piacentini, J. and Pittenger, C. and Plessen, K. and Ramensky, V. and Ramos, E. M. and Reus, V. and Richter, M. A. and Riddle, M. A. and Robertson, M. M. and Roessner, V. and Rosário, M. and Samuels, J. F. and Sandor, P. and Stein, D. J. and Tsetsos, F. and Van Nieuwerburgh, F. and Weatherall, S. and Wendland, J. R. and Wolanczyk, T. and Worbe, Y. and Zai, G. and Goes, F. S. and McLaughlin, N. and Nestadt, P. S. and Grabe, H. J. and Depienne, C. and Konkashbaev, A. and Lanzagorta, N. and Valencia-Duarte, A. and Bramon, E. and Buccola, N. and Cahn, W. and Cairns, M. and Chong, S. A. and Cohen, D. and Crespo-Facorro, B. and Crowley, J. and Davidson, M. and DeLisi, L. and Dinan, T. and Donohoe, G. and Drapeau, E. and Duan, J. and Haan, L. and Hougaard, D. and Karachanak-Yankova, S. and Khrunin, A. and Klovins, J. and Kučinskas, V. and Lee Chee Keong, J. and Limborska, S. and Loughland, C. and Lönnqvist, J. and Maher, B. and Mattheisen, M. and McDonald, C. and Murphy, K. C. and Nenadic, I. and van Os, J. and Pantelis, C. and Pato, M. and Petryshen, T. and Quested, D. and Roussos, P. and Sanders, A. R. and Schall, U. and Schwab, S. G. and Sim, K. and So, H. C. and Stögmann, E. and Subramaniam, M. and Toncheva, D. and Waddington, J. and Walters, J. and Weiser, M. and Cheng, W. and Cloninger, R. and Curtis, D. and Gejman, P. V. and Henskens, F. and Mattingsdal, M. and Oh, S. Y. and Scott, R. and Webb, B. and Breen, G. and Churchhouse, C. and Bulik, C. M. and Daly, M. and Dichgans, M. and Faraone, S. V. and Guerreiro, R. and Holmans, P. and Kendler, K. S. and Koeleman, B. and Mathews, C. A. and Price, A. and Scharf, J. and Sklar, P. and Williams, J. and Wood, N. W. and Cotsapas, C. and Palotie, A. and Smoller, J. W. and Sullivan, P. and Rosand, J. and Corvin, A. and Neale, B. M. and Schott, J. M. and Anney, R. and Elia, J. and Grigoroiu-Serbanescu, M. and Edenberg, H. J. and Murray, R. and Consortium, B.

(2018) 'Analysis of shared heritability in common disorders of the brain', *Science,* 360(6395).

Anzalone, A. V., Randolph, P. B., Davis, J. R., Sousa, A. A., Koblan, L. W., Levy, J. M., Chen, P. J., Wilson, C., Newby, G. A., Raguram, A. and Liu, D. R. (2019) 'Search-and-replace genome editing without double-strand breaks or donor DNA', *Nature,* 576(7785), pp. 149-157.

Arcellana-Panlilio, M. Y., Egeler, R. M., Ujack, E., Magliocco, A., Stuart, G. C., Robbins, S. M. and Coppes, M. J. (2002) 'Evidence of a role for the INK4 family of cyclin-dependent kinase inhibitors in ovarian granulosa cell tumours', *Genes Chromosomes Cancer,* 35(2), pp. 176-81.

Asthagiri, A. R., Parry, D. M., Butman, J. A., Kim, H. J., Tsilou, E. T., Zhuang, Z. and Lonser, R. R. (2009) 'Neurofibromatosis type 2', *Lancet,* 373(9679), pp. 1974-86.

Baser, M. E., Kuramoto, L., Woods, R., Joe, H., Friedman, J. M., Wallace, A. J., Ramsden, R. T., Olschwang, S., Bijlsma, E., Kalamarides, M., Papi, L., Kato, R., Carroll, J., Lázaro, C., Joncourt, F., Parry, D. M., Rouleau, G. A. and Evans, D. G. (2005) 'The location of constitutional neurofibromatosis 2 (NF2) splice site mutations is associated with the severity of NF2', *J Med Genet,* 42(7), pp. 540-6.

Berkowitz, O., Iyer, A. K., Kano, H., Talbott, E. O. and Lunsford, L. D. (2015) 'Epidemiology and Environmental Risk Factors Associated with Vestibular Schwannoma', *World Neurosurg,* 84(6), pp. 1674-80.

Biegel, J. A. (2006) 'Molecular genetics of atypical teratoid/rhabdoid tumour', *Neurosurg Focus,* 20(1), pp. E11.

Bigenzahn, J. W., Collu, G. M., Kartnig, F., Pieraks, M., Vladimer, G. I., Heinz, L. X., Sedlyarov, V., Schischlik, F., Fauster, A., Rebsamen, M., Parapatics, K., Blomen, V. A., Müller, A. C., Winter, G. E., Kralovics, R., Brummelkamp, T. R., Mlodzik, M. and Superti-Furga, G. (2018) 'LZTR1 is a regulator of RAS ubiquitination and signaling', *Science*.

Bikhazi, N. B., Slattery, W. H., Lalwani, A. K., Jackler, R. K., Bikhazi, P. H. and Brackmann, D. E. (1997) 'Familial occurrence of unilateral vestibular schwannoma', *Laryngoscope,* 107(9), pp. 1176-80.

Bivona, T. G., Hieronymus, H., Parker, J., Chang, K., Taron, M., Rosell, R., Moonsamy, P., Dahlman, K., Miller, V. A., Costa, C., Hannon, G. and Sawyers, C. L. (2011) 'FAS and NF-κB signalling modulate dependence of lung cancers on mutant EGFR', *Nature,* 471(7339), pp. 523-6.

Bogdanove, A. J. and Voytas, D. F. (2011) 'TAL effectors: customizable proteins for DNA targeting', *Science,* 333(6051), pp. 1843-6.

Bolotin, A., Quinquis, B., Sorokin, A. and Ehrlich, S. D. (2005) 'Clustered regularly interspaced short palindrome repeats (CRISPRs) have spacers of extrachromosomal origin', *Microbiology,* 151(Pt 8), pp. 2551-2561.

Boyd, C., Smith, M. J., Kluwe, L., Balogh, A., Maccollin, M. and Plotkin, S. R. (2008) 'Alterations in the SMARCB1 (INI1) tumour suppressor gene in familial schwannomatosis', *Clin Genet,* 74(4), pp. 358-66.

Brenner, A. V., Linet, M. S., Fine, H. A., Shapiro, W. R., Selker, R. G., Black, P. M. and Inskip, P. D. (2002) 'History of allergies and autoimmune diseases and risk of brain tumours in adults', *Int J Cancer,* 99(2), pp. 252-9.

Brieger, J., Bedavanija, A., Lehr, H. A., Maurer, J. and Mann, W. J. (2003) 'Expression of angiogenic growth factors in acoustic neurinoma', *Acta Otolaryngol,* 123(9), pp. 1040-5.

Bush, W. S. and Moore, J. H. (2012) 'Chapter 11: Genome-wide association studies', *PLoS Comput Biol,* 8(12), pp. e1002822.

Carlson, M. L., Smadbeck, J. B., Link, M. J., Klee, E. W., Vasmatzis, G. and Schimmenti, L. A. (2018) 'Next Generation Sequencing of Sporadic Vestibular Schwannoma: Necessity of Biallelic NF2 Inactivation and Implications of Accessory Non-NF2 Variants', *Otol Neurotol,* 39(9), pp. e860-e871.

Carrigan, P. E., Ballar, P. and Tuzmen, S. (2011) 'Site-directed mutagenesis', *Methods Mol Biol,* 700, pp. 107-24.

Carroll, D. (2014) 'Genome engineering with targetable nucleases', *Annu Rev Biochem,* 83, pp. 409-39.

Castellanos, E., Rosas, I., Solanes, A., Bielsa, I., Lázaro, C., Carrato, C., Hostalot, C., Prades, P., Roca-Ribas, F., Blanco, I., Serra, E. and HUGTiP-ICO-IMPPC, N. M. C. (2013) 'In vitro antisense therapeutics for a deep intronic mutation causing Neurofibromatosis type 2', *Eur J Hum Genet,* 21(7), pp. 769-73.

Cayé-Thomasen, P., Baandrup, L., Jacobsen, G. K., Thomsen, J. and Stangerup, S. E. (2003) 'Immunohistochemical demonstration of vascular endothelial growth factor in vestibular schwannomas correlates to tumour growth rate', *Laryngoscope,* 113(12), pp. 2129-34.

Cayé-Thomasen, P., Borup, R., Stangerup, S. E., Thomsen, J. and Nielsen, F. C. (2010) 'Deregulated genes in sporadic vestibular schwannomas', *Otol Neurotol,* 31(2), pp. 256-66.

Chen, C. H., Xiao, T., Xu, H., Jiang, P., Meyer, C. A., Li, W., Brown, M. and Liu, X. S. (2018) 'Improved design and analysis of CRISPR knockout screens', *Bioinformatics,* 34(23), pp. 4095-4101.

Chow, R. D., Chen, J. S., Shen, J. and Chen, S. (2021) 'A web tool for the design of prime-editing guide RNAs', *Nat Biomed Eng,* 5(2), pp. 190-194.

Chung, J., Jun, G. R., Dupuis, J. and Farrer, L. A. (2019) 'Comparison of methods for multivariate gene-based association tests for complex diseases using common variants', *Eur J Hum Genet,* 27(5), pp. 811-823.

Cioffi, J. A., Yue, W. Y., Mendolia-Loffredo, S., Hansen, K. R., Wackym, P. A. and Hansen, M. R. (2010) 'MicroRNA-21 overexpression contributes to vestibular schwannoma cell proliferation and survival', *Otol Neurotol,* 31(9), pp. 1455-62.

Clucas, J. and Valderrama, F. (2014) 'ERM proteins in cancer progression', *J Cell Sci,* 127(Pt 2), pp. 267-75.

Consortium, W. T. C. C. (2007) 'Genome-wide association study of 14,000 cases of seven common diseases and 3,000 shared controls', *Nature,* 447(7145), pp. 661-78.

Cui, Y., Groth, S., Troutman, S., Carlstedt, A., Sperka, T., Riecken, L. B., Kissil, J. L., Jin, H. and Morrison, H. (2019) 'The NF2 tumour suppressor merlin interacts with Ras and RasGAP, which may modulate Ras signaling', *Oncogene,* 38(36), pp. 6370-6381.

Cunnington, M. S., Santibanez Koref, M., Mayosi, B. M., Burn, J. and Keavney, B. (2010) 'Chromosome 9p21 SNPs Associated with Multiple Disease Phenotypes Correlate with ANRIL Expression', *PLoS Genet,* 6(4), pp. e1000899.

Das, S., Forer, L., Schönherr, S., Sidore, C., Locke, A. E., Kwong, A., Vrieze, S. I., Chew, E. Y., Levy, S., McGue, M., Schlessinger, D., Stambolian, D., Loh, P. R., Iacono, W. G., Swaroop, A., Scott, L. J., Cucca, F., Kronenberg, F., Boehnke, M., Abecasis, G. R. and Fuchsberger, C. (2016) 'Next-generation genotype imputation service and methods', *Nat Genet,* 48(10), pp. 1284-1287.

Davis, L. and Maizels, N. (2014) 'Homology-directed repair of DNA nicks via pathways distinct from canonical double-strand break repair', *Proc Natl Acad Sci U S A,* 111(10), pp. E924-32.

De Klein, A., Riegman, P. H., Bijlsma, E. K., Heldoorn, A., Muijtjens, M., den Bakker, M. A., Avezaat, C. J. and Zwarthoff, E. C. (1998) 'A G-->A transition creates a branch point sequence and activation of a cryptic exon, resulting in the hereditary disorder neurofibromatosis 2', *Hum Mol Genet,* 7(3), pp. 393-8.

de Vries, M., van der Mey, A. G. and Hogendoorn, P. C. (2015) 'Tumour Biology of Vestibular Schwannoma: A Review of Experimental Data on the Determinants of Tumour Genesis and Growth Characteristics', *Otol Neurotol,* 36(7), pp. 1128-36.

Evans, D. G. (2009) 'Neurofibromatosis type 2 (NF2): a clinical and molecular review', *Orphanet J Rare Dis,* 4, pp. 16.

Evans, D. G., Bowers, N. L., Tobi, S., Hartley, C., Wallace, A. J., King, A. T., Lloyd, S. K. W., Rutherford, S. A., Hammerbeck-Ward, C., Pathmanaban, O. N., Freeman, S. R., Ealing, J., Kellett, M., Laitt, R., Thomas, O., Halliday, D., Ferner, R., Taylor, A., Duff, C., Harkness, E. F. and Smith, M. J. (2018a) 'Schwannomatosis: a genetic and epidemiological study', *J Neurol Neurosurg Psychiatry,* 89(11), pp. 1215-1219.

Evans, D. G., Hartley, C. L., Smith, P. T., King, A. T., Bowers, N. L., Tobi, S., Wallace, A. J., Perry, M., Anup, R., Lloyd, S. K. W., Rutherford, S. A., Hammerbeck-Ward, C., Pathmanaban, O. N., Stapleton, E., Freeman, S. R., Kellett, M., Halliday, D., Parry, A., Gair, J. J., Axon, P., Laitt, R., Thomas, O., Afridi, S. K., Obholzer, R., Duff, C., Stivaros, S. M., Vassallo, G., Harkness, E. F., Smith, M. J. and group, E. S. N. r. (2019) 'Incidence of mosaicism in 1055 de novo NF2 cases: much higher than previous estimates with high utility of next-generation sequencing', *Genet Med*.

Evans, D. G., Huson, S. M., Donnai, D., Neary, W., Blair, V., Newton, V. and Harris, R. (1992) 'A clinical study of type 2 neurofibromatosis', *Q J Med,* 84(304), pp. 603-18.

Evans, D. G., King, A. T., Bowers, N. L., Tobi, S., Wallace, A. J., Perry, M., Anup, R., Lloyd, S. K. L., Rutherford, S. A., Hammerbeck-Ward, C., Pathmanaban, O. N., Stapleton, E., Freeman, S. R., Kellett, M., Halliday, D., Parry, A., Gair, J. J., Axon, P., Laitt, R., Thomas, O., Afridi, S., Ferner, R. E., Harkness, E. F., Smith, M. J. and Group, E. S. N. R. (2018b) 'Identifying the deficiencies of current diagnostic criteria for neurofibromatosis 2 using databases of 2777 individuals with molecular testing', *Genet Med*.

Evans, D. G., Moran, A., King, A., Saeed, S., Gurusinghe, N. and Ramsden, R. (2005) 'Incidence of vestibular schwannoma and neurofibromatosis 2 in the North West of England over a 10-year period: higher incidence than previously thought', *Otol Neurotol,* 26(1), pp. 93-7.

Evans, D. G., Raymond, F. L., Barwell, J. G. and Halliday, D. (2012) 'Genetic testing and screening of individuals at risk of NF2', *Clin Genet,* 82(5), pp. 416-24.

Evans, D. G., Trueman, L., Wallace, A., Collins, S. and Strachan, T. (1998a) 'Genotype/phenotype correlations in type 2 neurofibromatosis (NF2): evidence for more severe disease associated with truncating mutations', *J Med Genet,* 35(6), pp. 450-5.

Evans, D. G., Wallace, A. J., Hartley, C., Freeman, S. R., Lloyd, S. K., Thomas, O., Axon, P., Hammerbeck-Ward, C. L., Pathmanaban, O., Rutherford, S. A., Kellett, M., Laitt, R., King, A. T., Bischetsrieder, J., Blakeley, J. and Smith, M. J. (2018c) 'Familial unilateral vestibular schwannoma is rarely caused by inherited variants in the NF2 gene', *Laryngoscope*.

Evans, D. G., Wallace, A. J., Wu, C. L., Trueman, L., Ramsden, R. T. and Strachan, T. (1998b) 'Somatic mosaicism: a common cause of classic disease in tumour-prone syndromes? Lessons from type 2 neurofibromatosis', *Am J Hum Genet,* 63(3), pp. 727-36.

Firth, H. V., Richards, S. M., Bevan, A. P., Clayton, S., Corpas, M., Rajan, D., Van Vooren, S., Moreau, Y., Pettett, R. M. and Carter, N. P. (2009) 'DECIPHER: Database of Chromosomal Imbalance and Phenotype in Humans Using Ensembl Resources', *Am J Hum Genet,* 84(4), pp. 524-33.

Fisher, J. L., Pettersson, D., Palmisano, S., Schwartzbaum, J. A., Edwards, C. G., Mathiesen, T., Prochazka, M., Bergenheim, T., Florentzson, R., Harder, H., Nyberg, G., Siesjö, P. and Feychting, M. (2014) 'Loud noise exposure and acoustic neuroma', *Am J Epidemiol,* 180(1), pp. 58-67.

Fokkema, I. F. A. C., Kroon, M., López Hernández, J. A., Asscheman, D., Lugtenburg, I., Hoogenboom, J. and den Dunnen, J. T. (2021) 'The LOVD3 platform: efficient genome-wide sharing of genetic variants', *Eur J Hum Genet*.

Frattini, V., Trifonov, V., Chan, J. M., Castano, A., Lia, M., Abate, F., Keir, S. T., Ji, A. X., Zoppoli, P., Niola, F., Danussi, C., Dolgalev, I., Porrati, P., Pellegatta, S., Heguy, A., Gupta, G., Pisapia, D. J., Canoll, P., Bruce, J. N., McLendon, R. E., Yan, H., Aldape, K., Finocchiaro, G., Mikkelsen, T., Privé, G. G., Bigner, D. D., Lasorella, A., Rabadan, R. and Iavarone, A.

(2013) 'The integrated landscape of driver genomic alterations in glioblastoma', *Nat Genet,* 45(10), pp. 1141-9.

Gaudelli, N. M., Komor, A. C., Rees, H. A., Packer, M. S., Badran, A. H., Bryson, D. I. and Liu, D. R. (2017) 'Programmable base editing of A•T to G•C in genomic DNA without DNA cleavage', *Nature,* 551(7681), pp. 464-471.

Gautreau, A., Louvard, D. and Arpin, M. (2000) 'Morphogenic effects of ezrin require a phosphorylation-induced transition from oligomers to monomers at the plasma membrane', *J Cell Biol,* 150(1), pp. 193-203.

Gehlhausen, J. R., Park, S. J., Hickox, A. E., Shew, M., Staser, K., Rhodes, S. D., Menon, K., Lajiness, J. D., Mwanthi, M., Yang, X., Yuan, J., Territo, P., Hutchins, G., Nalepa, G., Yang, F. C., Conway, S. J., Heinz, M. G., Stemmer-Rachamimov, A., Yates, C. W. and Wade Clapp, D. (2015) 'A murine model of neurofibromatosis type 2 that accurately phenocopies human schwannoma formation', *Hum Mol Genet,* 24(1), pp. 1-8.

Genovese, G., Carugo, A., Tepper, J., Robinson, F. S., Li, L., Svelto, M., Nezi, L., Corti, D., Minelli, R., Pettazzoni, P., Gutschner, T., Wu, C. C., Seth, S., Akdemir, K. C., Leo, E., Amin, S., Molin, M. D., Ying, H., Kwong, L. N., Colla, S., Takahashi, K., Ghosh, P., Giuliani, V., Muller, F., Dey, P., Jiang, S., Garvey, J., Liu, C. G., Zhang, J., Heffernan, T. P., Toniatti, C., Fleming, J. B., Goggins, M. G., Wood, L. D., Sgambato, A., Agaimy, A., Maitra, A., Roberts, C. W., Wang, H., Viale, A., DePinho, R. A., Draetta, G. F. and Chin, L. (2017) 'Synthetic vulnerabilities of mesenchymal subpopulations in pancreatic cancer', *Nature,* 542(7641), pp. 362-366.

Glover, D. J., Lipps, H. J. and Jans, D. A. (2005) 'Towards safe, non-viral therapeutic gene expression in humans', *Nat Rev Genet,* 6(4), pp. 299-310.

Gondré-Lewis, M. C., Park, J. J. and Loh, Y. P. (2012) 'Cellular mechanisms for the biogenesis and transport of synaptic and dense-core vesicles', *Int Rev Cell Mol Biol,* 299, pp. 27-115.

Hadfield, K. D., Newman, W. G., Bowers, N. L., Wallace, A., Bolger, C., Colley, A., McCann, E., Trump, D., Prescott, T. and Evans, D. G. (2008) 'Molecular characterisation of SMARCB1 and NF2 in familial and sporadic schwannomatosis', *J Med Genet,* 45(6), pp. 332-9.

Hadfield, K. D., Smith, M. J., Urquhart, J. E., Wallace, A. J., Bowers, N. L., King, A. T., Rutherford, S. A., Trump, D., Newman, W. G. and Evans, D. G. (2010) 'Rates of loss of heterozygosity and mitotic recombination in NF2 schwannomas, sporadic vestibular schwannomas and schwannomatosis schwannomas', *Oncogene,* 29(47), pp. 6216-21.

Hammond, S. M. and Wood, M. J. (2011) 'Genetic therapies for RNA mis-splicing diseases', *Trends Genet,* 27(5), pp. 196-205.

Han, Y. Y., Berkowitz, O., Talbott, E., Kondziolka, D., Donovan, M. and Lunsford, L. D. (2012) 'Are frequent dental x-ray examinations associated with increased risk of vestibular schwannoma?', *J Neurosurg,* 117 Suppl, pp. 78-83.

Hanemann, C. O., Bartelt-Kirbach, B., Diebold, R., Kämpchen, K., Langmesser, S. and Utermark, T. (2006) 'Differential gene expression between human schwannoma and control Schwann cells', *Neuropathol Appl Neurobiol,* 32(6), pp. 605-14.

Hannan, C. J., Lewis, D., O'Leary, C., Donofrio, C. A., Evans, D. G., Roncaroli, F., Brough, D., King, A. T., Coope, D. and Pathmanaban, O. N. (2020) 'The inflammatory microenvironment in vestibular schwannoma', *Neurooncol Adv,* 2(1), pp. vdaa023.

Harvey, K. F., Zhang, X. and Thomas, D. M. (2013) 'The Hippo pathway and human cancer', *Nat Rev Cancer,* 13(4), pp. 246-57.

Hasegawa, T., Kida, Y., Kato, T., Iizuka, H., Kuramitsu, S., & Yamamoto, T. (2013). Long-term safety and efficacy of stereotactic radiosurgery for vestibular schwannomas: evaluation of 440 patients more than 10 years after treatment with Gamma Knife surgery. J Neurosurg, 118(3), 557-565.

Heineman, T. E., Evans, D. G., Campagne, F. and Selesnick, S. H. (2015) 'In Silico Analysis of NF2 Gene Missense Mutations in Neurofibromatosis Type 2: From Genotype to Phenotype', *Otol Neurotol,* 36(5), pp. 908-14.

Helgadottir, A., Thorleifsson, G., Magnusson, K. P., Grétarsdottir, S., Steinthorsdottir, V., Manolescu, A., Jones, G. T., Rinkel, G. J., Blankensteijn, J. D., Ronkainen, A., Jääskeläinen, J. E., Kyo, Y., Lenk, G. M., Sakalihasan, N., Kostulas, K., Gottsäter, A., Flex, A., Stefansson, H., Hansen, T., Andersen, G., Weinsheimer, S., Borch-Johnsen, K., Jorgensen, T., Shah, S. H., Quyyumi, A. A., Granger, C. B., Reilly, M. P., Austin, H., Levey, A. I., Vaccarino, V., Palsdottir, E., Walters, G. B., Jonsdottir, T., Snorradottir, S., Magnusdottir, D., Gudmundsson, G., Ferrell, R. E., Sveinbjornsdottir, S., Hernesniemi, J., Niemelä, M., Limet, R., Andersen, K., Sigurdsson, G., Benediktsson, R., Verhoeven, E. L., Teijink, J. A., Grobbee, D. E., Rader, D. J., Collier, D. A., Pedersen, O., Pola, R., Hillert, J., Lindblad, B., Valdimarsson, E. M., Magnadottir, H. B., Wijmenga, C., Tromp, G., Baas, A. F., Ruigrok, Y. M., van Rij, A. M., Kuivaniemi, H., Powell, J. T., Matthiasson, S. E., Gulcher, J. R., Thorgeirsson, G., Kong, A., Thorsteinsdottir, U. and Stefansson, K. (2008) 'The same sequence variant on 9p21 associates with myocardial infarction, abdominal aortic aneurysm and intracranial aneurysm', *Nat Genet,* 40(2), pp. 217-24.

Hemminki, K. and Li, X. (2003) 'Familial risks in nervous system tumours', *Cancer Epidemiol Biomarkers Prev,* 12(11 Pt 1), pp. 1137-42.

Hemminki, K., Tretli, S., Sundquist, J., Johannesen, T. B. and Granström, C. (2009) 'Familial risks in nervous-system tumours: a histology-specific analysis from Sweden and Norway', *Lancet Oncol,* 10(5), pp. 481-8.

Hsu, P. D., Lander, E. S. and Zhang, F. (2014) 'Development and applications of CRISPR-Cas9 for genome engineering', *Cell,* 157(6), pp. 1262-78.

Hulsebos, T. J., Plomp, A. S., Wolterman, R. A., Robanus-Maandag, E. C., Baas, F. and Wesseling, P. (2007) 'Germline mutation of INI1/SMARCB1 in familial schwannomatosis', *Am J Hum Genet,* 80(4), pp. 805-10.

Håvik, A. L., Bruland, O., Myrseth, E., Miletic, H., Aarhus, M., Knappskog, P. M. and Lund-Johansen, M. (2018) 'Genetic landscape of sporadic vestibular schwannoma', *J Neurosurg,* 128(3), pp. 911-922.

Ioannidis, N. M., Rothstein, J. H., Pejaver, V., Middha, S., McDonnell, S. K., Baheti, S., Musolf, A., Li, Q., Holzinger, E., Karyadi, D., Cannon-Albright, L. A., Teerlink, C. C., Stanford, J. L., Isaacs, W. B., Xu, J., Cooney, K. A., Lange, E. M., Schleutker, J., Carpten, J. D., Powell, I. J., Cussenot, O., Cancel-Tassin, G., Giles, G. G., MacInnis, R. J., Maier, C., Hsieh, C. L., Wiklund, F., Catalona, W. J., Foulkes, W. D., Mandal, D., Eeles, R. A., Kote-Jarai, Z., Bustamante, C. D., Schaid, D. J., Hastie, T., Ostrander, E. A., Bailey-Wilson, J. E., Radivojac, P., Thibodeau, S. N., Whittemore, A. S. and Sieh, W. (2016) 'REVEL: An Ensemble Method for Predicting the Pathogenicity of Rare Missense Variants', *Am J Hum Genet,* 99(4), pp. 877-885.

Jacob, A., Lee, T. X., Neff, B. A., Miller, S., Welling, B. and Chang, L. S. (2008) 'Phosphatidylinositol 3-kinase/AKT pathway activation in human vestibular schwannoma', *Otol Neurotol,* 29(1), pp. 58-68.

Jaganathan, K., Kyriazopoulou Panagiotopoulou, S., McRae, J. F., Darbandi, S. F., Knowles, D., Li, Y. I., Kosmicki, J. A., Arbelaez, J., Cui, W., Schwartz, G. B., Chow, E. D., Kanterakis, E., Gao, H., Kia, A., Batzoglou, S., Sanders, S. J. and Farh, K. K. (2019) 'Predicting Splicing from Primary Sequence with Deep Learning', *Cell,* 176(3), pp. 535-548.e24.

Jinek, M., Chylinski, K., Fonfara, I., Hauer, M., Doudna, J. A. and Charpentier, E. (2012) 'A programmable dual-RNA-guided DNA endonuclease in adaptive bacterial immunity', *Science,* 337(6096), pp. 816-21.

Johnston, J. J., van der Smagt, J. J., Rosenfeld, J. A., Pagnamenta, A. T., Alswaid, A., Baker, E. H., Blair, E., Borck, G., Brinkmann, J., Craigen, W., Dung, V. C., Emrick, L., Everman, D. B., van Gassen, K. L., Gulsuner, S., Harr, M. H., Jain, M., Kuechler, A., Leppig, K. A., McDonald-McGinn, D. M., Can, N. T. B., Peleg, A., Roeder, E. R., Rogers, R. C., Sagi-Dain, L., Sapp, J. C., Schäffer, A. A., Schanze, D., Stewart, H., Taylor, J. C., Verbeek, N. E., Walkiewicz, M. A., Zackai, E. H., Zweier, C., Zenker, M., Lee, B., Biesecker, L. G. and Network, M. o. t. U. D. (2018) 'Autosomal recessive Noonan syndrome associated with biallelic LZTR1 variants', *Genet Med,* 20(10), pp. 1175-1185.

Jörgensen, P. M., Gräslund, S., Betz, R., Ståhl, S., Larsson, C. and Höög, C. (2001) 'Characterisation of the human APC1, the largest subunit of the anaphase-promoting complex', *Gene,* 262(1-2), pp. 51-9.

Kadoch, C., Hargreaves, D. C., Hodges, C., Elias, L., Ho, L., Ranish, J. and Crabtree, G. R. (2013) 'Proteomic and bioinformatic analysis of mammalian SWI/SNF complexes identifies extensive roles in human malignancy', *Nat Genet,* 45(6), pp. 592-601.

Kaplan, J. C., Aurias, A., Julier, C., Prieur, M. and Szajnert, M. F. (1987) 'Human chromosome 22', *J Med Genet,* 24(2), pp. 65-78.

Karajannis, M. A., Hagiwara, M., Schreyer, M. and Haque, S. (2019) 'Sustained imaging response and hearing preservation with low-dose bevacizumab in sporadic vestibular schwannoma', *Neuro Oncol,* 21(6), pp. 822-824.

Kehrer-Sawatzki, H., Farschtschi, S., Mautner, V. F. and Cooper, D. N. (2017) 'The molecular pathogenesis of schwannomatosis, a paradigm for the co-involvement of multiple tumour suppressor genes in tumourigenesis', *Hum Genet,* 136(2), pp. 129-148.

Kent, W. J., Sugnet, C. W., Furey, T. S., Roskin, K. M., Pringle, T. H., Zahler, A. M. and Haussler, D. (2002) 'The human genome browser at UCSC', *Genome Res,* 12(6), pp. 996-1006.

Kentala, E. and Pyykkö, I. (2001) 'Clinical picture of vestibular schwannoma', *Auris Nasus Larynx,* 28(1), pp. 15-22.

Khera, A. V., Chaffin, M., Aragam, K. G., Haas, M. E., Roselli, C., Choi, S. H., Natarajan, P., Lander, E. S., Lubitz, S. A., Ellinor, P. T. and Kathiresan, S. (2018) 'Genome-wide polygenic scores for common diseases identify individuals with risk equivalent to monogenic mutations', *Nat Genet,* 50(9), pp. 1219-1224.

Kim, W. Y. and Sharpless, N. E. (2006) 'The regulation of INK4/ARF in cancer and aging', *Cell,* 127(2), pp. 265-75.

Kinnersley, B., Labussière, M., Holroyd, A., Di Stefano, A. L., Broderick, P., Vijayakrishnan, J., Mokhtari, K., Delattre, J. Y., Gousias, K., Schramm, J., Schoemaker, M. J., Fleming, S. J., Herms, S., Heilmann, S., Schreiber, S., Wichmann, H. E., Nöthen, M. M., Swerdlow, A., Lathrop, M., Simon, M., Bondy, M., Sanson, M. and Houlston, R. S. (2015) 'Genome-wide association study identifies multiple susceptibility loci for glioma', *Nat Commun,* 6, pp. 8559.

Kleijwegt, M., Ho, V., Visser, O., Godefroy, W. and van der Mey, A. (2016) 'Real Incidence of Vestibular Schwannoma? Estimations From a National Registry', *Otol Neurotol,* 37(9), pp. 1411-7.

Kluwe, L., MacCollin, M., Tatagiba, M., Thomas, S., Hazim, W., Haase, W. and Mautner, V. F. (1998) 'Phenotypic variability associated with 14 splice-site mutations in the NF2 gene', *Am J Med Genet,* 77(3), pp. 228-33.

Knudson, A. G. (1971) 'Mutation and cancer: statistical study of retinoblastoma', *Proc Natl Acad Sci U S A,* 68(4), pp. 820-3.

Komor, A. C., Kim, Y. B., Packer, M. S., Zuris, J. A. and Liu, D. R. (2016) 'Programmable editing of a target base in genomic DNA without double-stranded DNA cleavage', *Nature,* 533(7603), pp. 420-4.

Kruyt, I. J., Verheul, J. B., Hanssens, P. E. J., & Kunst, H. P. M. (2018). Gamma Knife radiosurgery for treatment of growing vestibular schwannomas in patients with neurofibromatosis Type 2: a matched cohort study with sporadic vestibular schwannomas. J Neurosurg, 128(1), 49-59.

Kshettry, V. R., Hsieh, J. K., Ostrom, Q. T., Kruchko, C. and Barnholtz-Sloan, J. S. (2015) 'Incidence of vestibular schwannomas in the United States', *J Neurooncol,* 124(2), pp. 223-8.

Kumar, P., Henikoff, S. and Ng, P. C. (2009) 'Predicting the effects of coding non-synonymous variants on protein function using the SIFT algorithm', *Nat Protoc,* 4(7), pp. 1073-81.

Kumar, R., Smeds, J., Lundh Rozell, B. and Hemminki, K. (1999) 'Loss of heterozygosity at chromosome 9p21 (INK4-p14ARF locus): homozygous deletions and mutations in the p16 and p14ARF genes in sporadic primary melanomas', *Melanoma Res,* 9(2), pp. 138-47.

Lacerra, G., Sierakowska, H., Carestia, C., Fucharoen, S., Summerton, J., Weller, D. and Kole, R. (2000) 'Restoration of hemoglobin A synthesis in erythroid cells from peripheral blood of thalassemic patients', *Proc Natl Acad Sci U S A,* 97(17), pp. 9591-6.

Lambert, S. A., Abraham, G. and Inouye, M. (2019) 'Towards clinical utility of polygenic risk scores', *Hum Mol Genet,* 28(R2), pp. R133-R142.

Landrum, M. J., Lee, J. M., Benson, M., Brown, G. R., Chao, C., Chitipiralla, S., Gu, B., Hart, J., Hoffman, D., Jang, W., Karapetyan, K., Katz, K., Liu, C., Maddipatla, Z., Malheiro, A., McDaniel, K., Ovetsky, M., Riley, G., Zhou, G., Holmes, J. B., Kattman, B. L. and Maglott, D. R. (2018) 'ClinVar: improving access to variant interpretations and supporting evidence', *Nucleic Acids Res,* 46(D1), pp. D1062-D1067.

Lassaletta, L., Torres-Martín, M., Peña-Granero, C., Roda, J. M., Santa-Cruz-Ruiz, S., Castresana, J. S., Gavilan, J. and Rey, J. A. (2013) 'NF2 genetic alterations in sporadic vestibular schwannomas: clinical implications', *Otol Neurotol,* 34(7), pp. 1355-61.

Lek, M., Karczewski, K. J., Minikel, E. V., Samocha, K. E., Banks, E., Fennell, T., O'Donnell-Luria, A. H., Ware, J. S., Hill, A. J., Cummings, B. B., Tukiainen, T., Birnbaum, D. P., Kosmicki, J. A., Duncan, L. E., Estrada, K., Zhao, F., Zou, J., Pierce-Hoffman, E., Berghout, J., Cooper, D. N., Deflaux, N., DePristo, M., Do, R., Flannick, J., Fromer, M., Gauthier, L., Goldstein, J., Gupta, N., Howrigan, D., Kiezun, A., Kurki, M. I., Moonshine, A. L., Natarajan, P., Orozco, L., Peloso, G. M., Poplin, R., Rivas, M. A., Ruano-Rubio, V., Rose, S. A., Ruderfer, D. M., Shakir, K., Stenson, P. D., Stevens, C., Thomas, B. P., Tiao, G., Tusie-Luna, M. T., Weisburd, B., Won, H. H., Yu, D., Altshuler, D. M., Ardissino, D., Boehnke, M., Danesh, J., Donnelly, S., Elosua, R., Florez, J. C., Gabriel, S. B., Getz, G., Glatt, S. J., Hultman, C. M., Kathiresan, S., Laakso, M., McCarroll, S., McCarthy, M. I., McGovern, D., McPherson, R., Neale, B. M., Palotie, A., Purcell, S. M., Saleheen, D., Scharf, J. M., Sklar, P., Sullivan, P. F., Tuomilehto, J., Tsuang, M. T., Watkins, H. C., Wilson, J. G., Daly, M. J., MacArthur, D. G. and Consortium, E. A. (2016) 'Analysis of protein-coding genetic variation in 60,706 humans', *Nature,* 536(7616), pp. 285-91.

Lewis, D., Roncaroli, F., Agushi, E., Mosses, D., Williams, R., Li, K. L., Zhu, X., Hinz, R., Atkinson, R., Wadeson, A., Hulme, S., Mayers, H., Stapleton, E., Lloyd, S. K. L., Freeman, S. R., Rutherford, S. A., Hammerbeck-Ward, C., Evans, D. G., Pathmanaban, O., Jackson, A., King, A. T. and Coope, D. (2018) 'Inflammation and Vascular Permeability Correlate With Growth in Sporadic Vestibular Schwannoma', *Neuro Oncol*.

Li, H., Chang, L. J., Neubauer, D. R., Muir, D. F. and Wallace, M. R. (2016) 'Immortalization of human normal and NF1 neurofibroma Schwann cells', *Lab Invest,* 96(10), pp. 1105-15.

Li, H., Yang, Y., Hong, W., Huang, M., Wu, M. and Zhao, X. (2020) 'Applications of genome editing technology in the targeted therapy of human diseases: mechanisms, advances and prospects', *Signal Transduct Target Ther,* 5(1), pp. 1.

Li, M. X., Yeung, J. M., Cherny, S. S. and Sham, P. C. (2012) 'Evaluating the effective numbers of independent tests and significant p-value thresholds in commercial genotyping arrays and public imputation reference datasets', *Hum Genet,* 131(5), pp. 747-56.

Li, Q., Wang, Z., Zong, L., Ye, L., Ye, J., Ou, H., Jiang, T., Guo, B., Yang, Q., Liang, W., Zhang, J., Long, Y., Zheng, X., Hou, Y., Wu, F., Zhou, L., Li, S., Huang, X. and Zhao, C. (2021) 'Allele-specific DNA methylation maps in monozygotic twins discordant for psychiatric disorders reveal that disease-associated switching at the EIPR1 regulatory loci modulates neural function', *Mol Psychiatry*.

Li, X., Burnight, E. R., Cooney, A. L., Malani, N., Brady, T., Sander, J. D., Staber, J., Wheelan, S. J., Joung, J. K., McCray, P. B., Bushman, F. D., Sinn, P. L. and Craig, N. L. (2013) 'piggyBac transposase tools for genome engineering', *Proc Natl Acad Sci U S A,* 110(25), pp. E2279-87.

Liu, X., Homma, A., Sayadi, J., Yang, S., Ohashi, J. and Takumi, T. (2016) 'Sequence features associated with the cleavage efficiency of CRISPR/Cas9 system', *Sci Rep,* 6, pp. 19675.

MacCollin, M., Chiocca, E. A., Evans, D. G., Friedman, J. M., Horvitz, R., Jaramillo, D., Lev, M., Mautner, V. F., Niimura, M., Plotkin, S. R., Sang, C. N., Stemmer-Rachamimov, A. and

Roach, E. S. (2005) 'Diagnostic criteria for schwannomatosis', *Neurology,* 64(11), pp. 1838-45.
Marchini, J. and Howie, B. (2010) 'Genotype imputation for genome-wide association studies', *Nat Rev Genet,* 11(7), pp. 499-511.
Marraffini, L. A. and Sontheimer, E. J. (2010) 'CRISPR interference: RNA-directed adaptive immunity in bacteria and archaea', *Nat Rev Genet,* 11(3), pp. 181-90.
Martin, J. H., Leonard, M. E. and Radzyner, H. (2003) *Neuroanatomy: text and atlas.*
Mathe, E., Olivier, M., Kato, S., Ishioka, C., Hainaut, P. and Tavtigian, S. V. (2006) 'Computational approaches for predicting the biological effect of p53 missense mutations: a comparison of three sequence analysis based methods', *Nucleic Acids Res,* 34(5), pp. 1317-25.
Mathieu, D., Kondziolka, D., Flickinger, J. C., Niranjan, A., Williamson, R., Martin, J. J., & Lunsford, L. D. (2007). Stereotactic radiosurgery for vestibular schwannomas in patients with neurofibromatosis type 2: an analysis of tumor control, complications, and hearing preservation rates. Neurosurgery, 60(3), 460-468; discussion 468-470.
Mautner, V. F., Lindenau, M., Baser, M. E., Hazim, W., Tatagiba, M., Haase, W., Samii, M., Wais, R. and Pulst, S. M. (1996) 'The neuroimaging and clinical spectrum of neurofibromatosis 2', *Neurosurgery,* 38(5), pp. 880-5; discussion 885-6.
Milev, M. P., Grout, M. E., Saint-Dic, D., Cheng, Y. H., Glass, I. A., Hale, C. J., Hanna, D. S., Dorschner, M. O., Prematilake, K., Shaag, A., Elpeleg, O., Sacher, M., Doherty, D. and Edvardson, S. (2017) 'Mutations in TRAPPC12 Manifest in Progressive Childhood Encephalopathy and Golgi Dysfunction', *Am J Hum Genet,* 101(2), pp. 291-299.
Molla, K. A. and Yang, Y. (2019) 'CRISPR/Cas-Mediated Base Editing: Technical Considerations and Practical Applications', *Trends Biotechnol,* 37(10), pp. 1121-1142.
Morris, K. A., Golding, J. F., Axon, P. R., Afridi, S., Blesing, C., Ferner, R. E., Halliday, D., Jena, R., Pretorius, P. M., Evans, D. G., McCabe, M. G., Parry, A. and group, U. N. R. (2016) 'Bevacizumab in neurofibromatosis type 2 (NF2) related vestibular schwannomas: a nationally coordinated approach to delivery and prospective evaluation', *Neurooncol Pract,* 3(4), pp. 281-289.
Morris, K. A., Golding, J. F., Blesing, C., Evans, D. G., Ferner, R. E., Foweraker, K., Halliday, D., Jena, R., McBain, C., McCabe, M. G., Swampillai, A., Warner, N., Wilson, S., Parry, A., Afridi, S. K. and group, U. N. r. (2017) 'Toxicity profile of bevacizumab in the UK Neurofibromatosis type 2 cohort', *J Neurooncol,* 131(1), pp. 117-124.
Morrison, H., Sherman, L. S., Legg, J., Banine, F., Isacke, C., Haipek, C. A., Gutmann, D. H., Ponta, H. and Herrlich, P. (2001) 'The NF2 tumour suppressor gene product, merlin, mediates contact inhibition of growth through interactions with CD44', *Genes Dev,* 15(8), pp. 968-80.
Motta, M., Fidan, M., Bellacchio, E., Pantaleoni, F., Schneider-Heieck, K., Coppola, S., Borck, G., Salviati, L., Zenker, M., Cirstea, I. C. and Tartaglia, M. (2018) 'Dominant Noonan syndrome-causing LZTR1 mutations specifically affect the kelch domain substrate-recognition surface and enhance RAS-MAPK signaling', *Hum Mol Genet*.
Muranen, T., Grönholm, M., Lampin, A., Lallemand, D., Zhao, F., Giovannini, M. and Carpén, O. (2007) 'The tumour suppressor merlin interacts with microtubules and modulates Schwann cell microtubule cytoskeleton', *Hum Mol Genet,* 16(14), pp. 1742-51.
Nacak, T. G., Leptien, K., Fellner, D., Augustin, H. G. and Kroll, J. (2006) 'The BTB-kelch protein LZTR-1 is a novel Golgi protein that is degraded upon induction of apoptosis', *J Biol Chem,* 281(8), pp. 5065-71.
'National Institutes of Health Consensus Development Conference Statement on Acoustic Neuroma, December 11-13, 1991. The Consensus Development Panel', (1994) *Arch Neurol,* 51(2), pp. 201-7.
Naviglio, S., Mattecucci, C., Matoskova, B., Nagase, T., Nomura, N., Di Fiore, P. P. and Draetta, G. F. (1998) 'UBPY: a growth-regulated human ubiquitin isopeptidase', *EMBO J,* 17(12), pp. 3241-50.

Network, C. G. A. R. (2008) 'Comprehensive genomic characterization defines human glioblastoma genes and core pathways', *Nature,* 455(7216), pp. 1061-8.

Ogata, T., Kozuka, T. and Kanda, T. (2003) 'Identification of an insulator in AAVS1, a preferred region for integration of adeno-associated virus DNA', *J Virol,* 77(16), pp. 9000-7.

Ostrom, Q. T., Cioffi, G., Waite, K., Kruchko, C. and Barnholtz-Sloan, J. S. (2021) 'CBTRUS Statistical Report: Primary Brain and Other Central Nervous System Tumours Diagnosed in the United States in 2014-2018', *Neuro Oncol,* 23(12 Suppl 2), pp. iii1-iii105.

Paganini, I., Chang, V. Y., Capone, G. L., Vitte, J., Benelli, M., Barbetti, L., Sestini, R., Trevisson, E., Hulsebos, T. J., Giovannini, M., Nelson, S. F. and Papi, L. (2015) 'Expanding the mutational spectrum of LZTR1 in schwannomatosis', *Eur J Hum Genet,* 23(7), pp. 963-8.

Parry, D. M., Eldridge, R., Kaiser-Kupfer, M. I., Bouzas, E. A., Pikus, A. and Patronas, N. (1994) 'Neurofibromatosis 2 (NF2): clinical characteristics of 63 affected individuals and clinical evidence for heterogeneity', *Am J Med Genet,* 52(4), pp. 450-61.

Pasmant, E., Laurendeau, I., Héron, D., Vidaud, M., Vidaud, D. and Bièche, I. (2007) 'Characterization of a germ-line deletion, including the entire INK4/ARF locus, in a melanoma-neural system tumour family: identification of ANRIL, an antisense noncoding RNA whose expression coclusters with ARF', *Cancer Res,* 67(8), pp. 3963-9.

Pasmant, E., Sabbagh, A., Masliah-Planchon, J., Ortonne, N., Laurendeau, I., Melin, L., Ferkal, S., Hernandez, L., Leroy, K., Valeyrie-Allanore, L., Parfait, B., Vidaud, D., Bièche, I., Lantieri, L., Wolkenstein, P., Vidaud, M. and Network, N. F. (2011a) 'Role of noncoding RNA ANRIL in genesis of plexiform neurofibromas in neurofibromatosis type 1', *J Natl Cancer Inst,* 103(22), pp. 1713-22.

Pasmant, E., Sabbagh, A., Vidaud, M. and Bièche, I. (2011b) 'ANRIL, a long, noncoding RNA, is an unexpected major hotspot in GWAS', *FASEB J,* 25(2), pp. 444-8.

Pathmanaban, O. N., Sadler, K. V., Kamaly-Asl, I. D., King, A. T., Rutherford, S. A., Hammerbeck-Ward, C., McCabe, M. G., Kilday, J. P., Beetz, C., Poplawski, N. K., Evans, D. G. and Smith, M. J. (2017) 'Association of Genetic Predisposition With Solitary Schwannoma or Meningioma in Children and Young Adults', *JAMA Neurol,* 74(9), pp. 1123-1129.

Perez-Becerril, C., Evans, D. G. and Smith, M. J. (2021) 'Pathogenic noncoding variants in the neurofibromatosis and schwannomatosis predisposition genes', *Hum Mutat,* 42(10), pp. 1187-1207.

Petrilli, A. M. and Fernández-Valle, C. (2016) 'Role of Merlin/NF2 inactivation in tumour biology', *Oncogene,* 35(5), pp. 537-48.

Piotrowski, A., Xie, J., Liu, Y. F., Poplawski, A. B., Gomes, A. R., Madanecki, P., Fu, C., Crowley, M. R., Crossman, D. K., Armstrong, L., Babovic-Vuksanovic, D., Bergner, A., Blakeley, J. O., Blumenthal, A. L., Daniels, M. S., Feit, H., Gardner, K., Hurst, S., Kobelka, C., Lee, C., Nagy, R., Rauen, K. A., Slopis, J. M., Suwannarat, P., Westman, J. A., Zanko, A., Korf, B. R. and Messiaen, L. M. (2014) 'Germline loss-of-function mutations in LZTR1 predispose to an inherited disorder of multiple schwannomas', *Nat Genet,* 46(2), pp. 182-7.

Plotkin, S. R., Merker, V. L., Halpin, C., Jennings, D., McKenna, M. J., Harris, G. J. and Barker, F. G. (2012) 'Bevacizumab for progressive vestibular schwannoma in neurofibromatosis type 2: a retrospective review of 31 patients', *Otol Neurotol,* 33(6), pp. 1046-52.

Plotkin, S. R., Stemmer-Rachamimov, A. O., Barker, F. G., Halpin, C., Padera, T. P., Tyrrell, A., Sorensen, A. G., Jain, R. K. and di Tomaso, E. (2009) 'Hearing improvement after bevacizumab in patients with neurofibromatosis type 2', *N Engl J Med,* 361(4), pp. 358-67.

Recillas-Targa, F. (2006) 'Multiple strategies for gene transfer, expression, knockdown, and chromatin influence in mammalian cell lines and transgenic animals', *Mol Biotechnol,* 34(3), pp. 337-54.

Richards, S., Aziz, N., Bale, S., Bick, D., Das, S., Gastier-Foster, J., Grody, W. W., Hegde, M., Lyon, E., Spector, E., Voelkerding, K., Rehm, H. L. and Committee, A. L. Q. A. (2015) 'Standards and guidelines for the interpretation of sequence variants: a joint consensus recommendation of the American College of Medical Genetics and Genomics and the Association for Molecular Pathology', *Genet Med,* 17(5), pp. 405-24.

Roberts, C. W. and Orkin, S. H. (2004) 'The SWI/SNF complex--chromatin and cancer', *Nat Rev Cancer,* 4(2), pp. 133-42.

Ron, E., Modan, B., Boice, J. D., Alfandary, E., Stovall, M., Chetrit, A. and Katz, L. (1988) 'Tumours of the brain and nervous system after radiotherapy in childhood', *N Engl J Med,* 319(16), pp. 1033-9.

Rong, R., Tang, X., Gutmann, D. H. and Ye, K. (2004) 'Neurofibromatosis 2 (NF2) tumour suppressor merlin inhibits phosphatidylinositol 3-kinase through binding to PIKE-L', *Proc Natl Acad Sci U S A,* 101(52), pp. 18200-5.

Rousseau, G., Noguchi, T., Bourdon, V., Sobol, H. and Olschwang, S. (2011) 'SMARCB1/INI1 germline mutations contribute to 10% of sporadic schwannomatosis', *BMC Neurol,* 11, pp. 9.

Ruttledge, M. H., Andermann, A. A., Phelan, C. M., Claudio, J. O., Han, F. Y., Chretien, N., Rangaratnam, S., MacCollin, M., Short, P., Parry, D., Michels, V., Riccardi, V. M., Weksberg, R., Kitamura, K., Bradburn, J. M., Hall, B. D., Propping, P. and Rouleau, G. A. (1996) 'Type of mutation in the neurofibromatosis type 2 gene (NF2) frequently determines severity of disease', *Am J Hum Genet,* 59(2), pp. 331-42.

Sadler, K. V., Bowers, N. L., Hartley, C., Smith, P. T., Tobi, S., Wallace, A. J., King, A., Lloyd, S. K. W., Rutherford, S., Pathmanaban, O. N., Hammerbeck-Ward, C., Freeman, S., Stapleton, E., Taylor, A., Shaw, A., Halliday, D., Smith, M. J. and Evans, D. G. (2020) 'Sporadic vestibular schwannoma: a molecular testing summary', *J Med Genet*.

Sainz, J., Huynh, D. P., Figueroa, K., Ragge, N. K., Baser, M. E. and Pulst, S. M. (1994) 'Mutations of the neurofibromatosis type 2 gene and lack of the gene product in vestibular schwannomas', *Hum Mol Genet,* 3(6), pp. 885-91.

Saito, K., Kato, M., Susaki, N., Nagatani, T., Nagasaka, T. and Yoshida, J. (2003) 'Expression of Ki-67 antigen and vascular endothelial growth factor in sporadic and neurofibromatosis type 2-associated schwannomas', *Clin Neuropathol,* 22(1), pp. 30-4.

Sargen, M. R., Merrill, S. L., Chu, E. Y. and Nathanson, K. L. (2016) 'CDKN2A mutations with p14 loss predisposing to multiple nerve sheath tumours, melanoma, dysplastic naevi and internal malignancies: a case series and review of the literature', *Br J Dermatol,* 175(4), pp. 785-9.

Sass, H. C., Borup, R., Alanin, M., Nielsen, F. C. and Cayé-Thomasen, P. (2017) 'Gene expression, signal transduction pathways and functional networks associated with growth of sporadic vestibular schwannomas', *J Neurooncol,* 131(2), pp. 283-292.

Sass, H. C. R., Hansen, M., Borup, R., Nielsen, F. C. and Cayé-Thomasen, P. (2020) 'Tumour miRNA expression profile is related to vestibular schwannoma growth rate', *Acta Neurochir (Wien),* 162(5), pp. 1187-1195.

Saydam, O., Senol, O., Würdinger, T., Mizrak, A., Ozdener, G. B., Stemmer-Rachamimov, A. O., Yi, M., Stephens, R. M., Krichevsky, A. M., Saydam, N., Brenner, G. J. and Breakefield, X. O. (2011) 'miRNA-7 attenuation in Schwannoma tumours stimulates growth by upregulating three oncogenic signaling pathways', *Cancer Res,* 71(3), pp. 852-61.

Schlehofer, B., Schlaefer, K., Blettner, M., Berg, G., Böhler, E., Hettinger, I., Kunna-Grass, K., Wahrendorf, J., Schüz, J. and Group, I. S. (2007) 'Environmental risk factors for sporadic acoustic neuroma (Interphone Study Group, Germany)', *Eur J Cancer,* 43(11), pp. 1741-7.

Schroeder, R. D., Angelo, L. S. and Kurzrock, R. (2014) 'NF2/merlin in hereditary neurofibromatosis 2 versus cancer: biologic mechanisms and clinical associations', *Oncotarget,* 5(1), pp. 67-77.

Schubert, M. S., Thommandru, B., Woodley, J., Turk, R., Yan, S., Kurgan, G., McNeill, M. S. and Rettig, G. R. (2021) 'Optimized design parameters for CRISPR Cas9 and Cas12a homology-directed repair', *Sci Rep,* 11(1), pp. 19482.

Schwarz, J. M., Cooper, D. N., Schuelke, M. and Seelow, D. (2014) 'MutationTaster2: mutation prediction for the deep-sequencing age', *Nat Methods,* 11(4), pp. 361-2.

Scrivens, P. J., Noueihed, B., Shahrzad, N., Hul, S., Brunet, S. and Sacher, M. (2011) 'C4orf41 and TTC-15 are mammalian TRAPP components with a role at an early stage in ER-to-Golgi trafficking', *Mol Biol Cell,* 22(12), pp. 2083-93.

Sestini, R., Bacci, C., Provenzano, A., Genuardi, M. and Papi, L. (2008) 'Evidence of a four-hit mechanism involving SMARCB1 and NF2 in schwannomatosis-associated schwannomas', *Hum Mutat,* 29(2), pp. 227-31.

Sharpless, N. E., Ramsey, M. R., Balasubramanian, P., Castrillon, D. H. and DePinho, R. A. (2004) 'The differential impact of p16(INK4a) or p19(ARF) deficiency on cell growth and tumourigenesis', *Oncogene,* 23(2), pp. 379-85.

Shaw, R. J., Paez, J. G., Curto, M., Yaktine, A., Pruitt, W. M., Saotome, I., O'Bryan, J. P., Gupta, V., Ratner, N., Der, C. J., Jacks, T. and McClatchey, A. I. (2001) 'The Nf2 tumour suppressor, merlin, functions in Rac-dependent signaling', *Dev Cell,* 1(1), pp. 63-72.

Sherry, S. T., Ward, M. H., Kholodov, M., Baker, J., Phan, L., Smigielski, E. M. and Sirotkin, K. (2001) 'dbSNP: the NCBI database of genetic variation', *Nucleic Acids Res,* 29(1), pp. 308-11.

Shete, S., Hosking, F. J., Robertson, L. B., Dobbins, S. E., Sanson, M., Malmer, B., Simon, M., Marie, Y., Boisselier, B., Delattre, J. Y., Hoang-Xuan, K., El Hallani, S., Idbaih, A., Zelenika, D., Andersson, U., Henriksson, R., Bergenheim, A. T., Feychting, M., Lönn, S., Ahlbom, A., Schramm, J., Linnebank, M., Hemminki, K., Kumar, R., Hepworth, S. J., Price, A., Armstrong, G., Liu, Y., Gu, X., Yu, R., Lau, C., Schoemaker, M., Muir, K., Swerdlow, A., Lathrop, M., Bondy, M. and Houlston, R. S. (2009) 'Genome-wide association study identifies five susceptibility loci for glioma', *Nat Genet,* 41(8), pp. 899-904.

Shimizu, T., Seto, A., Maita, N., Hamada, K., Tsukita, S. and Hakoshima, T. (2002) 'Structural basis for neurofibromatosis type 2. Crystal structure of the merlin FERM domain', *J Biol Chem,* 277(12), pp. 10332-6.

Shostak, K. and Chariot, A. (2015) 'EGFR and NF-κB: partners in cancer', *Trends Mol Med,* 21(6), pp. 385-93.

Sievers, F., Wilm, A., Dineen, D., Gibson, T. J., Karplus, K., Li, W., Lopez, R., McWilliam, H., Remmert, M., Söding, J., Thompson, J. D. and Higgins, D. G. (2011) 'Fast, scalable generation of high-quality protein multiple sequence alignments using Clustal Omega', *Mol Syst Biol,* 7, pp. 539.

Simanshu, D. K., Nissley, D. V. and McCormick, F. (2017) 'RAS Proteins and Their Regulators in Human Disease', *Cell,* 170(1), pp. 17-33.

Simon, M., Voss, D., Park-Simon, T. W., Mahlberg, R. and Köster, G. (2006) 'Role of p16 and p14ARF in radio- and chemosensitivity of malignant gliomas', *Oncol Rep,* 16(1), pp. 127-32.

Skol, A. D., Scott, L. J., Abecasis, G. R. and Boehnke, M. (2007) 'Optimal designs for two-stage genome-wide association studies', *Genet Epidemiol,* 31(7), pp. 776-88.

Smith, M. J., Bowers, N. L., Bulman, M., Gokhale, C., Wallace, A. J., King, A. T., Lloyd, S. K., Rutherford, S. A., Hammerbeck-Ward, C. L., Freeman, S. R. and Evans, D. G. (2017) 'Revisiting neurofibromatosis type 2 diagnostic criteria to exclude LZTR1-related schwannomatosis', *Neurology,* 88(1), pp. 87-92.

Smith, M. J., Isidor, B., Beetz, C., Williams, S. G., Bhaskar, S. S., Richer, W., O'Sullivan, J., Anderson, B., Daly, S. B., Urquhart, J. E., Fryer, A., Rustad, C. F., Mills, S. J., Samii, A., du Plessis, D., Halliday, D., Barbarot, S., Bourdeaut, F., Newman, W. G. and Evans, D. G. (2015) 'Mutations in LZTR1 add to the complex heterogeneity of schwannomatosis', *Neurology,* 84(2), pp. 141-7.

Smith, M. J., Kulkarni, A., Rustad, C., Bowers, N. L., Wallace, A. J., Holder, S. E., Heiberg, A., Ramsden, R. T. and Evans, D. G. (2012a) 'Vestibular schwannomas occur in schwannomatosis and should not be considered an exclusion criterion for clinical diagnosis', *Am J Med Genet A,* 158A(1), pp. 215-9.

Smith, M. J., Wallace, A. J., Bowers, N. L., Rustad, C. F., Woods, C. G., Leschziner, G. D., Ferner, R. E. and Evans, D. G. (2012b) 'Frequency of SMARCB1 mutations in familial and sporadic schwannomatosis', *Neurogenetics,* 13(2), pp. 141-5.

Spitali, P. and Aartsma-Rus, A. (2012) 'Splice modulating therapies for human disease', *Cell,* 148(6), pp. 1085-8.

Steklov, M., Pandolfi, S., Baietti, M. F., Batiuk, A., Carai, P., Najm, P., Zhang, M., Jang, H., Renzi, F., Cai, Y., Abbasi Asbagh, L., Pastor, T., De Troyer, M., Simicek, M., Radaelli, E., Brems, H., Legius, E., Tavernier, J., Gevaert, K., Impens, F., Messiaen, L., Nussinov, R., Heymans, S., Eyckerman, S. and Sablina, A. A. (2018) 'Mutations in LZTR1 drive human disease by dysregulating RAS ubiquitination', *Science,* 362(6419), pp. 1177-1182.

Stenson, P. D., Mort, M., Ball, E. V., Chapman, M., Evans, K., Azevedo, L., Hayden, M., Heywood, S., Millar, D. S., Phillips, A. D. and Cooper, D. N. (2020) 'The Human Gene Mutation Database (HGMD', *Hum Genet,* 139(10), pp. 1197-1207.

Stivaros, S. M., Stemmer-Rachamimov, A. O., Alston, R., Plotkin, S. R., Nadol, J. B., Quesnel, A., O'Malley, J., Whitfield, G. A., McCabe, M. G., Freeman, S. R., Lloyd, S. K., Wright, N. B., Kilday, J. P., Kamaly-Asl, I. D., Mills, S. J., Rutherford, S. A., King, A. T. and Evans, D. G. (2015) 'Multiple synchronous sites of origin of vestibular schwannomas in neurofibromatosis Type 2', *J Med Genet,* 52(8), pp. 557-62.

Su, F., Zhou, Z., Su, W., Wang, Z. and Wu, Q. (2016) 'A novel alternative splicing isoform of NF2 identified in human Schwann cells', *Oncol Lett,* 12(2), pp. 977-982.

Suckow, J., Markiewicz, P., Kleina, L. G., Miller, J., Kisters-Woike, B. and Müller-Hill, B. (1996) 'Genetic studies of the Lac repressor. XV: 4000 single amino acid substitutions and analysis of the resulting phenotypes on the basis of the protein structure', *J Mol Biol,* 261(4), pp. 509-23.

Sudlow, C., Gallacher, J., Allen, N., Beral, V., Burton, P., Danesh, J., Downey, P., Elliott, P., Green, J., Landray, M., Liu, B., Matthews, P., Ong, G., Pell, J., Silman, A., Young, A., Sprosen, T., Peakman, T. and Collins, R. (2015) 'UK biobank: an open access resource for identifying the causes of a wide range of complex diseases of middle and old age', *PLoS Med,* 12(3), pp. e1001779.

Sévenet, N., Sheridan, E., Amram, D., Schneider, P., Handgretinger, R. and Delattre, O. (1999) 'Constitutional mutations of the hSNF5/INI1 gene predispose to a variety of cancers', *Am J Hum Genet,* 65(5), pp. 1342-8.

Tai, A. L., Sham, J. S., Xie, D., Fang, Y., Wu, Y. L., Hu, L., Deng, W., Tsao, G. S., Qiao, G. B., Cheung, A. L. and Guan, X. Y. (2006) 'Co-overexpression of fibroblast growth factor 3 and epidermal growth factor receptor is correlated with the development of nonsmall cell lung carcinoma', *Cancer,* 106(1), pp. 146-55.

Tate, J. G., Bamford, S., Jubb, H. C., Sondka, Z., Beare, D. M., Bindal, N., Boutselakis, H., Cole, C. G., Creatore, C., Dawson, E., Fish, P., Harsha, B., Hathaway, C., Jupe, S. C., Kok, C. Y., Noble, K., Ponting, L., Ramshaw, C. C., Rye, C. E., Speedy, H. E., Stefancsik, R., Thompson, S. L., Wang, S., Ward, S., Campbell, P. J. and Forbes, S. A. (2019) 'COSMIC: the Catalogue Of Somatic Mutations In Cancer', *Nucleic Acids Res,* 47(D1), pp. D941-D947.

Taurone, S., Bianchi, E., Attanasio, G., Di Gioia, C., Ierinó, R., Carubbi, C., Galli, D., Pastore, F. S., Giangaspero, F., Filipo, R., Zanza, C. and Artico, M. (2015) 'Immunohistochemical profile of cytokines and growth factors expressed in vestibular schwannoma and in normal vestibular nerve tissue', *Mol Med Rep,* 12(1), pp. 737-45.

Tidyman, W. E. and Rauen, K. A. (2009) 'The RASopathies: developmental syndromes of Ras/MAPK pathway dysregulation', *Curr Opin Genet Dev,* 19(3), pp. 230-6.

Topalidou, I., Cattin-Ortolá, J., Hummer, B., Asensio, C. S. and Ailion, M. (2020) 'EIPR1 controls dense-core vesicle cargo retention and EARP complex localization in insulin-secreting cells', *Mol Biol Cell,* 31(1), pp. 59-79.

Trofatter, J. A., MacCollin, M. M., Rutter, J. L., Murrell, J. R., Duyao, M. P., Parry, D. M., Eldridge, R., Kley, N., Menon, A. G. and Pulaski, K. (1993) 'A novel moesin-, ezrin-, radixin-like gene is a candidate for the neurofibromatosis 2 tumour suppressor', *Cell,* 75(4), pp. 826.

Urnov, F. D., Miller, J. C., Lee, Y. L., Beausejour, C. M., Rock, J. M., Augustus, S., Jamieson, A. C., Porteus, M. H., Gregory, P. D. and Holmes, M. C. (2005) 'Highly efficient endogenous human gene correction using designed zinc-finger nucleases', *Nature,* 435(7042), pp. 646-51.

van Veen, E. M., Brentnall, A. R., Byers, H., Harkness, E. F., Astley, S. M., Sampson, S., Howell, A., Newman, W. G., Cuzick, J. and Evans, D. G. R. (2018) 'Use of Single-Nucleotide Polymorphisms and Mammographic Density Plus Classic Risk Factors for Breast Cancer Risk Prediction', *JAMA Oncol,* 4(4), pp. 476-482.

Visscher, P. M., Brown, M. A., McCarthy, M. I. and Yang, J. (2012) 'Five years of GWAS discovery', *Am J Hum Genet,* 90(1), pp. 7-24.

Visscher, P. M., Wray, N. R., Zhang, Q., Sklar, P., McCarthy, M. I., Brown, M. A. and Yang, J. (2017) '10 Years of GWAS Discovery: Biology, Function, and Translation', *Am J Hum Genet,* 101(1), pp. 5-22.

Vivanco, I. and Sawyers, C. L. (2002) 'The phosphatidylinositol 3-Kinase AKT pathway in human cancer', *Nat Rev Cancer,* 2(7), pp. 489-501.

Wang, H., Thomas, D. C., Pe'er, I. and Stram, D. O. (2006) 'Optimal two-stage genotyping designs for genome-wide association scans', *Genet Epidemiol,* 30(4), pp. 356-68.

Wang, K., Yamamoto, H., Chin, J. R., Werb, Z. and Vu, T. H. (2004) 'Epidermal growth factor receptor-deficient mice have delayed primary endochondral ossification because of defective osteoclast recruitment', *J Biol Chem,* 279(51), pp. 53848-56.

Watanabe, K., Taskesen, E., van Bochoven, A. and Posthuma, D. (2017) 'Functional mapping and annotation of genetic associations with FUMA', *Nat Commun,* 8(1), pp. 1826.

Weinberg, F., Peckys, D. B. and de Jonge, N. (2020) 'EGFR Expression in HER2-Driven Breast Cancer Cells', *Int J Mol Sci,* 21(23).

Welling, D. B., Lasak, J. M., Akhmametyeva, E., Ghaheri, B. and Chang, L. S. (2002) 'cDNA microarray analysis of vestibular schwannomas', *Otol Neurotol,* 23(5), pp. 736-48.

Whiffin, N., Minikel, E., Walsh, R., O'Donnell-Luria, A. H., Karczewski, K., Ing, A. Y., Barton, P. J. R., Funke, B., Cook, S. A., MacArthur, D. and Ware, J. S. (2017) 'Using high-resolution variant frequencies to empower clinical genome interpretation', *Genet Med,* 19(10), pp. 1151-1158.

Wiedemeyer, R., Brennan, C., Heffernan, T. P., Xiao, Y., Mahoney, J., Protopopov, A., Zheng, H., Bignell, G., Furnari, F., Cavenee, W. K., Hahn, W. C., Ichimura, K., Collins, V. P., Chu, G. C., Stratton, M. R., Ligon, K. L., Futreal, P. A. and Chin, L. (2008) 'Feedback circuit among INK4 tumour suppressors constrains human glioblastoma development', *Cancer Cell,* 13(4), pp. 355-64.

Wu, J., Kong, M. and Bi, Q. (2015) 'Identification of a novel germline SMARCB1 nonsense mutation in a family manifesting both schwannomatosis and unilateral vestibular schwannoma', *J Neurooncol,* 125(2), pp. 439-41.

Wu, X., Scott, D. A., Kriz, A. J., Chiu, A. C., Hsu, P. D., Dadon, D. B., Cheng, A. W., Trevino, A. E., Konermann, S., Chen, S., Jaenisch, R., Zhang, F. and Sharp, P. A. (2014) 'Genome-wide binding of the CRISPR endonuclease Cas9 in mammalian cells', *Nat Biotechnol,* 32(7), pp. 670-6.

Yeo, G. and Burge, C. B. (2004) 'Maximum entropy modeling of short sequence motifs with applications to RNA splicing signals', *J Comput Biol,* 11(2-3), pp. 377-94.

Yin, X., Huo, Z., Yan, S., Wang, Z., Yang, T., Wu, H. and Zhang, Z. (2021) 'MiR-205 Inhibits Sporadic Vestibular Schwannoma Cell Proliferation by Targeting Cyclin-Dependent Kinase 14', *World Neurosurg,* 147, pp. e25-e31.

Yoshida, K., Fujiwara, Y., Goto, Y., Kohno, T., Yoshida, A., Tsuta, K. and Ohe, Y. (2018) 'The first case of SMARCB1 (INI1) - deficient squamous cell carcinoma of the pleura: a case report', *BMC Cancer,* 18(1), pp. 398.

Yu, W., Gius, D., Onyango, P., Muldoon-Jacobs, K., Karp, J., Feinberg, A. P. and Cui, H. (2008) 'Epigenetic silencing of tumour suppressor gene p15 by its antisense RNA', *Nature,* 451(7175), pp. 202-6.

Zhang, M. Q. (1998) 'Statistical features of human exons and their flanking regions', *Hum Mol Genet,* 7(5), pp. 919-32.

Zhang, N., Bai, H., David, K. K., Dong, J., Zheng, Y., Cai, J., Giovannini, M., Liu, P., Anders, R. A. and Pan, D. (2010) 'The Merlin/NF2 tumour suppressor functions through the YAP oncoprotein to regulate tissue homeostasis in mammals', *Dev Cell,* 19(1), pp. 27-38.

Zhou, X., Han, X., Wittfeldt, A., Sun, J., Liu, C., Wang, X., Gan, L. M., Cao, H. and Liang, Z. (2016) 'Long non-coding RNA ANRIL regulates inflammatory responses as a novel component of NF-κB pathway', *RNA Biol,* 13(1), pp. 98-108.

Zondervan, K. T. and Cardon, L. R. (2007) 'Designing candidate gene and genome-wide case-control association studies', *Nat Protoc,* 2(10), pp. 2492-501.

Appendices

Appendix I: Table of *NF2* Missense Variant Classifications (chapter 4).

Sequence change	Genomic seq (GRCh38)	aa change	Exon	ClinPred scores	REVEL	Align GVGD	SIFT	Poly Phen	Splicing window Alamut	SpliceAI Score	rsID	gnomAD_v2.1.1 freq (ALL)	ClinVar (number subs)	Genetic origin	ACGS criteria	Classification ACGS guided	NF2 disease	PMID
c.1A>G	29603999	p.?	1	1.00	0.60	n/a	n/a	n/a		-	rs1319282473		VUS (1)	germline	PVS1(moderate), PM2, PM5(supporting)	VUS (hot)	Unknown	
c.2T>C	29604000	p.?	1	1.00	0.64	n/a	n/a	n/a		-	rs1555978325		Likely pathogenic (1)	germline	PVS1(moderate), PM2	VUS (warm)	Unknown	
c.4G>T	29604002	p.(Ala2Ser)	1	0.94	0.44	C0	0	0.98		-	rs1601515682		VUS (3)	Unknown	PM2	VUS (cool)	Associated	25741868
c.15C>G	29604013	p.(Ile5Met)	1	0.44	0.29	C0	0.1	0.8		-	rs998779035	4.8E-06	VUS (1)	germline	BP4	VUS (Ice cold)	Unknown	
c.16G>C	29604014	p.(Ala6Pro)	1	0.99	0.52	C0	0	0.91		-	rs1601515753		VUS (1)	germline	PM2	VUS (cool)	Unknown	
c.17C>A	29604015	p.(Ala6Asp)	1	0.97	0.50	C0	0	0.36		-			VUS (1)	germline	PM2	VUS (cool)	Unknown	
c.22C>T	29604020	p.(Arg8Cys)	1	0.99	0.54	C0	0	1		-			1	germline	PM2	VUS (cool)	Unknown	
c.25A>G	29604023	p.(Met9Val)	1	0.88	0.66	C0	0	0.99	New Donor Site?	-	rs1249717688	4.6E-06	VUS (1)	germline	None applied	VUS (ice cold)	Unknown	
c.32T>G	29604030	p.(Phe11Cys)	1	0.98	0.67	C0	0	0.94		-			1	germline	PM2	VUS (cool)	Unknown	
c.50A>G	29604048	p.(Lys17Arg)	1	0.96	0.41	C0	0.4	0.26		-					PM2	VUS (cool)	Unknown	
c.56C>G	29604054	p.(Pro19Arg)	1	0.99	0.46	C0	0.1	0.29		-	rs1601515928		VUS (1)	germline	PM2	VUS (cool)	Unknown	
c.58A>C	29604056	p.(Lys20Gln)	1	0.99	0.56	C0	0	0.45		-			VUS (1)	germline	PM2	VUS (cool)	Unknown	
c.67A>C	29604065	p.(Thr23Pro)	1	0.80	0.43	C0	0.1	0		-			1	germline	PM2	VUS (cool)	Unknown	
c.71T>C	29604069	p.(Val24Ala)	1	0.98	0.62	C0	0.4	0.85		-	rs773714780	0.000013	VUS (1)	germline	None applied	VUS (ice cold)	Unknown	
c.73A>G	29604071	p.(Arg25Gly)	1	1.00	0.70	C0	0	0.81		-					PM2, PP3	VUS (Tepid)	Unknown	
c.73A>T	29604071	p.(Arg25Trp)	1	0.99	0.75	C0	0	1		-			VUS (1)	germline	PM2, PP3	VUS (Tepid)	Unknown	
c.74G>A	29604072	p.(Arg25Lys)	1	0.85	0.33	C0	0.5	0	New Acceptor Site?	-	rs1569259813		VUS (2)	germline	PM2, BP4	VUS (cold)	Unknown	
c.77T>C	29604075	p.(Ile26Thr)	1	1.00	0.69	C0	0	1		-	rs1064795612		VUS (1)	germline	PM2	VUS (cool)	Unknown	
c.78C>G	29604076	p.(Ile26Met)	1	0.99	0.68	C0	0	1		-			VUS (1)	germline	PM2	VUS (cool)	Unknown	
c.85A>G	29604083	p.(Met29Val)	1	0.98	0.55	C0	0	0.01		-			VUS (1)	germline	PM2	VUS (cool)	Unknown	
c.88G>A	29604086	p.(Asp30Asn)	1	1.00	0.70	C0	0	0.98		-	rs1601516058		VUS (1)	germline	PM2	VUS (cool)	Unknown	
c.89A>G	29604087	p.(Asp30Gly)	1	0.99	0.66	C0	0	0.23		-	rs563168478	0.000004			None applied	VUS (ice cold)	Unknown	
c.94G>A	29604092	p.(Glu32Lys)	1	1.00	0.59	C0	0.1	0.95		-	rs373337083	0	VUS (2)	germline	PM2	VUS (cool)	Unknown	
c.100G>C	29604098	p.(Glu34Gln)	1	0.98	0.56	C0	0	0.28		-	rs753425376	0.000013			None applied	VUS (ice cold)	Unknown	

Supplementary table appendix I. Continued on next page.

c.107A>G	29604105	p.(Asn36Ser)	1	0.05	0.16	C0	1	0		-	rs372279458	0.000035	Likely benign/ VUS (4?)	germline	PP4, BS1, BP4	Likely benign	Yes	15684865 25931164
c.107A>T	29604105	p.(Asn36Ile)	1	0.87	0.18	C0	0.2	0.62		-	rs372279458		VUS (1)	germline	PM2, BP4	VUS (cold)	Unknown	
c.113A>C	29604111	p.(Glu38Ala)	1	1.00	0.75	C35	0	1	Possible effect	0.418				germline	PM2, PP3, PP4	VUS (Warm)	Yes	
c.113A>T	29604111	p.(Glu38Val)	1	1.00	0.77	C35	0	1	Disrupts donor?	0.492				Germline	PM2, PP3	VUS (Tepid)	Unknown	11779178
c.115A>G	29636751	p.(Met39Val)	2	0.23	0.13	C0	0.9	0	New Donor Site?	-	rs761188569		VUS (1)	germline	PM2, BP4	VUS (Cold)	Unknown	
c.123G>C	29636759	p.(Trp41Cys)	2	0.99	0.46	C15	0	1		-				Somatic	PM2 +	VUS (cool)	Associated	11779178 8698340
c.132G>C	29636768	p.(Lys44Asn)	2	0.99	0.52	C0	0	0.99		-				Somatic	PM2 +	VUS (cool)	No	10451704
c.133G>A	29636769	p.(Asp45Asn)	2	0.96	0.45	C0	0.1	0.97		-			1	germline	PM2	VUS (cool)	Unknown	
c.137T>A	29636773	p.(Leu46His)	2	1.00	0.96	C65	0	1		-			n/a		PM2, PP1, PP3	VUS (Warm)	Associated	
c.137T>G	29636773	p.(Leu46Arg)	2	1.00	0.97	C65	0	1		-			n/a	Somatic	PM2, PP3 +	VUS (Tepid)	Associated	21383154 11779178 25026211
c.141T>A	29636777	p.(Phe47Leu)	2	0.99	0.59	C15	0	1		0.121				Somatic	PM2	VUS (cool)	Associated	15980976
c.142G>A	29636778	p.(Asp48Asn)	2	0.99	0.49	C0	0	0.97		-	rs1352608076		VUS (1)	germline	PM2	VUS (cool)	Unknown	
c.154C>T	29636790	p.(Arg52Trp)	2	1.00	0.67	C25	0	1		0.194	rs764901064	0.000004	VUS (1)	germline	None applied	VUS (ice cold)	Unknown	
c.155G>A	29636791	p.(Arg52Gln)	2	0.97	0.34	C0	0.1	0.76	New Acceptor Site?	0.12	rs1185209056	0	n/a	Unknown	PM2, PP3	VUS (Tepid)	Associated	
c.157A>G	29636793	p.(Thr53Ala)	2	0.99	0.42	C0	0.1	0.09		0.168	rs1601578990		VUS (1)	germline	PM2	VUS (cool)	Unknown	
c.161T>C	29636797	p.(Leu54Pro)	2	1.00	0.89	C65	0	1		-				germline	PS4(supporting), PM2, PP3, PP4 +	VUS (Hot)	Yes	19715170
c.170G>A	29636806	p.(Arg57Gln)	2	0.99	0.65	C35	0	1		-	rs368773485	0.000016	VUS (2)	germline	None applied	VUS (ice cold)	Unknown	
c.180G>C	29636816	p.(Trp60Cys)	2	1.00	0.68	C65	0	1		-	rs780872661	0.000004		unknown	None applied +	VUS (ice cold)	Associated	12118253 18486129
c.182T>C	29636818	p.(Phe61Ser)	2	0.99	0.90	C55	0	1		-	rs1286915234	0.000007	1	germline	PP3	VUS (Cold)	Unknown	
c.185T>C	29636821	p.(Phe62Ser)	2	1.00	0.95	C65	0	1		-	rs121434261		Pathogenic (1)	germline/ somatic	PS3, PS4(moderate), PM2, PP1, PP3, PP4	Pathogenic (d)	Yes	16341811 10790209 10748301 8081368, 12118253

Supplementary table appendix I. Continued on next page.

c.191T>C	29636827	p.(Leu64Pro)	2	1.00	0.93	C65	0	1		-			VUS (1)	germline	PM2, PP3, PP4 +	VUS (Warm)	Yes	18033041 11448944 18086884 26073919
c.191T>G	29636827	p.(Leu64Arg)	2	1.00	0.93	C65	0	1		-				germline	PM2, PS4(supporting), PP3, PP4	VUS (Hot)	Yes	
c.196T>A	29636832	p.(Tyr66Asn)	2	1.00	0.84	C55	0	1	Cryptic acceptor activated?	-	rs772274240	0.000014	VUS (2)	germline	PP3	VUS (Cold)	Unknown	
c.208G>C	29636844	p.(Asp70His)	2	0.96	0.31	C15	0	0.02		0.168			1	germline	PM2, BP4	VUS (Cold)	Unknown	
c.215T>C	29636851	p.(Val72Ala)	2	0.39	0.19	C0	0.2	0.02		-	rs1260510937		VUS (5)?	germline/ unknown	PS4(supporting), PM2, BP4	VUS (cool)	Associated	
c.222G>T	29636858	p.(Trp74Cys)	2	1.00	0.79	C65	0	1		-			VUS (1)	germline	PM2, PP3	VUS (Tepid)	Unknown	
c.223C>A	29636859	p.(Leu75Ile)	2	0.96	0.67	C0	0	1		-					PM2	VUS (cool)	Unknown	33173047
c.229A>G	29636865	p.(Met77Val)	2	0.75	0.51	C0	0.4	0.06		-			n/a	germline/ somatic	PM2, PP4	VUS (Tepid)	Yes	
c.235A>C	29636871	p.(Lys79Gln)	2	0.99	0.64	C45	0	0.7		-				Somatic	PM2 +	VUS (cool)	Associated	11779178 11448944 7951231
c.235A>G	29636871	p.(Lys79Glu)	2	1.00	0.80	C55	0	1		-				somatic	PS3, PM2, PP3	Likely pathogenic (b)	Associated	7951231, 10712203 27285107 11448944 21402777 16324214
c.240G>C	29636876	p.(Lys80Asn)	2	0.99	0.58	C0	0	1	Disrupts donor?	0.844				Unknown	PM2, PP3 +	VUS (Tepid)	Unknown	21402777
c.245T>C	29639094	p.(Leu82Pro)	3	0.98	0.85	C0	0	1		-			1	germline	PM2, PP3	VUS (Tepid)	Unknown	
c.251A>G	29639100	p.(His84Arg)	3	0.52	0.32	C0	0.1	0.81	Cryptic Acceptor Strongly Activated?	-	rs773740023	0.000012	1	germline	BP4	VUS (Ice cold)	Unknown	
c.253G>C	29639102	p.(Asp85His)	3	0.99	0.48	C0	0	0.01	Cryptic Acceptor Strongly Activated?	-			1	germline	PM2	VUS (cool)	Unknown	
c.263A>G	29639112	p.(Lys88Arg)	3	0.42	0.28	C0	0.4	0.04	New Acceptor Site?	-	rs547255779	0.000004	VUS (1)	germline	BP4	VUS (Ice cold)	Unknown	
c.271C>A	29639120	p.(Pro91Thr)	3	0.99	0.55	C0	0.2	0		-	rs1555987645		VUS (1)	Germline	PM2	VUS (cool)	Unknown	
c.272C>A	29639121	p.(Pro91Gln)	3	0.99	0.53	C0	0.1	0.87		-	rs1569281659		VUS (1)	Germline	PM2	VUS (cool)	Unknown	

Supplementary table appendix I. Continued on next page.

c.272C>G	29639121	p.(Pro91Arg)	3	0.99	0.57	C0	0.1	0.95		-			VUS (1)	Germline	PM2	VUS (cool)	Unknown	
c.274G>A	29639123	p.(Val92Ile)	3	0.25	0.28	C0	0.9	0		-	rs145935225	0.000004	VUS (1)	Germline	BP4	VUS (Ice cold)	Unknown	
c.281T>G	29639130	p.(Phe94Cys)	3	1.00	0.84	C65	0	1		-	rs1601583588		VUS (1)	Germline	PM2, PP3	VUS (Tepid)	Unknown	
c.293C>A	29639142	p.(Ala98Asp)	3	1.00	0.84	C25	0	1		-	rs1060503668		VUS (1)	Germline	PM2, PP3	VUS (Tepid)	Unknown	
c.296A>G	29639145	p.(Lys99Arg)	3	0.91	0.78	C25	0	0.98	New Acceptor Site?	-	rs181794923	0.000012	VUS (2)	Germline	PP3	VUS (Cold)	Unknown	25931164
c.300T>A	29639149	p.(Phe100Leu)	3	1.00	0.74	C15	0	1		-	rs1555987677		VUS (1)	Germline	PM2, PP3	VUS (Tepid)	Unknown	
c.302A>T	29639151	p.(Tyr101Phe)	3	0.97	0.57	C0	0.3	0.16		-	rs1240469044		VUS (2)	Germline	PM2	VUS (cool)	Unknown	
c.305C>G	29639154	p.(Pro102Arg)	3	1.00	0.74	C65	0	1	New Donor Site?	-	rs1601583679		VUS (1)	Germline	PM2, PP3	VUS (Tepid)	Unknown	
c.311A>C	29639160	p.(Asn104Thr)	3	0.93	0.38	C25	0	0.05		-			VUS (1)	Germline	PM2, BP4	VUS (Cold)	Unknown	
c.317A>G	29639166	p.(Glu106Gly)	3	0.90	0.63	C0	0	0.88		-				Germline	PM2 +	VUS (cool)	Yes	11779178 11448944 8081368
c.319G>A	29639168	p.(Glu107Lys)	3	1.00	0.61	C0	0.1	1		-	rs1435118870		1	germline	PM2	VUS (cool)	Unknown	
c.321G>T	29639170	p.(Glu107Asp)	3	0.42	0.44	C0	0.2	0.07		-				Somatic	PM2	VUS (cool)	No	32494066
c.326T>C	29639175	p.(Leu109Pro)	3	1.00	0.92	C65	0	1		-	rs1601583740		VUS (1)	Germline	PM2, PP3	VUS (Tepid)	Unknown	
c.328G>C	29639177	p.(Val110Leu)	3	0.81	0.28	C0	0.1	0		-	rs1601583759		VUS (1)	Germline	PM2, BP4	VUS (cold)	Unknown	
c.332A>C	29639181	p.(Gln111Pro)	3	1.00	0.89	C0	0.1	1		-			VUS (1)	Germline	PM2, PP3	VUS (Tepid)	Unknown	
c.334G>A	29639183	p.(Glu112Lys)	3	0.98	0.60	C15	0.1	0.93		-	rs781593146	0.000012	VUS (1)	Germline	None applied	VUS (ice cold)	Unknown	
c.337A>C	29639186	p.(Ile113Leu)	3	0.90	0.48	C0	0.1	0.5		0.186			1	germline	PM2	VUS (cool)	Unknown	
c.343C>G	29639192	p.(Gln115Glu)	3	0.91	0.55	C0	0.1	0.92		-	rs1350618734	0.000032	VUS (1)	Germline	None applied	VUS (ice cold)	Unknown	
c.345A>T	29639194	p.(Gln115His)	3	0.98	0.58	C0	0.2	0.89		-	rs746369012	0.000004	VUS (2)	Germline	None applied	VUS (ice cold)	Unknown	
c.347A>G	29639196	p.(His116Arg)	3	0.82	0.69	C0	0.1	0.98		-	rs371373672		VUS (2)	Germline	PM2	VUS (cool)	Unknown	
c.349T>A	29639198	p.(Leu117Ile)	3	0.99	0.69	C0	0	1		-				somatic	PM2	VUS (cool)	Associated	8655144
c.349T>G	29639198	p.(Leu117Val)	3	1.00	0.67	C0	0	0.97		-	rs1569281810		VUS (1)	Unknown	PM2	VUS (cool)	Unknown	
c.352T>G	29639201	p.(Phe118Val)	3	1.00	0.83	C0	0.1	1		-			VUS (1)	Germline	PM2, PP3	VUS (Tepid)	Unknown	
c.361C>G	29639210	p.(Gln121Glu)	3	1.00	0.90	C25	0	0.91	New Acceptor Site?	-	rs1006294051	0.000004	VUS (1)	Germline	PP3	VUS (Cold)	Unknown	
c.370A>C	29642208	p.(Lys124Gln)	4	0.89	0.35	C0	0.3	0.14		-	rs1601589425		VUS (1)	Germline	PM2, BP4	VUS (Cold)	Unknown	
c.375G>C	29642213	p.(Gln125His)	4	0.92	0.62	C0	0.1	0.98		-			1	germline	PM2	VUS (cool)	Unknown	
c.376A>G	29642214	p.(Ile126Val)	4	0.69	0.56	C25	0	1	New Donor Site?	-	rs780483061				PM2	VUS (cool)	Unknown	
c.391A>C	29642229	p.(Ile131Leu)	4	0.86	0.39	C0	0.4	0.24		-	rs878853927		VUS (1)	Germline	PM2, BP4	VUS (cold)	Unknown	

Supplementary table appendix I. Continued on next page.

c.397T>C	29642235	p.(Cys133Arg)	4	1.00	0.95	C65	0	1		-				Germline	PM2, PP3	VUS (Tepid)	Associated	20445339
c.400C>T	29642238	p.(Pro134Ser)	4	0.94	0.32	C0	0.5	0.92		-	rs1555988776		VUS (1)	Germline	PM2, BP4	VUS (Cold)	Unknown	
c.401C>T	29642239	p.(Pro134Leu)	4	1.00	0.69	C0	0.1	0.96		-	rs1029716358		VUS (2)	Germline/ Unknown	PM2	VUS (cool)	Unknown	
c.422T>C	29642260	p.(Leu141Pro)	4	1.00	0.98	C65	0	1		-			n/a	Unknown	PM2, PP3, PP4 +	VUS (Warm)	Yes	16983642 21383154
c.422T>G	29642260	p.(Leu141Arg)	4	1.00	0.97	C65	0	1		-			n/a	germline	PM2, PP3, PP4	VUS (Warm)	Yes	20930055
c.433G>A	29642271	p.(Ala145Thr)	4	1.00	0.73	C55	0	1		-	rs1185977513	0.000004	VUS (1)	Germline	PP3	VUS (Cold)	Associated	
c.436G>A	29642274	p.(Val146Ile)	4	0.70	0.43	c25	0	1		-	rs771572024	0.000011	VUS (2)	Germline	None applied	VUS (ice cold)	Associated	
c.440A>C	29642278	p.(Gln147Pro)	4	1.00	0.93	C25	0	1		-			1	germline	PM2, PP3	VUS (Tepid)	Unknown	
c.447G>C	29642285	p.(Lys149Asn)	4	1.00	0.77	C0	0.1	0.99	Possible effect	0.798			n/a	germline/ somatic	PM2, PP3	VUS (Tepid)	Associated	18554169, 24030433
c.457T>C	29654666	p.(Tyr153His)	5	0.84	0.81	C0	0.1	1	Possible effect	-	rs1374299963	0.000012	VUS (2)	Germline	PP3	VUS (Cold)	Unknown	
c.463C>G	29654672	p.(Pro155Ala)	5	0.62	0.34	C0	0.3	0		-			1	unknown	PM2, BP4	VUS (Cold)	Unknown	
c.464C>T	29654673	p.(Pro155Leu)	5	0.99	0.46	C0	0.1	0.02	Cryptic acceptor activated?	-				Somatic	PM2	VUS (cool)	Unknown	
c.467G>A	29654676	p.(Ser156Asn)	5	0.05	0.16	C0	0.8	0		-				Somatic	PM2, BP4 +	VUS (Cold)	Associated	23921927
c.468T>A	29654677	p.(Ser156Arg)	5	0.17	0.27	C0	0.1	0	Cryptic acceptor activated?	-				Somatic	PM2, BP4	VUS (Cold)	Associated	16786152
c.473A>G	29654682	p.(His158Arg)	5	0.99	0.91	C0	0	0.99		-			VUS (1)	Germline	PM2, PP3	VUS (Tepid)	Unknown	
c.478C>T	29654687	p.(Arg160Trp)	5	0.98	0.40	C0	0	1		-	rs150667239	0.000011	VUS (1)	Germline	None applied	VUS (ice cold)	Unknown	
c.479G>A	29654688	p.(Arg160Gln)	5	0.83	0.27	C0	0.5	0.87		-	rs867595517		VUS (1)	Germline	PM2, BP4	VUS (cold)	Unknown	
c.484T>C	29654693	p.(Phe162Leu)	5	0.84	0.71	C0	1	0.13		-	rs1085307593	0.000004	VUS (1)	Germline	PP3	VUS (cold)	Unknown	
c.489G>T	29654698	p.(Leu163Phe)	5	0.98	0.69	C0	0	1		-	rs1232015629	0.000004		germline	None applied	VUS (ice cold)	No	31248416
c.497A>T	29654706	p.(Glu166Val)	5	0.99	0.66	C0	0	0.97		-	rs779353677	0.000004	VUS (1)	Germline	None applied	VUS (ice cold)	Unknown	
c.499G>C	29654708	p.(Glu167Gln)	5	0.93	0.47	C0	0	0.68		-			VUS (1)	Germline	PM2	VUS (cool)	Unknown	
c.501A>T	29654710	p.(Glu167Asp)	5	0.64	0.38	C0	0	0		-				Somatic	PM2, BP4	VUS (cold)	Associated	16786152
c.504G>C	29654713	p.(Leu168Phe)	5	0.98	0.61	C0	0.1	1		-			VUS (1)	Germline	PM2	VUS (cool)	Unknown	
c.506T>C	29654715	p.(Leu169Pro)	5	1.00	0.95	C65	0	1		-			1	germline	PM2, PP3	VUS (Tepid)	Unknown	
c.515G>A	29654724	p.(Arg172Lys)	5	0.84	0.36	C0	0.7	0.08	New Acceptor Site?	-	rs752963731	0.000004	VUS (1)	Germline	BP4	VUS (Ice cold)	Associated	
c.521T>C	29655598	p.(Ile174Thr)	6	0.87	0.51	C0	0.5	0.01		-	rs1346860299		VUS (1)	Germline	PM2	VUS (cool)	Unknown	

Supplementary table appendix I. Continued on next page.

c.524A>G	29655601	p.(Asn175Ser)	6	0.84	0.18	C0	0.1	0		-			1	germline	PM2, BP4	VUS (cold)	Unknown	
c.525T>A	29655602	p.(Asn175Lys)	6	0.71	0.22	C0	0.1	0.01		-	rs1601613495		VUS (1)	Germline	PM2, BP4	VUS (cold)	Unknown	
c.535A>G	29655612	p.(Met179Val)	6	0.93	0.64	C0	0.1	0.82	New Donor Site?	-	rs1601613523		VUS (1)	De novo	PM2, PP3	VUS (Tepid)	Unknown	
c.542C>T	29655619	p.(Pro181Leu)	6	0.93	0.29	C35	0	0.15		-	rs1362524399	0.000008	VUS (1)	Germline	BP4	VUS (Ice cold)	Unknown	
c.545A>G	29655622	p.(Glu182Gly)	6	0.99	0.55	C0	0	0.04		-			VUS (1)	Germline	PM2	VUS (Cool)	Unknown	
c.548T>C	29655625	p.(Met183Thr)	6	0.99	0.77	C0	0	1		-			n/a		PM2, PP3	VUS (Tepid)	Unknown	
c.558G>C	29655635	p.(Glu186Asp)	6	0.71	0.47	C0	0.4	0.04		-	rs1325902176	0.000004	VUS (1)	Germline	None applied	VUS (ice cold)	Unknown	
c.560G>A	29655637	p.(Arg187Lys)	6	0.41	0.24	C25	0	0.26		-	rs1234052589	0.000004	VUS (1)	Germline	BP4	VUS (Ice cold)	Unknown	
c.566C>T	29655643	p.(Thr189Ile)	6	0.99	0.64	C0	0.1	1		-			VUS (1)	Germline	PM2	VUS (Cool)	Unknown	
c.571T>A	29655648	p.(Trp191Arg)	6	1.00	0.75	C0	0	1		-				somatic	PM2, PP3	VUS (Tepid)	Associated	21727090
c.575A>G	29655652	p.(Tyr192Cys)	6	1.00	0.92	C15	0	1		-	rs1555993319		Not assigned (1)	Somatic	PM2, PP3	VUS (Tepid)	Associated	
c.577G>A	29655654	p.(Ala193Thr)	6	0.98	0.51	C0	0.1	0.95		-	rs1427589827	0.000007		somatic	None applied	VUS (ice cold)	No	29625052
c.587G>A	29655664	p.(Arg196Gln)	6	0.96	0.50	C0	0.2	1		-	rs749176138	0.000004	VUS (1)	Germline	None applied	VUS (ice cold)	Unknown	
c.589G>T	29655666	p.(Gly197Cys)	6	1.00	0.93	C25	0	1		-				Germline	PM2, PP3, PP4 +	VUS (Warm)	Yes	11779178 8698340, 32787631
c.595G>A	29655672	p.(Ala199Thr)	6	0.25	0.29	C0	1	0		-	rs1261707371	0.000008	VUS (2)	Germline	BP4	VUS (Ice cold)	Unknown	
c.598A>G	29655675	p.(Arg200Gly)	6	0.99	0.85	C65	0	0.91		-	rs1487106309	0.000004	1	germline	PP3	VUS (cold)	Unknown	
c.601G>T	29658190	p.(Asp201Tyr)	7	1.00	0.78	C25	0	1	New Donor Site?	-			n/a		PM2, PP3, PP4	VUS (Warm)	Yes	
c.602A>G	29658191	p.(Asp201Gly)	7	0.99	0.82	C15	0	0.96		-			1	germline	PM2, PP3	VUS (Tepid)	Unknown	
c.602A>T	29658191	p.(Asp201Val)	7	1.00	0.84	C25	0	1		-	rs1601618525		VUS (1)	Germline	PM2, PP3	VUS (Tepid)	Unknown	
c.610G>C	29658199	p.(Glu204Gln)	7	0.99	0.59	C0	0.1	0.96		-	rs1569295916		VUS (3)	Germline/ Unknown	PM2	VUS (Cool)	Unknown	32739965 32206572
c.613A>G	29658202	p.(Met205Val)	7	0.35	0.71	C0	0.2	0.97		-	rs141629512	0.000085	VUS (3)/ Benign (1)	Germline/ Unknown	BS1, PP3	Likely benign	Associated	25931164 26073919 16983642
c.614T>C	29658203	p.(Met205Thr)	7	0.98	0.85	C25	0	1		-	rs747871414	0.000012	VUS (1)	Germline	PP3	VUS (cold)	Unknown	
c.619T>C	29658208	p.(Tyr207His)	7	1.00	0.92	C0	0	1		-	rs1601618565		VUS (1)	Germline	PM2, PP3	VUS (Tepid)	Unknown	
c.623T>C	29658212	p.(Leu208Pro)	7	1.00	0.95	C65	0	1		-				Unknown/ somatic	PM2, PP3	VUS (Tepid)	Associated	23348505 32017710
c.623T>G	29658212	p.(Leu208Arg)	7	1.00	0.95	C65	0	1		-			n/a	germline	PM2, PP3	VUS (Tepid)	Associated	28409725

Supplementary table appendix I. Continued on next page.

c.631G>C	29658220	p.(Ala211Pro)	7	1.00	0.92	C0	0	1		-				germline	PS4(supporting), PM2, PP3, PP4	VUS (Hot)	Yes	
c.632C>A	29658221	p.(Ala211Asp)	7	1.00	0.94	C0	0	1		-					PM2, PP3, PP4 +	VUS (Warm)	Yes	21383154 20178741 10327069
c.641T>C	29658230	p.(Leu214Pro)	7	1.00	0.84	C0	0	1		-	rs1601618585		VUS (1)/ Likely path (1)		PS4(supporting), PM2, PP3, PP4	VUS (Hot)	Yes	
c.647T>C	29658236	p.(Met216Thr)	7	0.99	0.85	C35	0	1	Cryptic donor?	-			VUS (1)	Germline	PM2, PP3	VUS (Tepid)	Unknown	
c.647T>G	29658236	p.(Met216Arg)	7	1.00	0.83	C35	0	0.98	Cryptic donor?	0.749			n/a	somatic	PM2, PP3, PP4	VUS (Warm)	Yes	30325044
c.652G>A	29658241	p.(Gly218Ser)	7	1.00	0.94	C0	0.1	1		-	rs776818377	0.000021	VUS (1)	Germline	PP3	VUS (cold)	Unknown	
c.652G>T	29658241	p.(Gly218Cys)	7	1.00	0.94	C35	0	1		-	rs776818377	0.000032	1	germline	PP3	VUS (cold)	Unknown	
c.655G>A	29658244	p.(Val219Met)	7	0.95	0.72	C0	0	1	Cryptic donor?	0.783	rs1555994816		Likely pathogenic (1)	germline	PM2, PP3, PP4, PS4(moderate) +	Likely pathogenic (c)	Yes	11779178 17470137 12011146 8012353, 10669747
c.656T>A	29658245	p.(Val219Glu)	7	0.99	0.87	C0	0	1	Cryptic donor?	0.787			n/a	germline de novo	PM2, PM5(supporting), PP3, PP4	VUS (Hot)	Yes	18554169
c.658A>T	29658247	p.(Asn220Tyr)	7	1.00	0.85	C0	0.1	1	Cryptic donor?	0.787	rs1601618646		Pathogenic (1)	germline	PS4(supporting), PM2, PP3, PP1, PP4 +	Likely pathogenic (c)	Yes	11779178 10712203 8755919, 8230593
c.662A>G	29658251	p.(Tyr221Cys)	7	1.00	0.83	C45	0	1		-	rs746025177	0.000014	VUS (2)	Germline	PP3	VUS (cold)	Unknown	
c.670A>G	29658259	p.(Ile224Val)	7	0.88	0.43	C0	0.1	0.95	New Acceptor Site?	-	rs1555994825		VUS (1)	Germline	PM2, PP3	VUS (Tepid)	Unknown	
c.673C>T	29658262	p.(Arg225Trp)	7	0.98	0.66	C0	0	1	Possible effect	0.267	rs1386029079		VUS (1)	Germline	PM2, PP3	VUS (Tepid)	Unknown	
c.676A>C	29661205	p.(Asn226His)	8	1.00	0.82	C65	0	1		-	rs886057336		VUS (2)	Germline	PM2, PP3	VUS (Tepid)	Unknown	
c.683A>G	29661212	p.(Lys228Arg)	8	0.54	0.22	C0	0.1	0		-	rs145384260	0.000008	VUS (2)	Germline	BP4	VUS (Ice cold)	Unknown	25931164
c.685G>T	29661214	p.(Gly229Cys)	8	0.99	0.75	C15	0	1		-	rs1028670573	0.000008	VUS (2)	Germline	PP3	VUS (cold)	Unknown	
c.691G>C	29661220	p.(Glu231Gln)	8	0.63	0.40	C0	0.1	0.67		-	rs770019352	0.000004	VUS (1)	Germline	None applied	VUS (ice cold)	Unknown	
c.701T>G	29661230	p.(Leu234Arg)	8	1.00	0.96	C65	0	1		-				Germline	PM2, PP3 +	VUS (Tepid)	Yes	10369886 32787631
c.709G>C	29661238	p.(Asp237His)	8	0.99	0.83	C0	0	1		-			1	germline	PM2, PP3	VUS (Tepid)	Unknown	
c.713C>T	29661242	p.(Ala238Val)	8	0.99	0.86	C0	0	1		-	rs761195572	0.000004	VUS (2)	Germline	PP3	VUS (cold)	Unknown	22081132

Supplementary table appendix I. Continued on next page.

c.724C>G	29661253	p.(His242Asp)	8	0.88	0.68	C0	0.7	1		-				Somatic	PM2	VUS (cool)	No	16983642 11290539
c.726C>G	29661255	p.(His242Gln)	8	0.97	0.71	C0	0.2	1	New Acceptor Site?	-	rs1480040681		VUS (1)	Germline	PM2, PP3	VUS (Tepid)	Unknown	
c.727A>G	29661256	p.(Ile243Val)	8	0.93	0.34	C25	0	0.58		-	rs774996651		n/a		PM2, PP4, BP4	VUS (Cool)	Yes	
c.731A>G	29661260	p.(Tyr244Cys)	8	1.00	0.95	C65	0	1		-			1	germline	PM2, PP3	VUS (Tepid)	Unknown	
c.733G>A	29661262	p.(Asp245Asn)	8	0.81	0.30	C0	0	0		-			VUS (1)	Germline	PM2, BP4	VUS (cold)	Unknown	
c.736C>T	29661265	p.(Pro246Ser)	8	0.86	0.32	C0	0.6	0.14		-	rs1569297802		VUS (1)	Germline	PM2, BP4	VUS (cold)	Unknown	
c.743A>G	29661272	p.(Asn248Ser)	8	0.96	0.49	C15	0	0.72		-			VUS (1)	Germline	PM2	VUS (Cool)	Unknown	
c.749T>A	29661278	p.(Leu250Gln)	8	0.99	0.86	C65	0	1		-	rs1432132718	0.000004	VUS (1)	Germline	PP3	VUS (cold)	Unknown	
c.758A>G	29661287	p.(Lys253Arg)	8	0.52	0.53	C0	0.3	0.1		-	rs773573049	0.000004	VUS (1)	Germline	None applied	VUS (ice cold)	Unknown	
c.766T>C	29661295	p.(Phe256Leu)	8	1.00	0.96	C15	0	1		-	rs1474769404		VUS (1)	Germline	PM2, PP3	VUS (Tepid)	Unknown	
c.770C>G	29661299	p.(Pro257Arg)	8	0.98	0.76	C0	0.1	0.96		-	rs753300935		VUS (1)	Germline	PM2, PP3	VUS (Tepid)	Unknown	
c.770C>T	29661299	p.(Pro257Leu)	8	0.98	0.65	C0	0	0.99		-	rs753300935	0.000008	VUS (1)	Germline	None applied	VUS (ice cold)	Associated	
c.772T>G	29661301	p.(Trp258Gly)	8	1.00	0.91	C65	0	1		-	rs1601624186		VUS (1)	Germline	PM2, PP3	VUS (Tepid)	Unknown	
c.785G>A	29661314	p.(Arg262Gln)	8	0.96	0.82	C0	0	0.99		-	rs1450914413	0.000011	VUS (1)	Germline	PP3	VUS (cold)	Unknown	
c.789C>A	29661318	p.(Asn263Lys)	8	0.99	0.60	C0	0	1		-			VUS (1)	Germline	PM2	VUS (Cool)	Unknown	
c.794C>T	29661323	p.(Ser265Leu)	8	1.00	0.80	C15	0	0.95	Cryptic Acceptor Strongly Activated?	-	rs1601624241		VUS (1)	Germline	PM2, PP3	VUS (Tepid)	Unknown	
c.809A>G	29661338	p.(Glu270Gly)	8	0.99	0.86	C15	0	1	Possible effect	0.28				Germline	PM2, PP3, PP4 +	VUS (Warm)	Yes	9605590, 20178741 24726726
c.809A>T	29661338	p.(Glu270Val)	8	0.99	0.86	C15	0	0.95	Possible effect	0.769			n/a	germline	PM2, PP3	VUS (Tepid)	Associated	
c.810G>T	29661339	p.(Glu270Asp)	8	0.89	0.62	C0	0.1	0.95	Possible effect	0.9				somatic	PM2, PP3	VUS (Tepid)	Associated	17222329
c.812T>G	29664991	p.(Phe271Cys)	9	1.00	0.94	C0	0	1		-	rs1555997533		VUS (1)	germline	PM2, PP3	VUS (Tepid)	Unknown	
c.815C>T	29664994	p.(Thr272Ile)	9	0.76	0.56	C0	0.1	0.04		-	rs1555997534		VUS (1)	germline	PM2	VUS (Cool)	Unknown	
c.817A>G	29664996	p.(Ile273Val)	9	0.75	0.47	C0	0.1	0.19		-	rs1368184325	0.000004	VUS (3)	germline	None applied	VUS (ice cold)	Unknown	
c.817A>T	29664996	p.(Ile273Phe)	9	0.99	0.87	C0	0	0.68		-				Somatic	PM2, PP3 +	VUS (Tepid)	Unknown	11779178 8162073
c.820A>G	29664999	p.(Lys274Glu)	9	0.99	0.88	C0	0	1		-			VUS (1)	germline	PM2, PP3	VUS (Tepid)	Unknown	
c.831T>G	29665010	p.(Asp277Glu)	9	0.72	0.28	C0	0.2	0		-	rs762883753	0.000004	VUS (2)	germline	BP4	VUS (Ice cold)	Unknown	
c.845T>C	29665024	p.(Val282Ala)	9	0.74	0.36	C0	0.5	0.01		-	rs1601630493		VUS (1)	germline	PM2, BP4	VUS (cold)	Unknown	

Supplementary table appendix I. Continued on next page.

c.851A>G	29665030	p.(Lys284Arg)	9	0.52	0.34	C0	0.6	0	New Acceptor Site?	-	rs764034925	0.000004	VUS (1)	germline	PP3	VUS (cold)	Unknown	
c.857A>G	29665036	p.(Asn286Ser)	9	0.79	0.39	C0	0.3	0.07		-	rs757074151	0.000004	1	germline	BP4	VUS (Ice cold)	Unknown	
c.872G>A	29665051	p.(Arg291His)	9	0.88	0.75	C0	0.3	0.87		-	rs755200117	0.00002	VUS (2)	germline	PP3	VUS (cold)	Associated	
c.872G>T	29665051	p.(Arg291Leu)	9	0.99	0.86	C0	0	0.99		-					PM2, PP3	VUS (Tepid)	Unknown	
c.874G>A	29665053	p.(Val292Ile)	9	0.91	0.42	C0	0.8	0.01		-	rs1442581021	0	VUS (1)	germline	PM2	VUS (Cool)	Unknown	
c.896T>C	29668343	p.(Leu299Pro)	10	1.00	0.95	C65	0	1		-			VUS (1)	germline	PM2, PP3	VUS (Tepid)	Unknown	
c.899G>A	29668346	p.(Cys300Tyr)	10	1.00	0.86	C65	0	1		-				somatic	PM2, PP3	VUS (Tepid)	Associated	10712203 9538131
c.904G>A	29668351	p.(Gly302Arg)	10	0.98	0.87	C65	0	1		-	rs1255367068	0.000004	VUS (2)	germline	PP3	VUS (cold)	Unknown	
c.911A>G	29668358	p.(His304Arg)	10	1.00	0.95	C25	0	1		-	rs1555998800		VUS (1)	germline	PM2, PP3	VUS (Tepid)	Unknown	
c.916C>G	29668363	p.(Leu306Val)	10	0.98	0.83	C25	0	1		-	rs1399716137		1	germline	PM2, PP3	VUS (Tepid)	Unknown	
c.922A>G	29668369	p.(Met308Val)	10	0.95	0.74	C0	0	0.51	New Donor Site?	-			1	germline	PM2, PP3	VUS (Tepid)	Unknown	
c.932G>A	29668379	p.(Arg311Lys)	10	0.96	0.66	C25	0	1		-	rs1169276398	0.000004	VUS (1)	germline	None applied	VUS (ice cold)	Unknown	
c.940G>A	29668387	p.(Asp314Asn)	10	0.98	0.57	C15	0	0.93		-	rs1365006505	0.000032	VUS (1)	germline	None applied	VUS (ice cold)	Unknown	
c.947T>G	29668394	p.(Leu316Trp)	10	0.80	0.83	C35	0	1		-	rs750633919	0.000028	VUS (3)	germline/ unknown	PP3, PP4 +	VUS (Cool)	Yes	16532029 10561699 16983642
c.948G>C	29668395	p.(Leu316Phe)	10	0.73	0.73	C0	0	0.61						unknown	PM2, PP3 +	VUS (Tepid)	Unknown	16324214 11756419
c.952G>A	29668399	p.(Val318Ile)	10	0.49	0.29	C0	0.3	0.01		-	rs996057882	0.000004	VUS (1)	germline	BP4	VUS (Ice cold)	Unknown	
c.952G>T	29668399	p.(Val318Phe)	10	0.99	0.81	C0	0	0.99		-			VUS (1)	germline	PM2, PP3	VUS (Tepid)	Unknown	
c.956A>G	29668403	p.(Gln319Arg)	10	0.99	0.83	C35	0	0.95		-			VUS (1)	germline	PM2, PP3	VUS (Tepid)	Unknown	
c.957G>C	29668404	p.(Gln319His)	10	0.99	0.75	C15	0	1		-				somatic	PM2, PP3	VUS (Tepid)	No	29130106
c.970C>G	29668417	p.(Gln324Glu)	10	0.96	0.59	C25	0	0.82		-			VUS (1)	germline	PM2	VUS (Cool)	Unknown	
c.971A>T	29668418	p.(Gln324Leu)	10	0.98	0.59	C65	0	0.06		-				somatic	PM2 +	VUS (Cool)	Associated	21383154 11448944 24309211 7717450
c.974C>T	29668421	p.(Ala325Val)	10	0.99	0.72	C65	0	1		-			VUS (1)	germline	PM2, PP3	VUS (Tepid)	Unknown	
c.983A>T	29668430	p.(Glu328Val)	10	0.98	0.78	C35	0	0.99	New Donor Site?	-	rs200372028	0.000012	VUS (1)	germline	PP3	VUS (cold)	Associated	
c.992G>C	29668439	p.(Arg331Thr)	10	0.98	0.67	C65	0	1		-			VUS (1)	germline	PM2	VUS (Cool)	Unknown	
c.999G>C	29668446	p.(Gln333His)	10	0.91	0.45	C0	0	0.01	Possible effect	-	rs1469191017		VUS (1)	germline	PM2, PP3	VUS (Tepid)	Unknown	

Supplementary table appendix I. Continued on next page.

c.1000A>G	29671826	p.(Met334Val)	11	0.29	0.25	C0	1	0	New Donor Site?	-	rs1556000094		VUS (1)	germline	PM2, BP4	VUS (cold)	Unknown	
c.1003G>A	29671829	p.(Glu335Lys)	11	0.98	0.79	C0	0	0.9		-			1	germline	PM2, PP3	VUS (Tepid)	Unknown	
c.1006C>T	29671832	p.(Arg336Trp)	11	1.00	0.58	C25	0	1		-	rs140266312	0.000004	VUS (1)	germline	None applied	VUS (ice cold)	Unknown	
c.1007G>A	29671833	p.(Arg336Gln)	11	0.92	0.48	C0	0.3	0.96		-	rs587778554	0.000012	VUS (2)	germline	None applied	VUS (ice cold)	Unknown	
c.1012C>T	29671838	p.(Arg338Cys)	11	0.91	0.44	C25	0	0.01		-	rs761795291	0.000008	VUS (3)	germline	None applied	VUS (ice cold)	Associated	
c.1013G>A	29671839	p.(Arg338His)	11	0.69	0.38	C0	0.1	0.7		-	rs768053145	0.000016	VUS (2)	germline	BP4	VUS (Ice cold)	Unknown	18033041 28353378 18033041
c.1015C>T	29671841	p.(Leu339Phe)	11	0.91	0.60	C0	0.3	0.44		-				Somatic	PM2 +	VUS (Cool)	Associated	29130106 8655144, 16885985
c.1018G>A	29671844	p.(Ala340Thr)	11	0.32	0.34	C0	0.3	0.02		-	rs780430071	0.000016	VUS (2)	germline	BP4	VUS (ice cold)	Unknown	
c.1018G>T	29671844	p.(Ala340Ser)	11	0.72	0.32	C0	0.3	0		-	rs780430071		VUS (2)	germline	PM2, BP4	VUS (cold)	Unknown	
c.1021C>G	29671847	p.(Arg341Gly)	11	0.99	0.56	C0	0.1	0.99		-	rs74315499		1	germline	PM2	VUS (Cool)	Unknown	
c.1022G>A	29671848	p.(Arg341Gln)	11	0.95	0.48	C0	0.3	0.88		-	rs754087071	0.000008	VUS (2)	germline	None applied	VUS (ice cold)	Unknown	
c.1022G>T	29671848	p.(Arg341Leu)	11	0.98	0.64	C0	0.5	0.96		-	rs754087071	0.000004	VUS (2)	germline	None applied	VUS (ice cold)	Unknown	
c.1037G>A	29671863	p.(Arg346Lys)	11	0.97	0.49	C0	0.1	0.63		-	rs1556000154		VUS (1)	germline	PM2	VUS (Cool)	Unknown	
c.1038G>T	29671864	p.(Arg346Ser)	11	1.00	0.58	C0	0.2	0.75	New Donor Site?	-			VUS (1)	germline	PM2 +	VUS (Cool)	Associated	25026211 1481793, 33058421 18285426
c.1051C>T	29671877	p.(Arg351Cys)	11	0.99	0.51	C35	0	1		-	rs747756728	0.000012	VUS (1)	germline	None applied	VUS (ice cold)	Unknown	
c.1052G>A	29671878	p.(Arg351His)	11	0.66	0.45	C0	0.3	0.23		-	rs771675702	0.000039	VUS (2)	germline	BS1 +	Likely benign	Associated	7951231, 11401550
c.1055C>T	29671881	p.(Thr352Met)	11	0.76	0.52	C0	0.1	0.68		-	rs764441073	0.000012	VUS (1)	germline	PM6 +	VUS (Cool)	Associated	11779178 11448944 10712203 8081368
c.1059G>C	29671885	p.(Arg353Ser)	11	0.97	0.39	C0	0.1	0.09		-	rs1379674036		VUS (2)	germline/ unknown	PM2, BP4	VUS (cold)	Unknown	
c.1060G>A	29671886	p.(Asp354Asn)	11	0.88	0.41	C0	0.7	0.61		-	rs1435353346	0.000004	VUS (1)	germline	None applied	VUS (ice cold)	Unknown	
c.1063G>A	29671889	p.(Glu355Lys)	11	0.90	0.43	C0	0.1	0.03		-				Somatic	PM2	VUS (Cool)	No	29130106
c.1065G>C	29671891	p.(Glu355Asp)	11	0.43	0.32	C0	0.1	0		-	rs1277506366		VUS (1)	germline	PM2, BP4	VUS (cold)	Unknown	
c.1066T>A	29671892	p.(Leu356Met)	11	0.74	0.34	C0	0.3	0.34		-			1	germline	PM2, BP4	VUS (cold)	Unknown	

Supplementary table appendix I. Continued on next page.

c.1068G>T	29671894	p.(Leu356Phe)	11	0.98	0.64	C0	0	0.98		-				Somatic	PM2	VUS (Cool)	Associated	24030433
c.1069G>A	29671895	p.(Glu357Lys)	11	0.97	0.57	C0	0.4	0.91		-					PM2	VUS (Cool)	Unknown	
c.1079T>C	29671905	p.(Leu360Pro)	11	1.00	0.92	C0	0	1		-	rs74315492		Pathogenic (1)	Germline	PS3, PS4(supporting), PM2, PP3	Likely pathogenic (b)	Associated	8379998, 8882871, 11779178 31015291 10861283 11535133 9425229, 10669747 7535084
c.1088T>A	29671914	p.(Met363Lys)	11	0.92	0.35	C0	0	0.01		-			VUS (1)	germline	PM2, BP4	VUS (cold)	Unknown	
c.1088T>G	29671914	p.(Met363Arg)	11	0.93	0.38	C0	0	0.07		-			VUS (1)	germline	PM2, BP4	VUS (cold)	Unknown	
c.1091A>T	29671917	p.(Lys364Ile)	11	0.99	0.65	C0	0	0.45		-				somatic	PM2 +	VUS (Cool)	Unknown	11779178 8162073
c.1092A>T	29671918	p.(Lys364Asn)	11	0.73	0.35	C0	0.1	0.45		-	rs1601644296		VUS (1)	germline	PM2, BP4	VUS (cold)	Unknown	
c.1103C>T	29671929	p.(Thr368Ile)	11	0.38	0.13	C0	0.3	0.1		-	rs1556000214		VUS (1)	germline	PM2, BP4	VUS (cold)	Unknown	
c.1105A>G	29671931	p.(Met369Val)	11	0.17	0.30	C0	0.4	0		-	rs1325119842		VUS (1)	germline	PM2, BP4	VUS (cold)	Unknown	
c.1112A>G	29671938	p.(Asn371Ser)	11	0.39	0.43	C0	0.1	0.19		-	rs577940601	0.000028	VUS (1)	germline	None applied	VUS (ice cold)	Unknown	
c.1113C>G	29671939	p.(Asn371Lys)	11	0.90	0.46	C0	0.1	0.9		-	rs142459414		VUS (1)	unknown	PM2	VUS (Cool)	Unknown	
c.1123A>G	29673269	p.(Met375Val)	12	0.77	0.26	C0	0.4	0	New Donor Site?	-			VUS	Unknown	PM2, BP4	VUS (cold)	Unknown	
c.1124T>C	29673270	p.(Met375Thr)	12	0.73	0.32	C0	0.2	0.14		-	rs1556000763		VUS (1)	germline	PM2, BP4	VUS (cold)	Unknown	
c.1126C>T	29673272	p.(Arg376Trp)	12	1.00	0.68	C35	0	1		-	rs867367858	0.000011	VUS (1)	germline	None applied	VUS (ice cold)	Unknown	
c.1127G>A	29673273	p.(Arg376Gln)	12	0.98	0.62	C0	0	1		0.179	rs996964764	0.000011	VUS (2)	germline	None applied	VUS (ice cold)	Unknown	
c.1127G>T	29673273	p.(Arg376Leu)	12	0.96	0.71	C35	0	1		-	rs996964764	0.000006	VUS (1)	germline	PP3	VUS (cold)	Unknown	
c.1129T>G	29673275	p.(Ser377Ala)	12	0.93	0.53	C0	0.6	1		-	rs1569305865		VUS (1)	germline	PM2	VUS (Cool)	Unknown	
c.1148T>C	29673294	p.(Leu383Pro)	12	0.99	0.73	C0	0	1		-					PM2, PP3	VUS (Tepid)	Associated	
c.1159A>G	29673305	p.(Lys387Glu)	12	0.99	0.75	C0	0	1	Acceptor site?	-				somatic	PM2, PP3	VUS (Tepid)	Associated	10790227
c.1163C>T	29673309	p.(Ala388Val)	12	0.84	0.53	C0	0	0.45	Cryptic Acceptor Strongly Activated?	-	rs587778553		VUS (1)	germline	PM2	VUS (Cool)	Unknown	
c.1165C>G	29673311	p.(Gln389Glu)	12	0.86	0.38	C0	0	0.59		-			1	germline	PM2, BP4	VUS (cold)	Unknown	
c.1174G>A	29673320	p.(Glu392Lys)	12	0.91	0.66	C0	0	1		-	rs1026724985	0.000004	1	germline	PM2	VUS (Cool)	Unknown	24786638

Supplementary table appendix I. Continued on next page.

c.1175A>T	29673321	p.(Glu392Val)	12	1.00	0.71	C15	0	1		-				somatic	PM2, PP3	VUS (Tepid)	Associated	16983642 11448944 10606247
c.1183G>T	29673329	p.(Ala395Ser)	12	0.97	0.51	C0	0.5	0.98		-	rs1601648303		VUS (1)	germline	PM2	VUS (Cool)	Unknown	
c.1184C>T	29673330	p.(Ala395Val)	12	0.99	0.65	C0	0.4	1		-				somatic	PM2	VUS (Cool)	No	8069299
c.1193T>C	29673339	p.(Leu398Pro)	12	1.00	0.81	C0	0.1	1		-					PM2, PP3, PP4	VUS (Warm)	Yes	
c.1195G>C	29673341	p.(Ala399Pro)	12	0.79	0.35	C0	0.3	0.23		-			VUS	Unknown	PM2, BP4	VUS (cold)	Associated	26073919
c.1207G>A	29673353	p.(Ala403Thr)	12	0.90	0.31	C0	0.5	0.38		-			VUS (1)	germline	PM2, BP4	VUS (cold)	Unknown	
c.1207G>T	29673353	p.(Ala403Ser)	12	0.86	0.31	C0	0.7	0.45		-			1	germline	PM2, BP4	VUS (cold)	Unknown	
c.1231C>T	29673377	p.(Arg411Cys)	12	0.88	0.63	C65	0	1		-	rs773296925	0.000029	VUS (2)	germline/ unknown	None applied	VUS (ice cold)	Unknown	33173047
c.1232G>A	29673378	p.(Arg411His)	12	0.88	0.67	C25	0	1		-	rs201214090	0.000029	VUS (5)	germline/ unknown	None applied	VUS (ice cold)	Associated	
c.1234A>C	29673380	p.(Ile412Leu)	12	0.71	0.10	C0	1	0		-			VUS (1)	germline	PM2, BP4	VUS (cold)	Unknown	
c.1237A>G	29673383	p.(Lys413Glu)	12	0.36	0.38	C0	0.2	0		-	rs766974263	0.000004		germline	BP4 +	VUS (ice cold)	Associated	21383154 11448944 24309211 9466988, 9486775
c.1243A>G	29673389	p.(Thr415Ala)	12	0.92	0.30	C0	0.3	0.01		-			VUS (1)		PM2, BP4	VUS (cold)	Associated	16983642
c.1252C>T	29673398	p.(Arg418Cys)	12	0.97	0.68	C25	0	1		-	rs765540111	0.000025	VUS (2)	germline/ somatic	None applied +	VUS (ice cold)	Associated	8012353
c.1253G>A	29673399	p.(Arg418His)	12	0.95	0.45	C0	0.1	1		-	rs548217466	0.000008	VUS (2)	germline	None applied +	VUS (ice cold)	Associated	
c.1256C>T	29673402	p.(Thr419Met)	12	0.97	0.46	C0	0	0.94		-					PM2	VUS (Cool)	Associated	26342709
c.1264G>A	29673410	p.(Glu422Lys)	12	0.99	0.69	C0	0.2	0.95		-			VUS (1)	germline	PM2	VUS (Cool)	Unknown	
c.1270C>A	29673416	p.(Arg424Ser)	12	0.73	0.37	C15	0.1	0.04		-	rs763826793		VUS (2)	germline	PM2, BP4	VUS (cold)	Unknown	
c.1270C>G	29673416	p.(Arg424Gly)	12	0.54	0.55	C15	0.1	0.54		-	rs763826793		VUS (1)	germline	PM2	VUS (Cool)	Unknown	
c.1270C>T	29673416	p.(Arg424Cys)	12	0.76	0.58	C25	0	1		-	rs763826793	0.000004	VUS (1)	germline	None applied +	VUS (ice cold)	Unknown	33209614
c.1271G>A	29673417	p.(Arg424His)	12	0.39	0.31	C0	0.2	0.16		-	rs751182657	0.000024	VUS (3)	germline	BP4	VUS (ice cold)	Associated	
c.1271G>T	29673417	p.(Arg424Leu)	12	0.34	0.32	C0	0.4	0		-	rs751182657	0.00002	VUS (1)	germline	BP4	VUS (ice cold)	Unknown	
c.1280A>C	29673426	p.(Glu427Ala)	12	0.99	0.74	C15	0	0.99		-			VUS (1)	germline	PM2, PP3	VUS (Tepid)	Unknown	
c.1288G>T	29673434	p.(Val430Leu)	12	0.32	0.35	C0	0.4	0		0.129	rs1361867592	0.000004	VUS (1)	germline	BP4	VUS (ice cold)	Unknown	
c.1297G>A	29673443	p.(Ala433Thr)	12	0.80	0.38	C0	0.1	0.13		-	rs1449875899	0	1	germline	PM2, BP4	VUS (cold)	Unknown	
c.1298C>T	29673444	p.(Ala433Val)	12	0.70	0.56	C0	0	0.97		-	rs779721863	0.000029	VUS (1)	germline	None applied +	VUS (ice cold)	Unknown	

Supplementary table appendix I. Continued on next page.

c.1300G>A	29673446	p.(Glu434Lys)	12	0.60	0.46	C15	0	0.22	Cryptic Donor Strongly Activated?	0.316	rs992662337	0.000016	VUS (1)	germline	None applied +	VUS (ice cold)	Unknown	
c.1301A>G	29673447	p.(Glu434Gly)	12	0.99	0.78	C15	0	0.96		0.186	rs1601648832		VUS (1)	germline	PM2, PP3	VUS (Tepid)	Unknown	
c.1303G>A	29673449	p.(Val435Met)	12	0.75	0.39	C0	0.3	0		-	rs772334382		VUS (1)	germline	PM2, BP4	VUS (cold)	Associated	19234911
c.1303G>T	29673449	p.(Val435Leu)	12	0.17	0.35	C0	0.7	0		-	rs772334382	0.000008	VUS (1)	germline	BP4	VUS (ice cold)	Unknown	
c.1336A>G	29673482	p.(Arg446Gly)	12	0.97	0.73	C0	0.3	0.91	Possible effect	0.643			VUS (1)	germline	PM2, PP3	VUS (Tepid)	Unknown	
c.1340G>A	29673486	p.(Arg447Lys)	12	0.90	0.53	C0	0.6	1	Possible effect	0.614					PM2, PP3	VUS (Tepid)	Associated	
c.1340G>T	29673486	p.(Arg447Met)	12	0.99	0.81	C0	0.1	1	Possible effect	0.643			VUS (1)	germline	PM2, PP3	VUS (Tepid)	Associated	
c.1342G>A	29674837	p.(Ala448Thr)	13	0.87	0.24	C0	0.2	0.02		-			VUS (1)	germline	PM2, BP4	VUS (cold)	Unknown	
c.1343C>G	29674838	p.(Ala448Gly)	13	0.95	0.26	C0	0.1	0.01		-			1	germline	PM2, BP4	VUS (cold)	Unknown	
c.1351G>A	29674846	p.(Ala451Thr)	13	0.96	0.45	C0	0.2	0.48		-				somatic	PM2	VUS (Cool)	No	22081132
c.1357C>G	29674852	p.(Gln453Glu)	13	0.89	0.33	C0	0.1	0.02		-	rs1556001358		VUS (1)	germline	PM2, BP4	VUS (cold)	Unknown	
c.1364A>G	29674859	p.(Lys455Arg)	13	0.71	0.37	C0	0.4	0.33		-	rs1318882444	0.000006	VUS (1)	germline	BP4 +	VUS (ice cold)	Unknown	24166499
c.1366C>G	29674861	p.(Gln456Glu)	13	0.84	0.37	C0	0.4	0.02		-			VUS (1)	germline	PM2, BP4	VUS (cold)	Unknown	
c.1370A>T	29674865	p.(Asp457Val)	13	1.00	0.80	C25	0	0.98	New Donor Site?	-			1	germline	PM2, PP3	VUS (Tepid)	Unknown	
c.1373T>G	29674868	p.(Leu458Arg)	13	1.00	0.86	C15	0	1		-	rs1457638896	0	VUS (1)	germline	PM2, PP3	VUS (Tepid)	Unknown	
c.1384C>T	29674879	p.(Arg462Cys)	13	0.99	0.60	C25	0	1		-	rs771143279	0.000011	1	germline	PM2	VUS (Cool)	Unknown	
c.1385G>A	29674880	p.(Arg462His)	13	0.90	0.54	C0	0.1	1		-	rs373650983	0.000037	VUS (2)	germline	BS1	Likely benign	Unknown	31712784
c.1387G>A	29674882	p.(Glu463Lys)	13	0.06	0.43	C0	0.3	0.66		-	rs74315503	0.000138	VUS (1)/ Likely benign (2)	germline	BS1 +	Likely benign	Unknown	7829260, 26045165
c.1391C>T	29674886	p.(Ala464Val)	13	0.88	0.51	C0	0	0.99		-	rs776109136	0.000011	VUS (1)	germline	None applied	VUS (ice cold)	Associated	29975249
c.1396C>G	29674891	p.(Arg466Gly)	13	0.98	0.67	C25	0	0.94		-	rs74315504		VUS (1)	germline	PM2	VUS (Cool)	Unknown	
c.1397G>A	29674892	p.(Arg466Gln)	13	0.97	0.55	C0	0.3	0.99		-	rs866689896	0	VUS (2)	germline	PM2	VUS (Cool)	Unknown	
c.1397G>T	29674892	p.(Arg466Leu)	13	0.94	0.71	C25	0	0.11		-					PM2, PP3	VUS (Tepid)	Unknown	
c.1400G>A	29674895	p.(Arg467Lys)	13	0.41	0.30	C0	0.3	0.02		-	rs1294032875	0.000005	VUS (2)	germline	BP4	VUS (ice cold)	Unknown	22081132
c.1409A>G	29674904	p.(Gln470Arg)	13	0.89	0.38	C0	0.4	0.44		-				somatic	PM2, BP4	VUS (cold)	No	28524162
c.1409A>T	29674904	p.(Gln470Leu)	13	0.91	0.27	C0	0.2	0.01		-				somatic	PM2, BP4	VUS (cold)	No	21727090
c.1439C>A	29674934	p.(Thr480Lys)	13	0.50	0.30	C0	0.9	0.01		-	rs145666157		VUS (1)	germline	PM2, BP4	VUS (cold)	Unknown	
c.1439C>T	29674934	p.(Thr480Met)	13	0.07	0.22	C0	0.1	0.5		-	rs145666157	0.000113	VUS (2)	germline	PP4, BP4, BS1	Likely benign	Yes	25931164

Supplementary table appendix I. Continued on next page.

c.1442A>G	29674937	p.(Tyr481Cys)	13	0.97	0.58	C0	0.2	0.43		-			1	germline	PM2	VUS (Cool)	Unknown	
c.1445C>G	29674940	p.(Pro482Arg)	13	0.42	0.25	C0	0.1	0.03		-	rs766339217	0.000015	VUS (2)	germline	BP4	VUS (ice cold)	Unknown	
c.1445C>T	29674940	p.(Pro482Leu)	13	0.31	0.20	C0	0	0		-	rs766339217	0.000012	VUS (1?)	germline	BP4	VUS (ice cold)	Associated	
c.1447C>G	29678196	p.(Pro483Ala)	14	0.29	0.21	C0	1	0		-			VUS (1)	germline	PM2, BP4	VUS (Cold)	Unknown	
c.1450A>G	29678199	p.(Met484Val)	14	0.04	0.17	C0	0.3	0		-	rs1182896077	0.000008	VUS (2)	germline	BP4	VUS (ice cold)	Unknown	
c.1451T>C	29678200	p.(Met484Thr)	14	0.03	0.24	C0	0.5	0		-	rs141538143	0.000269	VUS (1)/ Likely benign (1)/ Benign (1)/ not provided (1)	germline/ unknown	BS1, BP4	Likely benign	Unknown	
c.1453A>T	29678202	p.(Asn485Tyr)	14	0.84	0.27	C0	0.1	0	Cryptic Acceptor Strongly Activated?	0.522	rs1601658875		VUS (2)	germline	PM2, PP3	VUS (Tepid)	Unknown	
c.1459A>C	29678208	p.(Ile487Leu)	14	0.06	0.20	C0	0.2	0	Cryptic Acceptor Strongly Activated?	-	rs147506929		VUS (2)	germline	PM2, BP4	VUS (Cold)	Unknown	
c.1459A>G	29678208	p.(Ile487Val)	14	0.05	0.16	C0	0.5	0		-	rs147506929	0.000008		somatic	BP4	VUS (Ice cold)	No	21727090
c.1460T>C	29678209	p.(Ile487Thr)	14	0.55	0.26	C0	0.1	0		-	rs1601658904		VUS (1)	germline	PM2, BP4	VUS (cold)	Unknown	
c.1463C>T	29678212	p.(Pro488Leu)	14	0.48	0.31	C0	0	0	Cryptic Acceptor Strongly Activated?	-	rs1173959854	0.000032	VUS (1)	germline	BP4	VUS (Ice cold)	Unknown	
c.1468C>T	29678217	p.(Pro490Ser)	14	0.07	0.16	C0	0.9	0		-	rs776076922	0.000012	VUS (1)	germline	BP4	VUS (ice cold)	Unknown	
c.1469C>T	29678218	p.(Pro490Leu)	14	0.14	0.21	C0	0.3	0		-	rs765100922	0.000016	VUS (2)	germline	BP4	VUS (ice cold)	Unknown	
c.1480G>C	29678229	p.(Asp494His)	14	0.70	0.59	C0	0.5	0.92		-			VUS (1)	germline	PM2	VUS (Cool)	Unknown	
c.1484T>G	29678233	p.(Ile495Arg)	14	0.57	0.21	C0	0.4	0.04	New Acceptor Site?	-	rs1556002511		VUS (1)	germline	PM2, PP3	VUS (Tepid)	Unknown	
c.1490G>C	29678239	p.(Ser497Thr)	14	0.34	0.41	C0	0.1	0		-	rs900545157	0.000008	VUS (3)	germline	PP4	VUS (cold)	Yes	15684865 16983642
c.1501A>G	29678250	p.(Ile501Val)	14	0.08	0.13	C0	0.9	0	Cryptic Acceptor Strongly Activated?	-	rs1315864916	0.000004	VUS (1)	germline	BP4	VUS (Ice cold)	Unknown	

Supplementary table appendix I. Continued on next page.

c.1502T>C	29678251	p.(Ile501Thr)	14	0.10	0.16	C0	0.5	0		-	rs767682136	0.000012	VUS (2)	germline	BP4	VUS (ice cold)	Unknown	
c.1511G>A	29678260	p.(Ser504Asn)	14	0.91	0.41	C0	0.6	0		-	rs756366940		VUS (1)	germline	PM2, PP3	VUS (Tepid)	Unknown	
c.1511G>T	29678260	p.(Ser504Ile)	14	0.34	0.46	C0	0	0.01		-	rs756366940	0.000008	1	germline	PP3	VUS (cold)	Unknown	
c.1517C>G	29678266	p.(Ser506Cys)	14	0.87	0.56	C0	0	0.7		-	rs970051210		VUS (1)	germline	PM2	VUS (Cool)	Unknown	
c.1522G>A	29678271	p.(Asp508Asn)	14	0.57	0.59	C0	0.5	0.95		-	rs749326764	0.00002	VUS (1)	germline	None applied	VUS (ice cold)	Unknown	27284491 30239046
c.1522G>T	29678271	p.(Asp508Tyr)	14	0.99	0.81	C0	0.1	0.11	Cryptic Acceptor Strongly Activated?	-	rs749326764		VUS (1)	germline	PM2, PP3	VUS (Tepid)	Unknown	
c.1529A>G	29678278	p.(Lys510Arg)	14	0.91	0.34	C0	0.2	0.01	New Acceptor Site?	-	rs886057337	0.000032	VUS (1)	germline	PP3	VUS (cold)	Unknown	
c.1531G>T	29678280	p.(Asp511Tyr)	14	0.99	0.85	C0	0	0.96		-					PM2, PP3	VUS (Tepid)	Associated	
c.1532A>G	29678281	p.(Asp511Gly)	14	0.95	0.79	C0	0	0.02	New Donor Site?	0.973					PS3, PM2, PP4	Likely path (b)	Yes	28409725
c.1540A>C	29678289	p.(Met514Leu)	14	0.88	0.32	C0	0.1	0		-			1	germline	PM2, BP4	VUS (cold)	Unknown	
c.1540A>G	29678289	p.(Met514Val)	14	0.07	0.66	C0	0.1	0		-	rs201527155	0.000099	VUS (4)/ benign (1)	germline	BS1, PP4 +	Likely benign	Yes	25931164 16983642 26045165 33058421
c.1544A>G	29678293	p.(Lys515Arg)	14	0.94	0.51	C0	0.1	0.61		-			VUS (1)	germline	PM2	VUS (Cool)	Unknown	
c.1547G>A	29678296	p.(Arg516Gln)	14	0.95	0.36	C0	0.4	0.24		-	rs1569309694		VUS (2)	germline	PM2, BP4	VUS (cold)	Unknown	
c.1550T>C	29678299	p.(Leu517Pro)	14	0.99	0.85	C0	0	0.38		-	rs1556002568		Pathogenic (1)	germline	PM2, PP3, PP4 +	VUS (Warm)	Yes	16983642 16983642 26045165 33058421
c.1557G>A	29678306	p.(Met519Ile)	14	0.92	0.40	C0	0.3	0.08	New Acceptor Site?	-	rs1601659358		VUS (1)	germline	PM2, PP3	VUS (Tepid)	Unknown	
c.1567A>G	29678316	p.(Lys523Glu)	14	0.96	0.39	C0	0	0.1		-			1	germline	PM2, BP4	VUS (cold)	Unknown	
c.1575A>C	29681439	p.(Lys525Asn)	15	0.91	0.42	C0	0	0.61	Close proximity, branch point disruption?	0.128			1	germline	PM2	VUS (Cool)	Unknown	
c.1585A>G	29681449	p.(Met529Val)	15	0.52	0.38	C0	0.2	0.12		-	rs1456599218				PM2, BP4	VUS (cold)	Unknown	
c.1585A>T	29681449	p.(Met529Leu)	15	0.40	0.26	C0	1	0		-				somatic	PM2, BP4	VUS (cold)	No	32483240
c.1586T>C	29681450	p.(Met529Thr)	15	0.51	0.43	C0	0.1	0.76		-	rs780818183	0.000028	VUS (2)	germline	None applied	VUS (ice cold)	Unknown	

Supplementary table appendix I. Continued on next page.

c.1598A>C	29681462	p.(Lys533Thr)	15	0.99	0.78	C0	0	0.85		-				germline/ somatic	PM2, PP3, PP4 +	VUS (Warm)	Yes	10790209 10748301
c.1600C>T	29681464	p.(His534Tyr)	15	0.95	0.54	C0	0.7	0.97		-	rs769370159	0.000004	VUS (1)	germline/ somatic	None applied	VUS (ice cold)	Associated	23921927
c.1601A>C	29681465	p.(His534Pro)	15	0.99	0.68	C0	0.2	0.92		-					PM2, PP4	VUS (Tepid)	Yes	
c.1604T>C	29681468	p.(Leu535Pro)	15	0.99	0.85	C0	0	1		-	rs74315493		Pathogenic (1)	germline	PS3, PM2, PS4(supporting), PP1, PP3, PP4 +	Pathogenic (d)	Yes	21383154 11779178 11448944 9931334, 26045165 11285248 17980164 11535133 10861283 16983642
c.1604T>G	29681468	p.(Leu535Arg)	15	0.99	0.81	C0	0	1		-					PM2, PP3, PP4	VUS (Warm)	Yes	
c.1611G>T	29681475	p.(Glu537Asp)	15	0.24	0.24	C0	0.1	0		-	rs946609084		VUS (1)	germline	PM2, BP4	VUS (cold)	Unknown	
c.1613A>C	29681477	p.(Gln538Pro)	15	1.00	0.86	C0	0	1		-	rs74315494		Pathogenic (1)	germline	PS3, PM2, PP3, PP4 +	Likely pathogenic (b)	Yes	11779178 11448944 8882871, 8566958, 26045165 10861283
c.1616T>A	29681480	p.(Leu539His)	15	0.99	0.96	C0	0	1		-				somatic	PM2, PP3, PP4	VUS (Warm)	Yes	8698340, 26045165
c.1616T>C	29681480	p.(Leu539Pro)	15	1.00	0.94	C0	0	1		-					PM2, PP3, PS4 (supporting), PP4	VUS (Hot)	Yes	
c.1619A>G	29681483	p.(Asn540Ser)	15	0.36	0.35	C0	0.2	0.12		-	rs774824164	0.000014	VUS (3)	germline/ unknown	BP4	VUS (ice cold)	Unknown	
c.1625T>A	29681489	p.(Leu542His)	15	0.99	0.97	C0	0	1		-				germline	PM2, PP3	VUS (Tepid)	Unknown	11779178 26045165
c.1630A>G	29681494	p.(Thr544Ala)	15	0.87	0.48	C0	0.4	0.42		-	rs762953921	0.000004	1	germline	None applied	VUS (ice cold)	Unknown	
c.1635A>T	29681499	p.(Glu545Asp)	15	0.88	0.69	C0	0.4	1		-	rs1556003698		VUS (2)	germline	PM2	VUS (Cool)	Unknown	
c.1639G>A	29681503	p.(Glu547Lys)	15	0.45	0.74	C0	0.1	0.95		-	rs199669486	0.000262	VUS (1)/ Likely benign (2)	germline	BS1, PP3 +	Likely benign	Associated	15692946 22325036
c.1642G>C	29681506	p.(Ala548Pro)	15	0.73	0.42	C0	0.4	0		-					PM2	VUS (Cool)	Associated	
c.1660A>G	29681524	p.(Arg554Gly)	15	0.98	0.63	C0	0.2	0.61		-			VUS (1)	germline	PM2	VUS (Cool)	Unknown	

Supplementary table appendix I. Continued on next page.

c.1660A>T	29681524	p.(Arg554Trp)	15	1.00	0.61	C0	0	0.99		-			1	germline	PM2	VUS (Cool)	Unknown	
c.1661G>A	29681525	p.(Arg554Lys)	15	0.71	0.37	C0	0.4	0		-			VUS (1)	germline	PM2, BP4	VUS (cold)	Unknown	
c.1663G>A	29681527	p.(Glu555Lys)	15	0.95	0.57	C0	0.2	0.24		-				somatic	PM2	VUS (Cool)	No	32494066
c.1675G>T	29681539	p.(Asp559Tyr)	15	0.98	0.64	C15	0	0.03		-	rs917012886	0.000004	VUS (2)	germline	None applied	VUS (ice cold)	Unknown	
c.1678A>G	29681542	p.(Ile560Val)	15	0.26	0.23	C0	0.7	0.02		-	rs557347747		VUS (2)	germline	PM2, BP4	VUS (cold)	Unknown	
c.1685A>G	29681549	p.(His562Arg)	15	0.99	0.90	C0	0.1	0.96		-				somatic	PM2, PP3	VUS (Tepid)	No	29130106
c.1685A>T	29681549	p.(His562Leu)	15	0.99	0.89	C0	0.1	0.63		-	rs878853926		VUS (1)	germline	PM2, PP3	VUS (Tepid)	Unknown	
c.1688A>G	29681552	p.(Asn563Ser)	15	0.10	0.24	C0	0.9	0.01	New Acceptor Site?	-	rs768303416		VUS (2)	germline	PM2, PP3	VUS (Tepid)	Unknown	
c.1690G>C	29681554	p.(Glu564Gln)	15	0.77	0.49	C0	0.4	0		-				somatic	PM2	VUS (Cool)	No	32494066
c.1693A>T	29681557	p.(Asn565Tyr)	15	0.91	0.54	C0	0.1	0.39		-	rs1601666359		VUS (1)	germline	PM2	VUS (Cool)	Unknown	
c.1699G>A	29681563	p.(Asp567Asn)	15	0.41	0.31	C0	0.3	0.11		-	rs757586383	0.000014	VUS (2)	germline/ unknown	BP4	VUS (ice cold)	Unknown	
c.1701C>G	29681565	p.(Asp567Glu)	15	0.04	0.21	C0	1	0		-	rs1049732514	0.000044	VUS (3)	germline/ unknown	BS1, BP4	Likely benign	Unknown	
c.1702A>G	29681566	p.(Arg568Gly)	15	0.94	0.45	C0	0.1	0.09		-	rs1318481716		VUS (1)	germline	PM2	VUS (Cool)	Unknown	
c.1706G>A	29681570	p.(Gly569Asp)	15	0.84	0.59	C0	0	0.94		-	rs781488145	0.000004	VUS (1)	germline	None applied	VUS (ice cold)	Unknown	
c.1712G>A	29681576	p.(Ser571Asn)	15	0.37	0.35	C0	0.6	0		-			VUS (1)	germline	PM2, BP4	VUS (cold)	Unknown	
c.1714A>C	29681578	p.(Ser572Arg)	15	0.80	0.58	C0	0	0.32		-	rs1379683835	0.000004	1	germline	None applied	VUS (ice cold)	Unknown	
c.1720C>T	29681584	p.(His574Tyr)	15	0.96	0.19	C0	0.6	0		-			1	germline	PM2, BP4	VUS (cold)	Unknown	
c.1721A>C	29681585	p.(His574Pro)	15	0.97	0.69	C0	0.1	0.18		-			1	germline	PM2	VUS (Cool)	Unknown	
c.1721A>G	29681585	p.(His574Arg)	15	0.90	0.49	C0	0.2	0		-	rs1601666509		VUS (1)	germline	PM2	VUS (Cool)	Unknown	
c.1724A>G	29681588	p.(Asn575Ser)	15	0.28	0.40	C0	0.6	0		-	rs1569312127		VUS (1)	unknown	PM2, BP4	VUS (cold)	Unknown	
c.1726A>T	29681590	p.(Thr576Ser)	15	0.85	0.61	C0	0.2	0.53		-	rs1601666549		VUS (2)	germline	PM2	VUS (Cool)	Unknown	
c.1732A>G	29681596	p.(Lys578Glu)	15	0.93	0.61	C0	0.1	0.01		-					PM2	VUS (Cool)	Unknown	
c.1733A>G	29681597	p.(Lys578Arg)	15	0.63	0.25	C0	0.3	0.01		-			VUS (1)	germline	PM2, BP4	VUS (cold)	Unknown	
c.1735A>C	29681599	p.(Lys579Gln)	15	0.77	0.49	C0	0.1	0.75		-			1	germline	PM2	VUS (Cool)	Unknown	
c.1736A>T	29681600	p.(Lys579Met)	15	0.98	0.78	C0	0	0.99	Possible effect	0.22				somatic	PM2, PP3, PP4	VUS (Warm)	Yes	10790209
c.1737G>T	29681601	p.(Lys579Asn)	15	0.96	0.51	C0	0	0.75	Possible effect	0.93				germline	PM2, PP3	VUS (Tepid)	Associated	8882871

Supplementary table appendix I. Continued on next page.

c.1741A>C	29694755	p.(Thr581Pro)	17	0.75	0.53	C0	0.2	0.4	Cryptic Acceptor Strongly Activated?	-	rs1601688849		VUS (1)	germline	PM2	VUS (Cool)	Unknown	
c.1745T>C	29694759	p.(Leu582Ser)	17	0.42	0.45	C0	0.6	0		-			VUS (1)	germline	PM2	VUS (Cool)	Unknown	
c.1753G>A	29694767	p.(Ala585Thr)	17	0.01	0.16	C0	0.6	0		-	rs145446060	0.00016	VUS (3)	germline	BS1, BP4	Likely benign	Unknown	25931164
c.1753G>T	29694767	p.(Ala585Ser)	17	0.37	0.24	C0	0.8	0.01		-			VUS (1)	germline	PM2, BP4	VUS (cold)	Unknown	
c.1763G>A	29694777	p.(Arg588Gln)	17	0.88	0.54	C0	0.1	0.96		-	rs766689587	0.000012	VUS (1)	germline	None applied	VUS (ice cold)	Unknown	
c.1765G>A	29694779	p.(Val589Met)	17	0.79	0.52	C0	0	0.8		-	rs1293851600	0.000008	VUS (2)	germline	None applied	VUS (ice cold)	Associated	
c.1769C>T	29694783	p.(Ala590Val)	17	0.85	0.54	C0	0.1	1	Cryptic Acceptor Strongly Activated?	-	rs1246154574	0.000004	1	germline	None applied	VUS (ice cold)	Unknown	
c.1774T>C	29694788	p.(Phe592Leu)	17	0.24	0.69	C0	0.3	1		-	rs764972504	0.000036	VUS (4)/ Likely benign (1)	germline	BS1	Likely benign	Unknown	
c.1783C>T	29694797	p.(Leu595Phe)	17	0.93	0.48	C0	0.1	0.79	Cryptic Acceptor Weakly Activated?	-	rs1601689027		VUS (2)	germline	PM2	VUS (Cool)	Unknown	

Supplementary table Appendix I. A comprehensive list of *NF2* missense variants and the evidence categories applied to their classification.

Variants were identified and re-evaluated as described in chapter 4. VUS = Variant of uncertain significance. ACGS criteria '+' indicates some functional work in literature but not considered sufficient for PS3 evidence.

Appendix II: Vector maps

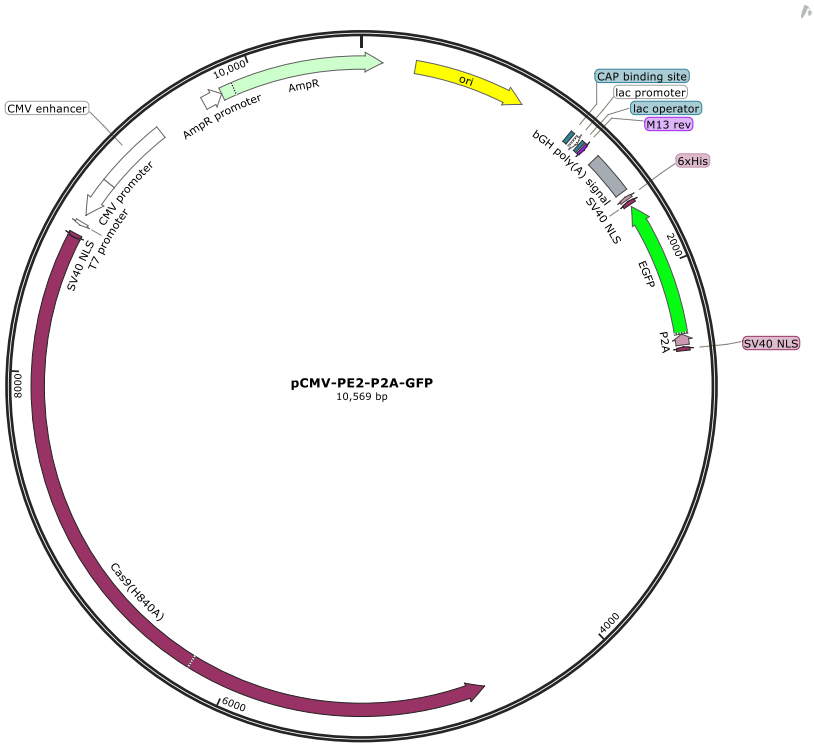

pCMV-PE2-P2A-GFP, a gift from David Liu (Addgene plasmid #132776)

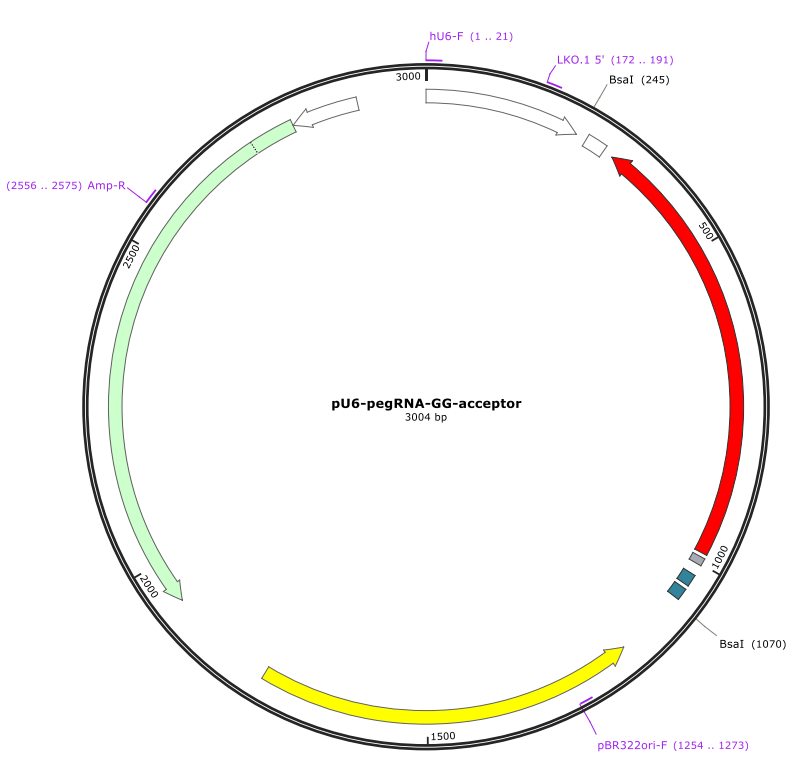

pU6-pegRNA-GG-acceptor, a gift from David Liu (Addgene plasmid #132777)

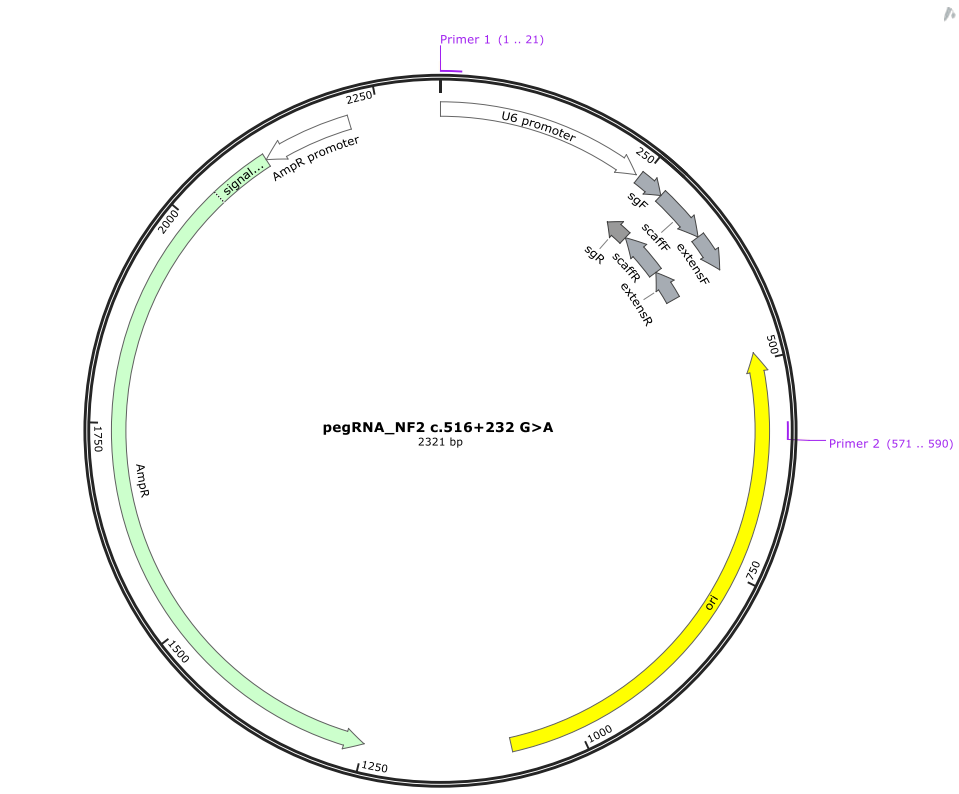

NF2 c.516+232 G>A specific pegRNA, assembled into digested pU6-pegRNA-GG-acceptor

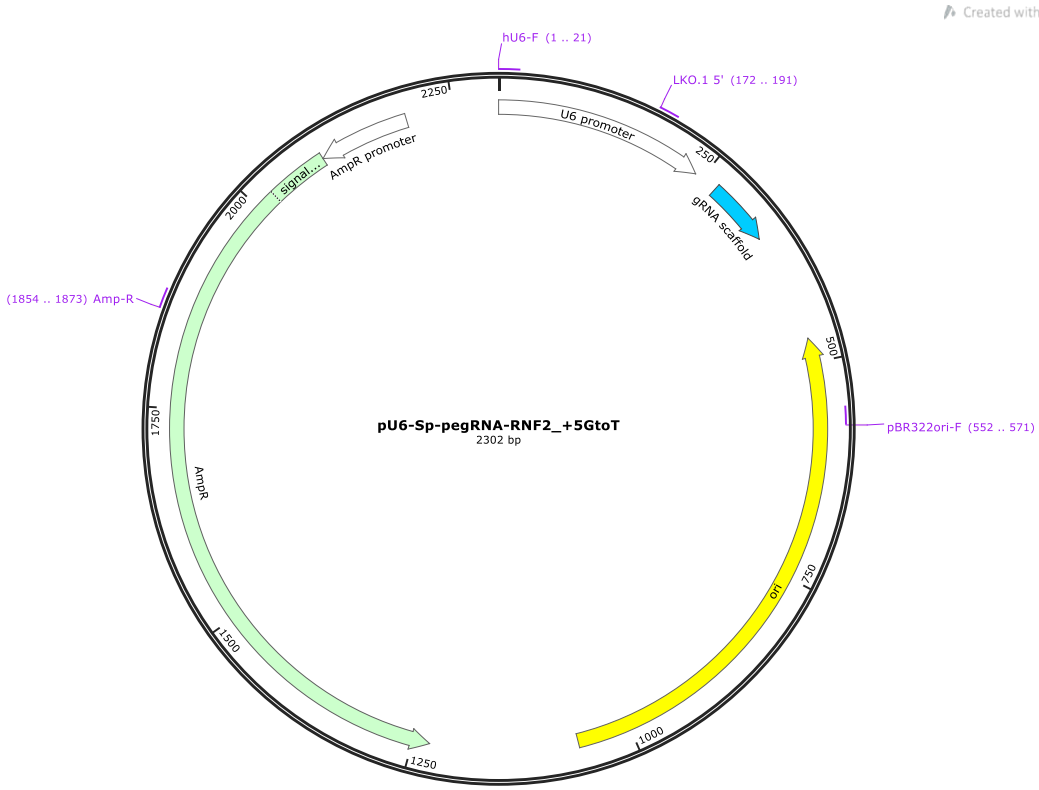

pU6-Sp-pegRNA-RNF2_+5GtoT, a gift from David Liu (Addgene plasmid #135957)

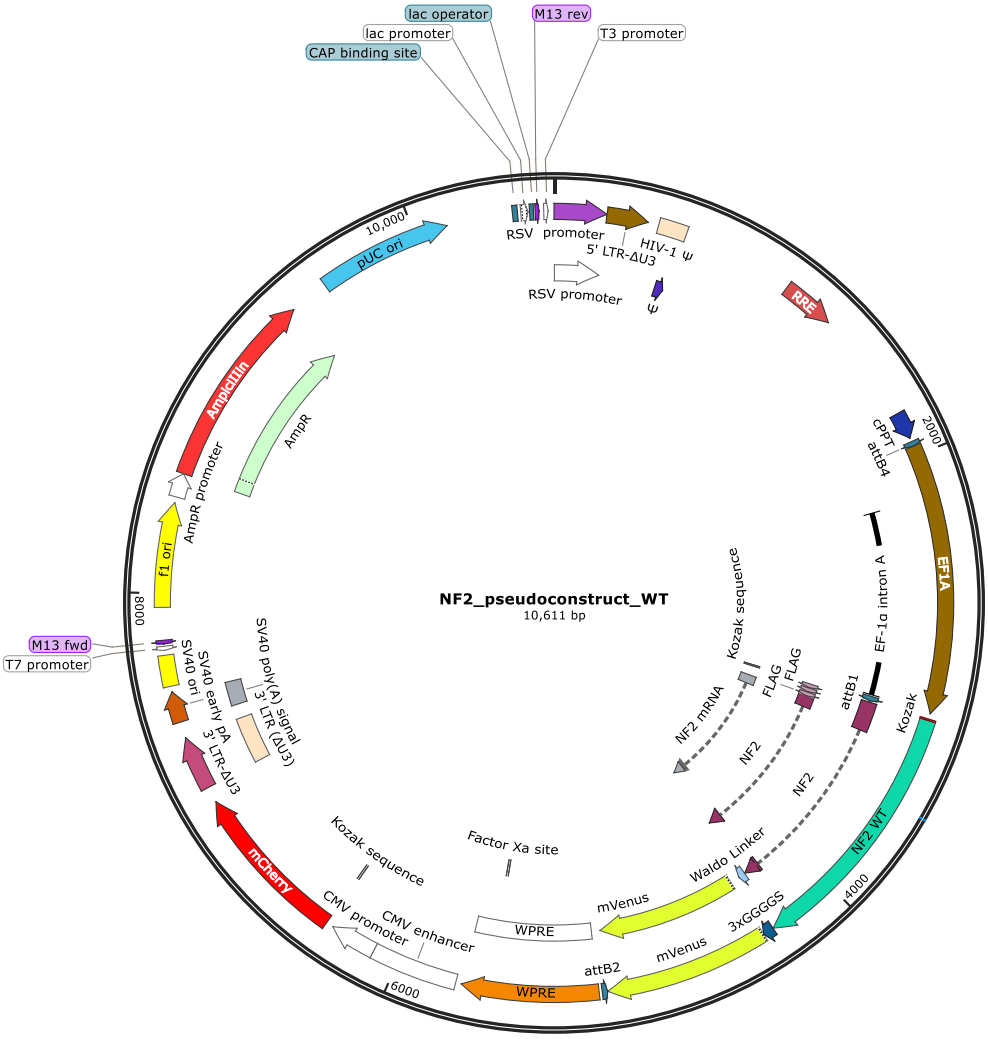

VectorBuilder *NF2* pseudo-construct reporter system, Wild Type.

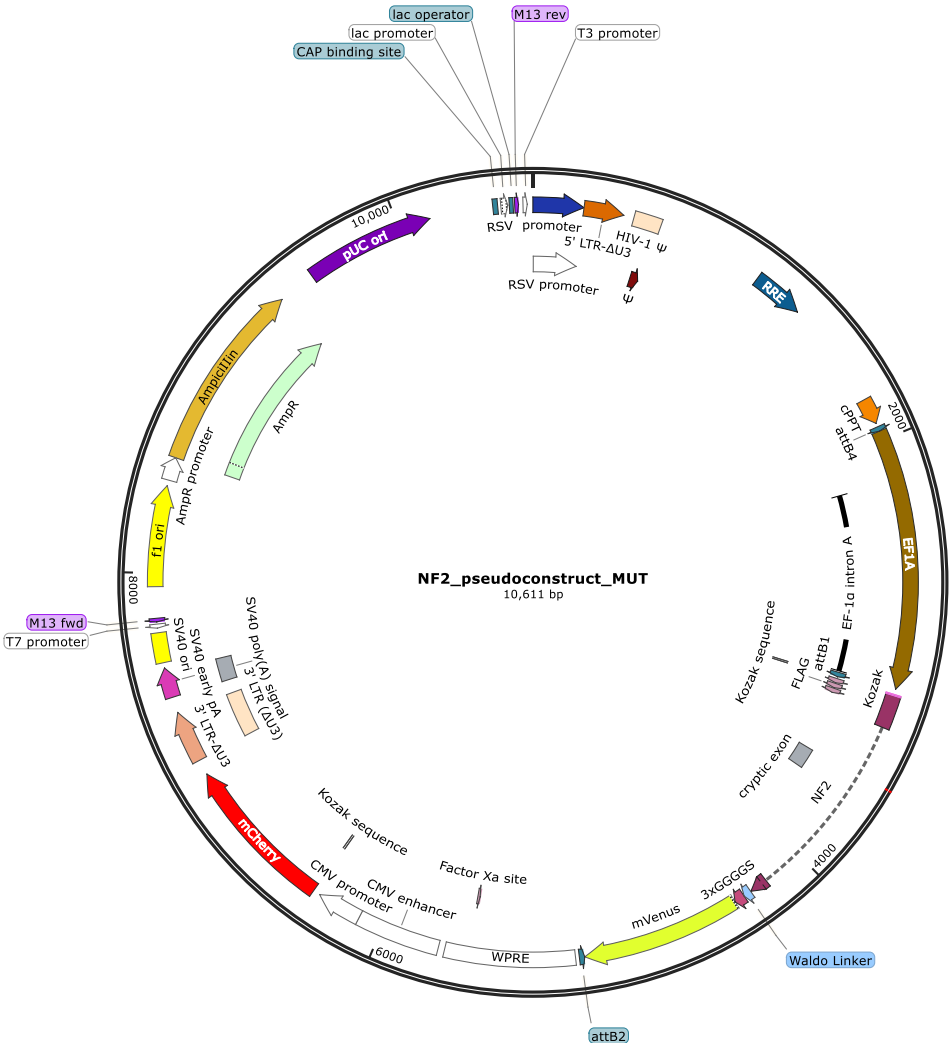

VectorBuilder *NF2* pseudo-construct reporter system, *NF2* c.516+232 G>A.